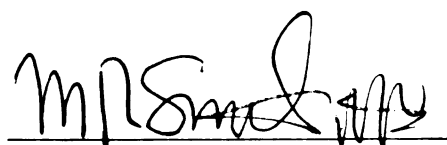This is to certify that the

dissertation entitled

INVESTIGATION OF STOICHIOMETRIC AND CATALYTIC

B-C BOND FORMATION BY GROUP 9 TRANSITION

METAL BORYL COMPLEXES

presented by

Jian-Yang Cho

has been accepted towards fulfillment
of the requirements for

_____Ph.D._____ degree in __Chemistry__

_____
Major professor

Date __12-9-02__

PLACE IN RETURN BOX to remove this checkout from your record.
TO AVOID FINES return on or before date due.
MAY BE RECALLED with earlier due date if requested.

DATE DUE	DATE DUE	DATE DUE

6/01 c:/CIRC/DateDue.p65-p.15

INVESTIGATION OF STOICHIOMETRIC AND CATALYTIC B-C BOND
FORMATION BY GROUP 9 TRANSITION METAL BORYL COMPLEXES

By

Jian-Yang Cho

A DISSERTATION

Submitted to
Michigan State University
in partial fulfillment of the requirement
for the degree of

DOCTOR OF PHILOSOPHY

Department of Chemistry

2002

ABSTRACT

INVESTIGATION OF STOICHIOMETRIC AND CATALYTIC B-C BOND
FORMATION BY GROUP 9 TRANSITION METAL BORYL COMPLEXES

By

Jian-Yang Cho

C-H bond activation has attracted considerable attention since hydrocarbon
feedstocks are ubiquitous. However, the catalytic functionalization of hydrocarbons still
represents a long-standing challenge in homogeneous and heterogeneous catalysis. Since
applications of arylboronate esters in cross-coupling chemistry are expansive, the
transformation depicted below would have broad appeal.

$$Ar\text{-}H + H\text{-}BX_2 \rightarrow Ar\text{-}BX_2 + H\text{-}H$$
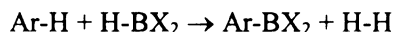
In 1999, our group demonstrated the first thermal, catalytic aromatic borylation
reaction catalyzed by Cp*Ir(PMe$_3$)(H)(BPin). In order to understand this important
transformation, detailed mechanistic studies were carried out. Through detailed
investigations, a remarkably selective iridium catalyst system was discovered for
aromatic borylation reactions.

Borylations of various mono-substituted arenes provide essentially a statistical
distribution of m- and p-C$_6$H$_4$(X)(BPin). This unique steric directing effect in aromatic
borylation provides a complementary means for regioselective functionalization of
aromatic compounds. For example, 1,3-disubstituted benzene rings are selectively
borylated at the 5-position. With the exception of electron-deficient arenes, this is
typically the least activated site towards aromatic substitution. Using this new
methodology, a variety of arylboronic esters can be synthesized in a relatively simple and

efficient way directly from corresponding arenes and pinacolborane or pinacol diboron catalyzed by the new iridium catalyst system.

The new iridium catalysts tolerate the entire range of aryl halides, ether, and ester functionalities and selectively functionalize aromatic C-H bonds. This remarkable selectivity broadens the potential applications for aromatic borylation.

Stoichiometric reactions of $(PMe_3)_4Ir(BPin)$ and fac-$(PMe_3)_3Ir(BPin)_3$ with arenes were examined. Both Ir^I and Ir^{III} boryl complexes can effect benzene borylation. However, their reactions with iodobenzene differ substantially under both stoichiometric and catalytic conditions.

In order to further investigate the possibility that metal boryl complexes are intermediates in borylation reactions, several derivatives containing alkyl, aryl, or silyl ligands were synthesized and fully characterized.

Preliminary mechanistic studies on the new iridium catalyst system were carried out and presently a mechanism involving Ir^{III} and Ir^V intermediates in an $Ir^{III/V}$ catalytic cycle is suggested. Correlations between the stoichiometric and catalytic reactions provided a deeper insight into the mechanism of aromatic borylation.

To my family and wife for their support and love

ACKNOWLEDGMENTS

First, I would like to thank my research advisor, Mitch Smith, for his guidance and assistance throughout my graduate career at Michigan State University. He taught me the qualities for pursuing the truth in science and gave me the opportunity to work on some exciting chemistry. Although the life for being a graduate student is tough, it equipped me with essential tools and knowledge to face future challenge. I will always appreciate that.

I am thankful to Dr. Odom and Dr. Maleczka for their stimulating discussions during our joint group meetings and Dr. Jackson and Dr. Pinnavaia for serving on my guidance committee.

My thanks also go out to Dr. Carl Iverson for his patient teaching and sharing of experiences during my first year here. I was very lucky to work with some talented postdoctoral associates, Dr. Man Kin Tse and Dr. Daniel Holmes. I learned a great deal from them. I will value the friendships I gained in my time at MSU. They are Chris Radano, Jim Ciszewski, Chen-Yu Yeh, Baixin Qian, Jie Fang, and Kuei-Fang Hsu. Their encouragement makes my graduate life more passable. Special thanks go to Jim and Kuei-Fang for their help in obtaining X-ray crystal structure. I also appreciate my best partners in Taiwan, Dr. Yih-Hsing Lo and Yi-Wei Chao, for their long-distance friendships.

Finally, I would like to thank my best friend, my soulmate, and my wonderful wife, Mi-Jin Chae, for her love, support, and sacrifice. Thank you for everything. I also

TABLE OF CONTENTS

CHAPTER 4

SYNTHESIS, CHARACTERIZATION, AND REACTIVITY OF IRIDIUM BORYL COMPLEXES

CHAPTER 5

PRELIMINARY MECHANISTIC STUDIES OF THE IRIDIUM/PHOSPHINE CATALYST SYSTEM FOR AROMATIC BORYLATION

CHAPTER 6

EXPERIMENTAL

APPENDIX A

APPENDIX B

APPENDIX C

LIST OF TABLES

LIST OF FIGURES

xv

LIST OF SYMBOLS AND ABBREVIATIONS

Å	Angstrom
BDAN	$B(NH)_2C_{10}H_6$
B_2Pin_2	bis(pinacolato)diboron, $Me_4C_2O_2B\text{-}BO_2C_2Me_4$
ClBCat	chloro-catecholborane
COD	1,5-cyclooctadiene
COE	cyclooctene
Cp*	pentamethylcyclopentadienyl, $\eta^5\text{-}C_5(CH_3)_5$
°C	degrees Celcius
d	doublet
dddd	doublet of doublet of doublet of doublet
D	deuterium
e.u.	entropy units
Et_2O	diethyl ether
equiv.	equivalent
fac	facial
GC	gas chromatography
h	hour
HBPin	pinacolborane, $HBO_2C_2Me_4$
Hz	hertz
IR	infrared
J	coupling constant

k	rate constant
K	temperature in Kelvin
kcal	kilocalorie
k_H/k_D	ratio of isotope effect on observed rate constant
k_{obs}	observed rate constant
L	liter, generic ligand
M	multiplet
Me	methyl, $-CH_3$
mer	meridional
min	minutes
mL	milliliters
mmol	millimole
mM	millimolar
mol	mole
MS	mass spectrometry
NMR	nuclear magnetic resonance
Ph	phenyl, $-C_6H_5$
PMe_3	trimethylphosphine
PPh_3	triphenylphosphine
Pin	pinacol, $1,2-O_2C_2Me_4^{2-}$
q	quartet
s	singlet, seconds
t	triplet

thf	tetrahydrofuran
δ	delta, ppm for NMR spectroscopy
$\Delta H^{\ddagger}$	change in enthalpy
$\Delta S^{\ddagger}$	change in entropy
η^{n}	ligand hapticity of number "n"
μL	microliters

CHAPTER 1

INTRODUCTION

C-H Bond Activation and Functionalization of Hydrocarbons

The selective transformation of carbon-hydrogen bonds to other functional groups represents a long-standing challenge in homogeneous and heterogeneous catalysis, because C-H bonds are the most ubiquitous chemical linkages in Nature. Elucidating the requirements necessary to effect their cleavage or their transformation into other bonds is based on our fundamental understanding of their chemical reactivity. Over the past two decades, many examples of C-H activation at transition metal centers were reported.[1] It has been a topic of great interest to the organometallic chemists. Saturated hydrocarbons are major constituents of natural gas and petroleum, but there are very few practical processes for converting them directly to more valuable chemicals. The lack of reactivity of alkane C-H bonds can be attributed to their high bond energies (typically 90-104 kcal/mol) and very low acidity or basicity. Despite the fact that C-H bonds are more difficult than other types of linkages to cleave, such as C-Cl and C-Br, they are not completely inert. Alkanes have been known to undergo a number of solution and gas-phase reactions that involve free radicals as intermediates. They exhibit some preference for reaction of tertiary C-H bonds over primary or secondary. There are also some examples of alkane reactions with superacids[2] or ozone[3]; however, they are usually very unselective. In recent years, considerable work with stoichiometric activation of C-H bonds suggests that homogeneous organometallic systems can overcome some of these

1

selectivity problems.[4] Many examples suggest that a regioselectivity pattern with (i.e., 1°

> 2° > 3°) can be obtained. Despite the success in this area, few systems are capable of

subsequent substrate functionalization and regeneration of the metal species as required

for catalytic turnover. Thus, developing a method not only to selectively activate but also

functionalize C-H bonds of hydrocarbons has been a "Holy Grail" in synthetic

chemistry.[1c]

Selective catalytic hydrocarbon functionalization is not unknown. In fact, Nature

performs ambient temperature alkane functionalization constantly, and sometimes with

excellent selectivity, through the use of oxygenase enzymes. Those, which belong to the

monooxygenase cytochrome P-450[5] and methane monooxygenase[6] (MMO) families,

have received a considerable amount of attention. These enzymes catalyze the

incorporation of molecular oxygen into alkane C-H bonds with the simultaneous loss of

water and oxidation of NADPH or NADH. In the case of cytochrome P-450, the enzyme

active site has been found to contain an iron porphyrin complex with a sulfur-bound

cysteine, which mediates the cleavage of O_2 to generate an iron-oxo complex. This oxo

complex is considered to be the active oxidant of alkane C-H bonds. The efficiency of

biological oxygenase systems has stimulated a significant body of research devoted to

developing both structural and functional mimics designed to oxidize alkane.[7]

Pathways discovered for activation of C-H bonds include (i) oxidative addition of

R-H to transition metal, (ii) σ bond metathesis between M-R' and R-H, 1,2-addition of R-

H to M=X (X=O, NR, CR$_2$), (iii) electrophilic activation in the reaction of M-X (X=

halide, hydroxide, triflate, etc.) and R-H to generate M-R and HX, and (iv) metalloradical

activation. Oxidative addition reactions are typical pathways for late transition metal

complexes. For example, Cp*Ir(PMe₃)(H)₂ (**2**, Cp* = η^5-C₅Me₅) loses H_2 under photo-irradiation to generate the reactive species "Cp*Ir(PMe₃)", which subsequently activate the C-H bonds of hydrocarbon substrates to form a metal alkyl hydride complex.[8] σ-Bond metathesis occurs mostly in early transition metal complexes. These reactions usually result in the interchange of metal and hydrocarbon alkyl fragments.[9] 1,2-addition reactions involve the addition of an alkane to metal-nonmetal multiple bond.[10] However, the scope of this type reaction and its potential for alkane functionalization remains unclear. Electrophilic activation reactions involve an electrophilic metal center, which attacks C-H bonds of alkanes to form functionalized alkanes directly. This type of reaction is usually carried out in a strongly polar medium such as water or anhydrous strong acid. One example in which the reaction between the Rh (II) porphyrin complexes and alkane C-H bonds with the involvement of free alkyl radical, generated through abstraction of a hydrogen atom from alkane by the Rh center is classified as metalloradical activation (Figure 1).[11]

Systems that can selectively and catalytically functionalize the C-H bonds of hydrocarbons are extremely rare. There are some examples of functionalization processes mediated by homogeneous transition metal complexes, including dehydrogenation of alkanes,[12] carbonylation of benzene,[13] carbonylation of pentane,[14] and acceptorless dehydrogenation of cyclic alkanes by iridium complex with PCP type ligand.[15]

Mechanistic insight into the fundamental processes and solutions of potential problems towards to the functionalization of hydrocarbons have been studied extensively and well developed in many stoichiometric reactions. Currently the biggest challenge in

3

this field is to develop better catalysts system to activate and functionalize the C-H bonds

of hydrocarbons for practical applications.

Oxidative addition

$$L_nM^x + R\text{-}H \longrightarrow L_nM^{x+2}(R)(H)$$

Sigma-bond metathesis

$$L_nM^x\text{-}R + R'\text{-}H \longrightarrow L_nM^x\text{-}R' + R\text{-}H$$

1,2-addition

$$L_nM^x{=}Y + R\text{-}H \longrightarrow L_nM^x\text{-}Y \quad\quad (Y = O, NR, CR_2)$$
$$\underset{R\ \ H}{}$$

Electrophilic activation

$$L_nM^x\text{-}Y + R\text{-}H \longrightarrow L_nM^x\text{-}R + H\text{-}Y \quad\quad (Y = \text{halide, hydroxide, triflate, etc.})$$

Metalloradical activation

$$\{(\text{porphyrin})Rh^{II}\}_2 \rightleftharpoons 2\,(\text{porphyrin})Rh^{II}\bullet \xrightarrow{R\text{-}H} \begin{array}{c}(\text{porphyrin})Rh^{III}(R)\\ +\\ (\text{porphyrin})Rh^{III}(H)\end{array}$$

Figure 1. Various pathways discovered for the activation of C-H bonds.

Thermodynamics of Borane Functionalization of C-H Bonds

Since the importance of boryl complexes as proposed intermediates in the

transition metal catalyzed functionalization of organic compounds, studies concerning the

4

fundamental properties and reaction chemistry of transition metal boryl complexes have been initiated since early 1990s. Transition metal-ligand covalent bond energies are important in understanding catalysis. However, there has been few data available for boranes and no thermochemical data for transition metal boryl complexes until 1994. In that year, Rablen and Hartwig[16] reported calculation of B-H and B-C bond dissociation energies (BDEs) for a series of boranes. From the established thermochemical and computational data of borane reagents, the reaction in equation 1 is essentially thermoneutral. Moreover, from calculated BDE's for B-H, C-H, and B-C bonds, synthesis of aryl boronic esters directly from boranes and arenes should be thermodynamically feasible.

$$CH_4 \cdot HBCat \rightleftharpoons CH_3BCat \cdot H_2 \quad \Delta H^\circ = \text{-2.1 kcal/mol} \quad (1)$$

Stoichiometric and Catalytic Borylation Reactions

In 1995, Hartwig et al.[17] reported the functionalization of hydrocarbons by the reaction of arenes and alkenes with $(CO)_5Mn(BCat)$, $(CO)_5Re(BCat)$, and $CpFe(CO)_2(BCat)$ under photochemical conditions (Figure 2). Although dehydrogenative borylation of benzene has not been observed previously before this report, dehydrogenative borylation of alkenes has been observed in catalytic chemistry.[18]

5

$(CO)_5M$—BCat $\xrightarrow{h\nu}$ ⬡—BCat + HBCat + $M_2(CO)_{10}$ + H_2 + $Re_3(CO)_{12}H_3$

M = Mn 45%   10-20%
M = Re 55%

Cp—Fe(CO)(OC)—BCat $\xrightarrow{h\nu,\ 1\ h}$ ⬡—BCat + Fp_2 + H_2

87%
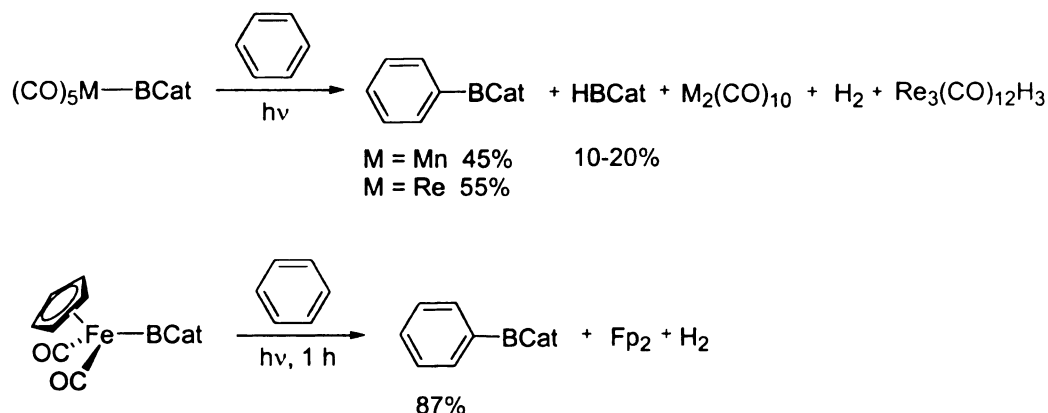
Figure 2. Functionalization of hydrocarbons by transition metal boryl complexes under photochemical conditions.

Waltz and Hartwig[19] in 1997 reported selective functionalization of alkane at terminal position to produce alkylboronate esters, which are common reagents in organic synthesis. They found that photochemical reaction of $Cp*Fe(CO)_2(BCat')$ ($Cp* = C_5Me_5$, $Cat' = 1,2,-O_2C_6H_2-3,5-(CH_3)_2$), $Cp*Ru(CO)_2(BCat')$, and $Cp*W(CO)_3(BCat')$ with a series of alkanes gives alkylboronate esters with functionalization of alkane exclusively at the terminal position (Figure 3). The boryl complexes are rare chemical reagents that react selectively at the terminal position of alkane to provide simple functionalized products. From their mechanistic analysis, they believe ligand dissociation is induced photochemically and that thermal reaction of the resulting intermediate occurs with alkanes. They pointed out that $CpFe(CO)_2(BCat)$ can functionalize arenes but not alkanes, presumably because of the presence of sp^2-hybridized C-H bond in the Cp ring, which is preferred to be functionalized than alkanes. Therefore, they prepared a derivative of this complex with the sp^2-hybridized position blocked to solve the problem.

6

Indeed, the elimination of all accessible sp^2 positions on the metal boryl complex does account for the unusual reactivity observed. Reaction with pentane gave 1-pentylboronate ester as the only functionalization product in 85% yield. Reaction with ethylcyclohexane gave (2-cyclohexyl)-1-ethylboronate ester as the only functionalization product in 74% yield. Interestingly, selectivity for the two terminal position of isopentane was good. Functionalization at the less hindered position occurred in 55% yield, whereas functionalization at the more hindered terminal position occurred in only 2% yield.
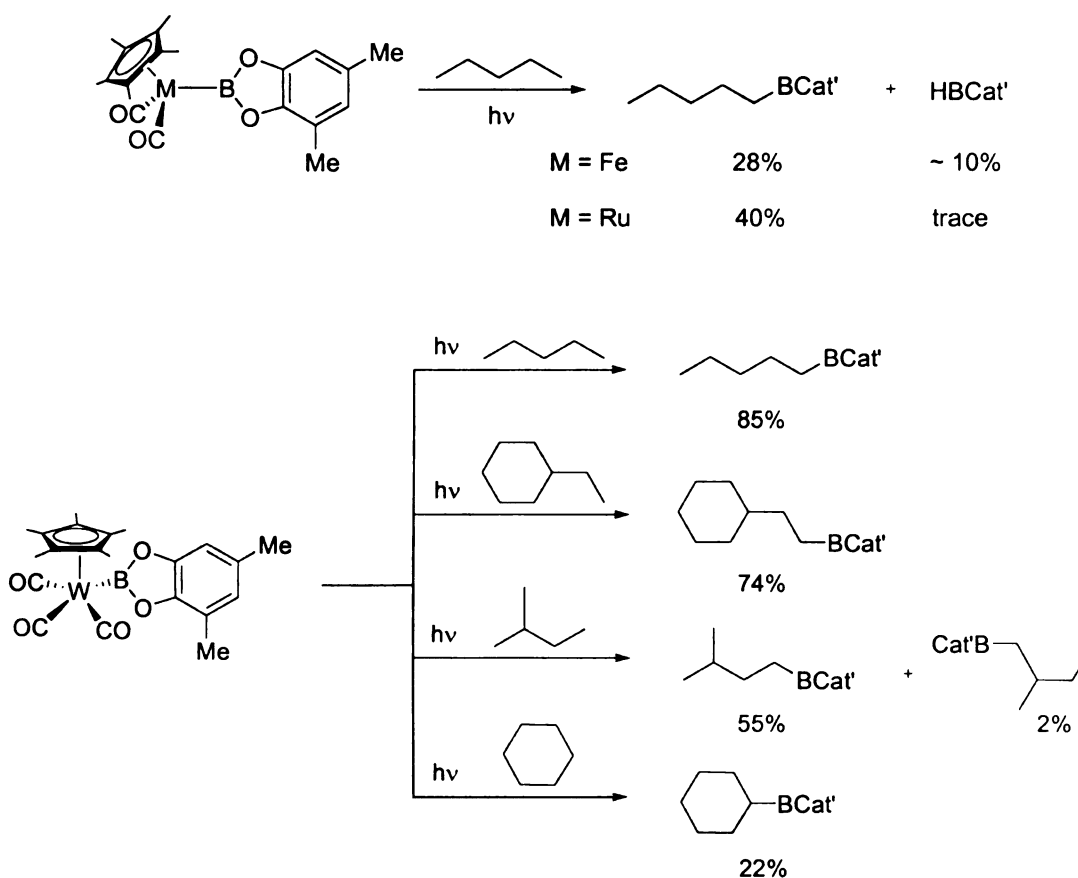
Figure 3. Selective functionalization of alkanes by transition metal boryl complexes.

7

Hartwig et al.[20] also examined the photochemical reaction of $CpFe(CO)_2(BCat)$ in a variety of mono-substituted arene solvents including $C_6H_5(Me)$, $C_6H_5(OMe)$, $C_6H_5(Cl)$, $C_6H_5(CF_3)$, and $C_6H_5(NMe_2)$. They found the reaction of $CpFe(CO)_2(BCat)$ with substituted arenes resulted in formation of only meta- and para-substituted arylboronate esters for all substituted except anisole, which showed substantial amounts of ortho-substituted product. For N,N-dimethylaniline, it showed a preference for reaction at the para position.

In 1999, Iverson and Smith[21] reported the first thermal, catalytic aromatic borylation reaction to synthesize aryl boronic esters directly from arenes and pinacolborane by pre-catalyst $Cp*Ir(PMe_3)(H)(BPin)$ (Figure 4). They demonstrated the catalytic viability of equation 2 for the first time.
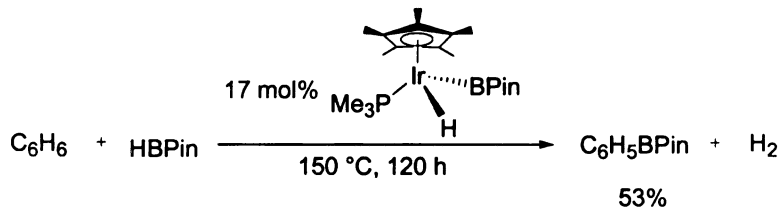
Figure 4. The first thermal, catalytic example of aromatic borylation reaction.

$$Ar{-}H + HBX_2 \rightleftharpoons Ar{-}BX_2 + H_2 \quad \Delta H^\circ \sim -3.1\ kcal/mol \qquad (2)$$
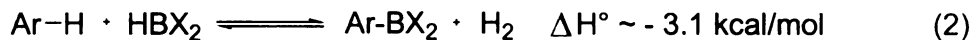
The findings was discovered in investigating stoichiometric B-C bond formation in reactions between $Cp*Ir(PMe_3)(Ph)(H)$ and HBPin in C_6D_6. They noticed the substantial quantities of arylboron products were produced from catalytic solvent activation.

Aside from methane-to-methanol conversion,[22] catalytic C-H functionalizations

for unactivated hydrocarbons are extremely rare. Since applications of boronate esters in

Miyaura-Suzuki cross-coupling chemistry are expansive,[23] the demonstration of catalytic

viability of equation 2 is significant.

Later in the same year, Chen and Hartwig[24] reported catalytic, regiospecific end-

functionalization of alkanes by the rhenium complex, Cp*Re(CO)₃, under photochemical

conditions. They suggested that the terminal boronate esters are kinetic products, and the

selective functionalization most likely results from a regiospecific reaction of the

rhenium bis-boryl complex with the alkane primary C-H bond (Figure 5).

$$R = n\text{-}C_5H_{11}$$
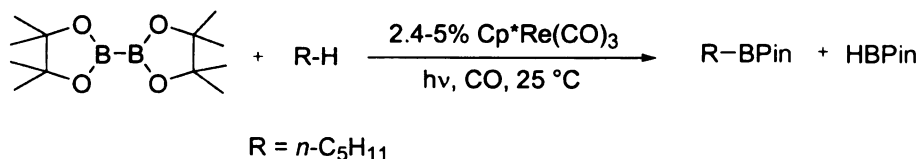
Figure 5. Reaction of B_2Pin_2 in pentane catalyzed by Cp*Re(CO)₃.

Synthetic Routes to Arylboronic Esters

The palladium-catalyzed cross-coupling reaction between organoboron

compounds and organic halides or triflates provides a powerful and general methodology

for the formation of C-C bonds. Arylboron reagents are typically synthesized in a

multistep process: (1) halogenations of arenes to form aryl halides, (2) treatment of aryl

halides with magnesium to generate their Grignard reagents, (3) reactions of Grignard

reagents with trialkyl borate to give final corresponding arylboronate esters. Miyaura et

al.[25] have described a clever arylboronate ester synthesis where the generation of Grignard and lithium reagents is avoided by using palladium catalysts to effect the desired transformation from borane reagents and halogenated arenes. Since halogenated arenes required for these approaches must be synthesized from hydrocarbon feedstock, direct routes to the arylboron reagents from hydrocarbons are attractive (Figure 6).

Traditional Method

Ar—H $\xrightarrow{[X]}$ Ar—X $\xrightarrow[\text{Ether}]{\text{Mg}}$ Ar—MgX $\xrightarrow[-\text{MgX(OR)}]{\text{B(OR)}_3}$ Ar—B(OR)$_2$

Miyaura et al.

Ar—H $\xrightarrow{[X]}$ Ar—X $\xrightarrow[\text{DMSO}]{\text{"Pd", B}_2\text{Pin}_2 \text{ or HBPin, Base}}$ Ar—BPin

Direct Method

Ar—H + H—B(OR)$_2$ $\xrightarrow[-\text{H}_2]{\text{catalyst}}$ Ar—B(OR)$_2$
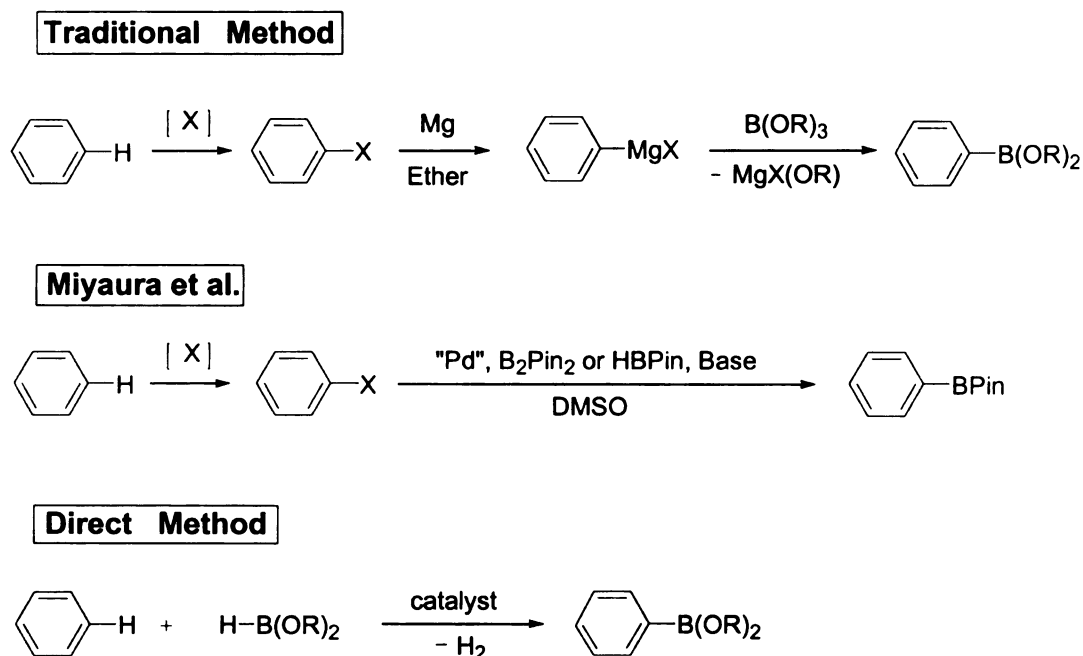
Figure 6. Traditional and direct routes to arylboronic esters from aromatic hydrocarbons.

Several research groups[26] including our group have achieved functionalization of hydrocarbons using a borane as an approach in stoichiometric and catalytic reactions under photochemical or thermal conditions. A milder reaction condition, higher turnover number, more efficient system is desirable. Furthermore, Knochel[27] and co-workers recently reported the kinetic and thermodynamic aspects in C-H bond activation by direct

borane-hydrocarbon dehydrogenation. On the basis of a better understanding of the role of transition metal boryl complexes in the organic transformation reactions, our ultimate goal is to develop a better catalytic system not only to activate but also functionalize hydrocarbon C-H bonds to well utilize ubiquitous hydrocarbon feedstock.
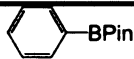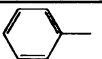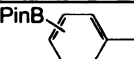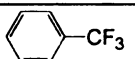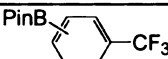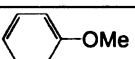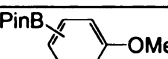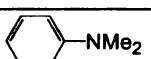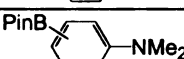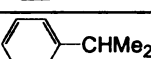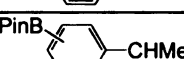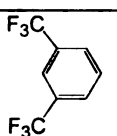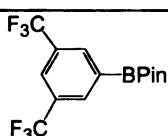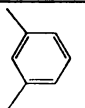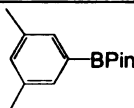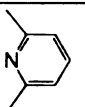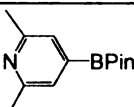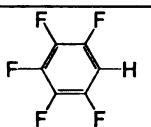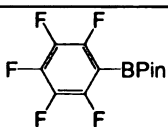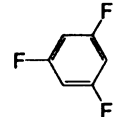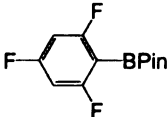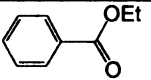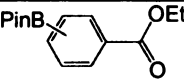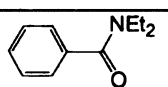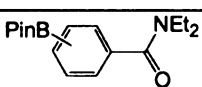
CHAPTER 2

MECHANISTIC INVESTIGATION OF Cp*Ir(PMe₃)(H)(BPin) CATALYZED

BORYLATION REACTIONS

Comparison between Cp*Ir(PMe$_3$)(H)(BPin) and Cp*Rh(η^4-C$_6$Me$_6$) Pre-catalyst

Systems in Borylation of Various Substituted Arenes

In 1999, our group reported the first thermal, catalytic example of aromatic

borylation reactions to generate arylboronic esters directly from unactivated arenes and

boranes by pre-catalyst Cp*Ir(PMe$_3$)(H)(BPin) (**1**, Cp* = η^5-C$_5$Me$_5$).[21] Subsequently,

Hartwig and co-workers reported alkane and arene borylations with the use of much more

reactive Rh pre-catalyst, such as Cp*Rh(η^4-C$_6$Me$_6$) (**3**).[26a] Given the broad utility of

arylboronic esters in Pd-catalyzed cross-couplings with aryl and alkyl halides,[23] we were

curious as to the extent of regioselectivity and functional group compatibility for

analogous transformations of substituted arenes.[26b] In an initial borylations of substituted

arenes, 20 mol% solutions of **1** or Cp*Ir(PMe$_3$)(H)$_2$ (**2**) were dissolved with HBPin in

neat arene solvents, and the reactions were run at 150 °C. Once borylation has

commenced, ^{31}P NMR spectroscopy indicated that compound **1** is the predominant Ir

species in solution with small quantities of compound **2** present in each case. Analogous

borylations were also performed using the more active pre-catalyst **3**. After the borane

was consumed, product ratios were determined by GC analysis of crude reaction

mixtures. Isolated yields of isomer mixtures are reported in Table 1, and the product

assignments were corroborated by comparisons to authentic samples.

Table 1. Isolated yields (based on HBPin) and isomer distributions for catalytic borylation of aromatic hydrocarbons catalyzed by solutions of compounds **1** and **3**.

Arene	Product(s)	% yield (*para:meta:ortho*), time[a]	% yield (*para:meta:ortho*), time[b]
(benzene)	(C₆H₅–BPin)	53, 120 h[c]	92, 2.5 h[d]
(toluene)	PinB–C₆H₄–CH₃	91 (33.9:62.0:4.1),[e] 51 h	72 (32.5:62.7:4.9),[f] 3.5 h
–CF₃	PinB–C₆H₄–CF₃	99 (33.3:66.7:0.0), 17 h	84 (33.3:66.7:0.0), 1.5 h
–OMe	PinB–C₆H₄–OMe	55 (19.5:79.0:1.6), 65 h	65 (25.4:66.9:7.6), 1 h
–NMe₂	PinB–C₆H₄–NMe₂	--	65 (42.9:54.9:2.1), 3.5 h
–CHMe₂	PinB–C₆H₄–CHMe₂	52 (31.1:68.0:0.9), 142 h	67 (33.2:66.1:0.7), 2 h
3,5-(F₃C)₂C₆H₄	(F₃C)₂C₆H₃–BPin	81,[c] 10 h	86, 3 h
(m-xylene)	(Me)₂C₆H₃–BPin	60,[g] 151 h	73,[h] 4 h
(2,6-dimethylpyridine)	N-heterocycle–BPin	--	41, 6 h
C₆F₅–H	C₆F₅–BPin	81,[i] 18 h	41,[j] 0.5 h
(1,3,5-trifluorobenzene)	F₃C₆H₂–BPin	--	46,[k,l] 0.5 h
–C(O)OEt	PinB–C₆H₄–C(O)OEt	--	-- (33.0:57.4:9.6),[m] 1 h
–C(O)NEt₂	PinB–C₆H₄–C(O)NEt₂	--	50 (14.0:27.7:58.3), 0.5 h

[a] 20 mol% **1**, generated *in situ* from compound **2** and HBPin at 150 °C. [b] 2 mol% **3** at 150 °C. [c] 20 mol% **1** at 150 °C. [d] GC yield reported in reference 18c. [e] < 1% of the isomer mixture is C₆H₅CH₂BPin. [f] 3% of the isomer mixture is C₆H₅CH₂BPin. [g] 3% of the isolated product is *m*-C₆H₄(Me)(CH₂BPin). [h] 12% of the product is *m*-C₆H₄(Me)(CH₂BPin). [i] 4% of the isolated product is isomers of C₆F₄H(BPin). [j] 16% of the isolated product is isomers of C₆F₄H(BPin). [k] Reaction was run in a 2:1 mixture of 1,3,5-C₆H₃F₃:*p*-xylene-*d₁₀*. [l] C₆HF₃(BPin)₂ (7%) and an isomer of C₆H₃F₂(BPin) (6%). [m] Products were not isolated.

13

In a simple assay of regioselectivity, toluene borylation primarily gave a statistical distribution of *m*- and *p*-$C_6H_4Me(BPin)$. In order to address the reversibility of the borylation reactions, the catalytic borylation of C_6D_6 by HBPin in the presence of *m*-$C_6H_4Me(BPin)$ was examined. Isomerization of *m*-$C_6H_4Me(BPin)$ to *p*-$C_6H_4Me(BPin)$ or generation of toluene would indicate that borylation is reversible. Under typical reaction conditions where C_6D_6 is converted to C_6D_5BPin, *m*-$C_6H_4Me(BPin)$ does not isomerize and toluene is not eliminated. Thus, the borylation products are kinetically determined. It is noteworthy that arene C-H bonds are functionalized in the presence of weaker benzylic C-H bonds. A range of monosubstituted arenes was examined to determine whether reaction conditions would tolerate heteroatom substituents and to assess the generality for statistical *meta/para* substitution. The results in Table 1 indicate that *meta/para* ratios are predominantly statistical with the largest deviations occurring for *N,N*-dimethylaniline, which favors *para* substitution, and anisole, which favors *meta* substitution. For Rh-catalyzed reactions, the deviations were relatively small, but *meta* borylation of anisole is pronounced for Ir system. Since cumene gave a statistical distribution of *meta* and *para* borylation products, electronic effects are responsible for enhanced *para* selectivity for *N,N*-dimethylaniline. Benzylic activation of toluene increased for Rh (~3 % $PhCH_2BPin$) versus Ir (~1 % $PhCH_2BPin$).

The aversion from borylation *ortho* to aromatic substituents suggested that selective borylation should be possible for 1,3-disubstituted arenes. We initially examined this possibility for 1,3-$C_6H_4(CF_3)_2$ and found exclusive borylation at the 5-position in reactions catalyzed by solutions of **1** or **3**. For the borylation of *m*-xylene mediated by compound **3**, benzylic activation increases significantly relative to that for

toluene. It appears that steric directing effects will extend to heterocycles as aromatic borylation of 2,6-lutidine occurs exclusively at the 4-position. Directing effects based on steric effects in aromatic substitution are uncommon, and electronic effects generally dictate the substitution pattern. For example, in the Friedel-Crafts alkylation of 3-chlorotoluene, no *meta*-substitution products are observed since Me group is an *ortho*- and *para*-directing activator and Cl is an *ortho*- and *para*-directing deactivator. Generally, selective *meta* functionalization is difficult and requires strong electron-withdrawing groups for electrophilic or –donating groups for nucleophilic aromatic substitution, respectively. The unique steric directing effect in aromatic borylation provides a complementary mean for regioselective functionalization of aromatic compounds.

Fluorinated arenes were also tested for compatibility. Ir- or Rh-catalyzed borylation of C_6HF_5 gave C_6F_5BPin as the primary product. Similarly, compound **3** catalyzes borylation in a 2:1 mixture of $1,3,5-C_6H_3F_3$ and *p*-xylene-d_{10} to yield $C_6H_2F_3BPin$ as the major product. Attempts to prepare the di- and triborated compounds, $C_6HF_3(BPin)_2$ and $C_6F_3(BPin)_3$, from stoichiometric amounts of $1,3,5-C_6H_3F_3$ in *p*-xylene-d_{10} yielded significant quantities of $C_6H_3F_2(BPin)$ (~60% of the borylated products). The selectivity for C-H activation is significant considering that Rh-catalyzed reactions of silane with C_6HF_5 give C-F activation products exclusively.[28]

For arenes bearing ester and amide functionality, reduction of the carbonyl groups could potentially compete with aromatic borylation. Since HBPin reacts sluggishly in uncatalyzed hydroborations, selective aromatic borylations of aryl esters and amides seemed possible. Hence, catalytic borylations of ethyl benzoate and diethyl benzamide by

compound **3** were examined. In both instances, the reactions gave primarily aromatic borylation. For ethyl benzoate, *meta/para* borylation dominates with a modest increase in *ortho* borylation (p:m:o = 1.00:1.74:0.29), whereas diethyl benzamide gave o-$C_6H_4(C(O)NEt_2)(BPin)$ as the major isomer (p:m:o = 1.00:1.98:4.17). The shift in substitution pattern is consistent with chelate-directed borylation at the *ortho* position. Since resonance structure B has a larger contribution for an amide relative to an ester (Figure 7), chelation of the amide oxygen to Rh or B in the catalytically active species is more favorable for the amide. The statistical *meta*:*para* ratio for the minor isomers suggests that chelate and sterically directed pathways compete.

$$
\underset{\textbf{A}}{\underset{\displaystyle Ph \diagup\!\!\!\overset{\displaystyle \cdot\overset{\cdot\cdot}{O}\cdot}{\diagdown} E}{}} \longleftrightarrow \underset{\textbf{B}}{\underset{\displaystyle Ph \diagup\!\!\!\overset{\displaystyle :\overset{\cdot\cdot}{\underset{\cdot\cdot}{O}}:^{\ominus}}{\diagdown} E^{\oplus}}{}} \qquad E = NEt_2, OEt
$$
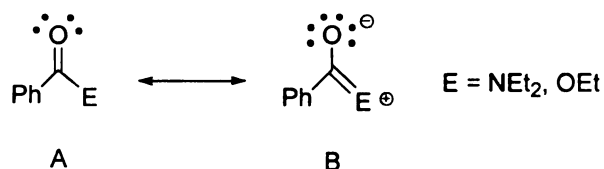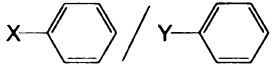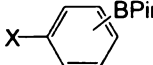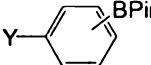
Figure 7. Resonance structures of ethyl benzoate and N,N-diethyl benzamide.

To probe the role of electronic effects, relative product ratios from catalytic borylations in equimolar mixtures of substituted arenes were determined (Table 2). Electron-deficient arenes are generally more reactive in both systems, and relative rate differences for Ir are slightly more pronounced than those for Rh. Ir-catalyzed borylation in neat N,N-dimethylaniline was extremely slow. Factors besides deactivation of the arene ring may be responsible for the reduced reaction rate; such as, possible coordination of the nitrogen lone-pair electrons of aniline to the Ir metal center, which

would block the active site around Ir. This may explain why cumene borylation in *N,N*-dimethylaniline/cumene mixtures was suppressed relative to borylation in neat cumene.

Table 2. Relative ratios of arylboronic esters for borylations of equimolar mixtures of substituted arenes catalyzed by compounds **2** and **3**.

X—⟨ ⟩/ Y—⟨ ⟩	X—⟨ ⟩-BPin : Y—⟨ ⟩-BPin (Catalyzed by solutions of 2)	(Catalyzed by solutions of 3)
X = CF$_3$, Y = CH$_3$	89.0:11.0	73.0:27.0
X = OCH$_3$, Y = CH$_3$	62.0:38.0	51.0:49.0
X = N(CH$_3$)$_2$, Y = CH$_3$	--	40.8:59.2
X = N(CH$_3$)$_2$, Y = CH(CH$_3$)$_2$	31.0:69.0	40.1:59.9

A comparison of pre-catalysts **1** and **3** in borylations of various substituted arenes revealed that the Ir system was more selective toward arene C-H activation. Given the importance of selectivity in chemical synthesis, these findings spurred a detailed investigation of the original Ir system.

Metathesis Reactions between Cp*M(PMe₃)(Ph)(H) (M = Ir, Rh) and Pinacolborane in C₆D₆

Fundamental understanding of hydrocarbon activation by "Cp*M(PMe₃)" (Cp* = C₅Me₅, M = Ir, Rh) has been studied extensively by Jones' and Bergman's research groups. In the iridium system, Bergman[1a] and co-workers showed that, upon irradiation, an excited state of Cp*Ir(PMe₃)H₂ is formed. This rapidly extrudes H₂, and leaves behind the reactive, coordinately unsaturated intermediate "Cp*Ir(PMe₃)". The intermediate inserts into a C-H bond of R-H via a three-center transition state, and leads to the formation of Cp*Ir(PMe₃)(R)(H) complexes. At the same period of time, Jones and co-workers studied the related rhodium complexes[1b] to determine the relative stabilities of the Cp*Rh(PMe₃)(Alkyl)(H) and Cp*Rh(PMe₃)(Aryl)(H). They found a slight kinetic preference for benzene over propane and overwhelming thermodynamic preference for benzene oxidative addition. For the Cp*Rh(PMe₃)(Ph)(H) (4) complex, a reversible reductive elimination of benzene was found to occur at convenient rate upon heating to ~ 60 °C in C₆D₆ solvent, producing Cp*Rh(PMe₃)(C₆D₅)(D). With a detailed picture of transition metal mediated C-H activation established by several research groups, we chose a Lewis acidic reagent, boranes, as an approach to convert activated alkyl and aryl groups to functionalized organic products. Our initial proposed catalytic cycle is shown below (Figure 8).

$$R-H \quad + \quad H-BX_2 \quad \longrightarrow \quad R-BX_2 \quad + \quad H_2 \quad \Delta H^\circ \sim -3.1 \text{ kcal/mol}$$
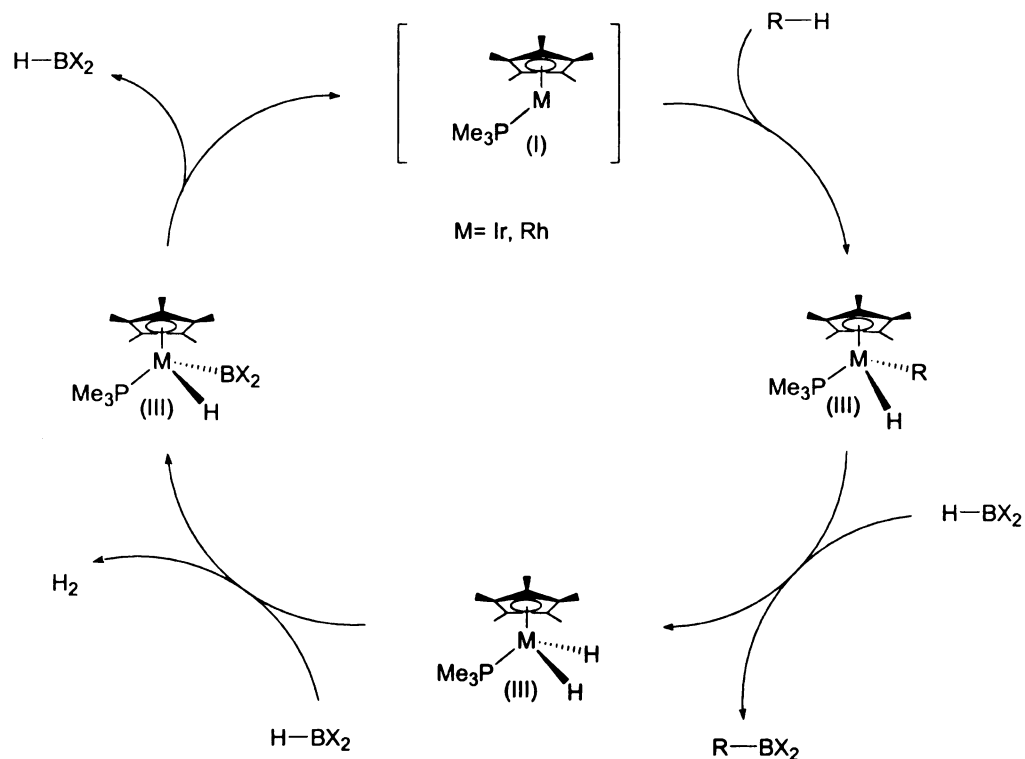
Figure 8. Initial proposed catalytic cycle for catalytic functionalization of hydrocarbon C-H bonds.

In the proposed catalytic cycle, the reactive unsaturated intermediate "$Cp^*M(PMe_3)$" can activate the C-H bond of hydrocarbons to form $Cp^*Ir(PMe_3)(R)(H)$. Hopefully the metathesis reaction between HBX_2 and $Cp^*Ir(PMe_3)(R)(H)$ can release R-BX_2 and generate $Cp^*Ir(PMe_3)H_2$. Then the dihydride complex can react further with HBX_2 to generate $Cp^*Ir(PMe_3)(H)(BX_2)$, followed by reductive elimination of HBX_2 to

19

regenerate the reactive 16 electron intermediate "Cp*M(PMe₃)" to complete the catalytic

cycle. In order to test the viability of this proposed catalytic cycle, the metathesis reaction

between Cp*M(PMe₃)(Ph)(H) (M = Ir, Rh) and HBPin in C₆D₆ were examined. For the

reaction between Cp*Ir(PMe₃)(Ph)(H) (5) and HBPin in C₆D₆ at 150 °C, after around

37% conversion (based on ¹H NMR spectra) from Cp*Ir(PMe₃)(Ph)(H) to

Cp*Ir(PMe₃)(H)(BPin), the ratio between C₆H₅BPin and C₆D₅BPin was found to be

around 1:23 (Figure 9).

(a)

Cp*Ir(PMe₃)(H)(BPin) (1)

Cp*Ir(PMe₃)(Ph)(H) (5)

2.20   2.10   2.00   1.90   1.80   1.70

(b)

PhBPin   5   PhBPin   5

8.00   7.80   7.60   7.40   7.20   7.00
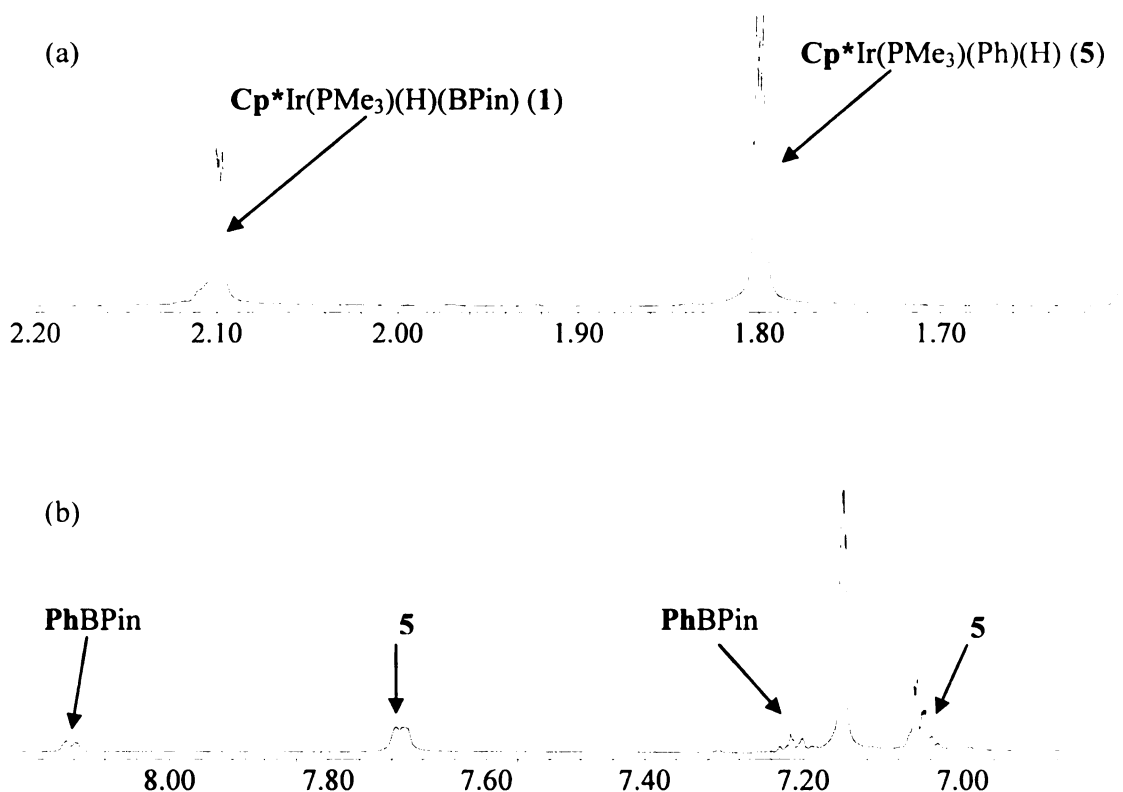
Figure 9. The reaction between Cp*Ir(PMe₃)(Ph)(H) (5) and HBPin in C₆D₆ at 150 °C

after around 37% conversion from Cp*Ir(PMe₃)(Ph)(H) to Cp*Ir(PMe₃)(H)(BPin): (a) ¹H

NMR spectrum of Cp* region; (b) ¹H NMR spectrum of aromatic region.

Substantial quantities of arylboron products were produced from catalytic solvent activation. Hence, we conclude that catalytic borylation is much faster than metathesis reaction between compound **5** and HBPin in C_6D_6, even though the metathesis process is viable (Figure 10).
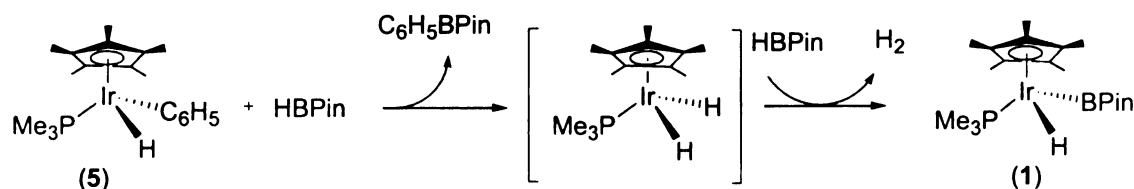
Figure 10. The metathesis reaction between compound **5** and HBPin in C_6D_6 at 150 °C.

Thermal borane elimination from Cp*Ir(PMe₃)(H)(BPin) (**1**) was assessed by heating C_6D_6 solution of the pure compounds. After two weeks at 200 °C and one day at 280 °C, the formation of C_6D_5BPin was not detected (Figure 11). If HBPin is reductively eliminated from compound **1**, the reactive intermediate "Cp*Ir(PMe₃)" can activate C-D bond of C_6D_6 to form Cp*Ir(PMe₃)(C_6D_5)(D), which can react further with HBPin through metathesis process to generate C_6D_5BPin. Since only small quantities of Cp*Ir(PMe₃)(C_6D_5)(D) (**6**) were generated in the reaction after prolonged thermolysis, the HBPin reductive elimination pathway is not kinetically competent to account for catalysis. Therefore, a pathway involving HBPin reductive elimination to generate an active catalyst can be eliminated. The final ^1H NMR and ^{31}P NMR spectra of the reaction are shown in Figure 12. The moderate quantities of BPin-O-BPin observed may result from the reaction between trace moisture and HBPin.
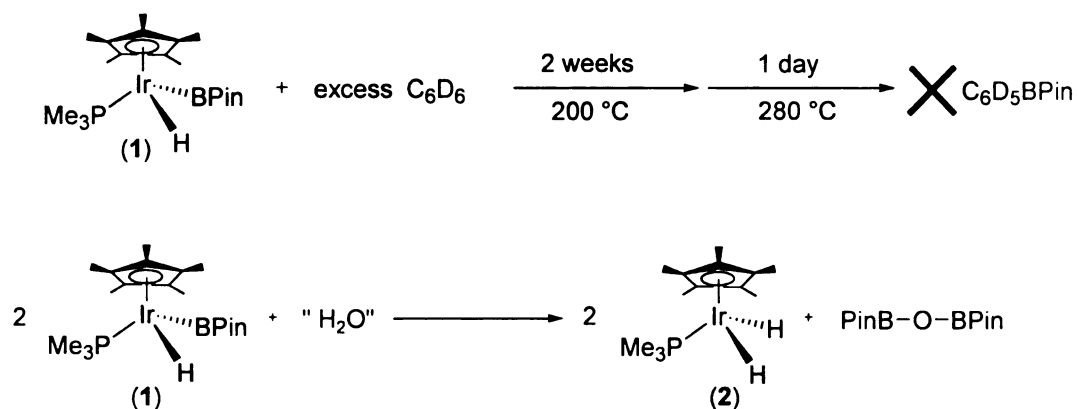
Figure 11. Thermolysis of Cp*Ir(PMe$_3$)(H)(BPin) (**1**) in C$_6$D$_6$.
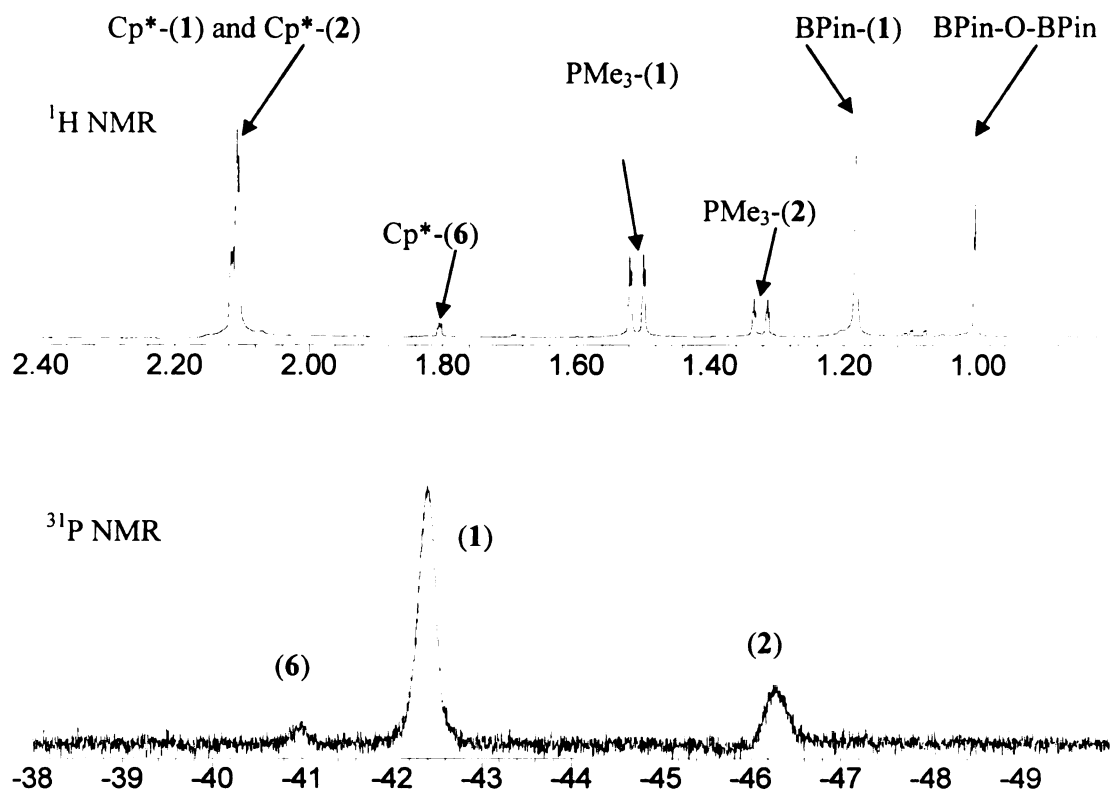
Figure 12. ^{1}H NMR and ^{31}P{^{1}H} NMR spectra of the thermolysis of compound **1** in C$_6$D$_6$.

The analogous reaction in the Rh system was also examined. Benzene reductive elimination from Cp*Rh(PMe₃)(Ph)(H) (**4**) occurred before metathesis reaction took place. In the reaction of compound **4** with HBPin in C₆D₆ at elevated temperature, compound **4** reductively eliminated C₆H₆, followed by oxidative addition of HBPin to form Cp*Rh(PMe₃)(H)(BPin) (**7**) (Figure 13).

Simplified rate expressions can be derived by applying the steady-state approximation. Application of the steady-state approximation to Figure 13 gives the rate law and k_{obs} expression shown in Equations 3 and 4.
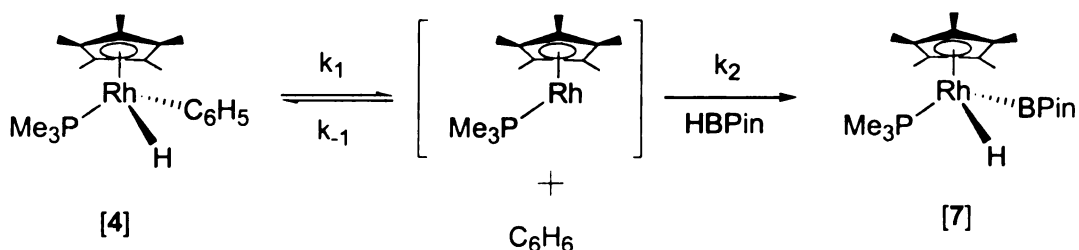
Figure 13. The reaction of compound **4** with HBPin in C₆D₆ at elevated temperature.

$$\frac{- d[4]}{dt} = k_{obs} [4] \tag{3}$$

$$k_{obs} = \frac{k_1 k_2 [HBPin]}{k_{-1}[C_6H_6] + k_2[HBPin]} \tag{4}$$

$$\text{If } k_{-1}[C_6H_6] \gg K_2[HBPin] \qquad k_{obs} = \frac{k_1 k_2 [HBPin]}{k_{-1}[C_6H_6]} \tag{5}$$

If $k_{-1}[C_6H_6] \gg k_2[HBPin]$, k_{obs} is expected to exhibit a first order dependance on [HBPin] as shown in equation 5. This is indeed the case as shown in Figure 14. The kinetic data are consistent with this proposed rate law. The k_{obs} was measured from 65 to 115 °C, and activation parameters were determined from the temperature dependence of k_{obs}. From the Eyring plot (Figure 15) over this temperature range, activation parameters were obtained: $\Delta H^{\ddagger} = 25.6$ kcal/mol and $\Delta S^{\ddagger} = -5.3$ e.u. For a comparison, Jones and co-workers found that a reversible reductive elimination of benzene from compound **4** in C_6D_6 solvent at ~60 °C to form $Cp^*Rh(PMe_3)(C_6D_5)(D)$ followed first-order kinetics over a 46-degree temperature range. From the Eyring plot of the first–order rate constants, they obtained the activation parameters for arene loss: $\Delta H^{\ddagger} = 30.5$ (8) kcal/mol and $\Delta S^{\ddagger} = 14.9$ (2.5) e.u. They stated that the positive value for the entropy of activation is consistent with the formation of an intact, dissociating benzene molecule in the transition state.[29] In the reaction of compound **4** with HBPin in C_6D_6, the small negative value for the entropy of activation suggests that the transition state of the reaction is more ordered than the ground state. From the activation parameters established by Jones and co-workers, the k_{obs} for benzene elimination at 75 °C is calculated to be 6.98×10^{-4} s^{-1} and the k_{obs} for the reaction of compound **4** with HBPin in C_6D_6 at 75 °C is 5×10^{-5} s^{-1}. Since the overall rate k_{obs} for the reaction of compound **4** with HBPin at 75 °C (5×10^{-5} s^{-1}) is smaller than k_{obs} for benzene elimination at 75 °C (6.98×10^{-4} s^{-1}), the rate determining step must involve a process other than benzene elimination. This piece of evidence suggests that H-B activation is the rate-determining step in this reaction.
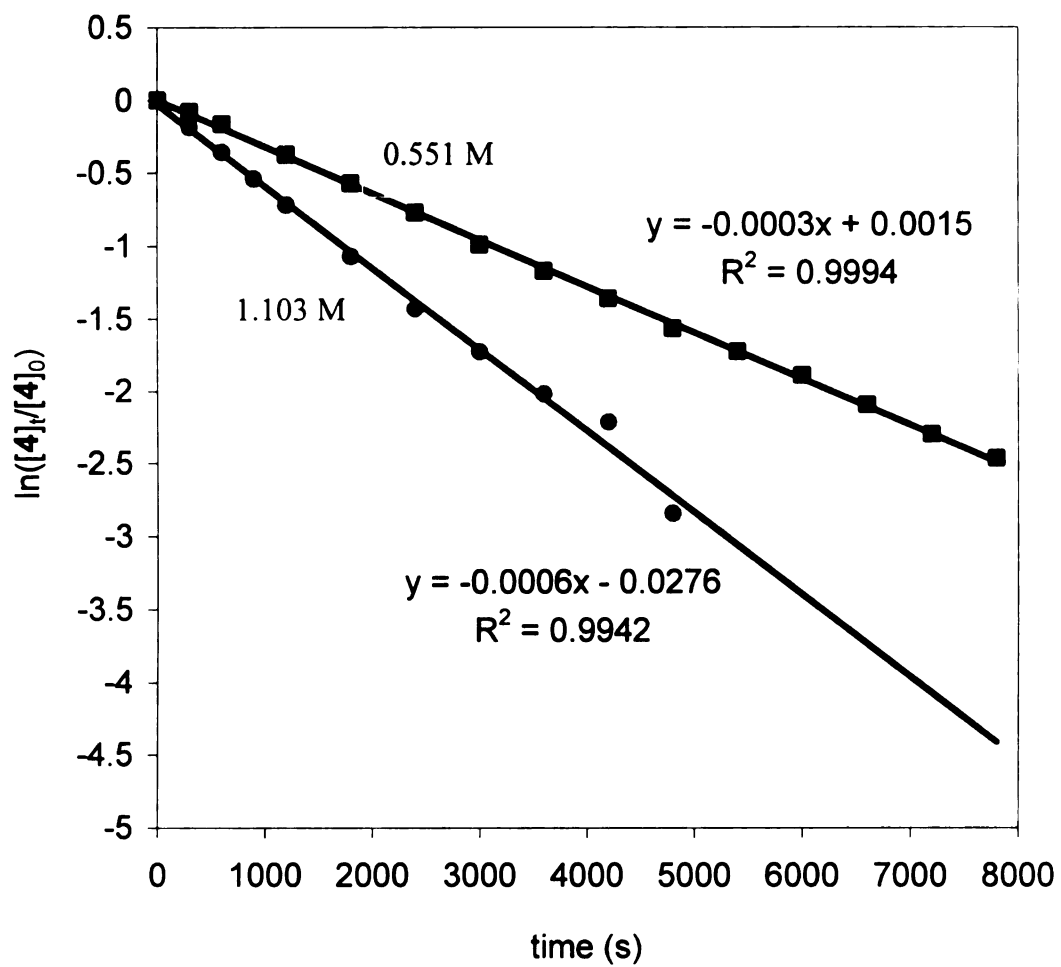
Figure 14. Plot of $\ln([4]_t/[4]_0)$ vs. time (s) for the reaction of compound **4** with [HBPin] = 0.551 M and [HBPin] = 1.103 M in C_6D_6 at 95 °C, respectively.
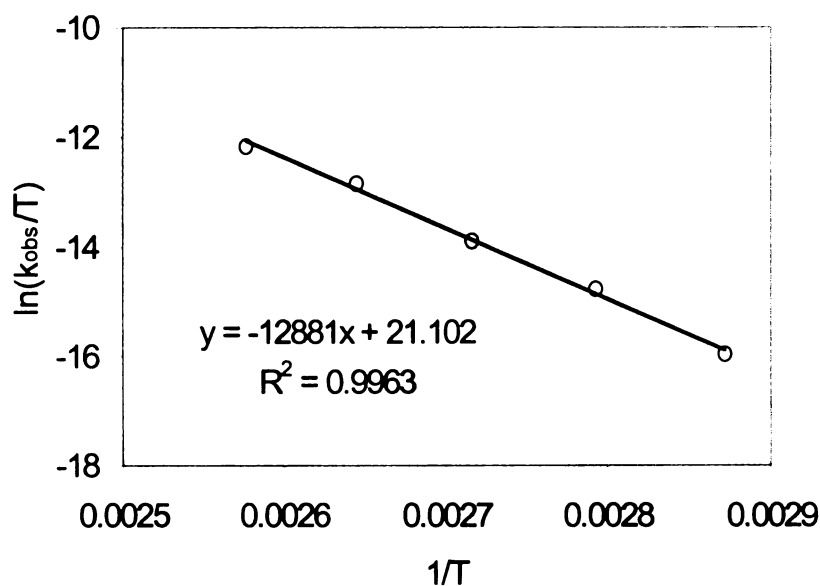
Figure 15. Eyring plot for the reaction of compound **4** with HBPin in C_6D_6. ($[4]_o$ = 0.046 M; $[HBPin]_o$ = 0.551 M; T = 338.15 to 388.15 K, $\Delta H^{\ddagger}$ = 25.6 kcal/mol and $\Delta S^{\ddagger}$ = -5.3 e.u.).

Mechanistic Studies of The Original Iridium System

Compound **1** was stable in benzene solution after prolonged thermolysis, which excludes the pathway involving the elimination of HBPin from $Cp^*Ir(PMe_3)(H)(BPin)$ (**1**). Regarding the possibility of PMe_3 dissociation pathway to generate $Cp^*Ir(H)(BPin)$, an analog of Hartwig's proposed intermediate in the Rh system,[26a] we designed a pseudo double-labeling crossover experiment to probe the PMe_3 dissociation pathway. Two labeled complexes $Cp^*Ir(P(CD_3)_3)(H)_2$ (**8**) and $(C_5Me_4Et)Ir(PMe_3)(H)_2$ (**9**) were prepared. If phosphine does dissociate from $Cp^*Ir(PMe_3)(H)(BPin)$, we expect to see the

two crossover products, Cp*Ir(PMe₃)(H)₂ **(2)** and (C₅Me₄Et)Ir(P(CD₃)₃)(H)₂ **(10)** (Figure 16). Surprisingly, those iridium complexes can be easily quantified by GC-MS (Figure 17).
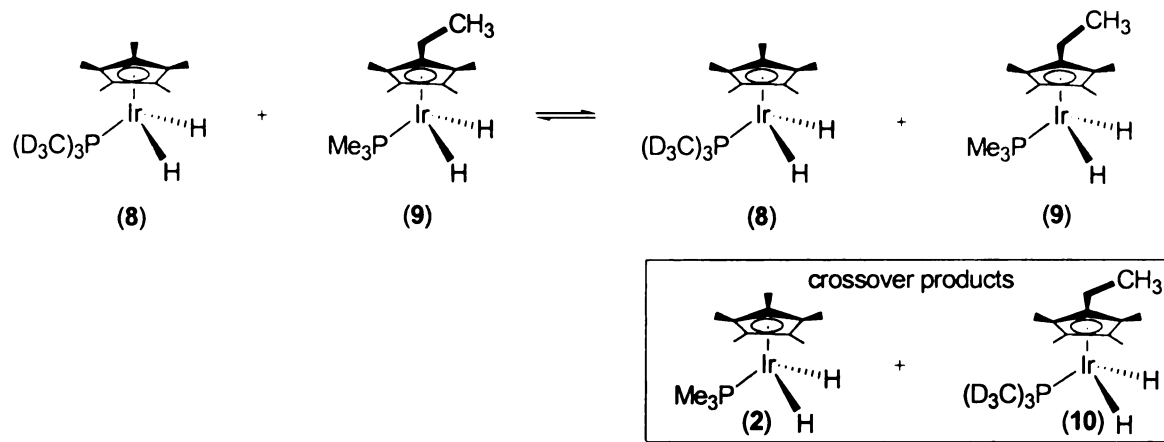
Figure 16. Potential crossover products from pseudo double-labeling crossover experiment.

Figure 17. Separation of compounds **2**, **8**, and **9** in a GC-MS chromatogram.
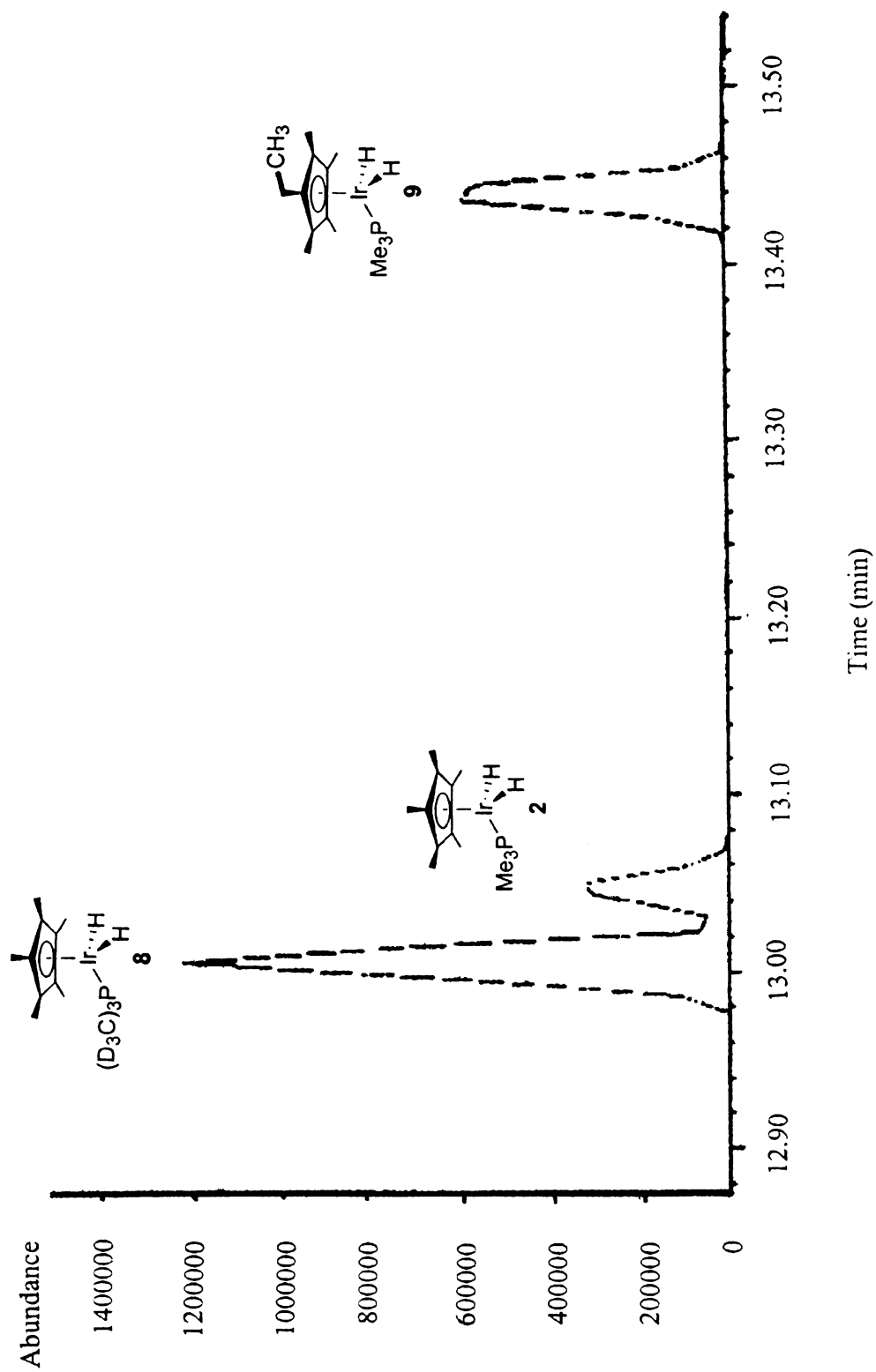
28

Benzene borylation with pinacolborane in the presence of 10 mol% of compound

8 and 10 mol% of compound 9 was carried out (Figure 18). The reaction proceeded

smoothly to generate C_6H_5BPin and H_2 as products. From the chromatogram of the crude

mixture (Figure 19) there was no crossover products observed. Crossover during catalytic

borylation was minimal. Therefore, phosphine dissociation pathway is unlikely.

$$HBPin \ + \ C_6H_6 \xrightarrow[150\ °C]{10\ mol\%\ \textbf{8}\ and\ 10\ mol\%\ \textbf{9}} C_6H_5BPin \ + \ H_2$$
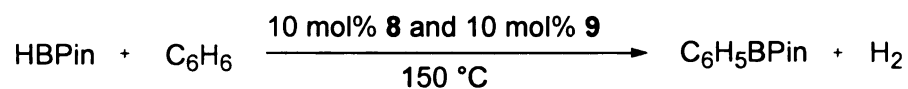
Figure 18. Pseudo double-labeling crossover experiment.

Figure 19-1. The chromatogram of the crude mixture from benzene borylation with pinacolborane in the presence of 10 mol% of compound **8** and 10 mol% of compound **9**.
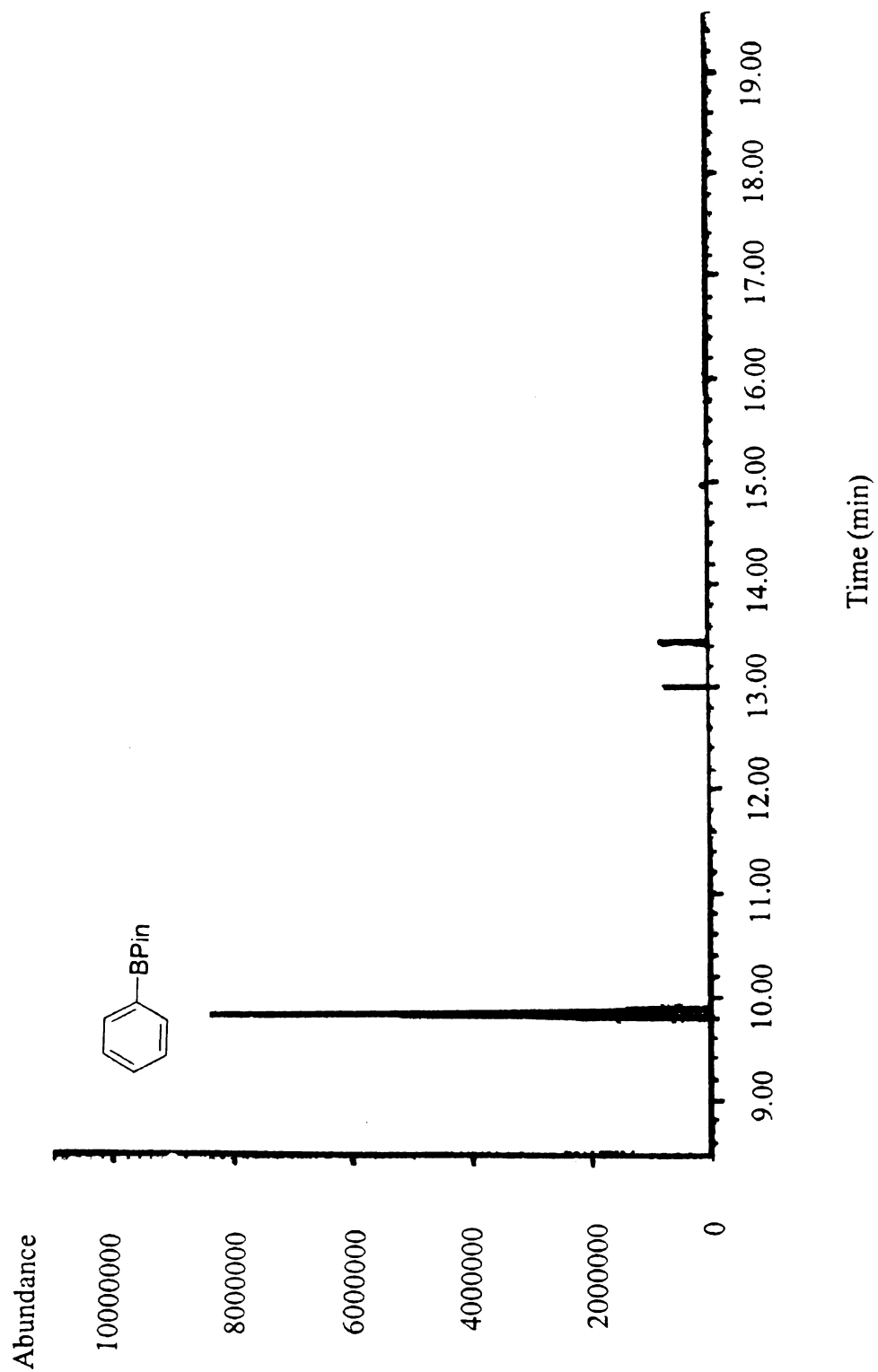
Figure 19-2. The chromatogram of the crude mixture from benzene borylation with pinacolborane in the presence of 10 mol% of compound **8** and 10 mol% of compound **9**.

31
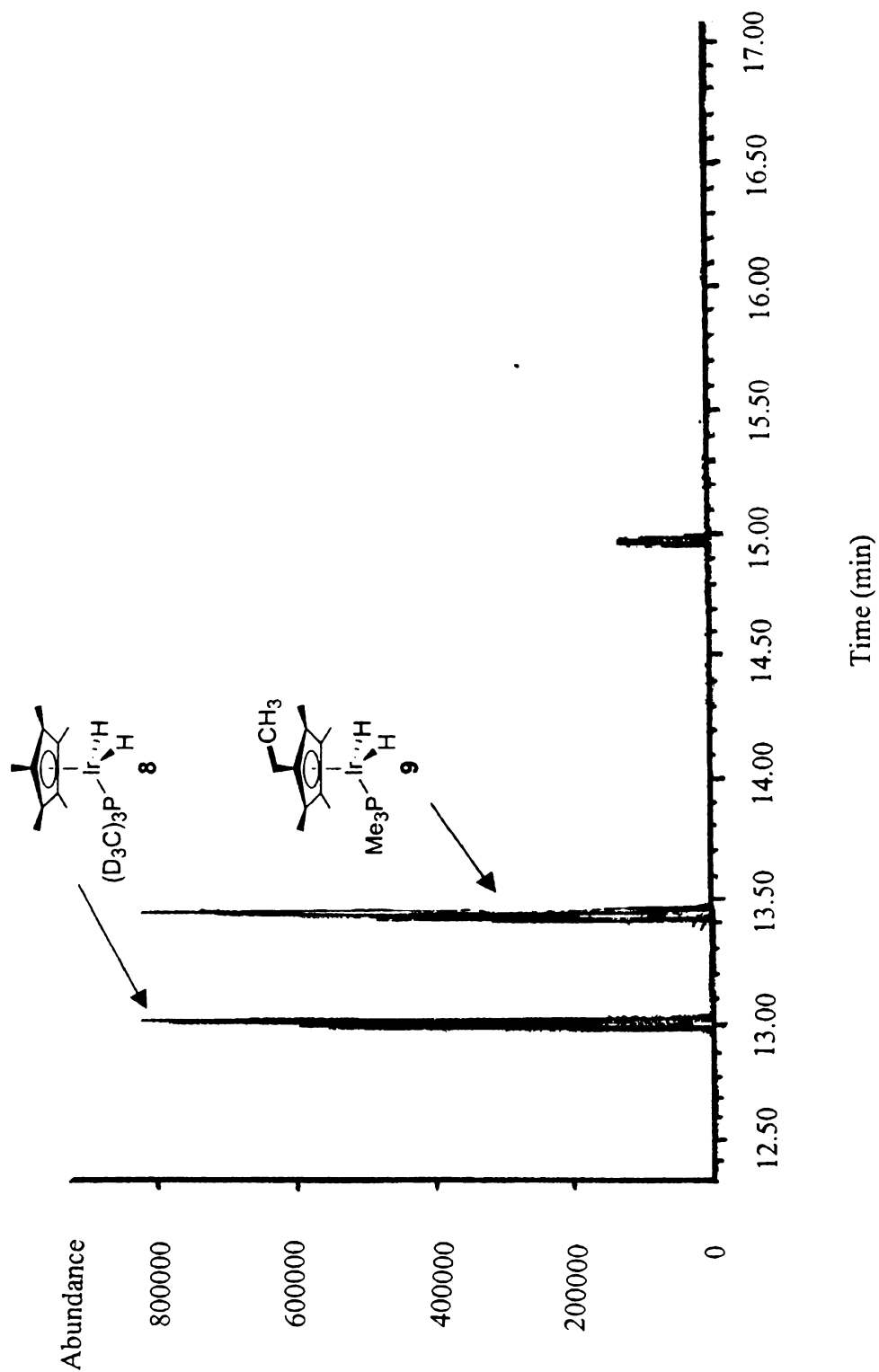
However, added PMe$_3$ strongly inhibited catalysis where HBPin was present. The finding raised possibility that small quantities of phosphine free Ir^V species could be active. Cp*IrH$_{4-x}$(BPin)$_x$ species[30] (where x = 1, 2) formed in the thermolysis of Cp*IrH$_4$ (11) and HBPin and Cp*Ir(H)$_2$(BPin)$_2$ (12) are Ir analogs of other intermediates proposed by Hartwig in the Rh system. Anisole borylation with 20 mol% loadings of compound 11 and 1 were compared (Figure 20). The isomer ratios for 11, *o:m:p* = 3:49:48; for 1, *o:m:p* = 2:79:19. From this experiment, Cp*IrH$_{4-x}$(BPin)$_x$ intermediates could be eliminated because the borylation regioselectivities for 11 and 1 differed substantially.

o : m : p = 2 : 79 : 19

o : m : p = 3 : 49 : 48
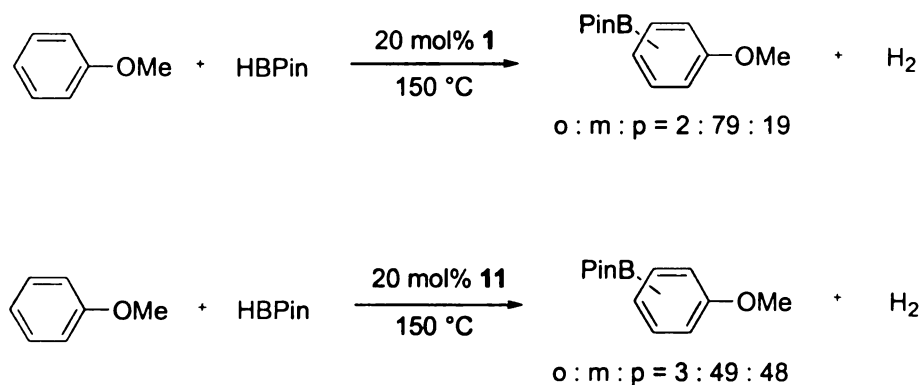
Figure 20. Borylation reactions of anisole with 20 mol% loading of compound 1 and compound 11, respectively.

Exclusion of a simple phosphine dissociative pathway narrows the plausible catalysts to two choices: (1) Ir phosphine species arising from Cp* loss or (2) species where both Cp* and PMe$_3$ have been lost. The latter possibility is intriguing in light of Marder's synthesis of (η^6-arene)Ir(BCat)$_3$ complexes (where Cat = *ortho*-catecholate) from (Ind)Ir(COD) (13, where Ind = η^5-C$_9$H$_7$, COD = 1,5-cyclooctadiene) and HBCat in

arene solvents.[31] Using an analogous route, we prepared (MesH)Ir(BPin)₃ (14, where

MesH = η⁶-mesitylene) in 19% yield from compound 13 and HBPin in mesitylene

solvent.[26e] Single crystals of 14 were grown from pentane at –30 °C and the structure was

further confirmed by single–crystal X-ray crystallographic analysis. The molecular

structure of 14 is shown in Figure 21 and the distance from Ir(1) to the center of the

mesitylene ring is 1.880 Å.
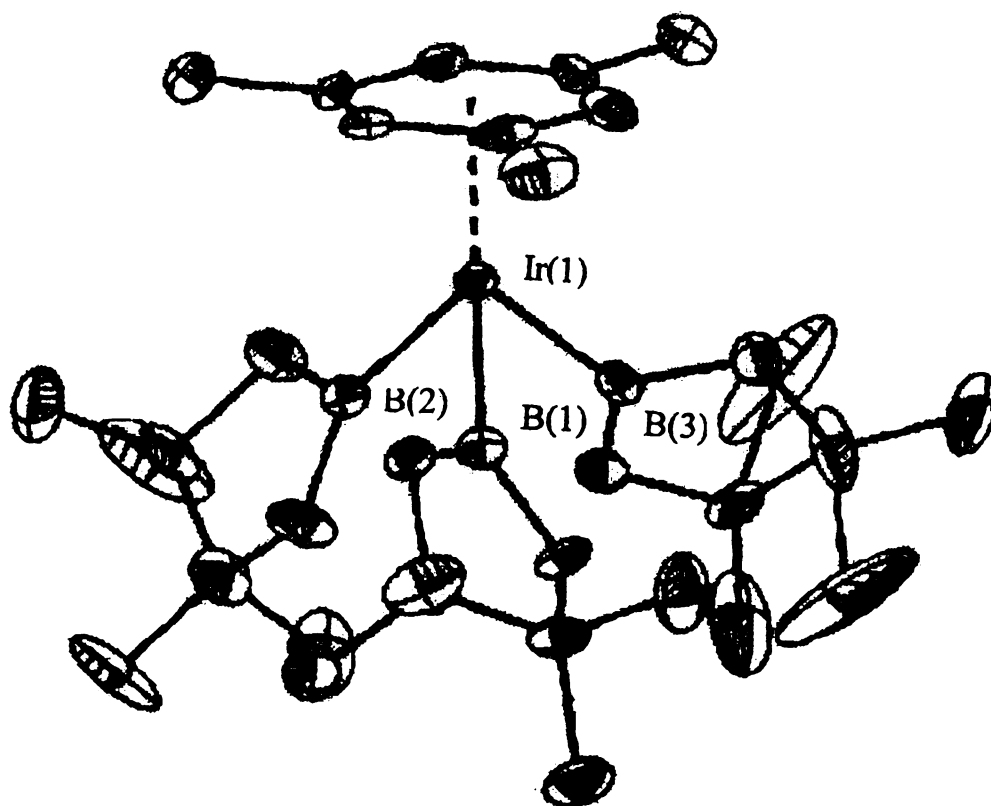
Figure 21. ORTEP diagram of (MesH)Ir(BPin)₃ (14). Thermal ellipsoids are shown at
25% probability.

Table 3. Selected bond lengths [Å] and angles [°] for **14**.

Bond	Distance [Å]	Bonds	Angle [°]
Ir(1)-B(1)	2.051(1)	B(1)-Ir(1)-B(2)	80.6(4)
Ir(1)-B(2)	2.021(1)	B(1)-Ir(1)-B(3)	81.7(4)
Ir(1)-B(3)	2.039(1)	B(2)-Ir(1)-B(3)	83.8(4)

Compound **14** reacts with benzene at 150 °C to produce Ir metal and three equivalents of C_6H_5BPin, but it does not catalyze C_6H_5BPin formation from benzene and HBPin. Thus, it appears that phosphines or related donor ligands are required for catalysis. Using the lability of the mesitylene ligand in **14**, Ir phosphine species can be generated *in situ* from **14** and appropriate phosphines. Borylation of benzene with the use of 2 mol% **14** and 4 mol% PMe_3 was found to be a viable pre-catalyst for aromatic borylation reactions (Figure 22).

$$C_6H_6 \ + \ HBPin \ \xrightarrow[\text{150 °C, 15 h}]{\text{2 mol\% } \mathbf{14}, \text{ 4 mol\% } PMe_3} \ C_6H_5BPin \ + \ H_2$$
$$98\% \text{ GC yield}$$
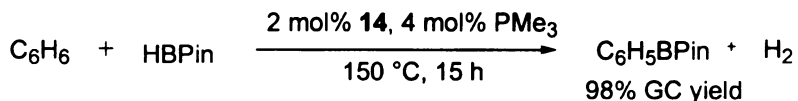
Figure 22. Benzene borylation with HBPin catalyzed by 2 mol% **14** and 4 mol% PMe_3.

From the experiments discussed previously, we ruled out a H-B elimination pathway, PMe_3 dissociation pathway, and a pathway where the active species is generated from both Cp* and PMe_3 loss. The remaining candidates for active species are iridium phosphine boryl complexes. Syntheses of some model complexes to examine their stoichiometric reactions with arenes and screening for different metal complexes

and ligands combination for catalysis would hopefully help to determine the identity of the active species and understand the mechanism of the aromatic borylation in this system.

In this chapter, through detailed mechanistic studies of the original Ir pre-catalyst system, we suggest that active species are iridium phosphine boryl complexes.

CHAPTER 3

CATALYTIC BORYLATION REACTIONS OF AROMATIC COMPOUNDS

Screenings of Phosphine Ligands, Other Donor Ligands, and Metal Complexes for Catalytic Benzene Borylation

From mechanistic investigation of the initial Cp*Ir(PMe₃)(H)(BPin) (1) pre-catalyst system, it was found that the use of 2 mol% (MesH)Ir(BPin)₃ (14) and 4 mol% PMe₃ was a viable pre-catalyst for aromatic borylation reactions. The low isolated yield of **14** hampered screening efforts and precluded practical applications despite dramatic improvement in catalytic activity. Hence, we sought alternative means for generating active catalysts. Because NMR indicated virtually quantitative generation of **14** from (Ind)Ir(COD) (13), *in situ* generation of active catalysts by phosphine addition to **13** was examined.[32] This approach was successful and we were able to conduct systematic studies of the effects of different phosphine ligands, various donor ligands, and metal complexes on catalytic activity.

First, as shown in Table 4 different ratios between PMe₃ and "Ir" were examined for catalytic activity. The results showed that borylation rates were appreciable when [P]:[Ir] < 3:1 but decreased dramatically when [P]:[Ir] ratio equaled or exceeded 3:1 (Entries 2-5). Several other mono-dentate phosphine ligands including PEt₃, PⁱPr₃, PᵗBu₃, PCy₃, and PPh₃ were also tested as ligands for the catalytic borylation of benzene giving moderate GC yields (Entries 6-10).

36

$$\text{benzene} + \text{HBPin} \xrightarrow[\text{150 °C}]{\text{2 mol\% \textbf{13} or \textbf{14}, x mol\% PR}_3} \text{Ph–BPin} + H_2$$
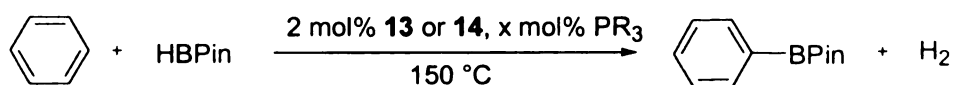
Table 4. Summary of borylation of benzene with HBPin in the presence of 2 mol% pre-catalyst at 150 °C.[33]
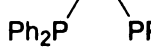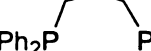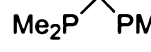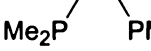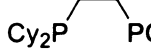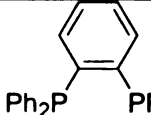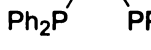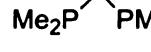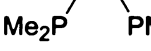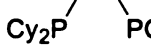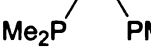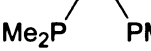
Entry	Pre-catalyst	[P]:[Ir] Ratio	Reaction Time (h)	Yield (%)
1	14 PMe$_3$	2:1	15	98
2	13 PMe$_3$	1:1	5	87
3	13 PMe$_3$	2:1	18	87
4	13 PMe$_3$	3:1	57	0.4
5	13 PMe$_3$	4:1	20	0
6	13 PEt$_3$	2:1	13	79
7	13 P^{i}Pr$_3$	2:1	93	80
8	13 P^{t}Bu$_3$	2:1	21	71
9	13 PCy$_3$	2:1	46	79
10	13 PPh$_3$	2:1	58	69

Reactions run in neat benzene. GC yields based on HBPin.

In addition to mono-dentate phosphine ligands, chelating bidentate phosphine ligands were examined (Table 5). A dramatic increase in catalytic activity and turnover numbers were observed for the bidentate phosphines.

$$\text{benzene} + \text{HBPin} \xrightarrow[\Delta]{2 \text{ mol\% } \mathbf{13}, \ 2 \text{ mol\% } R_2P \wedge PR_2} \text{Ph-BPin} + H_2$$
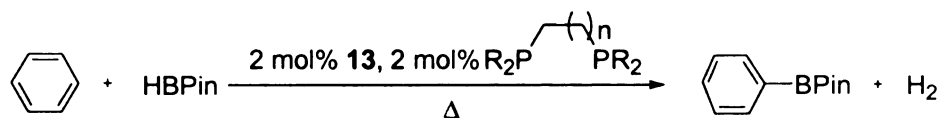
Table 5. Borylation reaction of benzene with HBPin in the presence of 2 mol% **13** and 2 mol% chelating phosphine ligand.[33]

Entry	Ligand	Pre-catalyst Loading	Temperature (°C)	Reaction Time (h)	Yield (%)
1	Ph$_2$P⌒PPh$_2$	2 mol%	150	2	95
2	Ph$_2$P⌒PPh$_2$	2 mol%	150	16	87
3	Me$_2$P⌒PMe$_2$	2 mol%	150	3	79
4	Me$_2$P⌒PMe$_2$	2 mol%	150	2	84*
5	Cy$_2$P⌒PCy$_2$	2 mol%	150	3	86
6	Ph$_2$P⌒PPh$_2$	2 mol%	150	0.8	78
7	Ph$_2$P⌒PPh$_2$	2 mol%	100	7	88
8	Me$_2$P⌒PMe$_2$	2 mol%	100	77	18
9	Me$_2$P⌒PMe$_2$	2 mol%	100	31	96
10	Cy$_2$P⌒PCy$_2$	2 mol%	100	96	86
11	Me$_2$P⌒PMe$_2$	0.2 mol%	150	9	85*
12	Me$_2$P⌒PMe$_2$	0.02 mol%	150	61	90

Reactions run in neat benzene. GC yields based on HBPin.*Isolated yield.

Chelating phosphines as ligands substantially increased catalytic activity and TONs as highlighted for 1,2-bis(dimethylphosphino)ethane (dmpe) (Entry 12), where the effective TON of 4500 represents an improvement of more than 1000-fold over pre-catalyst Cp*Ir(PMe$_3$)(H)(BPin) (**1**). Furthermore, the borylation reactions can be run at

38
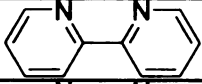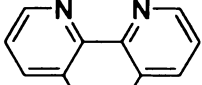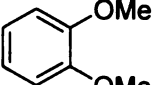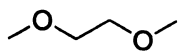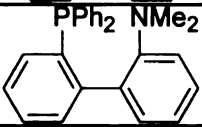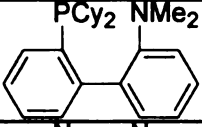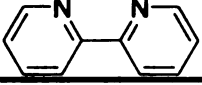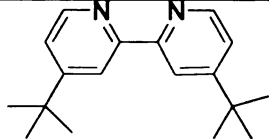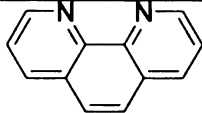
100 °C with a reasonable rate by using 1,2-bis(diphenylphosphino)ethane (dppe) as the ligand (Entry 7).

Besides phosphorous containing ligands, nitrogen, oxygen, and sulfur containing ligands were also screened for catalytic activity as shown in Table 6.
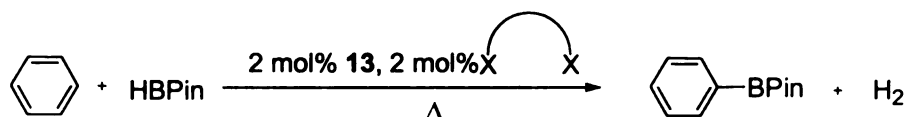
Table 6. Borylation reaction of benzene with HBPin (0.7 M) in the presence of 2 mol% **13** and nitrogen, oxygen, or sulfur containing ligands.

Entry	Ligand	Ligand Loading	Temperature (°C)	Reaction Time (h)	Yield (%)
1		4 mol%	100	31	69
2		4 mol%	150	15	8
3		2 mol%	150	0.2	85
4		2 mol%	150	<1	85
5	Me₂N NMe₂	2 mol%	150	6	52
6	OMe / OMe	2 mol%	150	14	11
7	O O	2 mol%	150	14	7
8		2 mol%	150	1	6
9	PPh₂ NMe₂	2 mol%	150	2.7	73
10	PCy₂ NMe₂	2 mol%	150	16.3	66
11		2 mol%	100	1.5	86

Entry	Pre-catalyst	Pre-catalyst Loading	Temperature (°C)	Reaction Time (h)	Yield (%)
12		2 mol%	100	1	82
13		2 mol%	100	1	84
14		2 mol%	50	16	85

Reactions run in neat benzene. GC yields based on HBPin.

2,2'-bipyridine (bpy), 1,10-phenanthroline, 4,4'-di-*tert*-butyl-2,2'-bipyridine (dtbpy)[26f] were found to be good ligands for borylation (Entries 3, 4, 11, 12, and 13). For bpy, the borylation occurred at relatively low temperature (50 °C) at an appreciable rate, and good yield (Entry 14, 85% yield). Attempts to reduce pre-catalyst loading to 0.02 mol% yielded significant quantities of decomposition and PinB-O-BPin. The use of thiophene, veratrole, DME, and 2,2'-bithiophene were inefficient as ligands for borylation of benzene (Entries 2, 6, 7, and 8). Ligands containing both "hard" N and "soft" P were also examined (Entries 9 and 10). Catalysts containing 2-(diphenylphosphino)-2'-(N,N-dimethylamino)biphenyl and 2-(dicyclohexylphosphino)-2'-(N,N-dimethylamino)biphenyl did not exhibit any advantages in catalysis over chelating phosphine ligands, dppe and dmpe, or chelating nitrogen ligands, bpy, 1,10-phenanthroline, and dtbpy. N,N,N,N-tetramethylethylenediamine (TMEDA) performed marginally as a ligand (Entry 5, 52% yield).

Besides **13**, different metal complex precursors were investigated. Since the approach where we generated active catalysts *in situ* from (Ind)Ir(COD) (**13**) and phosphine ligands was successful, we were interested if the active catalysts can be

40

generated *in situ* from the precursor [Ir(COD)Cl]$_2$, which is the starting material for the preparation of **13**, or even IrCl$_3$·xH$_2$O. In addition, some of the related Rh complexes were also screened for catalysis. The results are summarized in Table 7.
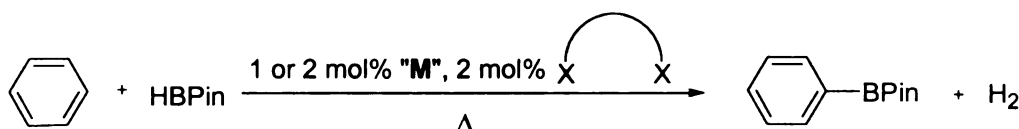
Table 7. Borylation of benzene with HBPin in the presence of various metal precursors (M) and ligands.

Entry	Pre-catalyst	Pre-catalyst Loading	Temperature (°C)	Reaction Time (h)	Yield (%)
1	[Ir(COD)Cl]$_2$ dmpe	1 mol% 2 mol%	150	8	74
2	[Ir(COD)Cl]$_2$ dppe	1 mol% 2 mol%	100	23	93
3	[Ir(COD)Cl]$_2$ bpy	1 mol% 2 mol%	100	8	82
4	IrCl$_3$·xH$_2$O dppe	2 mol% 2 mol%	150	63	1
5	[Rh(COD)Cl]$_2$ dppe	1 mol% 2 mol%	100	15	--
6	[Rh(COD)Cl]$_2$ dppe	1 mol% 2 mol%	150	63	8
7	[Rh(COD)Cl]$_2$ bpy	1 mol% 2 mol%	100	72	55
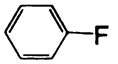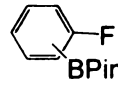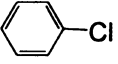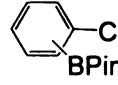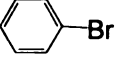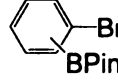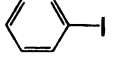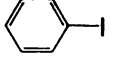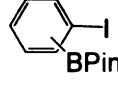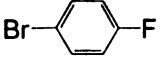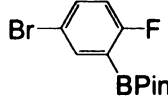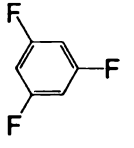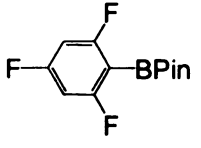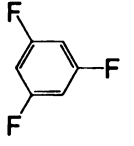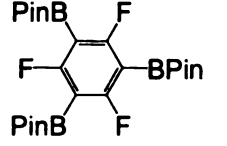
Reactions run in neat benzene. GC yields based on HBPin.
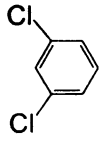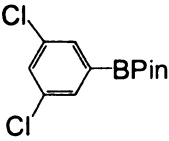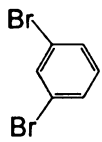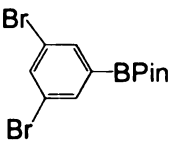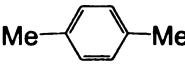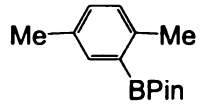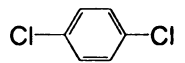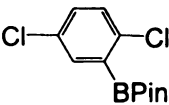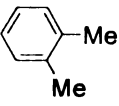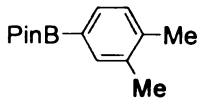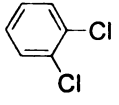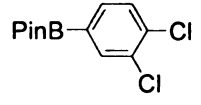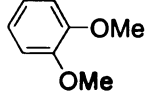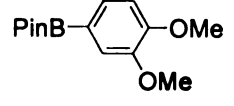
[Ir(COD)Cl]$_2$ is an air-stable, commercially available iridium(I) compound and has been demonstrated to be a good catalyst system in conjunction with dmpe,[33] bpy or dtbpy (Entries 1, 2, and 3).[34] In contrast, IrCl$_3$·xH$_2$O and [Rh(COD)Cl]$_2$ were poor metal precursors for catalytic borylation (Entries 4, 5, 6 and 7), and no borylation occurred for the [Rh(COD)Cl]$_2$/dppe pre-catalyst system after 15 hours at 100 °C (Entry 5).

Borylation of Substituted Benzenes

Since applications of boronate esters in cross-coupling chemistry are extensive,[23] a convenient way to expand the library of boronate esters is desired. With this goal in mind, borylations of a variety of arenes were carried out. The results are summarized in Table 8.

Table 8. Ir-catalyzed aromatic borylations. Reactions are run in neat arene, [Ir] = 2 mol%, [P]:[Ir] = 2:1, and yields are reported for isolated materials.[33]

Entry	Substrate	Product	Arene:HBPin	Catalyst	Temp (°C)	Time (h)	Yield (%)
1	C6H5–F	F, BPin substituted benzene	10:1	13/dppe	100	17	84
2	C6H5–Cl	Cl, BPin substituted benzene	10:1	13/dppe	100	17	83
3	C6H5–Br	Br, BPin substituted benzene	10:1	13/dppe	100	17	90
4	C6H5–I	--	10:1	13/dppe	100	60	--
5	C6H5–I	I, BPin substituted benzene	10:1	14/dppe	100	57	77
6	Br–C6H4–F	Br, F, BPin substituted benzene	4:1	13/dppe	100	14	81
7	1,3,5-trifluorobenzene	F3 C6H–BPin	4:1	13/dmpe	150	1	63
8	1,3,5-trifluorobenzene	F3, (BPin)3 substituted benzene	1:5	13/dmpe	150	62	76

Entry	Substrate	Product	Arene:HBPin	Catalyst	Temp (°C)	Time (h)	Yield (%)
9	(3,4-dichlorobenzene)	(Cl, Cl substituted arene)—BPin	1:1.5	13/dppe	100	14	89
10	(3,5-dibromobenzene)	(Br, Br substituted arene)—BPin	1:1.5	13/dppe	100	17	92
11	Me—⟨ ⟩—Me	Me—⟨ ⟩—Me, BPin	12:1	13/dmpe	150	112	68
12	Cl—⟨ ⟩—Cl	Cl—⟨ ⟩—Cl, BPin	4:1	13/dmpe	150	39	76
13	⟨ ⟩—Me, Me	PinB—⟨ ⟩—Me, Me	12:1	13/dmpe	150	10	85
14	⟨ ⟩—Cl, Cl	PinB—⟨ ⟩—Cl, Cl	9:1	13/dmpe	150	12	98
15*	⟨ ⟩—OMe, OMe	PinB—⟨ ⟩—OMe, OMe	1:3	13/dmpe	150	95	62

Isolated yields based on HBPin. *Reaction run in cyclohexane.
13: (Ind)Ir(COD); **14**: (MesH)Ir(BPin)$_3$; dppe: 1,2-bis(diphenylphosphino)ethane; dmpe: 1,2-bis(dimethylphosphino)ethane.

Dramatic differences in chemoselectivities between Ir and Rh catalysts were found for halogenated substrates, where the Ir catalysts preferentially activate C-H bonds. Thus, good yields of mono- or triborated products of 1,3,5-trifluorobenzene were obtained by adjusting the arene:HBPin ratio (Entries 7 and 8). In contrast, previous attempts to effect multiple borylations of 1,3,5-trifluorobenzene with the use of Rh catalysts **3** led to increased defluorination.[26b] Ir-catalyzed borylations of 1,3-

dichlorobenzene and 1,3-dibromobenzene generate meta-functionalized products in high yields (Entries 9 and 10), whereas dehalogenation is the dominant pathway in Rh-catalyzed reactions.[35] A dramatic example of the difference between Rh- and Ir-catalyzed borylation is shown in Figure 23 where the GC chromatograms of 1,3-dichlorobenzene borylations catalyzed by a Rh pre-catalyst and catalyzed by a Ir pre-catalyst are compared. In the Rh-catalyzed borylation, dechloronation is a competitive side reaction pathway; on the contrary, in the Ir-catalyzed borylation a clean single product was obtained. The finding that aromatic C-Br bonds survive in the Ir-catalyzed reactions contrasts Pd-catalyzed reactions of boranes and aryl bromides, where the C-Br bonds are converted to C-B or C-H bonds.[36] Because aryl iodides have the weakest carbon-halogen bonds, they are susceptible to reductive cleavage by transition metals. Hence it is not surprising that the Ir catalysts generated from **13** are ineffective for the aromatic borylation of iodobenzene (Entry 4). However, iodobenzene and HBPin reacted smoothly to yield a mixture of $C_6H_4(I)(BPin)$ isomers when active catalysts are generated from the Ir^{III} source, $(MesH)Ir(BPin)_3$ **(14)**, and dppe (Entry 5). With the success in borylating iodobenzene, Ir catalysts have been shown to be compatible with the entire range of aryl halides.[33] We also demonstrated that cyclohexane can function as an inert solvent (Entry 15), which is useful in borylations of more valuable substrates.

Ir catalysts selectively borylate symmetrical 1,2-disubstituted arenes including o-xylene, 1,2-dichlorobenzene, and veratrole at the 4-position to give a single borylation product (Entries 13, 14, and 15). Symmetrical 1,4-disubstituted arenes can also be selectively borylated at the 2-position (Entries 11 and 12). Borylations of 1,4-disubstituted arenes proceed slower than the corresponding 1,2- and 1,3-disubstituted

arenes presumably due to steric bulkiness of the two substituents in 1,4-disubstituted arenes. Attempts to borylate 1,3,5-trichlorobenzene led to unidentified decomposition species and PinB-O-BPin. Borylation of $1,4\text{-}C_6H_4(Br)(F)$ occurred selectively at the postion *ortho* to F most likely due to the different steric bulkiness between Br and F (Entry 6).

Figure 23-1. GC chromatogram of borylation of 1,3-dichlorobenzene catalyzed by the Rh pre-catalyst **3**.
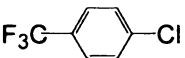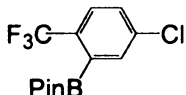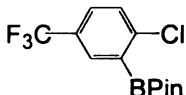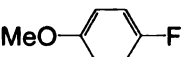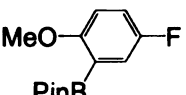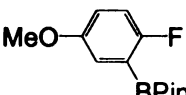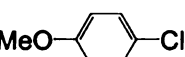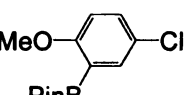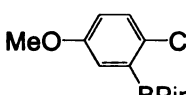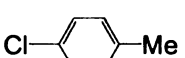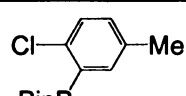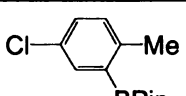
Figure 23-2. GC chromatogram of borylation of 1,3-dichlorobenzene catalyzed by the Ir pre-catalyst **13** and dppe.
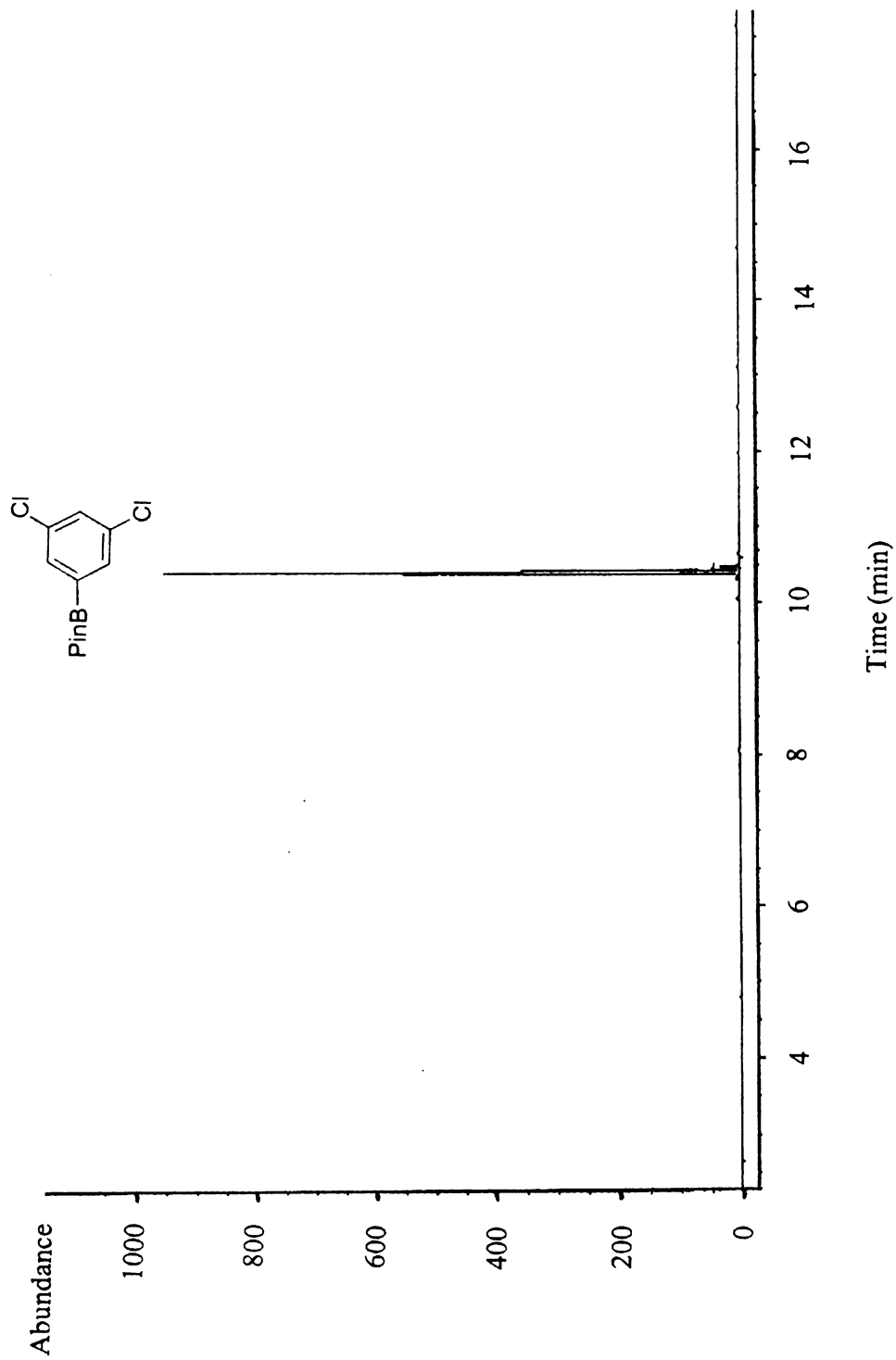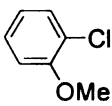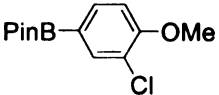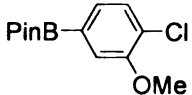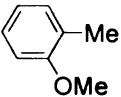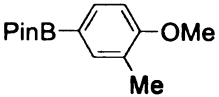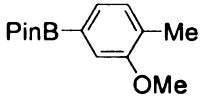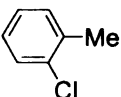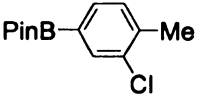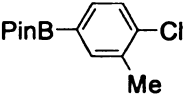
Steric, Electronic, and Directing Effects in Aromatic Borylation

From previous studies as shown in Table 8, borylations of symmetrical 1,2- and 1,4-disubstituted arenes give a single borylation product. In order to study the roles of steric and electronic effects on the selectivity for the borylation reactions, borylations of unsymmetrical 1,2- and 1,4-disubstituted arenes were compared. The results are summarized in Table 9.

Table 9. Borylations of unsymmetrical 1,2- and 1,4-disubstituted arenes with HBPin in the presence of 2 mol% **13** and 2 mol% dmpe. Reactions run in neat arene, and yields are reported for isolated materials.

Entry	Substrate	Product Distribution (%)*	Time (h)	Yield (%)
1	F_3C—⟨⟩—Cl	F_3C—⟨⟩—Cl F_3C—⟨⟩—Cl PinB BPin 11.8:88.2	5	78
2	MeO—⟨⟩—F	MeO—⟨⟩—F MeO—⟨⟩—F PinB BPin 6.6:93.4	23	62
3	MeO—⟨⟩—Cl	MeO—⟨⟩—Cl MeO—⟨⟩—Cl PinB BPin 68.0:32.0	23	62
4	Cl—⟨⟩—Me	Cl—⟨⟩—Me Cl—⟨⟩—Me PinB BPin 43.5:56.5	44	88

Entry	Substrate	Product Distribution (%)*	Time (h)	Yield (%)
5	[structure: benzene with Cl and OMe (ortho)]	PinB—⟨⟩—OMe PinB—⟨⟩—Cl (with Cl and OMe substituents) 48.5:51.5	12	73
6	[structure: benzene with Me and OMe (ortho)]	PinB—⟨⟩—OMe PinB—⟨⟩—Me (with Me and OMe substituents) 36.3:63.7	12	77
7	[structure: benzene with Me and Cl (ortho)]	PinB—⟨⟩—Me PinB—⟨⟩—Cl (with Cl and Me substituents) 62.2:37.8	16	89

* The product distribution was determined from the area ratio of each isomer in the GC chromatogram of the crude reaction mixture. One of the products from borylation of an unsymmetrical 1,2- or 1,4-disubstituted arene was independently synthesized according to the literature.[25]

Calculated ligand repulsive energies, E_R, have been demonstrated in White and co-workers report[37] to provide reliable steric parameters for ligands in organometallic systems. E_R is defined as the amount of pure steric repulsion between a ligand and the prototypical molecular fragment to which it is bonded [Cr(CO)$_5$] or [CpRh(CO)]. Other parameters such as Taft-Dubois steric parameter, E's, and A-values[38] are used as standard measures of steric effects in organic chemistry. However, the experimentally based measures, E's and A-values, are a product of both steric and electronic effects. Therefore, E_R values are applied here in order to assess the pure steric effect on borylation reactions. Selected E_R values and A-values are listed in Table 10.

Table 10. Ligand repulsive energies (in kcal/mol) computed using the universal force field and A-values (in kcal/mol) for a variety of organic substituents.

Substituent	E_R (kcal/mol)	A-value (kcal/mol)
F	0.28	0.25
Cl	1	0.53
Me	18	1.74
OMe	37	0.75
CF$_3$	44	2.5
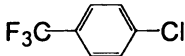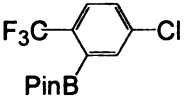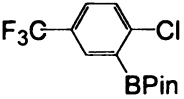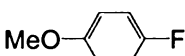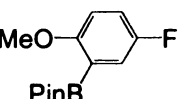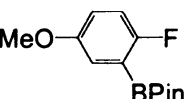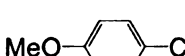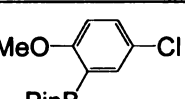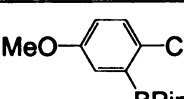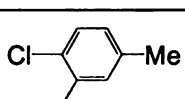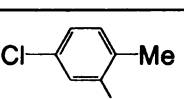
If only steric effects are considered, we can calculate and predict the isomer distribution for borylation of unsymmetrical 1,4-disubstituted arenes and compare that to experimental data. Since, for a 1,4-disubstituted arene, both substituents have two *ortho* sites, the calculated isomer distribution ratio can be determined by using the relative E_R values of the two different substituents. For present purposes, it was assumed that *ortho* substitution would preferably occur adjacent to the substituent with the smaller steric factor (E_R). For example, the E_R value for CF$_3$ group is 44 and the E_R value for Cl is 1; therefore, the isomer distribution for 1,4-C$_6$H$_4$(Cl)(CF$_3$) borylation is expected to be 1:44 (2.2:97.8) for 1,3,4-C$_6$H$_3$(Cl)(BPin)(CF$_3$) to 1,2,4-C$_6$H$_3$(Cl)(BPin)(CF$_3$) on the basis of E_R values as illustrated in Figure 24. The result differs from the experimental value of 11.8:88.2 (Entry 1). Apparently, other factors are also involved in determining the isomer distribution. In order to determine if a trend exists for various unsymmetrically 1,4-disubstituted arenes, their borylation chemistry was investigated. The comparison of isomer distribution between the experimental values and the calculated values derived

50

from E_R values for other unsymmetrical 1,4-disubstituted arenes are summarized in Table 11.

$$F_3C-\langle \rangle-Cl$$

E_R value: 44 (CF$_3$)   1 (Cl)

substitution *ortho* to CF$_3$ substitution *ortho* to Cl

$$F_3C-\langle \rangle-Cl$$ $$F_3C-\langle \rangle-Cl$$
PinB   BPin

Expected ratio: 1   :   44

                   =   2.2%   :   97.8%
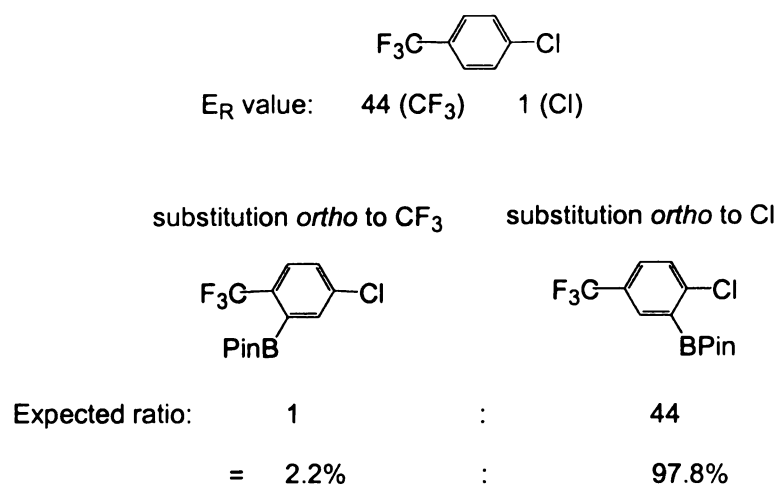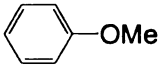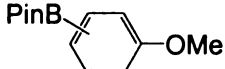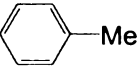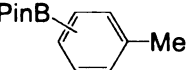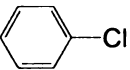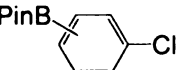
Figure 24. The calculated value of isomer distribution of the borylation of 1,4-C$_6$H$_4$(Cl)(CF$_3$).

51

Table 11. Comparison of isomer distribution between the experimental values and the calculated values derived from pure steric effect (E_R).

Entry	Substrate	Isomer Mixture (%)	Calculated (from E_R) (%)
1	F₃C—⟨⟩—Cl	F₃C—⟨⟩—Cl (PinB) F₃C—⟨⟩—Cl (BPin) 11.8:88.2	2.2:97.8
2	MeO—⟨⟩—F	MeO—⟨⟩—F (PinB) MeO—⟨⟩—F (BPin) 6.6:93.4	0.8:99.2
3	MeO—⟨⟩—Cl	MeO—⟨⟩—Cl (PinB) MeO—⟨⟩—Cl (BPin) 68.0:32.0	2.6:97.4
4	Cl—⟨⟩—Me	Cl—⟨⟩—Me (PinB) Cl—⟨⟩—Me (BPin) 43.5:56.5	94.7:5.3

The data summarized above suggest that the electronic effects and other effects such as chelate-directed effects of substituents also contribute to the resulting isomer distributions. It was therefore seemed of interest to evaluate borylations of unsymmetrical 1,2-disubstituted arenes to assess the electronic effects of substituents for these aromatic borylation reactions. In order to obtain a qualitative understanding of electronic effects, the experimental data are compared to the calculated isomer distribution data, which are derived from the selectivities observed in borylation of mono-substituted arenes (Table 12).

Table 12. Borylations of mono-substituted arenes with HBPin in the presence of 2 mol% **13** and 2 mol% dmpe. Reactions run in neat arene. Isomer distribution is obtained from area ratios in GC-FID chromatograms.

Arene	Products	Isomer Distribution (*para:meta:ortho*) (%)	Selectivity (*para:meta:ortho*) (%)
⟨benzene⟩—OMe	PinB—⟨benzene⟩—OMe	19.1:76.0:5.0	32.1:63.8:4.2
⟨benzene⟩—Me	PinB—⟨benzene⟩—Me	31.6:67.1:1.3	48.1:51.0:1.0
⟨benzene⟩—Cl	PinB—⟨benzene⟩—Cl	23.1:76.9:0.0	37.5:62.5:0.0

The isomer distribution of borylation of each substrate including anisole, toluene, and chlorobenzene is determined from the area ratio of each isomer in the GC chromatogram. For present purposes, it was assumed that the response factors were similar because the molecules are isomers. Therefore, we deemed it unnecessary to make calibration curves for these screening experiments. In each mono-substituted arene, borylation can occur at either of two *meta* positions, two *ortho* positions, and one *para* position. The reported selectivities are obtained by dividing the GC isomer distribution for each isomer by the potential number of sites of borylation (e.g. for *meta* position divide by 2). Then the selectivity of *para* substitution is normalized to 1.00, and *meta* and *ortho* selectivities are based on the normalized value. For example, for anisole borylation the selectivity for *para:meta:ortho* is 1.00:1.99:0.13 (= 32.1:63.8:4.2) and for chlorobenzene borylation the selectivity for *para:meta:ortho* is 1.00:1.67:0.00 (= 37.5:62.5:0.0). The method for calculating the estimated value of isomer distribution for unsymmetrical 1,2-disubstituted arenes is illustrated for the borylation of 2-chloroanisole (Figure 25). For isomer (A), the borylation occurs at the position *meta* to Cl and *para* to
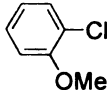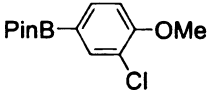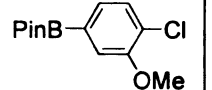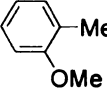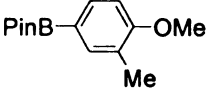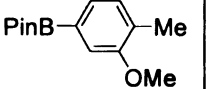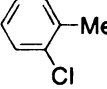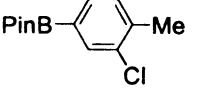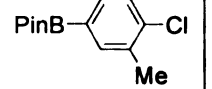
OMe group, the estimated selectivity for isomer (A) is the sum of the two normalized selectivities of the mono-substituted arenes (1.67 and 1.00). For isomer (B), the borylation occurs at the position *meta* to OMe group and *para* to Cl, the estimated selectivity for isomer (B) is the sum of the two normalized selectivities of the mono-substituted arenes (1.99 and 1.00). The estimated selectivity for borylation of 2-chloroanisole is obtained as 2.67:2.99, which is equal to 47.2:52.8.

$$(A):(B) = 2.67:2.99 = 47.2\%:52.8\%.$$
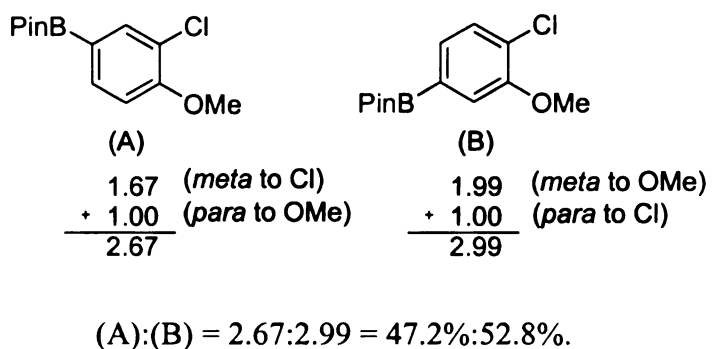
Figure 25. The estimated value of isomer distribution of the borylation of 2-chloroanisole.

Table 13. Comparison of isomer distribution between the experimental values and the estimated values derived from selectivity in borylation of mono-substituted arenes.

Entry	Substrate	Isomer Mixture		Observed (%)	Estimated (%)
1				48.5:51.5	47.2:52.8
2				36.3:63.7	40.8:59.2
3				62.2:37.8	56.4:43.6
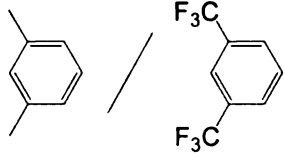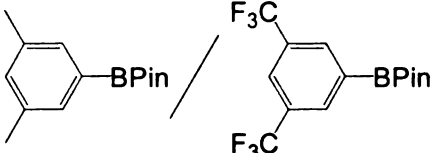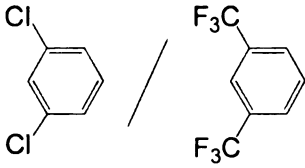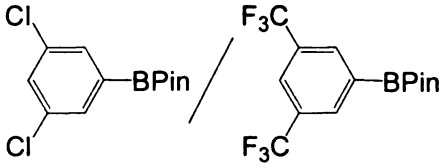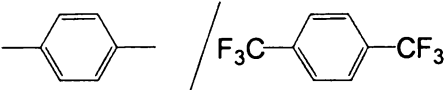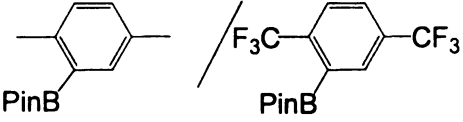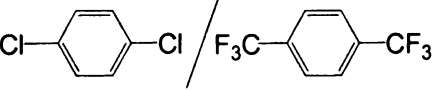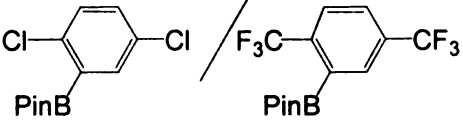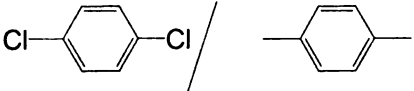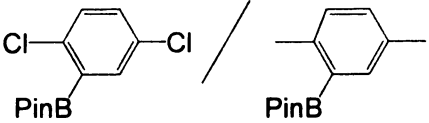
From the comparison in Table 13, the experimental isomer distribution data observed for those three 1,2-disubstituted arenes are similar to the estimated ones. The small deviations between the observed values and estimated values might result from the different dielectric constants of these substrates since the borylation reactions were carried out in neat arenes solvents (ε (chlorobenzene): 5.69; ε (anisole): 4.30; ε (toluene): 2.38; ε (2-chlorotoluene): 4.72; ε (2-methylanisole): 3.50; ε (2-chloroanisole): N/A).[39]

The results for borylations of 1,2-disubstituted arenes give some indication of the electronic effects of various substituents. It is clear from assessing and comparing the electronic effects for borylation of 1,2-disubstituted arenes and the steric effects from the ligand repulsive energies, E_R, that the methoxy group has a *meta* directing effect contributing to the isomer distribution in borylation of 2-methylanisole and 2-chloroanisole.

Competition Reactions

To probe the role of electronic effects in the new Ir catalyst system (2 mol% **13** and 2 mol% of dmpe), relative product ratios from catalytic borylations in equimolar mixtures of substituted arenes were determined (Table 14).

Table 14. Relative ratios of arylboronic esters for borylations of equimolar mixtures of substituted arenes catalyzed by 2 mol% **13** and 2 mol% dmpe.

Entry	Equimolar Mixtures of Substituted Arenes	Borylation Product Distribution
1		3.5:96.5
2		48.5:51.5
3		51.9:48.1
4		99.3:0.7
5		98.7:1.3

For borylation of 1,3-disubstituted arenes, steric effect directs borylation in the *meta* position. Therefore, in the competition reaction between *m*-xylene and 1,3-$C_6H_4(CF_3)_2$, the arene selectivity, 3.5:96.5 (Entry 1), is solely governed by the relative electronic nature of the two arenes. As mentioned previously, it was found that electron-deficient arenes borylate faster than electron-rich arenes. In the competition reaction between 1,3-$C_6H_4(Cl)_2$ and 1,3-$C_6H_4(CF_3)_2$, the arene selectivity was found to be 48.5:51.5 (Entry 2). Switching substrates from 1,3-disubstituted arenes to 1,4-disubstituted arenes, dramatically different arene selectivities were observed. In the competition reaction between *p*-xylene and 1,4-$C_6H_4(CF_3)_2$, the selectivity changed from 3.5:96.5 for the 1,3-disubstituted variants to 51.9:48.1 (Entry 3). Similarly, in the competition reaction between 1,4-$C_6H_4(Cl)_2$ and 1,4-$C_6H_4(CF_3)_2$, the selectivity is changed from 48.5:51.5 for 1,3-disubstituted variants to 99.3:0.7 (Entry 4). These results undoubtedly demonstrate that steric effects play a crucial role in the borylation of 1,4-disubstituted arenes.

The results from screening experiments show that any changes in phosphine ligands, other donor ligands, or metal complexes have dramatic effect on the catalytic activity. Steric effect governs the regioselectivity of aromatic borylation. For borylation of symmetric 1,2-, 1,4- and symmetric or unsymmetric 1,3-disubstituted arenes, a single borylation product is obtained. In addition, for borylation of unsymmetric 1,2- or 1,4-disubstituted arenes, product distribution is the result of steric, electronic, and some type of chelate-directed effect depending on the substituents such as a OMe group.

CHAPTER 4

SYNTHESIS, CHARACTERIZATION, AND REACTIVITY OF IRIDIUM BORYL

COMPLEXES

Synthesis and Characterization of an Ir^I Boryl Complex

In order to gain mechanistic insight into the Ir-catalyzed borylation reaction and establish the most likely overall mechanistic pathway, it is important to examine the viability and determine the rates of each individual stage. Halpern's[40] stepwise analysis of the mechanism by which Wilkinson's catalyst catalyzes olefin hydrogenation provides a significant "take home lesson"; namely, that the identification of a dominant or detectable species in a catalytic system may lead to incorrect interpretations of the reaction mechanism. Only when kinetic and thermodynamic measurements define the role of the complexes along the actual reaction path can the mechanism be defined. A multi-step reaction is very complicated, and the dominant mechanism changes when the nature of the pre-catalyst, the ligand, and/or the substrate is altered.

From a mechanistic standpoint, there are two potential catalytic cycles involving oxidative addition and reductive elimination from $Ir^{I/III}$ and/or $Ir^{III/V}$ intermediates with Ir^I and Ir^{III} boryl intermediates being the most likely C-H activating species in the $Ir^{I/III}$ and/or $Ir^{III/V}$ cycles, respectively as shown in Figure 26.
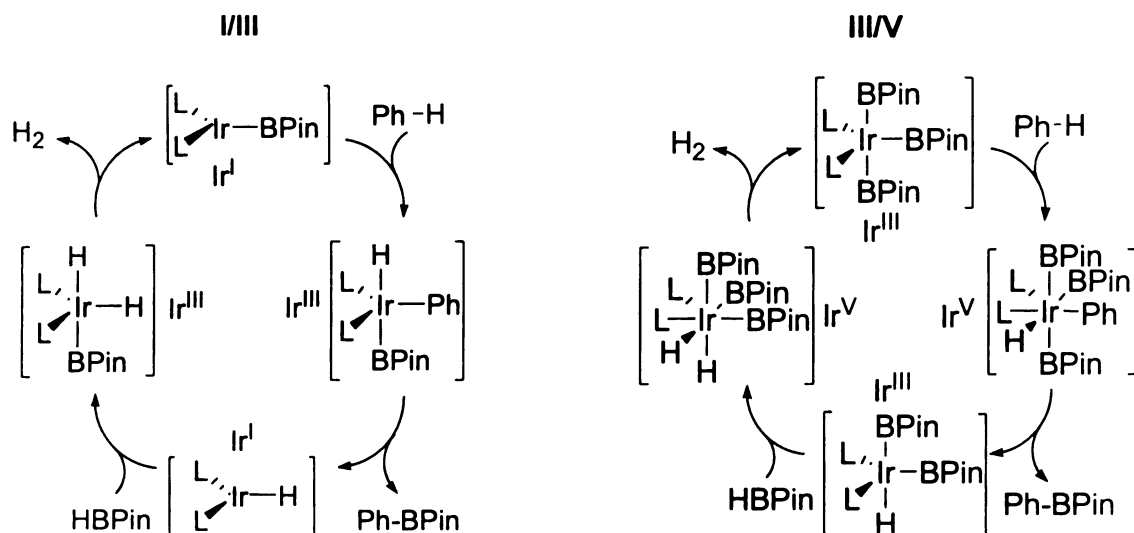
Figure 26. Two potential catalytic cycles for aromatic borylation: (Left) involving Ir$^{I/III}$ intermediates; (right) involving Ir$^{III/V}$ intermediates.

From competition reactions of mono-substituted arenes, it was found that electron-deficient arenes borylate faster than electron-rich arenes. The general observed trend suggests that the iridium metal center is electron rich, which implies that Ir^I intermediates may be the active species in the catalytic borylation reactions. In order to examine that possibility, the Ir^I boryl complex, (PMe$_3$)$_4$Ir(BPin), was first synthesized to evaluate its stoichiometric reaction with arenes.

Flood[41] and co-workers' studies on the mechanism of cyclometallation, i.e. oxidative addition of a C-H bond of a ligand to form a chelate complex, of tris(trimethylphosphine)neopentyliridium(I) compound showed that the mechanism involves direct, concerted oxidative addition and reductive elimination of the C-H bond

59

interconverting the square-planar Ir^I and octahedral Ir^{III} centers without PMe$_3$ dissociation (Figure 27).

$$Me_3P\overset{PMe_3}{\underset{Me_3P}{\Longrightarrow}}Ir\text{-}PMe_3 \quad \overset{+}{\Big]} \; Cl^- \; + \; Me_3CCH_2Li \quad \xrightarrow[\text{pentane, -20 °C}]{} \quad Me_3P\overset{PMe_3}{\underset{Me_3P}{\Longrightarrow}}Ir \quad \xrightarrow{0 \text{ °C}} \quad Me_3P\overset{H}{\underset{Me_3P}{\Longrightarrow}}Ir$$
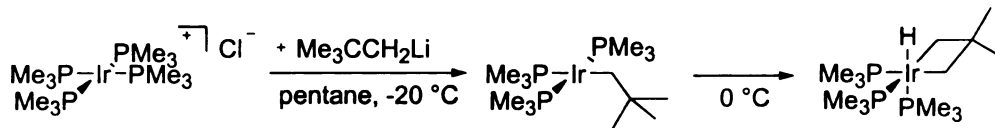
Figure 27. Cyclometallation of tris(trimethylphosphine)neopentyliridium(I) complex.

At first, the 16-electron square planar complex, [(PMe$_3$)$_3$Ir(BPin)], the proposed key intermediate in the borylation reactions, was the target complex to be synthesized. Initially, we attempted to use a dehydrohalogenation route to synthesize [(PMe$_3$)$_3$Ir(BPin)] from the reaction between *mer*-(PMe$_3$)$_3$Ir(BPin)(H)(Cl) (**15**)[42] and KO^{t}Bu (Figure 28). However, there was no reaction at room temperature, and at elevated temperature the reaction proceeded slowly to generate a complex mixture of Ir products. Several other reagents including NaN(SiMe$_3$)$_2$ and ^{t}BuLi were also used and these attempts were unsuccessful. Presumably, [(PMe$_3$)$_3$Ir(BPin)], a coordinatively unsaturated 16-electron square planar complex, is unstable, thus rendering its isolation and characterization difficult.

$$Me_3P\overset{BPin}{\underset{Me_3P}{\Longrightarrow}}Ir\text{-}H \quad + \quad KO^tBu \quad \overset{\times}{\longrightarrow} \quad \left[Me_3P\overset{PMe_3}{\underset{Me_3P}{\Longrightarrow}}Ir\text{-}BPin \right] \quad + \quad ^tBuOH \quad + \quad KCl$$

(15)
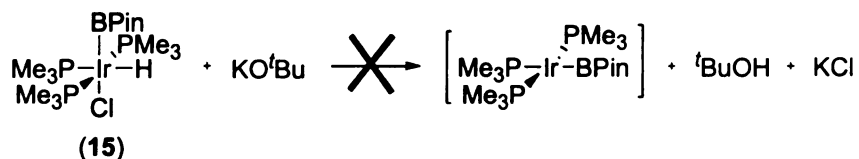
Figure 28. The reaction between *mer*-(PMe$_3$)$_3$Ir(BPin)(H)(Cl) (**15**) and KO^{t}Bu.

In 1997, Marder, Norman, and co-workers reported the synthesis of a low valent, electron-rich, late transition metal boryl complex, $(PMe_3)_4Rh(BCat)$,[43] from the reaction between $(PMe_3)_4Rh(Me)$ and B_2Cat_2 with MeBCat as byproduct. With this information in hand, we targeted $(PMe_3)_4Ir(BPin)$, which is a coordinatively saturated 18-electron complex and is presumably more stable than the original 16-electron target. In 1982, Thorn and Tulip[44] reported the preparation of $(PMe_3)_4Ir(H)$ from the reaction of $[(PMe_3)_4IrH_2]Cl$, which can be prepared at ambient temperature by purging dihydrogen gas into a THF solution of $(PMe_3)_4Ir(Cl)$, and KO^tBu through a dehydrohalogenation route. A similar reaction was carried out to first synthesize $[(PMe_3)_4Ir(H)(BPin)]Cl$ (16) by addition of HBPin instead of H_2 to the THF solution of $(PMe_3)_4Ir(Cl)$. This attempt was successful and compound 16 was prepared in 71% yield. The structure of 16 was assigned according to ^1H, ^{11}B, and $^{31}P\{^1H\}$ NMR spectroscopy. In the ^1H NMR spectrum, a doublet of quartet is observed in the hydride region at –13.16 ppm ($^2J_{HP}$ = 119.0 Hz, 18.7 Hz), indicating a *trans* relationship to a PMe_3 group and a *cis* to three PMe_3 groups. A singlet at 1.22 ppm integrating to 12 protons is assigned as the resonance of BPin group. There are two sets of doublets and one triplet corresponding to three different PMe_3 groups at 1.61 ppm (d, $^2J_{HP}$ = 8.2 Hz, 9H), 1.63 ppm (d, $^2J_{HP}$ = 7.3 Hz, 9H), and 1.74 ppm (t, $^2J_{HP}$ = 3.4 Hz, 18H, two mutually *trans* PMe_3). In the $^{31}P\{^1H\}$ NMR spectrum, there are three different phosphorous resonances. A broad peak is observed at -67.2 ppm (the PMe_3 *trans* to BPin group), a quartet is observed at –60.1 ppm ($^2J_{pp}$ = 20.8 Hz, the PMe_3 *trans* to hydride), and a triplet is observed at -55.2 ppm ($^2J_{pp}$ = 22.9 Hz, two mutually *trans* PMe_3 groups). In the ^{11}B NMR, a broad peak is observed at 32.8 ppm. Unfortunately, its reaction with KO^tBu proceeded through an undesired

deborylhalogenation pathway instead of dehydrohalogenation pathway to give

(PMe₃)₄Ir(H) and 'BuOBPin as products (Figure 29). Presumably the formation of

'BuOBPin is thermodynamically favored. Since deborylhalogenation is a dominant

reaction pathway, a process involving the synthesis of a diboryl complex in the first step,

and the reaction with KO'Bu through the deborylhalogenation pathway to give a Ir^I boryl

complex would be a possible synthetic route.
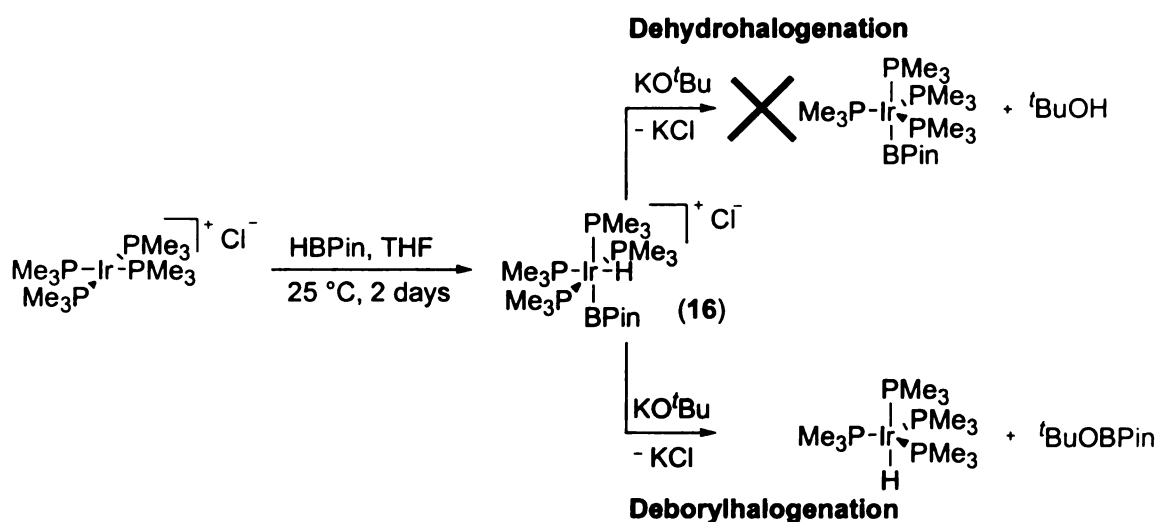
Figure 29. Deborylhalogenation reaction between complex **16** and KO'Bu.

mer,cis-(PMe₃)₃Ir(BPin)₂Cl (**17**) was prepared from the reaction between B₂Pin₂

and (PMe₃)₄Ir(Cl) in a THF solution at 70 °C for one day. The complex was purified by

recrystallization from a pentane solution at -30 °C to give spectroscopically pure

compound **17** in 74% yield (Figure 31). The ^{11}B NMR spectrum shows two boryl

resonances at 28.0 and 36.5 ppm and the ^{31}P{^{1}H} NMR spectrum exhibits a broad singlet

at –51.4 ppm due to trans coupling to a boron nucleus (^{11}B, spin 3/2, 80.4% natural

abundance, ^{10}B, spin 3, 19.6% natural abundance)[45] and a doublet at –41.1 ppm ($^2J_{pp}$ = 26.9 Hz). The catecholate analogue, *mer,cis*-(PMe$_3$)$_3$Ir(BCat)$_2$Cl, was previously prepared via a different route by Dai and co-workers.[46]

Single crystals of **17** and B$_2$Pin$_2$ co-crystallized from pentane at –30 °C and the structures were established by X-ray crystallographic analysis. The molecular structure of **17** is shown in Figure 30. Selected bond distances and bond angles are given in Table 15. The molecular structure of **17** consists of an octahedral geometry with phosphines ligands in a *meridional* arrangement. The two BPin groups are *cis* to each other with the B(1)-Ir(1)-B(2) angle of 77.97(19). The boron *trans* to chloride has an Ir-B bond distance of 2.057(5) Å, which is the same (within statistical error) as that in the compound *mer*-(PMe$_3$)$_3$Ir(BPin)(H)(Cl) **(15)** (2.054(3) Å). The other Ir-B bond distance is 2.114(5) Å. Among those Ir-P bond distances in complex **17**, the two trans phosphine ligands have Ir-P distances of 2.328(1) and 2.320(1) Å, respectively, which are very similar to the two *trans* Ir-P distances in compound **15** (2.3277(8) and 2.3147(8) Å). Furthermore, the PMe$_3$ ligand *trans* to BPin in compound **17** has a substantially longer Ir-P distance of 2.3921(13) Å. This suggests that the BPin group has a larger trans influence than a PMe$_3$ ligand.
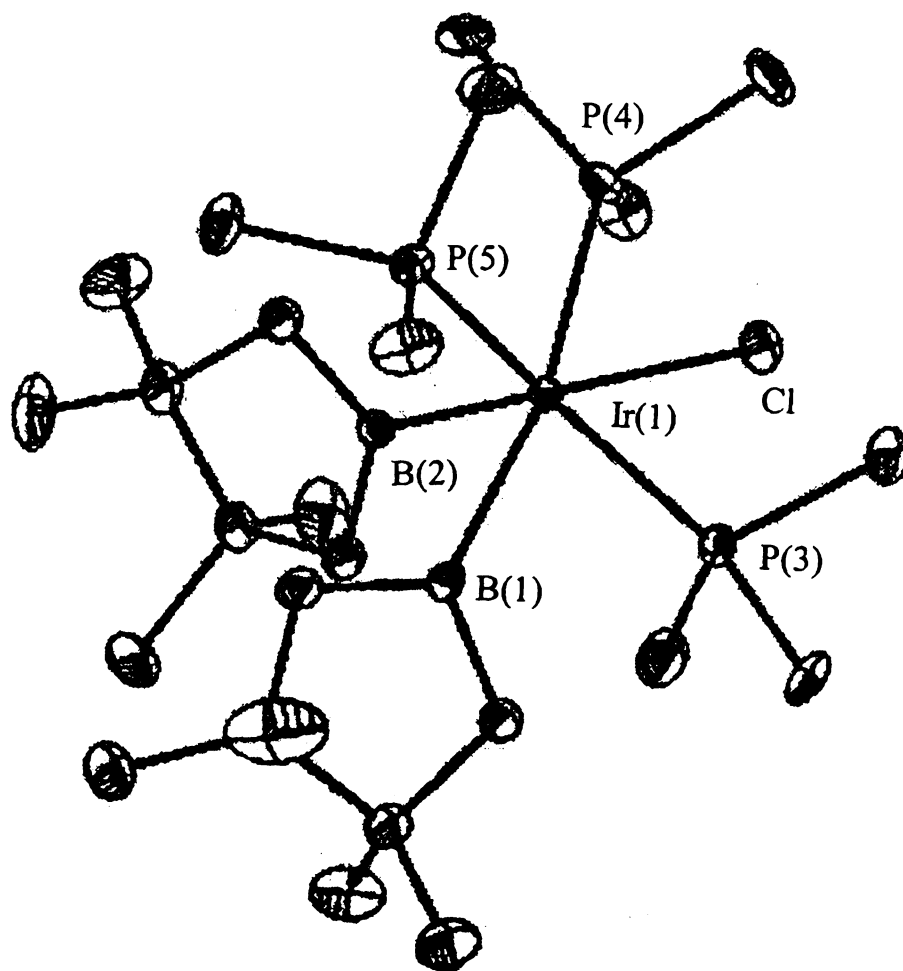
Figure 30. ORTEP diagram of *mer,cis*-(PMe₃)₃Ir(BPin)₂Cl (**17**). Thermal ellipsoids are shown at 25% probability.

Table 15. Selected bond lengths [Å] and angles [°] for **17**.

Bond	Distance [Å]	Bonds	Angle [°]
Ir(1)-B(1)	2.114(5)	B(1)-Ir(1)-B(2)	78.0(2)
Ir(1)-B(2)	2.057(5)	B(1)-Ir(1)-P(3)	87.9(1)
Ir(1)-P(3)	2.328(1)	B(1)-Ir(1)-P(4)	164.3(1)
Ir(1)-P(4)	2.392(1)	B(1)-Ir(1)-P(5)	86.3(1)
Ir(1)-P(5)	2.320(1)	B(1)-Ir(1)-Cl	102.7(1)
Ir(1)-Cl	2.560(1)	B(2)-Ir(1)-P(3)	96.8(1)
		B(2)-Ir(1)-P(4)	86.5(2)
		B(2)-Ir(1)-P(5)	97.2(1)
		B(2)-Ir(1)-Cl	179.3(2)
		P(3)-Ir(1)-P(4)	96.0(4)
		P(3)-Ir(1)-P(5)	163.33(4)
		P(3)-Ir(1)-Cl	83.05(4)
		P(4)-Ir(1)-P(5)	93.84(5)
		P(4)-Ir(1)-Cl	92.88(4)
		P(5)-Ir(1)-Cl	83.03(4)

The reaction between compound **17** and KO^{t}Bu in the presence of 2 equivalent PMe$_3$ was carried out at ambient temperature to give (PMe$_3$)$_4$Ir(BPin) (**18**) in good yield (The product always contained a small amount of (PMe$_3$)$_4$Ir(H) (ca. 3% by ^{1}H NMR) due to its considerable moisture sensitivity) (Figure 31). Complex **18** is fluxional in solution as evidenced by the appearance of a singlet at –57.5 ppm at 298.15 K (25 °C) in the ^{31}P{^{1}H} NMR spectrum where it displays a doublet (-56.2 ppm, ^2Jpp = 32.8 Hz, 3P) and a broad quartets (-57.7 ppm, 1P) at 213 K (-60 °C). The low temperature-limiting spectrum indicates a trigonal bipyramidal geometry with the BPin group occupying an axial site.

$$(\text{PMe}_3)_4\text{Ir(Cl)} \cdot \text{B}_2\text{Pin}_2 \xrightarrow[\text{70 °C, 12 h}]{\text{THF}}$$

$$\underset{\substack{| \\ \text{Me}_3\text{P}}}{\overset{\substack{\text{BPin} \\ |}}{\text{Me}_3\text{P}\!-\!\text{Ir}\!-\!\text{BPin}}} \overset{\text{PMe}_3}{\underset{\text{Cl}}{}}$$

(17)

74% yield

$$\textbf{17} \xrightarrow[\text{25 °C, 90 min, – KCl}]{\text{KO}^t\text{Bu, PMe}_3\text{, THF}} \underset{\substack{| \\ \text{PMe}_3}}{\overset{\substack{\text{BPin} \\ |}}{\text{Me}_3\text{P}\!-\!\text{Ir}\!-\!\text{PMe}_3}} \overset{\text{PMe}_3}{} + {}^t\text{BuOBPin}$$

(18)

92% yield
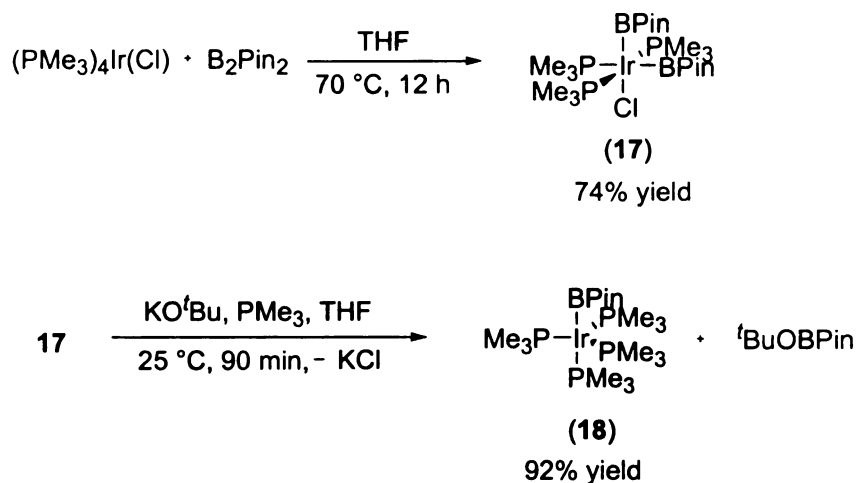
Figure 31. Syntheses of *mer,cis*-(PMe₃)₃Ir(BPin)₂Cl (**17**) and (PMe₃)₄Ir(BPin) (**18**).

Single crystals of **18** were grown from pentane at –30 °C and the structure was further confirmed by single–crystal X-ray crystallographic analysis. The molecular structure of **18** is shown in Figure 32. Selected bond distances and bond angles are given in Table 16. From the X-ray structure, the Ir(1)-P(1) distance of 2.334(2) Å, is significantly longer than Ir(1)-P bonds of the other equatorial PMe₃ ligands (Ir(1)-P(2), 2.287(2) Å, Ir(1)-P(3), 2.282(2) Å, and Ir(1)-P(4), 2.270(2) Å). The result can be rationalized by assuming a large trans influence of BPin group.
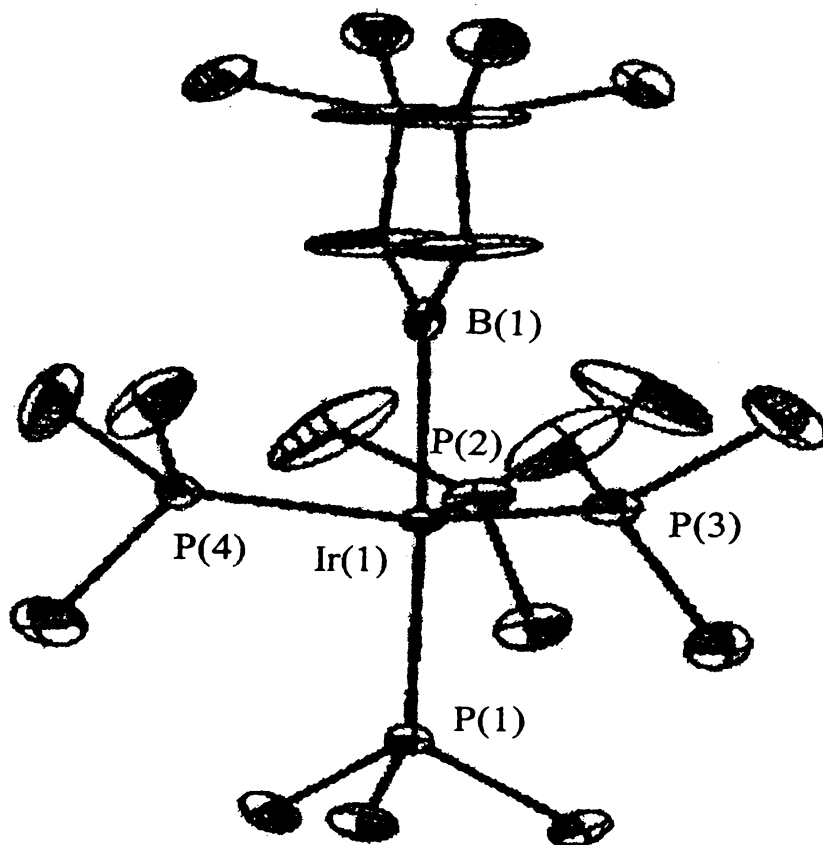
Figure 32. ORTEP diagram of (PMe₃)₄Ir(BPin) (**18**). Thermal ellipsoids are shown at 25% probability.

Table 16. Selected bond lengths [Å] and angles [°] for **18**.

Bond	Distance [Å]	Bonds	Angle [°]
Ir(1)-B(1)	2.147(9)	B(1)-Ir(1)-P(1)	178.0(2)
Ir(1)-P(1)	2.334(2)	B(1)-Ir(1)-P(2)	85.1(2)
Ir(1)-P(2)	2.287(2)	B(1)-Ir(1)-P(3)	85.0(2)
Ir(1)-P(3)	2.282(2)	B(1)-Ir(1)-P(4)	82.2(2)
Ir(1)-P(4)	2.270(2)	P(2)-Ir(1)-P(3)	119.8(1)
		P(2)-Ir(1)-P(4)	119.1(1)
		P(3)-Ir(1)-P(4)	118.0(1)
		P(1)-Ir(1)-P(2)	95.8(7)
		P(1)-Ir(1)-P(3)	96.1(7)
		P(1)-Ir(1)-P(4)	95.8(8)

(PMe$_3$)$_4$Ir(BPin) (**18**) underwent a variety of substitution and oxidative addition reactions. It reacted with dppe in C$_6$D$_6$ at room temperature for 3 days to give Ir(PMe$_3$)$_2$(dppe)(BPin) (**19**) as the major iridium containing complex as shown in Figure 33. The reaction resulted in the replacement of 2 PMe$_3$ ligands with the chelating phosphine ligand, 1,2-bis(diphenylphosphino)ethane (dppe). The structure of **19** was assigned according to ^{1}H, ^{11}B, and ^{31}P{^{1}H} NMR spectroscopy. In the ^{1}H NMR spectrum, a singlet at 1.10 ppm is assigned as the resonance of the BPin group. There is a triplet corresponding to two PMe$_3$ groups at 1.33 ppm ($^2J_{HP}$ = 3.3 Hz, 18H) and a multiplet in the region of 1.92-2.18 ppm corresponding to four protons of the two CH$_2$ groups on the backbone of dppe ligand. In the aromatic region (6.98-7.12, 7.16-7.28, 7.72-7.89, and 7.91-7.98 ppm) there are 20 protons corresponding to the protons for the four phenyl groups of the dppe ligand. In the ^{11}B NMR, a broad peak is observed at 38.8 ppm. In the ^{31}P{^{1}H} NMR spectrum, there are three different phosphorous resonances. A broad peak is observed at 46.1 ppm for the PPh$_2$ *trans* to BPin, a doublet of triplet is observed at 39.1 ppm (J = 141.6 Hz, 13.4 Hz) for the PPh$_2$ *cis* to BPin, and a doublet of doublet is observed at –58.9 ppm (J = 141.6 Hz, 26.8 Hz) corresponding to two PMe$_3$ groups.
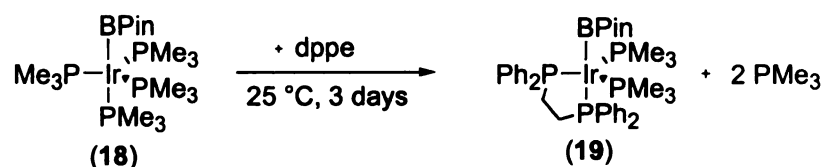
Figure 33. The reaction between compound **18** and dppe.

Compound **18** reacted with HBPin in C_6D_6 to give *mer,trans*-$(PMe_3)_3Ir(BPin)_2(H)$ **(20)** as the initial predominant species, and this kinetic product gradually isomerized to *fac*-$(PMe_3)_3Ir(BPin)_2(H)$ **(21)** after heating at 70 °C for 11 hours. The structure of **20** was assigned according to ^1H, ^{11}B, and $^{31}P\{^1H\}$ NMR spectroscopy. In the ^1H NMR spectrum, a doublet of triplet is observed in the hydride region at –12.36 ppm ($^2J_{HP}$ = 117.0 Hz, 21.7 Hz), indicating a *trans* relationship to a PMe_3 group and a *cis* orientation to two PMe_3 groups. A singlet at 1.22 ppm is assigned as the resonance of the two mutually *trans* BPin groups. A doublet is observed at 1.49 ppm (J = 8.0 Hz, 9H) corresponding to the PMe_3 *trans* to hydride and a triplet is observed at 1.74 (J = 3.4 Hz, 18H) corresponding to the two PMe_3 groups, which are *trans* to each other. In the ^{11}B NMR, a broad peak is observed at 38.9 ppm. In the $^{31}P\{^1H\}$ NMR spectrum, there are two different phosphorous resonances. A triplet is observed at –59.6 ppm (J = 22.0 Hz) for the PMe_3 *trans* to H and a doublet is observed at –50.8 ppm (J = 22.0 Hz) for the two mutually *trans* PMe_3 groups. The structure of **21** was also assigned according to ^1H, ^{11}B, and $^{31}P\{^1H\}$ NMR spectroscopy. In the ^1H NMR spectrum, a doublet of triplet is observed in the hydride region at –11.66 ppm ($^2J_{HP}$ = 118.1 Hz, 18.1 Hz), indicating a *trans* relationship to a PMe_3 group and a *cis* to two PMe_3 groups. A singlet at 1.29 ppm is assigned as the resonance of the two chemically equivalent BPin groups. A virtual triplet is observed at 1.41 ppm corresponding to the two PMe_3 groups *trans* to BPin and a doublet is observed at 1.58 ppm (J = 8.0 Hz) assigned as the PMe_3 *trans* to hydride. In the ^{11}B NMR, a broad peak is observed at 38.6 ppm. The $^{31}P\{^1H\}$ NMR spectrum of **21** displays a triplet at –56.6 ppm (J = 22.0 Hz) for the PMe_3 *trans* to H and a broad resonance at –61.8 ppm for the two PMe_3 groups *trans* to BPin.

Eisenberg and co-workers[47] reported that the oxidative addition of catecholborane (HBCat) to the Ir(I) cis-phosphine complexes IrX(CO)(dppe) (X = Br, I; dppe = 1,2-bis(diphenylphosphino)ethane) proceeds stereoselectively under kinetic control. In their original studies on H_2, R_3SiH, and HX' oxidative additions to IrX(CO)(dppe) complexes,[48] they reasoned that both H_2 and R_3SiH add to the IrX(CO)(dppe) complexes as nucleophiles. The addition occurs over the OC-Ir-P axis because the π^* orbital of CO is able to stabilize the developing transition state by reduction of electron density of the Ir d_z^2 orbital, thus minimizing the repulsive 4e$^-$ interaction between the filled d_z^2 and σ^b orbitals of H_2 and R_3SiH. On the contrary, hydrogen halides (HX') approach IrX(CO)(dppe) in aprotic media as electrophiles. Therefore, interactions that retain or enhance electron density at the metal center will favor addition along that pathway. Thus, HX' addition is preferred by bending the X-Ir-P axis because this pathway leads to an antibonding interaction between an occupied p_z orbital of X and the d_z^2 orbital of Ir, thus enhancing the ability of Ir to donate electrons to the incoming electrophile (Figure 34).[49] Since oxidative addition of catecholborane to IrX(CO)(dppe) complexes (X = Br, I) resembles HX' additions, the result implies that catecholborane approaches the metal center as an electrophile in accord with the view that the vacant B p_z orbital can overlap with the filled d_z^2 of Ir (Figure 35).

70
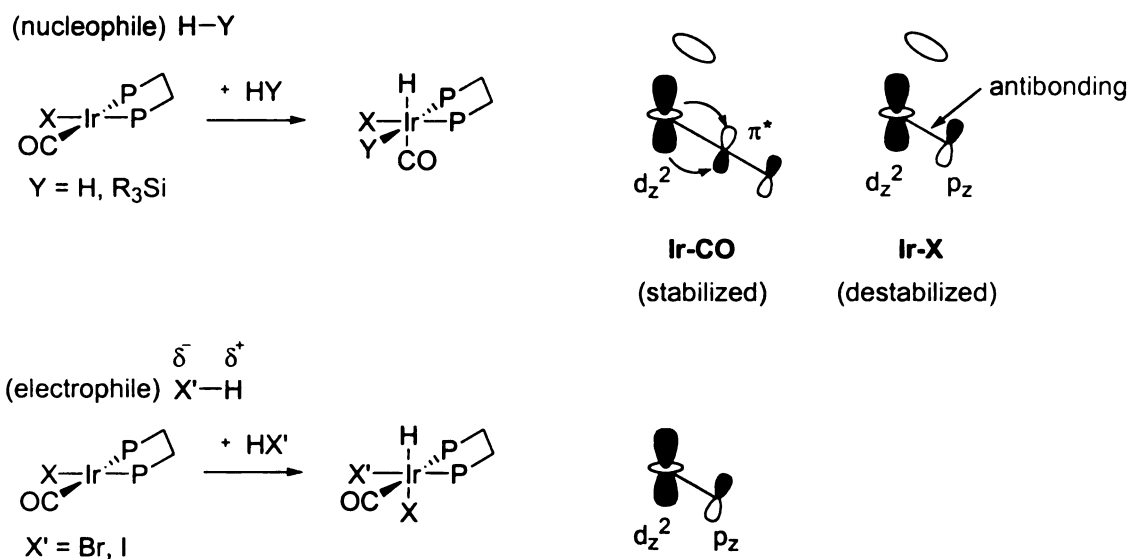
Figure 34. H_2, R_3SiH, and HX' oxidative additions to IrX(CO)(dppe) complexes.
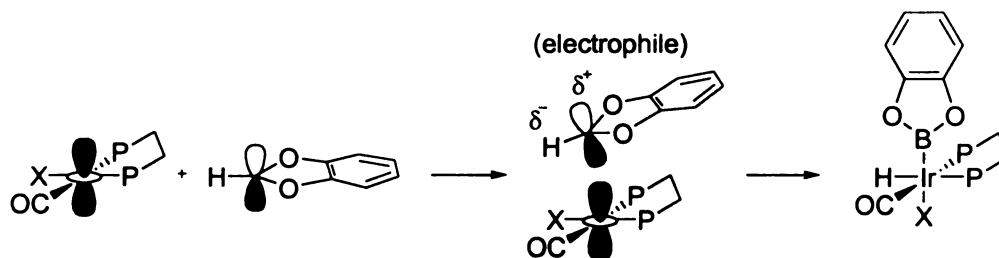
Figure 35. Catecholborane (HBCat) oxidative addition to IrX(CO)(dppe) complexes.

Pinacolborane (HBPin) oxidative addition to compound **18** gives complex **20** as the kinetic product with the two BPin groups *trans* to each other. The result can be rationalized by assuming that pinacolborane (HBPin) approaches the Ir metal center as an electrophile in accord with the results for HBCat. Furthermore, the backbonding interaction between the filled Ir metal d_z^2 orbital and the empty B p_z orbital, as HBPin

71

adds in the P-Ir-B plane, provides additional stabilization to the five-coordinate species, as shown in Figure 36.
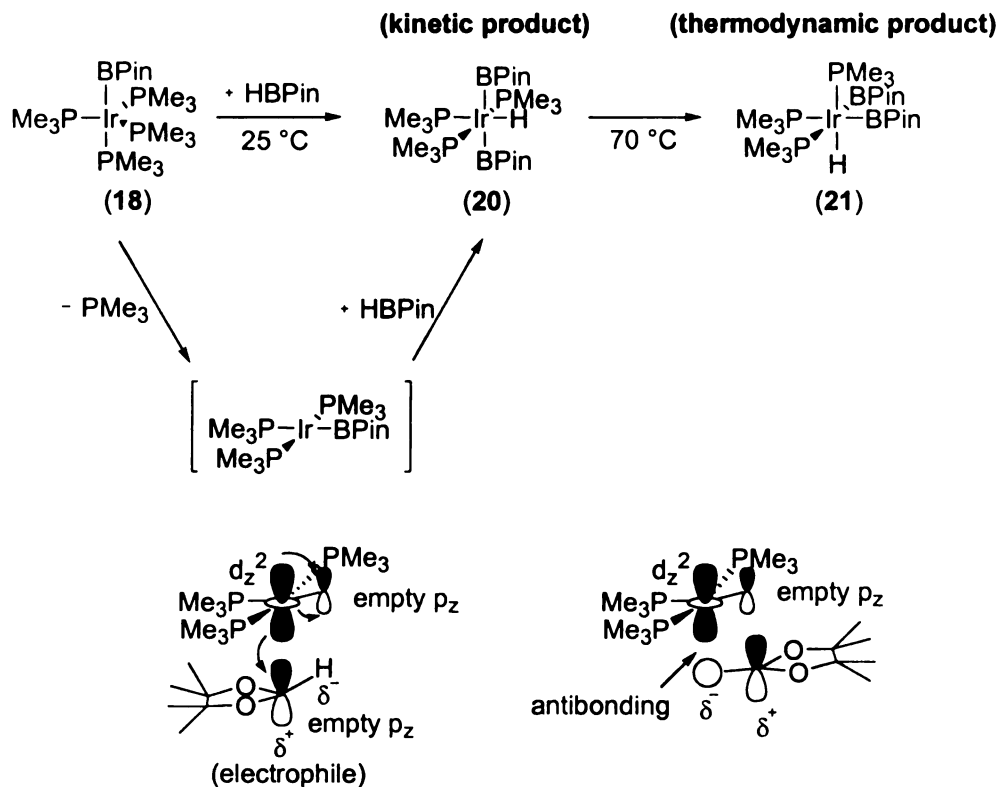
Figure 36. Pinacolborane (HBPin) oxidative addition to compound **18**.

The reaction of **18** with chlorocatecholborane (ClBCat) proceeded at room temperature to give *mer*-(PMe₃)₃Ir(BPin)(BCat)(Cl) (**22**) as the major product with the BPin group *trans* to the chloride ligand as shown in Figure 37. The geometry of **22** was assigned according to ^{1}H, ^{11}B, and ^{31}P{^{1}H} NMR spectroscopy. In the ^{1}H NMR spectrum, a singlet at 1.18 ppm is assigned as the resonance of the BPin group. There is a doublet at 1.29 ppm (J = 7.3 Hz) corresponding to the PMe₃ *trans* to BCat and a triplet at

1.47 ppm corresponding to two mutually *trans* PMe₃ groups. An AA'BB' pattern is observed at 6.84 and 7.19 ppm in the aromatic region, which corresponds to the four protons of the catecholate. The ^{11}B NMR spectrum displays two well-separated resonances at 28.1 and 41.6 ppm, respectively. By comparing the resonances of boryl groups in compound **15**, **17**, *mer*-(PMe₃)₃Ir(BCat)(H)Cl (**23**),[42] and *mer,cis*-(PMe₃)₃Ir(BCat)₂Cl (**24**)[46] as summarized in Table 17, we assigned the resonance at 28.1 ppm as the BPin group and the resonance at 41.6 ppm as the BCat group. The ^{31}P{^{1}H} NMR spectrum of **22** displays a broad peak at -56.2 ppm assigned as the PMe₃ *trans* to BCat and a doublet at -39.3 ppm (J = 29.3 Hz) corresponding to two mutually *trans* PMe₃ groups.

$$
\begin{array}{ccc}
\underset{\textstyle(18)}{\overset{\textstyle BPin}{\underset{\textstyle PMe_3}{Me_3P-\overset{\textstyle|\ ,PMe_3}{\underset{\textstyle|}{Ir},PMe_3}}}} & \xrightarrow[\textstyle 25\ ^\circ C,\ 3\ days]{\textstyle +\ ClBCat,\ -\ PMe_3} & \underset{\textstyle(22)}{\overset{\textstyle BPin}{\underset{\textstyle Me_3P}{Me_3P-\overset{\textstyle|,PMe_3}{\underset{\textstyle Cl}{Ir}-BCat}}}}
\end{array}
$$
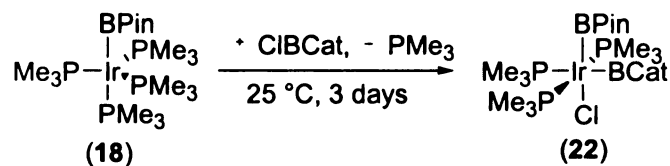
Figure 37. Chlorocatecholborane (ClBCat) oxidative addition to compound **18**.

Table 17. Comparison of boryl resonances of complexes **15**, **17**, **22**, **23**, and **24** in ^{11}B NMR spectra.

Complex	15	17	22	23	24
BPin *trans* to Cl (ppm)	28.5	28.0	**28.1**	--	--
BCat *trans* to Cl (ppm)	--	--		32.8	32.6
BPin *trans* to PMe₃ (ppm)	--	36.5	--	--	--
BCat *trans* to PMe₃ (ppm)	--	--	**41.6**	--	41.7

Synthesis and Characterization of an Ir^{III} Boryl Complex

The Ir^{III} boryl complex, *fac*-(PMe$_3$)$_3$Ir(BPin)$_3$ (25) can be easily prepared in essentially quantitative yield by addition of a slight excess of PMe$_3$ to (MesH)Ir(BPin)$_3$ (14) in benzene solution at ambient temperature (Figure 38).
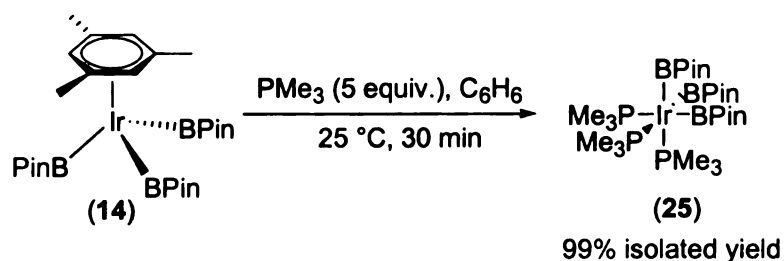
Figure 38. Synthesis of *fac*-(PMe$_3$)$_3$Ir(BPin)$_3$ (25).

Crystals suitable for X-ray analysis of 25 were grown from pentane at –30 °C. The molecular structure of 25 is shown in Figure 39. Selected bond distances and bond angles are given in Table 18. The complex adopts a *facial* geometry with all three PMe$_3$ ligands *trans* to the BPin groups. The ^{11}B NMR spectrum shows only one boryl resonance at 36 ppm and the ^{31}P{^{1}H} NMR spectrum shows one broad singlet at -64 ppm due to a trans coupling to the boron nucleus. A similar compound, *fac*-(PEt$_3$)$_3$Ir(BCat)$_3$, was previously prepared by Marder and co-workers via the displacement of the mesitylene ligand of (MesH)Ir(BCat)$_3$ with 3 equivalent of PEt$_3$.^{31} *fac*-(PEt$_3$)$_3$Ir(BCat)$_3$ has similar spectroscopic properties as compound 25. In the ^{11}B NMR spectrum, a broad peak was observed at 44.7 ppm corresponding to the three BCat groups and in ^{31}P{^{1}H}

74

NMR spectrum, a broad peak was observed at −32.1 ppm corresponding to the three PMe₃ groups.
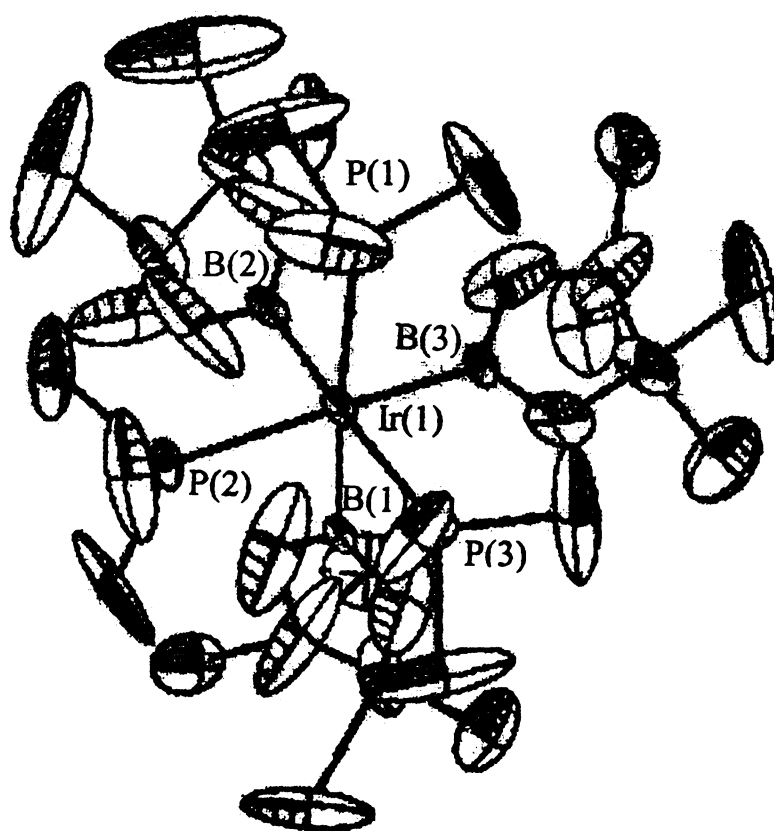
Figure 39. ORTEP diagram of *fac*-(PMe₃)₃Ir(BPin)₃ (**25**). Thermal ellipsoids are shown at 25% probability. All oxygen and carbon labels are omitted for clarity. Hydrogen atoms are also omitted for clarity.

Table 18. Selected bond lengths [Å] and angles [°] for **25**.

Bond	Distance [Å]	Bonds	Angle [°]
Ir(1)-B(1)	2.106(2)	B(1)-Ir(1)-B(2)	82.3(7)
Ir(1)-B(2)	2.148(2)	B(1)-Ir(1)-B(3)	79.4(6)
Ir(1)-B(3)	2.082(2)	B(2)-Ir(1)-B(3)	81.9(7)
Ir(1)-P(1)	2.352(4)	B(1)-Ir(1)-P(1)	169.2(5)
Ir(1)-P(2)	2.353(4)	B(1)-Ir(1)-P(2)	91.5(5)
Ir(1)-P(3)	2.347(4)	B(1)-Ir(1)-P(3)	89.6(5)
		B(2)-Ir(1)-P(1)	90.8(5)
		B(2)-Ir(1)-P(2)	90.9(5)
		B(2)-Ir(1)-P(3)	169.6(5)
		B(3)-Ir(1)-P(1)	91.4(5)
		B(3)-Ir(1)-P(2)	169.0(5)
		B(3)-Ir(1)-P(3)	90.1(5)
		P(1)-Ir(1)-P(2)	97.1(2)
		P(1)-Ir(1)-P(3)	96.2(2)
		P(2)-Ir(1)-P(3)	95.9(2)

Synthesis and Characterization of Novel Metal Boryl Complexes Containing Alkyl, Aryl, or Silyl Ligands

In transition metal catalyzed hydroboration of unsaturated hydrocarbons and borylation reactions of alkanes and arenes, an intermediate containing a boryl ligand and a σ-bound carbon ligand has been proposed. Several theoretical studies also support the intermediacy of such metal complex. However, only a few of this type of metal complexes have appeared in literature (Figure 40). One of them, reported by Crabtree[50] and co-workers in 1993, was an unprecedented Ir^{IV} boryl complex, $[Ir(PMe_3)_3(biphBF)Cl]^+I^-$. Knorr and Merola[42] reported the preparation and characterization of mer-$(PMe_3)_3Ir(BCat)(trans-\{CO_2CH_3\}=CH\{CO_2CH_3\})(Cl)$ in which the vinyl group arises from insertion of dimethyl acetylenedicarboxylate into the Ir-H

bond of *mer*-(PMe₃)₃Ir(BCat)(H)(Cl). Another case is the report by Roper, Wright, and co-workers of the synthesis of *cis*- and *trans*-[Os(BCat)(*o*-tolyl)(CO)₂(PPh₃)₂].[51] The complex with *o*-tolyl and BCat groups *cis* to each other was unstable at room temperature. *o*-tolylBCat was slowly eliminated from the complex at room temperature in benzene solution to give the orthometallation product, [Os(C₆H₄PPh₂)(H)(CO)₂(PPh₃)]. On the other hand, the complex with *o*-tolyl and BCat groups *trans* to each other was stable under reflux in benzene for 2 hours. Their observations indicate that the requirement for facile reductive elimination is that the aryl and BCat ligands be adjacent to one another.

R = C(O)OCH₃

R = *o*-tolyl

R = *o*-tolyl
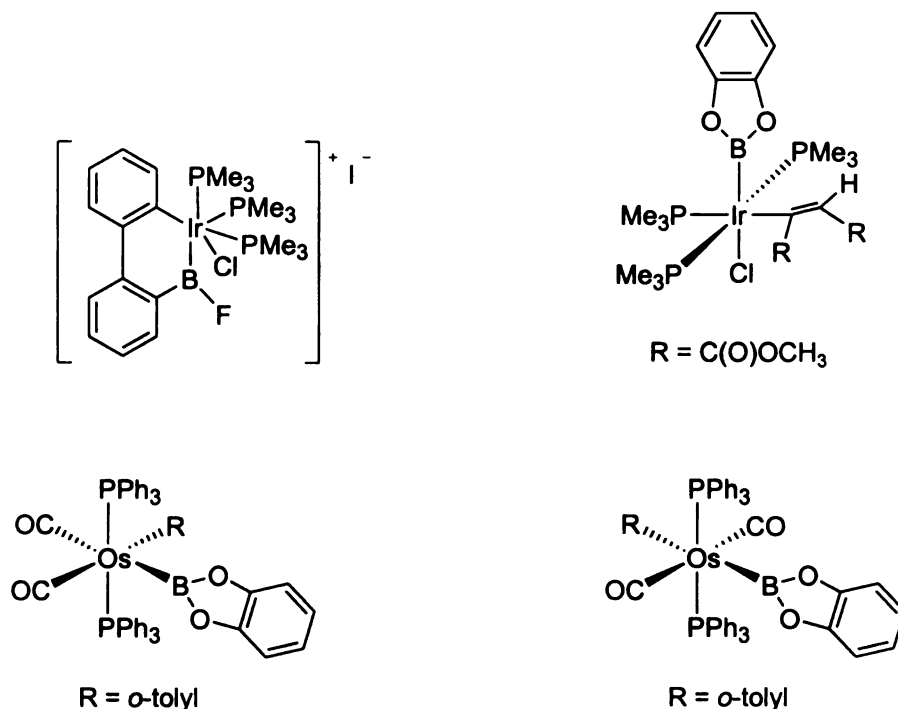
Figure 40. Reported complexes containing a boryl ligand and a σ-bound carbon ligand.

There are several cases where the authors imply the intermediacy of such a complex. For example, the reaction of (PMe₃)₄Rh(Me) with B₂Cat₂ resulted in the formation of MeBCat and (PMe₃)₄Rh(BCat).[43] The authors reasoned that the reaction proceeded via oxidative addition of the B-B bond followed by rapid reductive elimination of MeBCat (Figure 43).

$$(PMe_3)_4Rh(Me) \; + \; B_2Cat_2 \xrightarrow{\; -PMe_3 \;} \left[\begin{array}{c} PMe_3 \\ CatB_{\text{,}} \cdot \underset{\displaystyle Me}{\overset{\displaystyle |}{Ir}} \cdot PMe_3 \\ CatB^{\prime} \; | \; PMe_3 \end{array} \right]$$

↓ MeBCat

$$(PMe_3)_4Rh(BCat) \xleftarrow{\; +PMe_3 \;} [(PMe_3)_3Rh(BCat)]$$
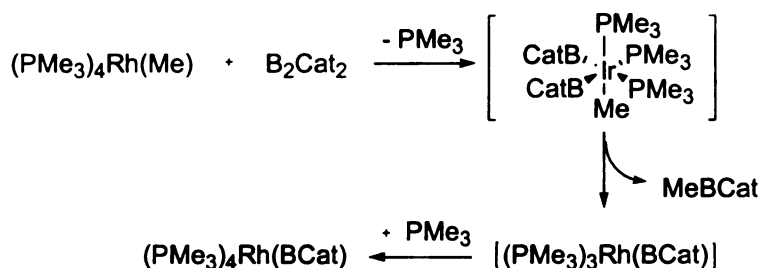
Figure 41. The reaction between (PMe₃)₄Rh(Me) and B₂Cat₂.

Although transition metal alkyl boryl complexes have been proposed as intermediates in stoichiometric and catalytic alkane borylation reactions, no such species have ever been isolated. In an attempt to synthesize this type of species in the "Ir(PMe₃)ₙ" system, we examined the reaction between (PMe₃)₄Ir(Me)[52] and HBPin in pentane solution. The reaction occurred immediately at ambient temperature to generate an isomer mixture of *fac*-(PMe₃)₃Ir(H)(Me)(BPin) **(26)** (83%) and *mer*-(PMe₃)₃Ir(Me)(H)(BPin) **(27)** (17%) in 75% yield (Figure 42).[53]
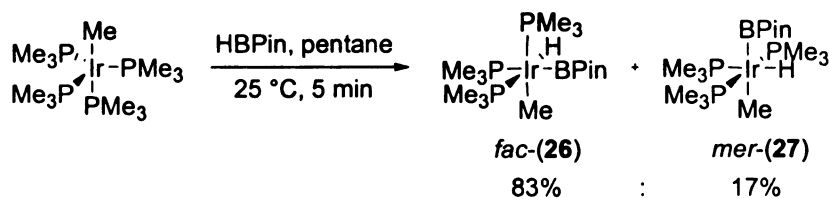
Figure 42. The reaction between $(PMe_3)_4Ir(Me)$ and HBPin in pentane.

Complex **26** adopts a *facial* geometry with BPin, H, and Me groups all *trans* to a

PMe$_3$ group. The geometry of **26** was assigned according to ^{1}H, ^{11}B, and ^{31}P$\{^1$H$\}$ NMR

spectroscopy. In the ^{1}H NMR spectrum, a doublet of triplet is observed in the hydride

region at -11.30 ppm ($^2J_{HP}$ = 140.4 Hz, 18.9 Hz), indicating a *trans* relationship to a

PMe$_3$ group and a *cis* to two PMe$_3$ groups. From 0.37 to 0.42 ppm, there is a peak with a

dddd pattern corresponding to a methyl group which is *cis* to three different PMe$_3$ groups

and a hydride ligand as shown in Figure 43. A singlet at 1.25 ppm is assigned as the

resonance of BPin group, and there are three sets of doublets corresponding to three

different PMe$_3$ groups at 1.17 ppm ($^2J_{HP}$ = 6.4 Hz, PMe$_3$ *trans* to BPin), 1.35 ppm ($^2J_{HP}$ =

7.3 Hz, PMe$_3$ *trans* to hydride), and 1.47 ppm ($^2J_{HP}$ = 7.9 Hz, PMe$_3$ *trans* to Me) as

shown in Figure 44. In the ^{31}P$\{^1$H$\}$ NMR spectrum, there are three different phosphorous

resonances for complex **26** as shown in Figure 47. A broad peak is observed at -63.3 ppm

(the PMe$_3$ *trans* to BPin group), a doublet of doublet is observed at -56.83 ppm ($^2J_{pp}$ =

13.4 Hz, 23.2 Hz, PMe$_3$ *trans* to hydride), and a doublet of doublet is observed at -55.16

ppm ($^2J_{pp}$ = 13.4 Hz, 18.3 Hz, PMe$_3$ *trans* to Me). The assignment of different PMe$_3$

groups in ^{1}H NMR spectra was established by one-dimensional Nuclear Overhauser

Effect (NOE) experiments (Figures 45 and 46). In the NOE experiment, the hydride and

79

the methyl resonances of compound **26** were irradiated in order to establish the through space relationships to identify their *trans* PMe$_3$ groups. Irradiation of the hydride resonance at δ -11.30 resulted in enhancement of the peaks at 0.40, 1.17, 1.25, and 1.47 ppm. Therefore, the peak at δ 1.35 is the PMe$_3$ *trans* to hydride. Irradiation of the methyl resonance at δ 0.40 resulted in enhancement of the peaks at δ -11.30, 1.17, 1.25, and 1.35. Therefore, the peak at δ 1.47 is the PMe$_3$ *trans* to the methyl group. The assignment of the different PMe$_3$ groups in ^{31}P$\{^1$H$\}$ NMR spectra is based on two-dimensional Heteronuclear Chemical Shift Correlation (HETCOR) experiment (^{1}H, ^{31}P) to correlate the resonances of PMe$_3$ groups in the ^{1}H NMR spectra to those in the ^{31}P$\{^1$H$\}$ NMR spectra (Figure 48). The cross peak (a) presumably comes from a ^3J coupling. In two-dimensional heteronuclear NMR, couplings through two or more bonds are very much smaller than directly bonded couplings but do not necessarily fall off regularly with the number of bonds, ^3J being sometimes larger than ^2J. To our knowledge, this is the first structural characterization of a transition metal alkyl boryl complex.

PMe₃
Me₃P–Ir–BPin
Me₃P
Me
fac-(26)

0.50   0.48   0.46   0.44   0.42   0.40   0.38   0.36   0.34   0.32
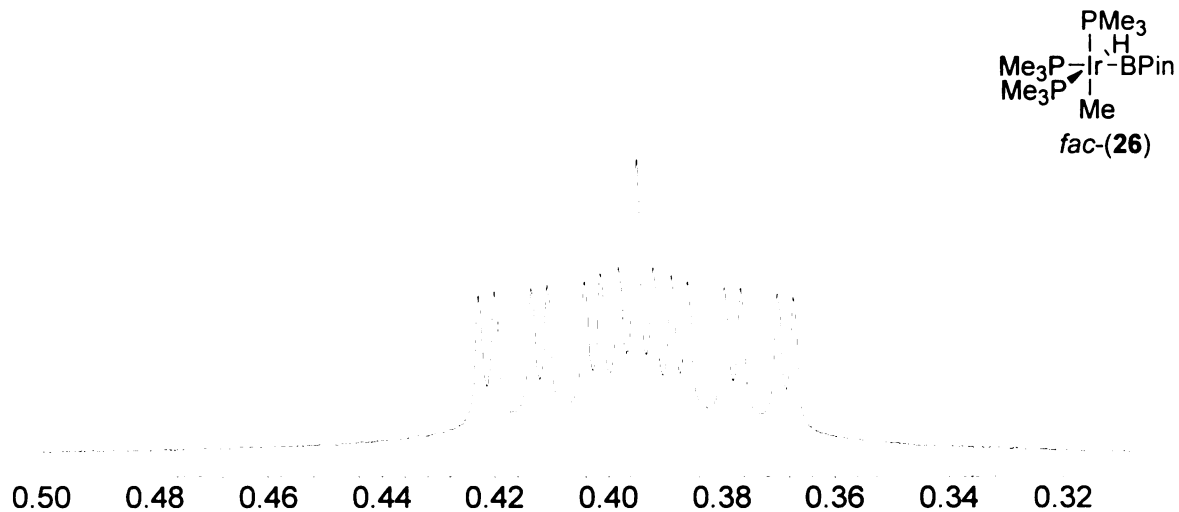
Figure 43. The resonance of the methyl group of *fac*-(PMe₃)₃Ir(Me)(H)(BPin) **(26)** in the

¹H NMR spectrum.

PMe₃
Me₃P–Ir–BPin
Me₃P
Me
fac-(26)

BPin of **26**

PMe₃ of **26**

PMe₃ of **26**

PMe₃ of **26**

*   *

1.60   1.50   1.40   1.30   1.20
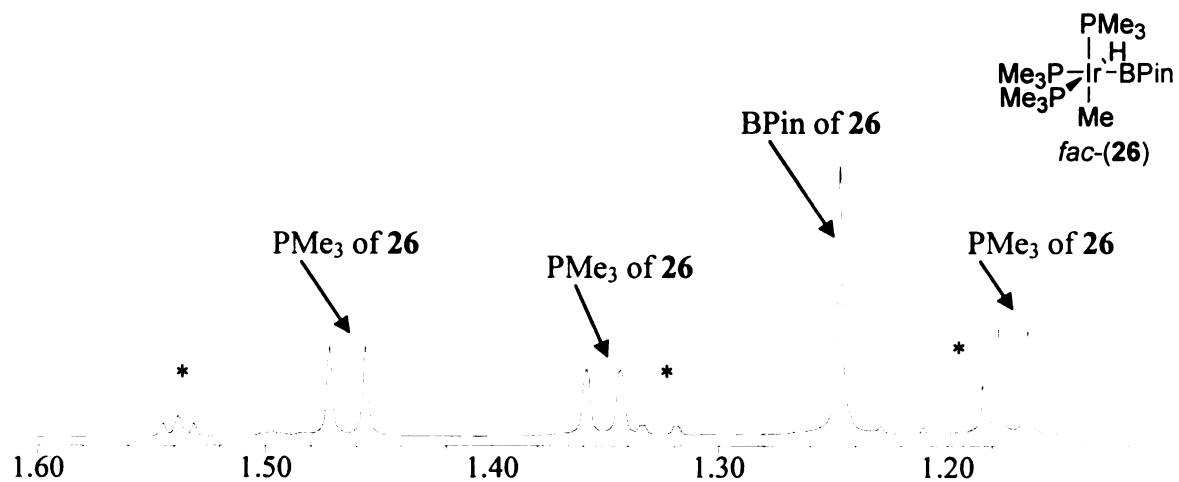
Figure 44. The resonances of PMe₃ groups of *fac*-(PMe₃)₃Ir(Me)(H)(BPin) **(26)** in the ¹H

NMR spectrum. The peaks denoted with an asterisk (*) are due to PMe₃ and BPin

resonances of compound **27**.

81

Figure 45. NOE experiments of compound **26** (Irradiation of the hydride resonance at -11.30 ppm).

Normal ^{1}H NMR spectrum

Irradiation of the hydride
resonance at -11.30 ppm

PMe$_3$ *trans* to H
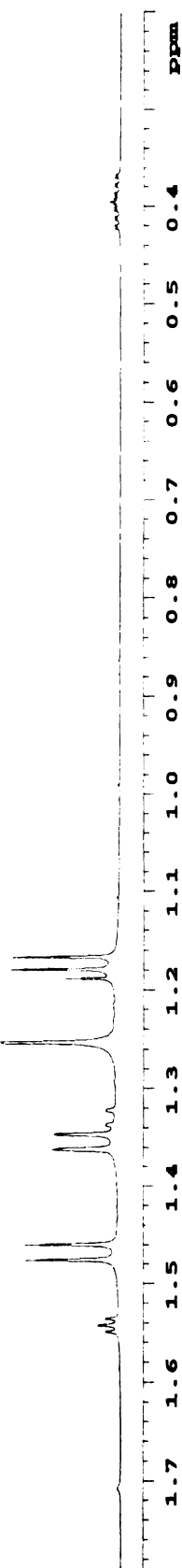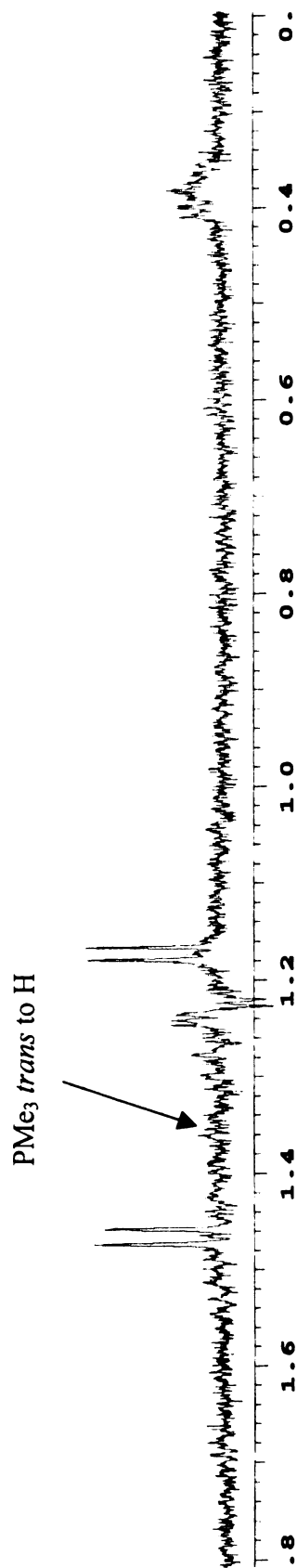
Figure 46. NOE experiments of compound **26** (Irradiation of the Me resonance at 0.40 ppm).

Irradiation of the Me
resonance at 0.40 ppm

PMe₃ *trans* to Me
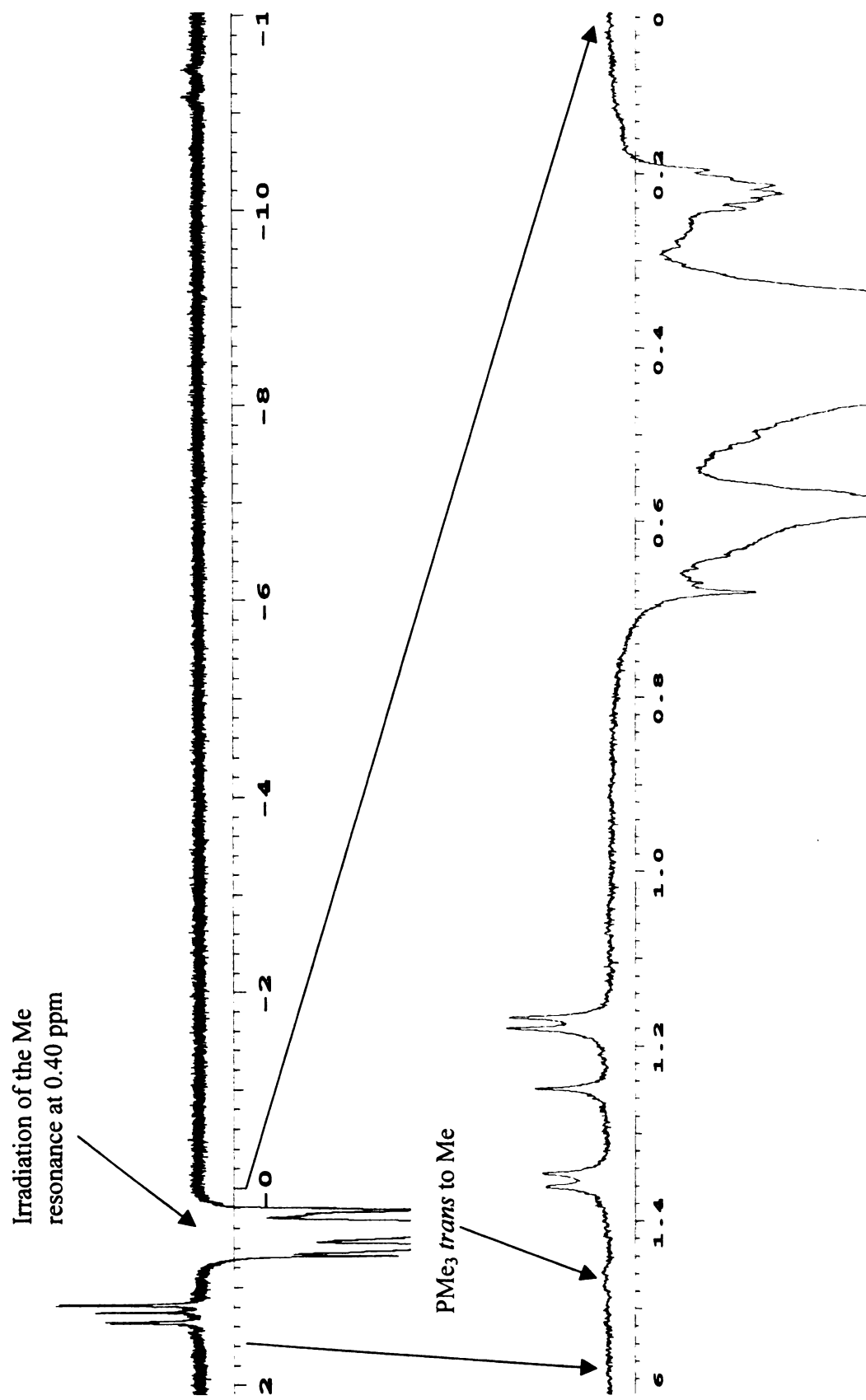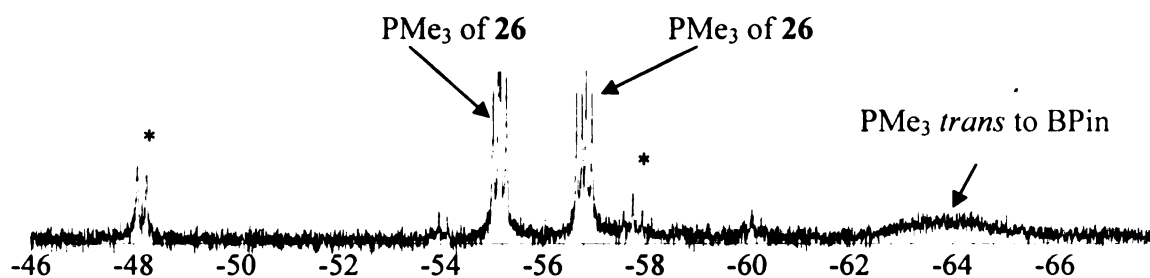
Figure 47. The resonances of PMe₃ groups of *fac*-(PMe₃)₃Ir(Me)(H)(BPin) (**26**) in the ³¹P{¹H} NMR spectrum. The peaks denoted with an asterisk (*) are due to PMe₃ resonances of compound **27**.
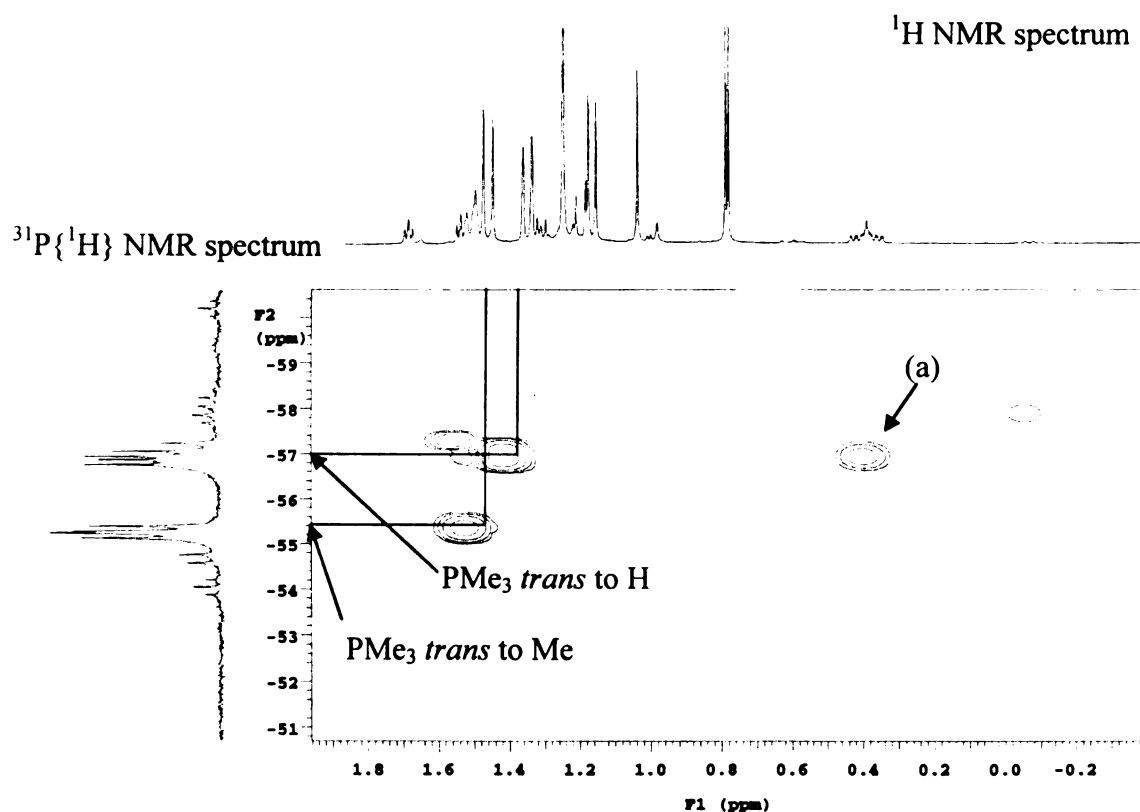
Figure 48. HETCOR experiment (¹H, ³¹P) to correlate the resonances of PMe₃ groups in the ¹H NMR spectra to those in the ³¹P{¹H} NMR spectra.

In the reaction of (PMe₃)₄Ir(Me) with 9-BBN reported by Baker and co-workers, the reaction led to the isolation of a boroethyl-metal compound, which most likely results from C-H activation of transient $MeBC_8H_{14}$, formed by borane oxidative addition and alkylborane reductive elimination or via a direct σ-bond metathesis pathway (Figure 49).[54]
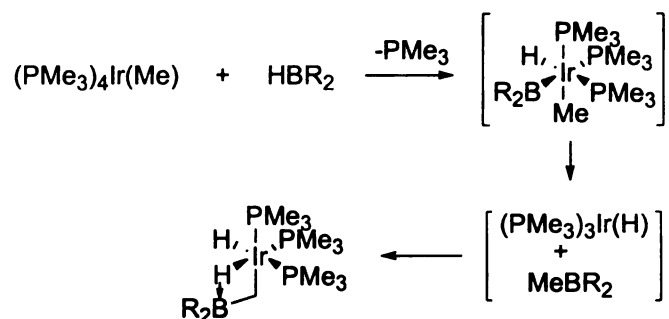
Figure 49. The reaction between (PMe₃)₄Ir(Me) with 9-BBN.

A complex with the formula *fac*-(PMe₃)₃Ir(BPin)(D)(C₆D₅) was proposed as an intermediate in the stoichiometric reaction between (PMe₃)₄Ir(BPin) **(18)** and C₆D₆. Attempts to synthesize this target compound were undertaken. Therefore, a NMR reaction between (PMe₃)₃Ir(Ph)[55] and HBPin in toluene-d₈ was carried out. The reaction occurred immediately at room temperature to yield *mer*-(PMe₃)₃Ir(BPin)(H)(Ph) **(28)** (~95%), *fac*-(PMe₃)₃Ir(D)(H)(tolyl-d₇) (~5%), and less than 5% of PhBPin as byproduct. The trace amount of PhBPin was presumably formed by reductive elimination from the isomers with the BPin and Ph groups *cis* to each other (Figure 50). In a larger scale reaction in pentane, the product was isolated in 95% yield. The crude product can be further purified by recrystallization from pentane at -30 °C to give colorless crystals

suitable for X-ray analysis. From the ORTEP plot of complex **28** (Figure 51), the structure consists of an octahedral arrangement of ligands with the three PMe₃ groups in a *meridional* arrangement, the hydride *trans* to one of the PMe₃ groups, and the phenyl group *trans* to the BPin group. Examination of the ^{1}H NMR spectrum of the complex is consistent with the X-ray data. Thus, the hydride resonance shows as a doublet of triplet at -11.32 ppm ($^2J_{HP}$ = 131 Hz, 20 Hz), indicating it is *trans* to a PMe₃ group and *cis* to two mutually *trans* PMe₃ groups. A singlet corresponding to the resonance of the BPin group is observed at 1.16 ppm, and an overlapped doublet and triplet is observed at 1.41 ppm, which corresponds to the resonance of the three PMe₃ groups. For the phenyl group protons, a multiplet from 7.17 to 7.20 ppm and a broad peak at 7.98 ppm integrate in a 3 to 2 ratio. Surprisingly, a broad peak at 7.98 ppm is observed, which may result from the hindered rotation about the iridium phenyl bond. The single crystal of **28** shows that the iridium atom is at the center of a distorted octahedral geometry with a P(2)-Ir(1)-P(3) angle of 166.29 (8) and C(41)-Ir(1)-B(5) angle of 167.7 (3). Selected bond distances and bond angles are given in Table 19. From the space-filling model of **28**, it is clear that there is steric interactions between the protons of the phenyl group and the protons of the PMe₃ groups (P(2) and P(3)), which may impede rotation. The ^{31}P{^{1}H} NMR spectrum shows a triplet at −57.8 ppm ($^2J_{PP}$ = 22.9 Hz), which is the resonance of the PMe₃ *trans* to hydride and a doublet at -45.6 ppm ($^2J_{PP}$ = 22.0 Hz), which is the resonance of two mutually *trans* PMe₃ groups. This is a rare example of a stable transition metal complex containing boryl and σ-bound phenyl ligands.
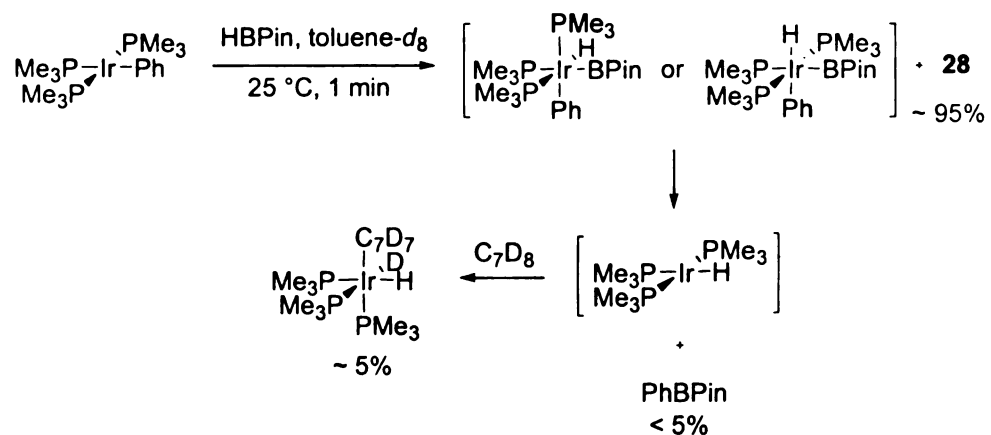
Figure 50. The NMR reaction of (PMe₃)₃Ir(Ph) with HBPin in toluene-d_8 at room temperature.
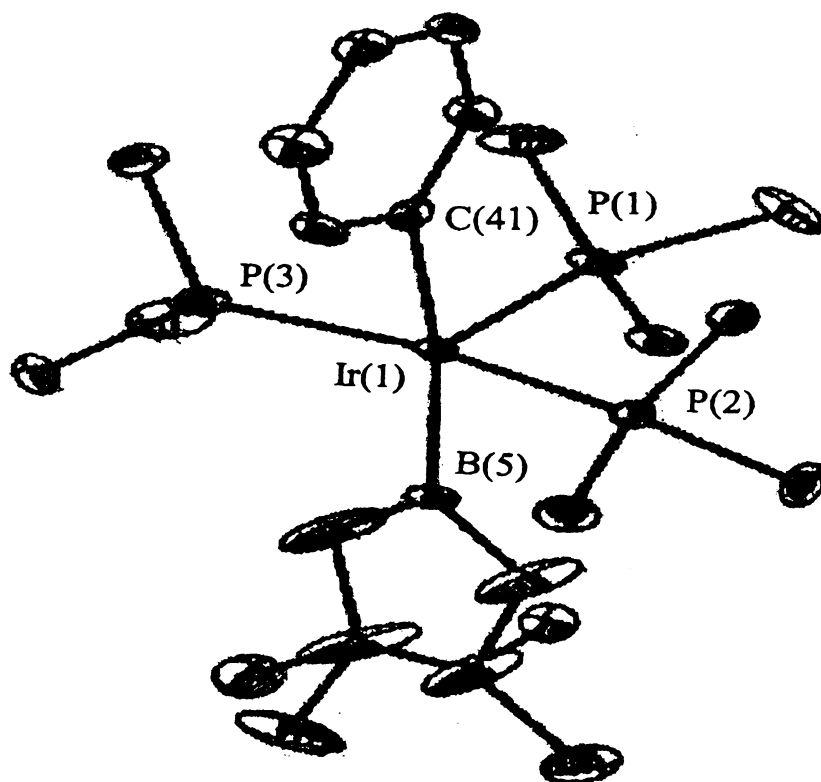
Figure 51. ORTEP of *mer*-(PMe₃)₃Ir(BPin)(H)(Ph) **(28)**. Thermal ellipsoids are shown at 25% probability.

Table 19. Selected Bond lengths [Å] and angles [°] for **28**.

Bond	Distance [Å]	Bonds	Angle [°]
Ir(1)-B(5)	2.097(6)	B(5)-Ir(1)-P(1)	94.6(2)
Ir(1)-P(1)	2.328(2)	B(5)-Ir(1)-P(2)	90.0(2)
Ir(1)-P(2)	2.288(2)	B(5)-Ir(1)-P(3)	90.5(2)
Ir(1)-P(3)	2.288(2)	B(5)-Ir(1)-C(41)	167.7(3)
Ir(1)-C(41)	2.194(5)	P(2)-Ir(1)-P(1)	96.8(7)
		P(2)-Ir(1)-P(3)	166.4(6)
		P(3)-Ir(1)-P(1)	96.75(6)
		C(41)-Ir(1)-P(1)	97.7(2)
		C(41)-Ir(1)-P(2)	88.2(2)
		C(41)-Ir(1)-P(3)	88.4(2)

In their synthetic study of *fac*-(PMe$_3$)$_3$Ir(Me)(H)(SiR$_3$)[55] by Aizenberg and Milstein, they established the order of trans influence: SiEt$_3$ > SiPh$_3$ > H > CH$_3$ based on X-ray structural data. A good trans-influence ligand could weaken the bond between the metal and the *trans* ligand. This is a thermodynamic effect. The study shows that silyl group has stronger trans influence than hydride. Moreover, in the computational study by Sakaki and co-workers,[56] they noted that the trans influence of the boryl group is stronger than the very strong trans influence of silyl group. We deemed it of interest to establish experimentally the stronger trans influence of a boryl group than that of a silyl group. Thus, we decided to explore the reaction between (PMe$_3$)$_4$Ir(BPin) (**18**) and HSiEt$_3$. The reaction proceeded slowly at room temperature over 2.5 days to give *fac*-(PMe$_3$)$_3$Ir(H)(BPin)(SiEt$_3$) (**29**) as the only observed product (Figure 52).

BPin
Me$_3$P, Ir–PMe$_3$ 25 °C, 2.5 days   PMe$_3$
Me$_3$P PMe$_3$ · HSiEt$_3$ ——————→   Me$_3$P—Ir–BPin   ·   PMe$_3$
                                    C$_6$H$_6$ Me$_3$P H
                                                        SiEt$_3$
(18)   fac-(29)
                                                        86% yield
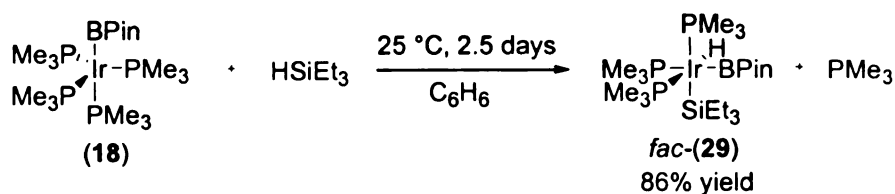
Figure 52. The reaction between (PMe$_3$)$_4$Ir(BPin) **(18)** and HSiEt$_3$.

The product was then recrystallized from a concentrated pentane solution at –30 °C to give 83 mg of colorless crystals in 86% yield. The structure of **29** was established by ^{1}H, ^{11}B, ^{31}P{^{1}H} NMR spectroscopy. In the ^{1}H NMR spectrum, a doublet of triplet is observed in the hydride region at –12.30 ppm (hydride, 1H, $^2J_{HP}$ = 117.0 Hz, 17.0 Hz), indicating that it is *trans* to a PMe$_3$ group and *cis* to two PMe$_3$ groups. A singlet at 1.29 ppm is assigned as the resonance of the BPin group. There are three sets of doublets corresponding to three different PMe$_3$ groups at 1.25 ppm ($^2J_{HP}$ = 6.7 Hz, PMe$_3$ *trans* to BPin), 1.37 ppm ($^2J_{HP}$ = 7.3 Hz, PMe$_3$ *trans* to SiEt$_3$), and 1.46 ppm ($^2J_{HP}$ = 7.6 Hz, PMe$_3$ *trans* to Me). There is no symmetry about the Ir metal center, which renders the molecule chiral. Thus, the CH$_2$ groups of SiEt$_3$ are diastereotopic and should exhibit complex coupling patterns. Indeed, three diastereotopic protons of the CH$_2$ groups of SiEt$_3$ are observed from 0.84 to 0.95 ppm and there are twelve protons in the region of 1.35-1.45 ppm which include the other three diastereotopic protons of the CH$_2$ groups of SiEt$_3$ and nine protons from the CH$_3$ groups of SiEt$_3$. In the ^{31}P{^{1}H} NMR spectrum, there are three different phosphorous resonances. A broad peak is observed at -66.4 ppm corresponding to the PMe$_3$ *trans* to BPin group, a doublet of doublet is observed at –64.2 ppm ($^2J_{pp}$ = 31.3 Hz, 19.8 Hz, PMe$_3$ *trans* to SiEt$_3$), and another doublet of doublet is observed at

−58.1 ppm ($^2J_{pp}$ = 19.8 Hz, 19.8 Hz, PMe$_3$ *trans* to H). The assignment of the PMe$_3$ groups in the ^{1}H NMR spectrum is established by one-dimensional Nuclear Overhauser Effect (NOE) experiments and the assignment of the PMe$_3$ groups in the ^{31}P{^{1}H} NMR spectrum is based on two-dimensional selective decoupling experiments (^{1}H, ^{31}P) to correlate the resonances of PMe$_3$ groups in the ^{1}H NMR spectrum to those in the ^{31}P{^{1}H} NMR spectrum. Complex **29** adopts a *facial* geometry with BPin, SiEt$_3$, and H groups all *trans* to different PMe$_3$ groups. Single crystals of **29** were grown from pentane at −30 °C and the structure was further confirmed by single–crystal X-ray crystallographic analysis. The molecular structure of **29** is shown in Figure 53. Selected bond distances and bond angles are given in Table 20. From the single X-ray structure of **29**, Ir(1)-P(3)$_{trans\ to\ BPin}$ bond length is 2.359(2) Å, Ir(1)-P(4)$_{trans\ to\ SiEt3}$ bond length is 2.334(2) Å, and Ir(1)-P(2)$_{trans\ to\ H}$ bond length is 2.319(2) Å. The Ir-P bond length is directly proportional to the magnitude of the trans influence of the trans ligand; namely, the longer the Ir-P bond, the stronger the trans influence. It obviously shows that the order of trans influence is BPin> SiEt$_3$ > H. To our knowledge, this is the first structural characterization of a transition metal boryl complex containing a silyl group.

90
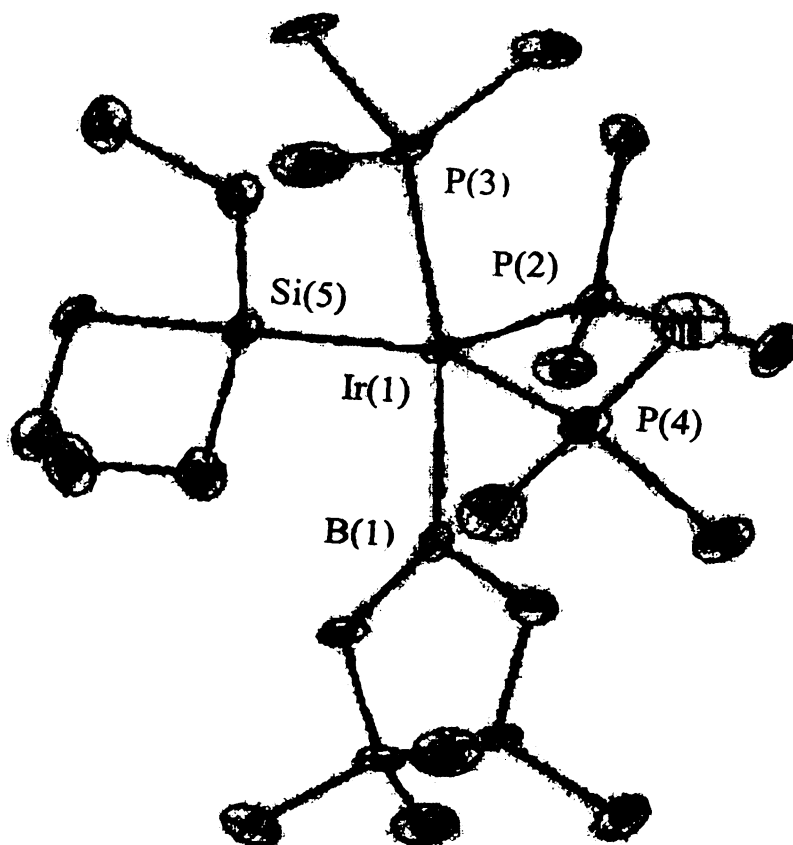
Figure 53. ORTEP of *fac*-(PMe₃)₃Ir(H)(BPin)(SiEt₃) (**29**). Thermal ellipsoids are shown at 25% probability.

Table 20. Selected Bond lengths [Å] and angles [°] for **29**.

Bond	Distance [Å]	Bonds	Angle [°]
Ir(1)-B(1)	2.077(8)	B(1)-Ir(1)-P(2)	92.5(2)
Ir(1)-P(2)	2.319(2)	B(1)-Ir(1)-P(3)	166.5(2)
Ir(1)-P(3)	2.359(2)	B(1)-Ir(1)-P(4)	82.9(2)
Ir(1)-P(4)	2.334(2)	B(1)-Ir(1)-Si(5)	85.1(2)
Ir(1)-Si(5)	2.422(2)	P(2)-Ir(1)-P(3)	100.9(7)
		P(2)-Ir(1)-P(4)	102.6(8)
		P(2)-Ir(1)-Si(5)	94.5(7)
		P(3)-Ir(1)-Si(5)	91.9(7)
		P(4)-Ir(1)-P(3)	95.9(7)
		P(4)-Ir(1)-Si(5)	159.4(7)

Several novel iridium boryl complexes have been synthesized, and a strong trans influence of the boryl ligand has been observed in those complexes by comparing Ir-P bond distances to the Ir-P$_{trans\ to\ BPin}$ bond distance. In those complexes, significantly longer Ir-P$_{trans\ to\ BPin}$ bonds were observed compared to other Ir-P bonds in the complex. Ir-P$_{trans\ to\ BPin}$ bond distances in those complexes are compared and summarized in Table 21 with the angles of PinB-Ir-PMe$_3$(trans).

Table 21. Comparisons of X$_2$B-**Ir-PMe$_3$**$_{trans\ to\ BPin}$ bond distances of iridium boryl complexes.

Complex	Bond	Bond Length (Å)	*Trans* Ligands	Angle (°)
17	PinB-**Ir-PMe$_3$**	2.392(1)	PinB-Ir-PMe$_3$	164.3(1)
18	PinB-**Ir-PMe$_3$**	2.334(2)	PinB-Ir-PMe$_3$	178.0(2)
24	CatB-**Ir-PMe$_3$**	2.399(1)	CatB-Ir-PMe$_3$	172.2(2)
25	PinB-**Ir-PMe$_3$**	2.352(4)	PinB-Ir-PMe$_3$	169.2(5)
	PinB-**Ir-PMe$_3$**	2.353(4)	PinB-Ir-PMe$_3$	169.0(5)
	PinB-**Ir-PMe$_3$**	2.347(4)	PinB-Ir-PMe$_3$	169.6(5)
29	PinB-**Ir-PMe$_3$**	2.359(2)	PinB-Ir-PMe$_3$	166.5(2)

Oxidation Chemistry of Ir^I complex with Boranes

In contrast to the catecholboryl complexes, the corresponding compounds with other substituents (e.g. N, S) on boron are rather rare. In the past, B-H oxidative addition was exploited as a general synthetic method for preparing boryl compounds. A common theme in these reactions is the use of low-valent metal precursors containing readily dissociable ligands. This creates vacant sites in the metal coordination sphere, which allows for the oxidative addition of the boron reagents to the electron-rich metal center. This method was exploited to examine the reaction of several nitrogen-containing boranes including $H[B(NH)_2C_6H_4]$, $H[B(NH)_2C_{10}H_6]$ (HBDAN), and $H[B(NMe)_2C_6H_4]$ with $(PMe_3)_3Ir(COE)(Cl)$ (**30**). The results are summarized in Figure 54. Similar to the reactions of compound **30** with HBPin and HBCat, $H[B(NH)_2C_6H_4]$ reacts with compound **30** to give *mer*-$(PMe_3)_3Ir[B(NH)_2C_6H_4](H)(Cl)$ (**31**) with the boryl group *trans* to Cl and H *trans* to PMe_3 as the only observed product. Since, as discussed earlier, the borane approaches the metal center as an electrophile, H-B addition is preferred by bending Cl-Ir-P axis to form compound **31**. Therefore, compound **31** is the kinetic product of the reaction. Consideration of the trans influence for the various ligands in compound **31** suggests that it is also the thermodynamic product. Changing the borane source to HBDAN gives two isomers *mer*-$(PMe_3)_3Ir(BDAN)(H)(Cl)$ (**32**) and *mer*-$(PMe_3)_3Ir(H)(BDAN)(Cl)$ (**33**) in a 90.4:9.6 ratio. The geometries of these two complexes were determined by ^1H, ^{11}B, and $^{31}P\{^1H\}$ NMR spectroscopy. The formation of the other isomer is presumably due to the bulkiness of the BDAN group, which might have interactions with methyl groups of a PMe_3 ligand. It is expected that replacing the H

atoms on the N atoms of -[B(NH)$_2$C$_6$H$_4$] with methyl groups would increase the steric bulkiness of the boryl group. We, therefore, examined the reaction of (PMe$_3$)$_3$Ir(COE)(Cl) (**30**) with H[B(NMe)$_2$C$_6$H$_4$]. This reaction produced an isomer mixture of *mer*-(PMe$_3$)$_3$Ir[B(NMe)$_2$C$_6$H$_4$](H)(Cl) (**34**) and *mer*-(PMe$_3$)$_3$Ir(H)[B(NMe)$_2$C$_6$H$_4$](Cl) (**35**) in a ratio of 14.4:85.6. The geometries of these two complexes were determined by ^{1}H, ^{11}B, and ^{31}P{^{1}H} NMR spectroscopy. Characterization details of compounds **31, 32, 33, 34,** and **35** are included in the experimental section. The reaction between compound **30** and H[B(NMe)$_2$C$_6$H$_4$] suggests that steric factors can influence the outcome of boryl complex formation.

(PMe$_3$)$_4$Ir(BPin) and *fac*-(PMe$_3$)$_3$Ir(BPin)$_3$ have been prepared in order to examine their viability to be the C-H activating species in the catalytic borylation reactions. Furthermore, Several novel Ir boryl complexes containing alkyl, aryl, or silyl ligands were synthesized and fully characterized.
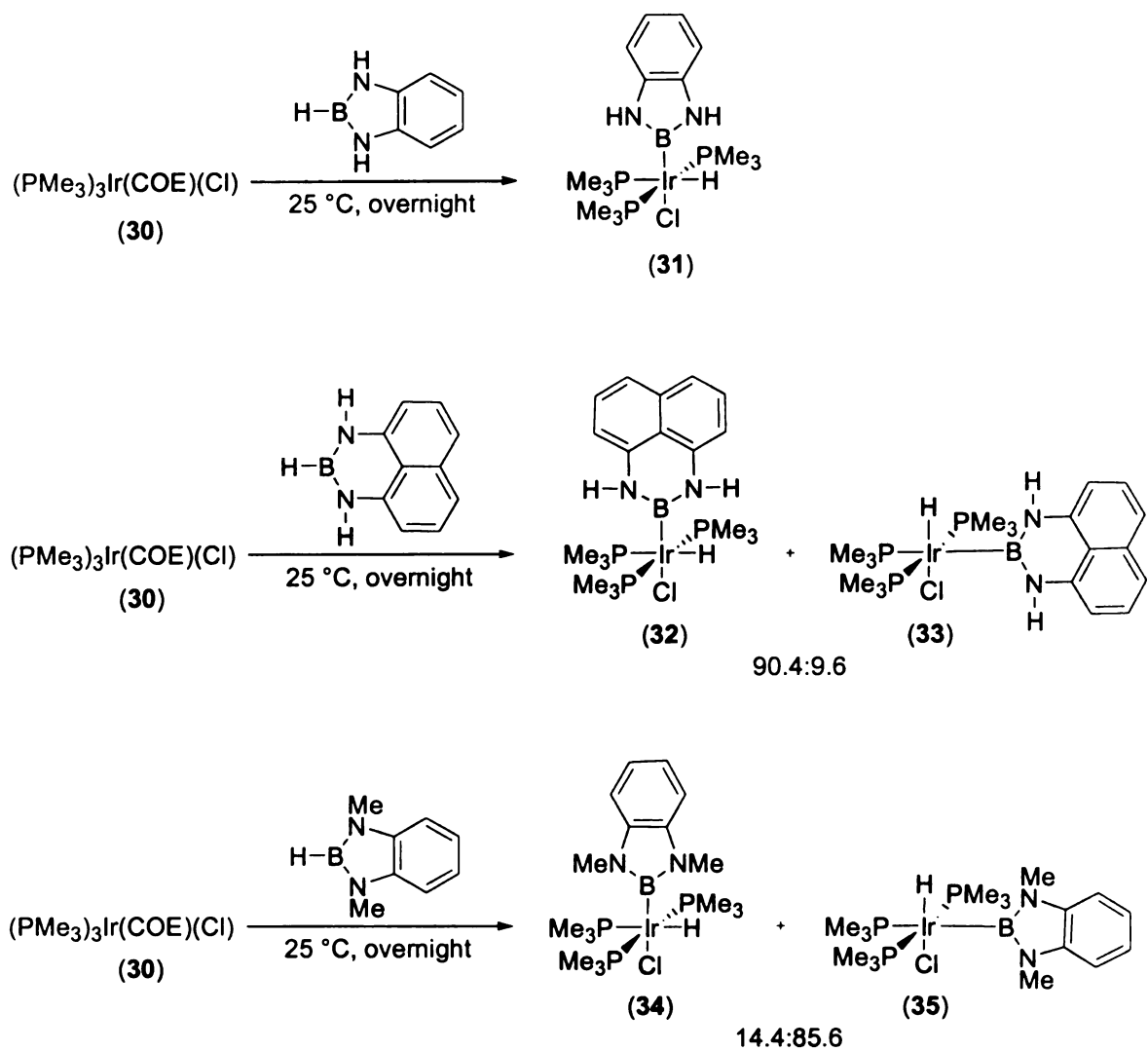
Figure 54. The reactions of $(PMe_3)_3Ir(COE)(Cl)$ **(30)** with nitrogen-containing boranes including $H[B(NH)_2C_6H_4]$, $H[B(NH)_2C_{10}H_6]$ (HBDAN), and $H[B(NMe)_2C_6H_4]$.

CHAPTER 5

PRELIMINARY MECHANISTIC STUDIES OF THE IRIDIUM/PHOSPHINE CATALYST SYSTEM FOR AROMATIC BORYLATION

For many systems, catalysis by organometallic compounds is known to go through several of the following reactions: coordination of ligands to metals, oxidative addition, insertion and reductive elimination. In order to elucidate the mechanism of a homogeneously catalyzed reaction, it is a good idea to study the mechanism of each individual step in a series of relatively elementary chemical reactions by using tools such as kinetics, stereochemical studies, and spectroscopy. Importantly, each step must be shown to be kinetically and thermodynamically reasonable. Preliminary mechanistic studies of the Ir-catalyzed aromatic borylation were carried out and discussed in the previous chapter. Initially, it was deemed of importance to determine the viability of Ir^I and Ir^{III} boryl intermediates as the C-H activating species in the $Ir^{I/III}$ and/or $Ir^{III/V}$ cycles, respectively. Thus, the stoichiometric reactions of compounds **18**nd **25** with benzene were examined.

Stoichiometric Reactions of Ir^I and Ir^{III} Boryl Complexes with Arenes

Thermolysis of (PMe$_3$)$_4$Ir(BPin) **(18)** was carried out in C$_6$D$_6$ at 150 °C, the reaction proceeded smoothly to give the corresponding iridium deuteride complex, (PMe$_3$)$_4$Ir(D), and C$_6$D$_5$BPin (Figure 55).

96

BPin
| \PMe3
Me3P—Ir•PMe3   +   C6D6   —150 °C→   Me3P—Ir•PMe3   ·   C6D5BPin
| |
PMe3   PMe3
(18)

                                              D
                                              | \PMe3
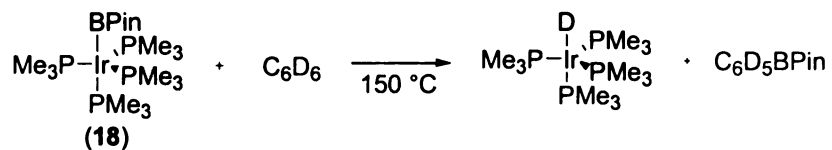
Figure 55. Thermolysis of **18** in C_6D_6 at 150 °C.

From ^{1}H NMR spectra, more than 95% (PMe$_3$)$_4$Ir(D) was generated from stoichiometric reaction between **18** and C_6D_6 as shown in Figures 56 and 57.

Figure 56. Thermolysis of **18** in C_6D_6 at 150 °C: ^{1}H NMR spectrum before thermolysis.

(PMe$_3$)$_4$Ir(**BPin**)

(**PMe$_3$**)$_4$Ir(BPin)

0.7   0.8   0.9   1.0   1.1   1.2   1.3   1.4   1.5   1.6   1.7   1.8
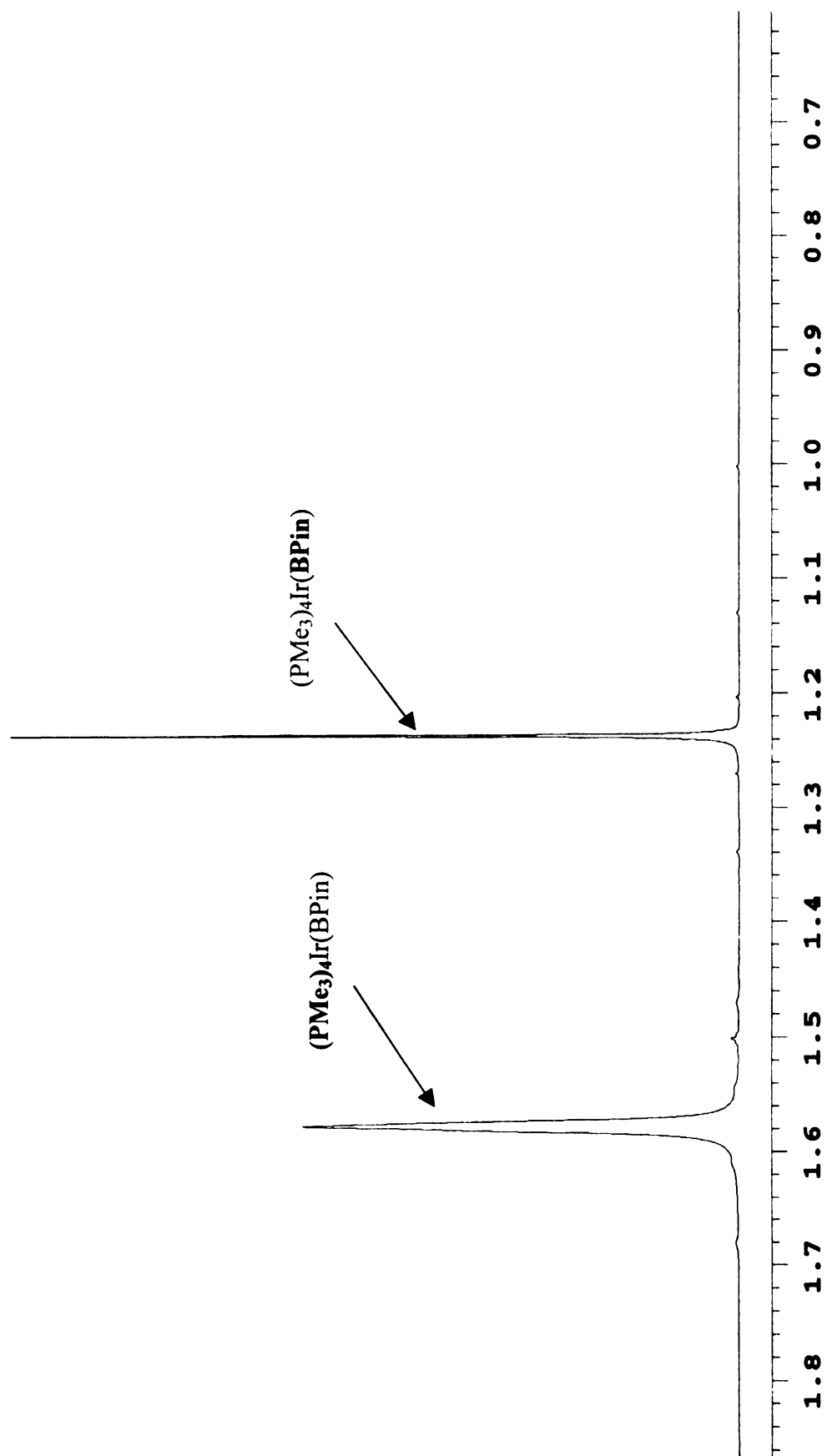
Figure 57. Thermolysis of **18** in C_6D_6 at 150 °C: ^{1}H NMR spectrum after thermolysis. Small peaks around 1.28-1.42 ppm and 1.57-1.60 ppm were not identified.

PhBPin

$(PMe_3)_4Ir(H)$

1.8 1.7 1.6 1.5 1.4 1.3 1.2 1.1 1.0 0.9 0.8 0.7
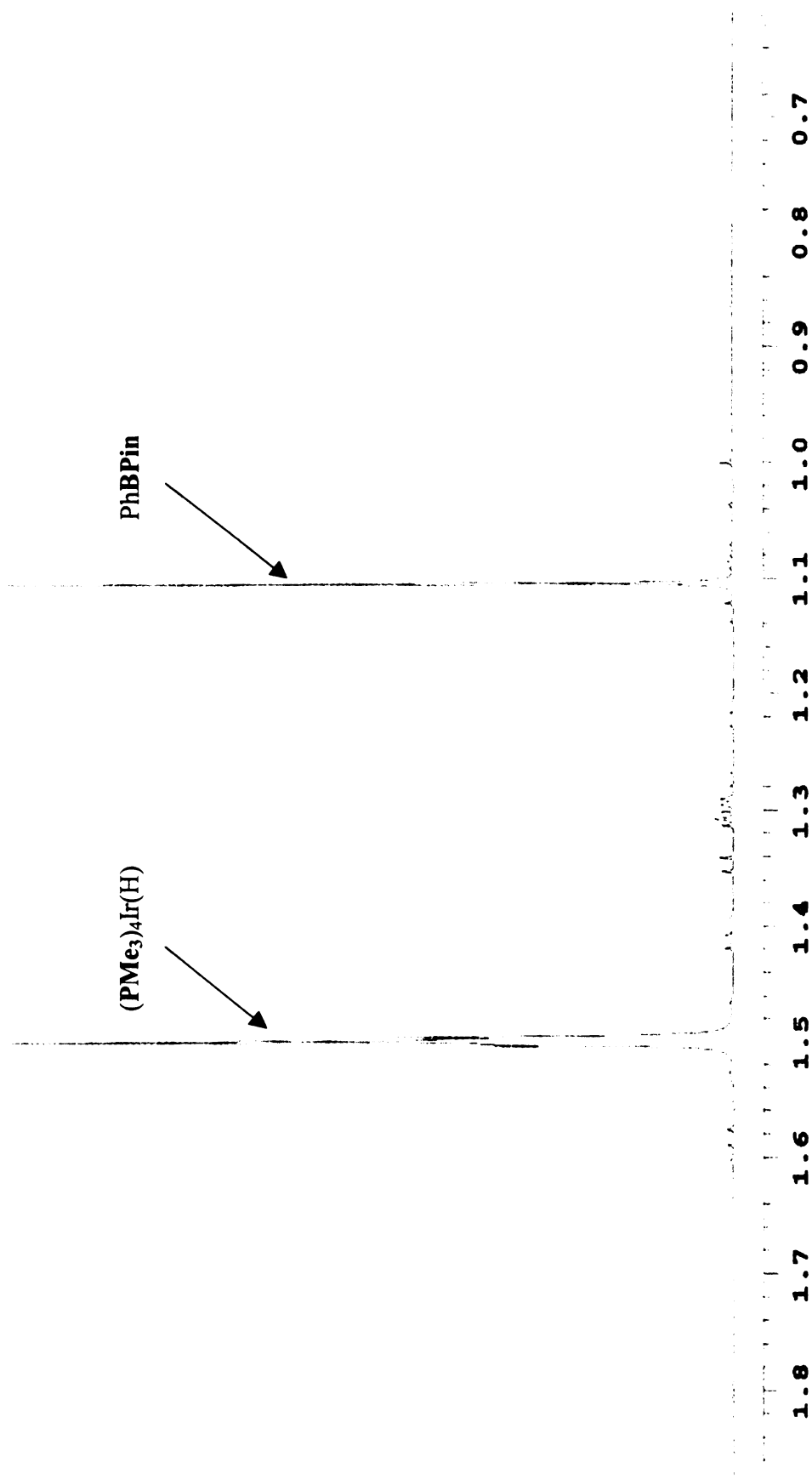
Kinetic studies of the thermolysis of **18** in C_6D_6 were carried out and the reaction

rate of the thermolysis was found to follow first-order kinetics as shown in Figure 58.

$$y = -0.0416x - 0.0978$$
$$R^2 = 0.9962$$
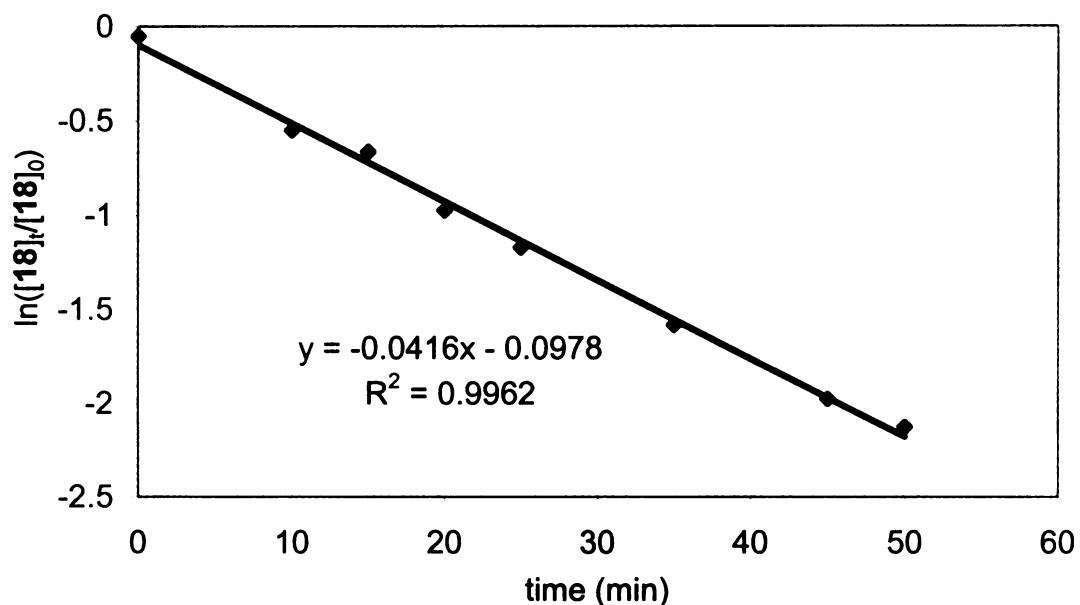
Figure 58. Plot of $\ln([18]_t/[18]_0)$ vs. time (min) for the thermolysis of **18** in C_6D_6 at 130

°C.

There are two potential pathways to account for the stoichiometric transformation

between **18** and C_6D_6 (Figure 59). One of them involves dissociation of PMe_3 to generate

a 16-electron intermediate, $[(PMe_3)_3Ir(BPin)]$, followed by reaction with C_6D_6 to give

products. The other potential pathway involves dissociation of two PMe_3 ligands and

generation of a 14-electron intermediate, $[(PMe_3)_2Ir(BPin)]$, which subsequently reacts

with C_6D_6 to give the final products.

$$18 \underset{k_{-1}}{\overset{k_1}{\rightleftharpoons}} \left[(PMe_3)_3Ir(BPin) + PMe_3 \right] \underset{k_{-2}}{\overset{k_2}{\rightleftharpoons}} \left[(PMe_3)_2Ir(BPin) + PMe_3 \right]$$

16 e⁻   14 e⁻

k_3 | C_6D_6 k_4 | C_6D_6

$(PMe_3)_4Ir(D) + C_6D_5BPin$ $(PMe_3)_4Ir(D) + C_6D_5BPin$
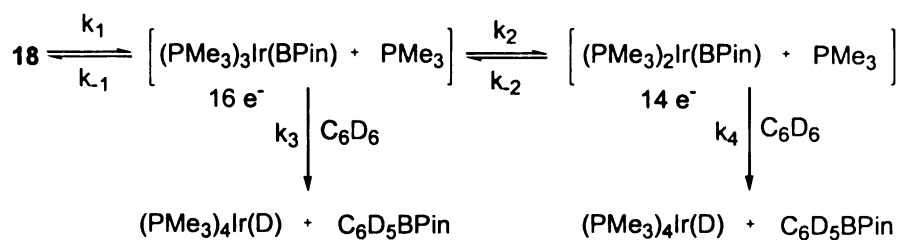
Figure 59. Two potential pathways to account for the stoichiometric reaction between **18** and C_6D_6.

From the steady-state approximation, the rate law of the reaction is derived as below.

$$-\frac{d[18]}{dt} = k_{obs}[18] \tag{6}$$

$$k_{obs} = \frac{k_1 k_{-2} k_3 [C_6D_6][PMe_3] + k_1 k_4 [C_6D_6](k_2 + k_3[C_6D_6])}{k_{-1}k_{-2}[PMe_3]^2 + (k_{-1}k_4 + k_{-2}k_3)[C_6D_6][PMe_3] + k_4[C_6D_6](k_2 + k_3[C_6D_6])} \tag{7}$$

Phosphine inhibition experiments were carried out to determine whether the reaction goes through a 16-electron intermediate or a 14-electron intermediate. Experiments of thermolysis of **18** in C_6D_6 in the presence of various concentrations of [PMe₃] were examined. From $1/k_{obs}$ vs. [PMe₃] plot (Figure 60), $1/k_{obs}$ obviously shows first order dependence on [PMe₃]; therefore, the experimental data are consistent with the mechanism involving a 16-electron intermediate.
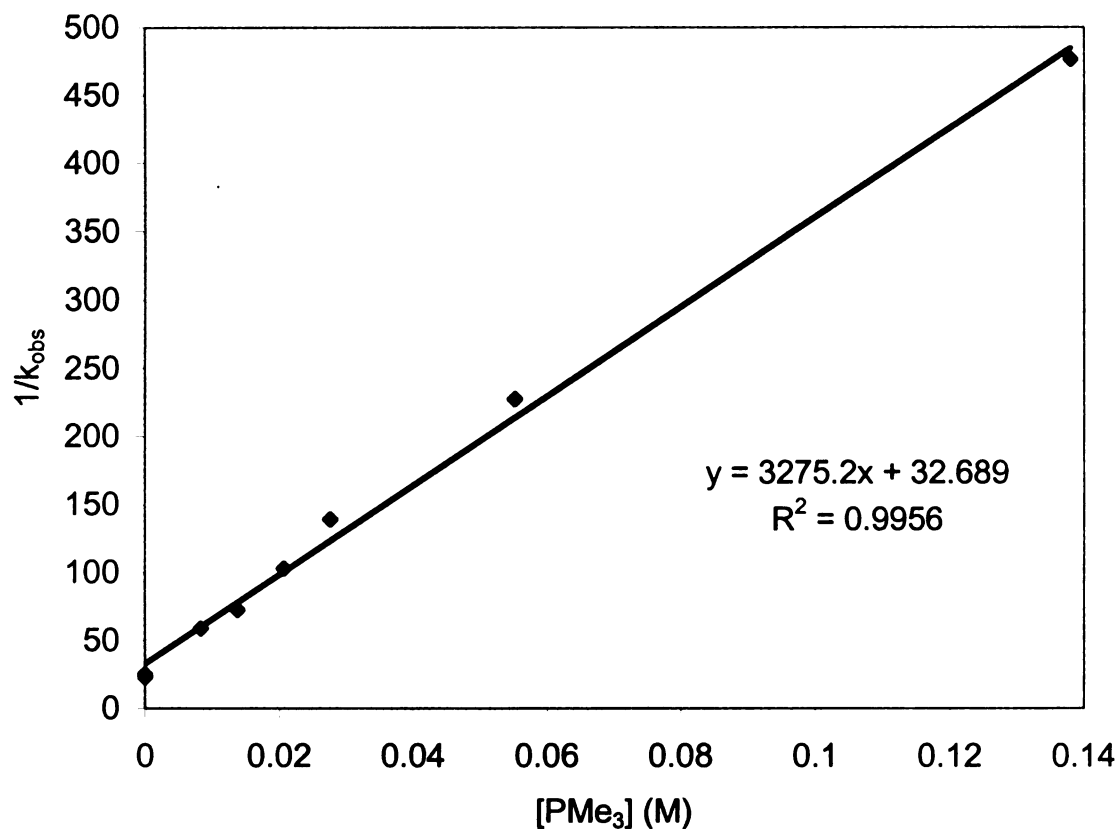
Figure 60. Plot of $1/k_{obs}$ vs. [PMe$_3$] of the thermolysis of **18** in C_6D_6 in the presence of various concentrations of PMe$_3$.

From the results of phosphine inhibition experiments, a mechanism of the stoichiometric transformation is proposed in Figure 61. In the proposed mechanism, the reaction goes through phosphine dissociation to generate a 16-electron intermediate, [(PMe$_3$)$_3$Ir(BPin)], which can activate the C-D bond of C_6D_6 to form [(PMe$_3$)$_3$Ir(BPin)(C$_6$D$_5$)(D)]. This intermediate reductively eliminate C$_6$D$_5$BPin to generate [(PMe$_3$)$_3$Ir(D)], which is followed by re-coordination of PMe$_3$ to form the observed product, (PMe$_3$)$_4$Ir(D).
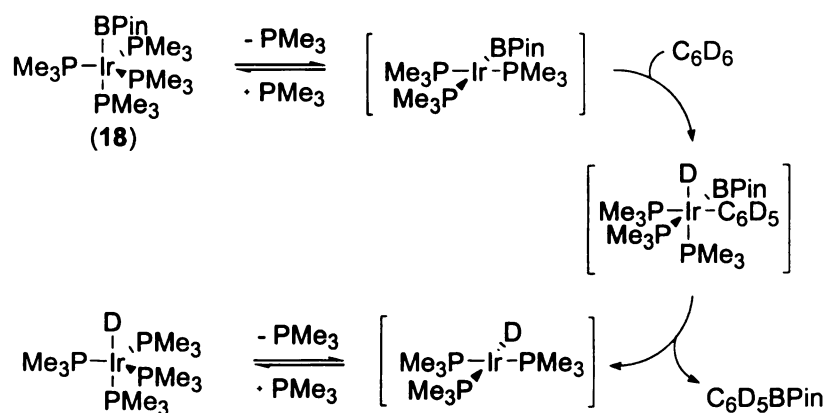
Figure 61. Our proposed mechanism for the thermolysis of **18** in C_6D_6.

Stoichiometric reaction of **25** with arenes was investigated by the thermolysis of **25** in C_6D_6 at 150 °C. The thermolysis of **25** gave *fac*-(PMe$_3$)$_3$Ir(D)$_3$ as the final iridium containing product and generated 3 equivalents of C_6D_5BPin. The thermolysis of **25** proceeded in a stepwise procedure as shown in Figure 62.
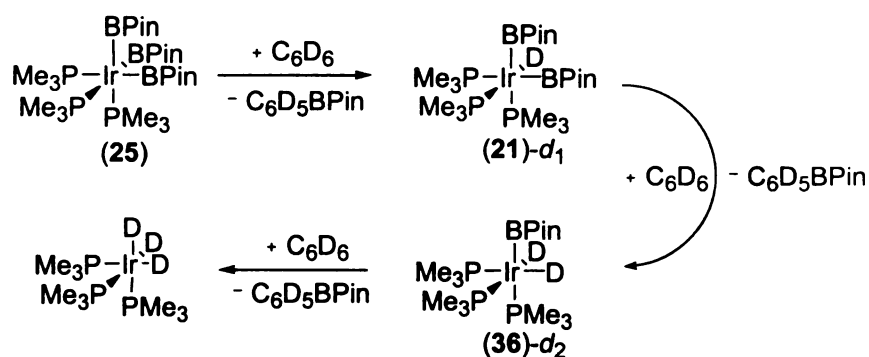
Figure 62. The process of thermolysis of **25** in C_6D_6 at 150 °C.

The process of thermolysis of **25** was monitored by ^1H, ^{11}B, and $^{31}P\{^1H\}$ NMR spectra. Figure 63 displays the course of the reaction (the relative concentration of each species to C_6Me_6 (as an internal standard) versus time (in minutes)) as monitored by ^1H NMR.
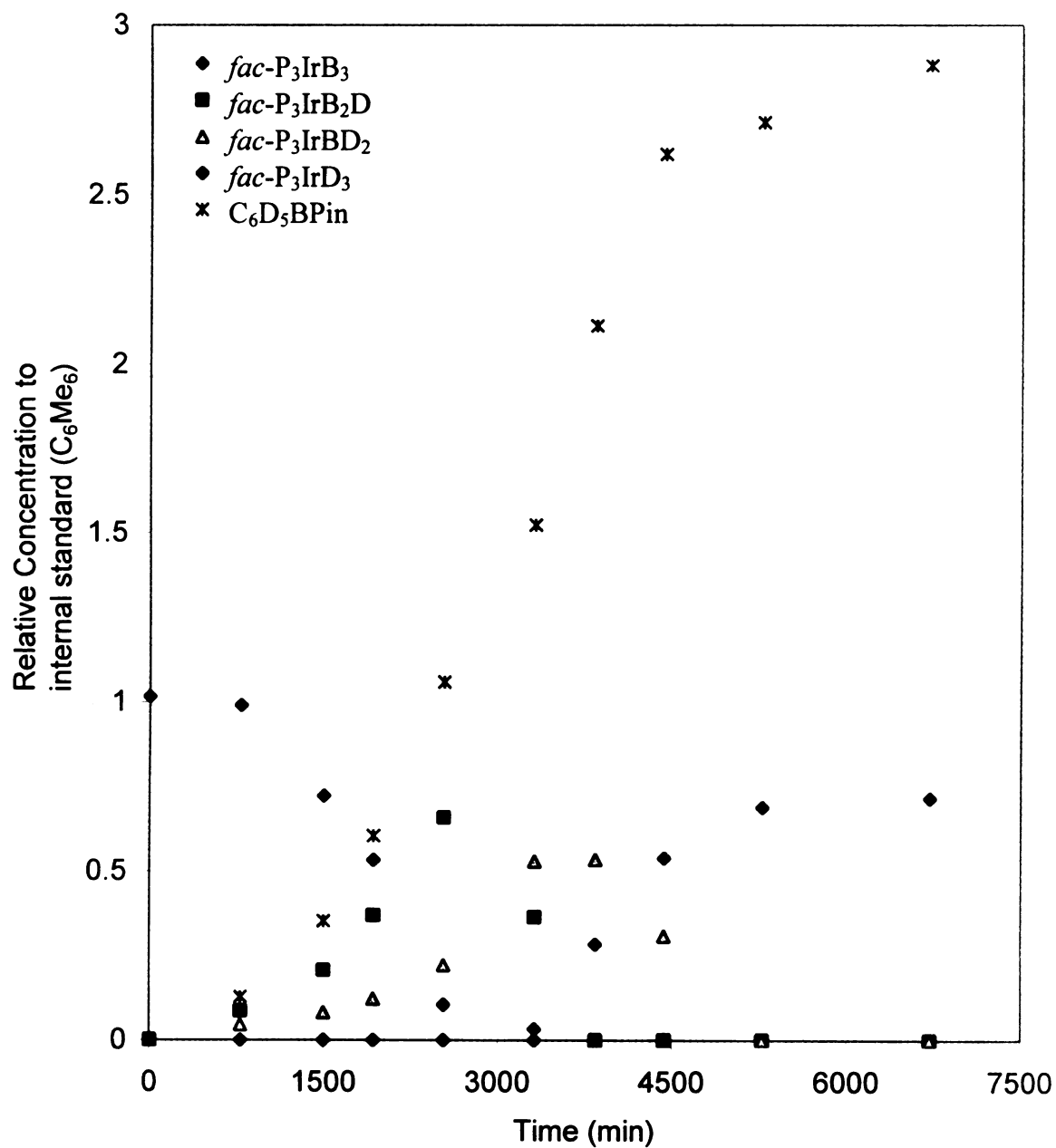
Figure 63. Concentration of each species relative to internal standard (C_6Me_6) vs. time (min) for the thermolysis of **25** in C_6D_6 at 150 °C measured by ^1H NMR.

The results showed that there was an induction period in the beginning of the thermolysis. Complex **25** was gradually converted to fac-(PMe$_3$)$_3$Ir(BPin)$_2$(D) (**21**-d_1) and generated 1 equiv. of C$_6$D$_5$BPin in the first step. Then fac-(PMe$_3$)$_3$Ir(BPin)$_2$(D) (**21**-d_1) was converted to fac-(PMe$_3$)$_3$Ir(BPin)(D)$_2$ (**36**-d_2) and the reaction generated a second equiv. of C$_6$D$_5$BPin. Finally, fac-(PMe$_3$)$_3$Ir(BPin)(D)$_2$ (**36**-d_2) was transformed to fac-(PMe$_3$)$_3$Ir(D)$_3$ as the final iridium containing product and the reaction generated the third equiv. of C$_6$D$_5$BPin.

The kinetic data for the thermolysis of **25** in C$_6$D$_6$ showed that the reaction did not follow first order kinetics (Figure 64). Furthermore, the thermolysis was strongly inhibited by external phosphine ligands. The inhibition phenomena are consistent with the observations in catalytic reactions where the reaction rate decreases dramatically when [P]:[Ir] ratio equals or exceeds 3:1. Detailed discussions will be included in the section followed by next paragraph.
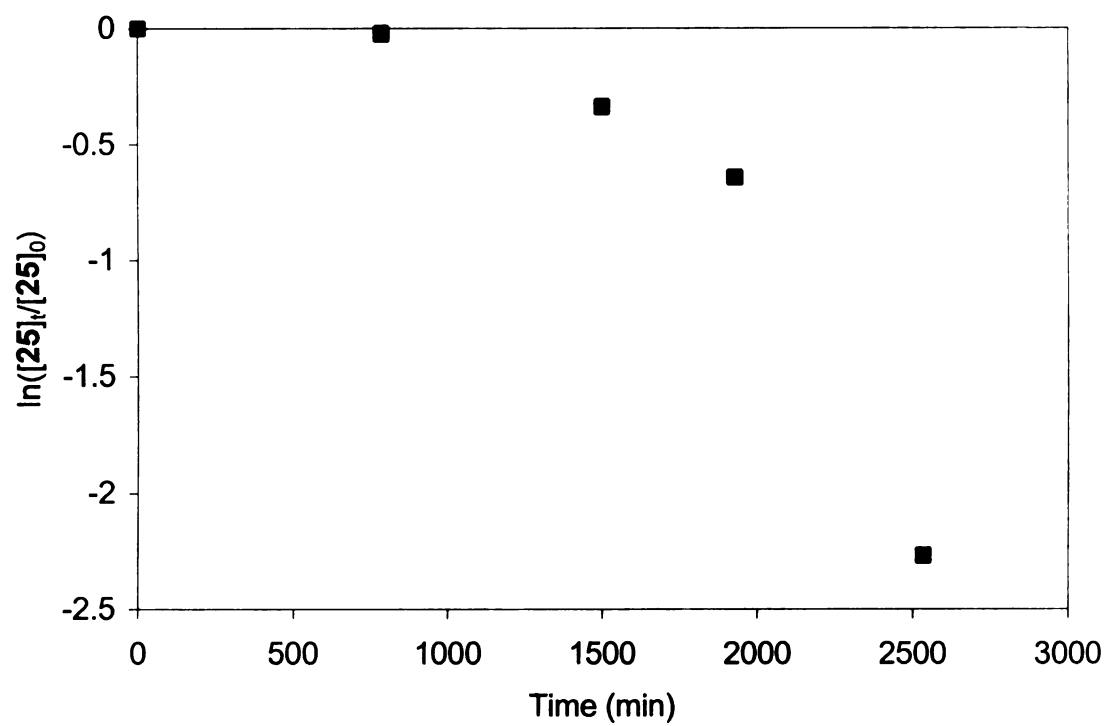
Figure 64. Plot of ln([25]$_t$/[25]$_0$) vs. time (min) for the thermolysis of **25** in C$_6$D$_6$ at 150

°C.

fac-(PMe₃)₃Ir(BPin)(H)₂ **(36)** and *fac*-(PMe₃)₃Ir(BPin)₂(H) **(21)** were prepared independently from the reaction of (PMe₃)₄Ir(H) **(37)** with HBPin and B₂Pin₂, respectively (Figure 65). Compound **37** reacted with HBPin at room temperature and generated a mixture of *mer,cis*-(PMe₃)₃Ir(BPin)(H)₂ **(38)** and *fac*-(PMe₃)₃Ir(BPin)(H)₂ **(36)**. After 6 days at room temperature, compound **36** was the predominant species in the reaction mixture. Similarly, compound **37** reacted with B₂Pin₂ at 60 °C and yielded a mixture of *mer,trans*-(PMe₃)₃Ir(BPin)₂(H) **(20)** and *fac*-(PMe₃)₃Ir(BPin)₂(H) **(21)**. Compound **21** was the predominant species after the temperature was increased to 100 °C for 7 hours. The geometries of **20**, **21**, **36**, and **38** were determined by ^{1}H, ^{11}B, and ^{31}P{^{1}H} NMR spectroscopy and summarized in the experimental section.
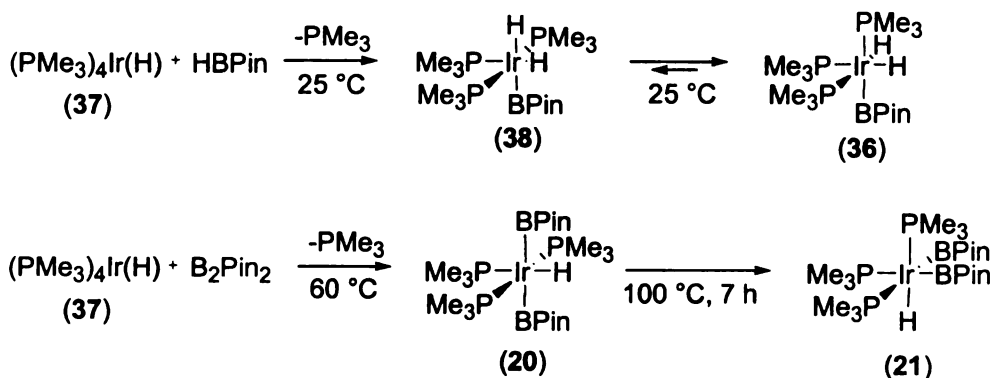
Figure 65. The reaction of (PMe₃)₄Ir(H) **(37)** with HBPin and B₂Pin₂.

Correlation between Phosphine Ligands and Catalytic Activity

Since both Ir^I and Ir^{III} boryl complexes can effect stoichiometric borylation of benzene, they are potentially viable candidates to be the C-H activating species for

catalytic borylation reactions. However, the stoichiometric reactions of $(PMe_3)_4Ir(BPin)$ (18) and $fac\text{-}(PMe_3)_3Ir(BPin)_3$ (25) with benzene exhibit dramatically different reactivities in terms of phosphine dependence. The thermolysis of Ir^{III} complex 25 in C_6D_6 is strongly inhibited by external phosphine ligands, whereas the thermolysis of Ir^{I} complex 25 shows inverse first-order dependence on $[PMe_3]$. For catalysis to occur it is usually required to produce vacant coordination sites in organometallic complexes. Since both compounds are coordinatively saturated 18-electron complexes, it is not surprising that the stoichiometric reaction of 18 or 25 with benzene proceeds slowly at elevated temperature. As previously mentioned it was shown that a phosphine dissociation pathway is responsible for generating active species to activate C-H bonds of benzene in the stoichiometric reaction of 18 with benzene. Furthermore, in the catalytic borylation reactions, the reaction rate was shown to be dependent on the nature of phosphine ligands and the relative concentration between phosphine ligands and iridium metal complex.[57] In particular, borylation rates were appreciable when $[P]:[Ir] < 3:1$ but decreased dramatically when $[P]:[Ir]$ ratio equaled or exceeded $3:1$. The fact that phosphine inhibition is observed in the thermolysis of complex 25, which contains three PMe_3 ligands, in the presence of external phosphine ligands is consistent with the inhibition phenomena seen in catalytic reactions when $[P]:[Ir]$ ratio equals or exceeds $3:1$. The thermolysis of Ir^{I} complex 18, however, shows inverse first order dependence on $[PMe_3]$. The reaction rate decreases when the concentration of PMe_3 increases. Since the thermolysis of 18 is not completely shut down when $[P]:[Ir] >> 3$, the observation is not not consistent with that in catalytic reactions. These experimental observations support a

109

mechanism involving an Ir^{III} boryl intermediate being the C-H activating species in these catalytic borylation reactions.

Substantially improved catalytic activity was observed with the use of bidentate chelating phosphine ligands including 1,2-bis(diphenylphosphino)ethane (dppe) and 1,2-bis(dimethylphosphino)ethane (dmpe). This observation strongly supports the viability of bisphosphine intermediates. A further piece of evidence is that the 18-electron bisphosphine compound, $(PMe_3)_2Ir(H)_5$, is an effective pre-catalyst for aromatic borylation. Those data imply a mechanism involving Ir^{III} and Ir^V intermediates in a $Ir^{III/V}$ catalytic cycle.

Stoichiometric and Catalytic Borylations of Iodobenzene

Previously it was found that iridium catalysts generated from an Ir^I source, (Ind)Ir(COD) (13) and dppe, were ineffective for the aromatic borylation of iodobenzene. However, iodobenzene and HBPin reacted smoothly to yield an isomer mixture of $C_6H_4(I)(BPin)$ when active catalysts were generated from an Ir^{III} source, $(MesH)Ir(BPin)_3$ (14) and dppe. Both the Ir^I boryl complex, $(PMe_3)_4Ir(BPin)$ (18), and the Ir^{III} boryl complex, fac-$(PMe_3)_3Ir(BPin)_3$ (25) can effect stoichiometric reactions with benzene to produce PhBPin and the corresponding hydride complexes. However, the arene products from stoichiometric reactions of 18 and 25 with iodobenzene differ substantially. Specifically, compound 18 reacted rapidly with iodobenzene at room temperature to form an off-white precipitate, but isomers of $C_6H_4(I)(BPin)$ were not detected, even after prolonged thermolysis. Analysis of the ^1H and $^{31}P\{^1H\}$ NMR spectra of the off-white

precipitate from the reaction indicated that the material contained a number of species, which could not be identified (Figure 66). Presumably, the reaction proceeded via oxidative addition of iodobenzene to complex **18** to form [(PMe₃)₃Ir(I)(C₆H₅)(BPin)] followed by several potential reaction pathways to generate a variety of products. For example, [(PMe₃)₃Ir(I)(C₆H₅)(BPin)] could eliminate C-B or I-B bonds.

^{1}H NMR spectrum

2.60   2.40   2.20   2.00   1.80   1.60   1.40   1.20

^{11}B NMR spectrum

70 60 50 40 30 20 10 0 -10 -20 -30 -40 -50 -60 -70

^{31}P{^{1}H} NMR spectrum

-10   -20   -30   -40   -50   -60   -70
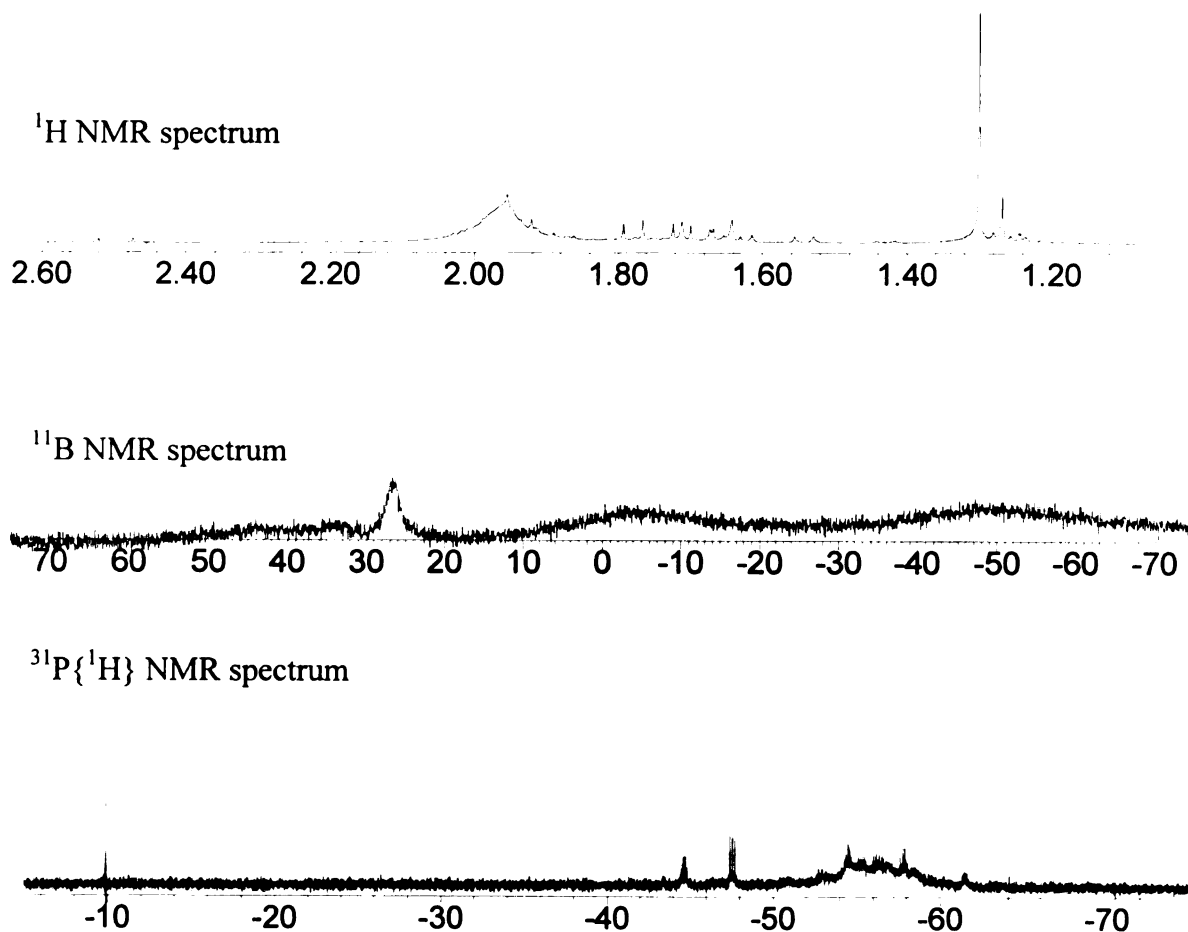
Figure 66. ^{1}H, ^{11}B, and ^{31}P{^{1}H} NMR spectra of the off-white precipitate from the reaction between **18** and C₆H₅I.

Conversely, thermolysis of **25** in iodobenzene at 150 °C produced, in addition to a

45% yield of PhBPin, *m*- and *p*-C₆H₄(I)(BPin) in 54% yield (Figure 67). The significant

quantities of PhBPin formed were presumably generated from a competitive C-I

activation pathway followed by PhBPin reductive elimination.

$$fac\text{-(PMe}_3)_3\text{Ir(BPin)}_3 \quad \xrightarrow[150\ °C]{} $$

(25)

(54% GC yield)   (45% GC yield)
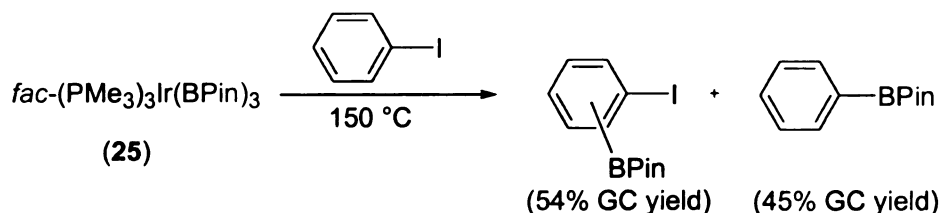
Figure 67. Thermolysis of **25** in iodobenzene.

The previous paragraph demonstrates that borylation products of iodobenzene are

not obtained when Ir^I sources are used under stoichiometric and catalytic conditions,

whereas, Ir^{III} complexes effect both stoichiometric and catalytic borylations. Furthermore,

in situ generation of "Ir^{III} species" from an Ir^I source, compound **13**, and dppe has been

demonstrated to be a viable way to generate effective catalysts for borylation of

iodobenzene. These experimental observations are consistent with a mechanism

involving Ir^{III} and Ir^V intermediates.

Kinetic Isotope Effects in Aromatic Borylation

The isotope effects involved in the activation of arene C-H bonds by the intermediate [Cp*Rh(PMe₃)] have been investigated by Jones and Feher.[58] In their study of reductive elimination of arenes from aryl hydride complexes Cp*Rh(PMe₃)(Aryl)(H), they discovered that a low–energy pathway existed for the interconversion of the carbon attached to the metal. The isomerization was found to occur in a sequential [1,2] fashion, and it can be accommodated by the reversible formation of an π^2-arene complex as shown in Figure 68.
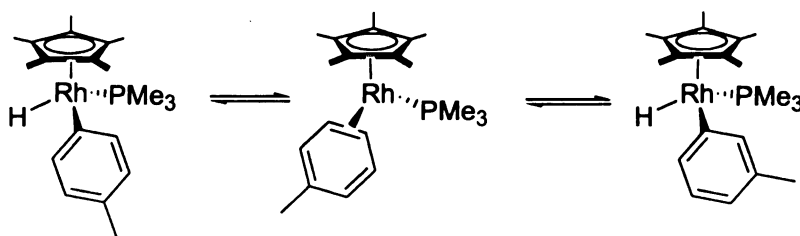
Figure 68. The process of reversible formation of π^2-arene complexes proposed by Jones and Feher.

The photolysis of Cp*Rh(PMe₃)(H)₂ offers a convenient method for the photoinduced generation of the coordinatively unsaturated intermediate [Cp*Rh(PMe₃)] by elimination of dihydrogen. The active species is able to activate C-H or C-D bonds under conditions of kinetic control. Jones et al. conducted a kinetic isotope experiment by irradiating Cp*Rh(PMe₃)(H)₂ in a 1:1 (v:v) mixture of C₆H₆/C₆D₆ at 10 °C, which resulted in the evolution of H₂ and the formation of the benzene C-H/C-D activation products Cp*Rh(PMe₃)(C₆H₅)(H) (**4**) and Cp*Rh(PMe₃)(C₆D₅)(D). Quenching of the reaction with CCl₄ forms the corresponding chloro derivatives Cp*Rh(PMe₃)(C₆H₅)(Cl)

113

and Cp*Rh(PMe₃)(C₆D₅)(Cl). Mass spectral analysis of this mixture revealed a 1.05:1 ratio of the products in which C_6H_6 versus C_6D_6 has been activated (Figure 69). Since benzene is not labile in the products Cp*Rh(PMe₃)(C₆H₅)(H) and Cp*Rh(PMe₃)(C₆D₅)(D) under the condition of the experiment (10 °C), this ratio reflects the kinetic isotope effect for arene complexation and/or C-H bond activation. This small value of $k_H{:}k_D$ was consistent with there being little or no C-H bond breaking in the rate-determining step.

$$k_H{:}k_D = \quad 1.05 \quad : \quad 1.00$$
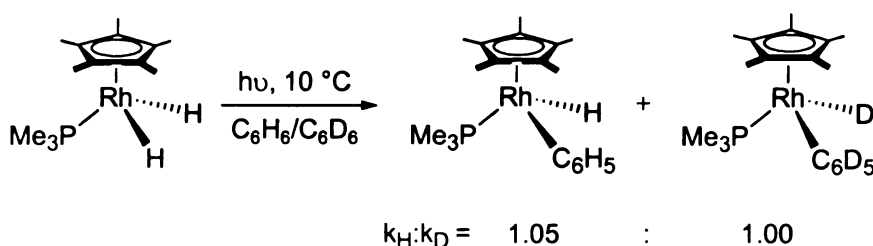
Figure 69. Observed k_H/k_D in the activation of a 1:1 mixture of C_6H_6/C_6D_6 by the intermediate [Cp*Rh(PMe₃)].

In order to access the C-H bond-breaking step, Jones et al. carried out a similar kinetic isotope effect experiment with 1,3,5-$C_6D_3H_3$ and k_H/k_D was determined to be 1.4. Because complexation of [Cp*Rh(PMe₃)] to 1,3,5-$C_6D_3H_3$ can produce one possible π^2-arene complex, the ratio k_H/k_D for this reaction reflects only the isotope effect involved in the cleavage of the C-H. Since both experiments involve bimolecular activation of the benzene C-H/C-D bond ([Cp*Rh(PMe₃)] + benzene), their observation of different kinetic isotope effects for these two experiments prove that a direct insertion of [Cp*Rh(PMe₃)] into the C-H bond of benzene is not occurring. In other words, they have

determined that the activation of arene C-H bonds by [Cp*Rh(PMe₃)] proceeds through an intermediate complex, [Cp*Rh(PMe₃)(η^2-C₆H₆)].

In order to have a deeper understanding of the mechanism of borylation by (Ind)Ir(COD) (**13**)/2 PMe₃ or (MesH)Ir(BPin)₃ (**14**)/2 PMe₃ pre-catalyst system and hopefully identify the rate-determining step in the catalytic borylation reactions, borylation reactions in a molar ratio 1:1 mixture of C_6H_6/C_6D_6 and separately in 1,3,5-$C_6D_3H_3$ were carried out. If a kinetic isotope effect is observed for the borylation reaction in a molar ratio 1:1 mixture of C_6H_6/C_6D_6, it may result from coordination of C_6H_6 vs. C_6D_6 or from the C-H/C-D bond breaking step. On the other hand, the kinetic isotope effect for the borylation reaction of 1,3,5-$C_6D_3H_3$ can only result from the C-H bond activation step since there is only one arene for coordination. The results from experiments of catalytic reactions are summarized in Table 22.

Table 22. Borylation reactions with HBPin in a molar ratio 1:1 mixture of C_6H_6/C_6D_6 or $1,3,5-C_6D_3H_3$ catalyzed by Ir^I and Ir^{III} sources at 150 °C, [Ir] = 2 mol%, [PMe₃]:[Ir] = 2:1.

Entry	Pre-catalysts	Substrate	Product Distribution[59]
1	(MesH)Ir(BPin)₃ **(14)**	Molar ratio 1:1	$C_6D_5BPin:C_6H_5BPin$
	Ir^{III}	C_6H_6/C_6D_6	1.00:2.28 (100% conversion)
2	**14**	$1,3,5,-C_6D_3H_3$	$C_6D_2H_3(BPin):C_6D_3H_2(BPin)$
	Ir^{III}		1.00:1.94 (100% conversion)
3	(Ind)Ir(COD) **(13)**	Molar ratio 1:1	$C_6D_5BPin:C_6H_5BPin$
	Ir^I	C_6H_6/C_6D_6	1.00:2.29 (100% conversion)
4	**13**	$1,3,5,-C_6D_3H_3$	$C_6D_2H_3(BPin):C_6D_3H_2(BPin)$
	Ir^I		1.00:2.06 (100% conversion)

Comparison of the results in Table 22 shows similar k_H/k_D values for the borylations of C_6H_6/C_6D_6 (1:1) and of $1,3,5-C_6D_3H_3$ by Ir^I or Ir^{III}. Furthermore, it appears that the kinetic isotope effect is essentially identical from the Ir^I and Ir^{III} pre-catalyst sources, which suggests a similar or same active species. The large observed kinetic isotope effect in borylations of C_6H_6/C_6D_6 (1:1), which is different from Jones' case, suggests that arene coordination cannot be the rate-determining step. If the arene coordination is the rate-determing step, we expect to see no or, at most, a very small kinetic isotope effect since it does not involve the C-H bond breaking event. However, current data cannot distinguish whether C-H bond breaking or reductive elimination of the arylboronic ester is the rate-determining step (see Figure 73). If reductive elimination

of the arylboronic ester were the rate-determining step, we would expect to see a small secondary isotope effect because the reaction does not involve cleavage of C-H/C-D bonds. The expected small isotope effect differs from relatively large observed k_H/k_D (2.06 and 1.94) for the borylations in $1,3,5\text{-}C_6D_3H_3$ from Ir^I and Ir^{III} sources, respectively. However, it is important to remember that any step prior to the rate-determining step can contribute to the observed kinetic isotope effect. Therefore, the current data cannot definitely determine the actual rate-determining step in the borylation reactions.

Stoichiometric borylations of $(PMe_3)_4Ir(BPin)$ (**18**) and *fac*-$(PMe_3)_3Ir(BPin)_3$ (**25**) in a 1:1 mixture of C_6H_6/C_6D_6 and separately in $1,3,5\text{-}C_6D_3H_3$ were also examined. Thermolysis of **25** in a 1:1 mixture of C_6H_6/C_6D_6 and separately in $1,3,5\text{-}C_6D_3H_3$ at 150 °C gave similar kinetic isotopes effect k_H/k_D as compared to the catalytic borylation reactions, whereas thermolysis of **18** in a 1:1 mixture of C_6H_6/C_6D_6 and separately in $1,3,5\text{-}C_6D_3H_3$ at 150 °C gave relatively larger kinetic isotope effect k_H/k_D than those observed in catalysis as shown in Table 23.

117

Table 23. Stoichiometric borylation reactions of **18** and **25** with a molar ratio 1:1 mixture of C_6H_6/C_6D_6 or $1,3,5-C_6D_3H_3$ at 150 °C.

Entry	Iridium Complex	Substrate	Product Distribution[59]
1	*fac*-(PMe$_3$)$_3$Ir(BPin)$_3$ **(25)** Ir^{III}	Molar ratio 1:1 C_6H_6/C_6D_6	C_6D_5BPin:C_6H_5BPin 1.00:2.53 (100% conversion)
2	**25** Ir^{III}	$1,3,5,-C_6D_3H_3$	$C_6D_2H_3$(BPin) : $C_6D_3H_2$(BPin) 1.00:1.93 (100% conversion)
3	(PMe$_3$)$_4$Ir(BPin) **(18)** Ir^{I}	Molar ratio 1:1 C_6H_6/C_6D_6	C_6D_5BPin:C_6H_5BPin 1.00:2.67 (100% conversion)
4	**18** Ir^{I}	$1,3,5,-C_6D_3H_3$	$C_6D_2H_3$(BPin):$C_6D_3H_2$(BPin) 1.00:2.37 (100% conversion)

Mechanistic Discussions

The existence of an arene coordination step in the catalytic cycle of aromatic borylation by **13**/2 PMe$_3$ or **14**/2 PMe$_3$ pre-catalyst systems cannot be completely ruled out based on the present data. However, Miyaura[26f] and co-workers reported the isolation of a trisboryl complex [Ir((dtbpy)(COE)(BPin)$_3$] as shown in Figure 70, which is chemically and kinetically competent to be an intermediate in the catalytic process in their pre-catalyst system (3 mol% 1/2[IrCl(COE)$_2$]$_2$/dtbpy). Based on a lesson from

118

Halpern's work in elucidating the mechanism of the hydrogenation reaction catalyzed by Wilkinson's catalyst, $(PPh_3)_3Rh(Cl)$, isolation of a stable olefin complex is inconsistent with an η^2-arene complex pathway. Therefore, the arene coordination step prior to C-H bond activation seems unlikely.

$$[Ir(COE)_2Cl]_2 \ + \quad \text{(dtbpy)} \ + \ B_2Pin_2 \ \xrightarrow[\text{mesitylene}]{} \quad \text{(trisboryl complex)}$$
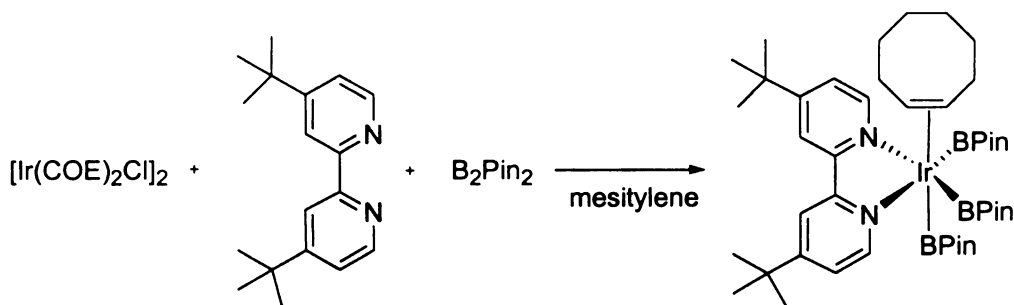
Figure 70. A trisboryl complex $[Ir((dtbpy)(COE)(BPin)_3]$ isolated by Miyaura and co-workers.

There are two potential pathways for the active species to react with an arene. One possibility is that it proceeds through oxidative addition of a C-H bond of an arene to give an Ir^V intermediate followed by reductive elimination of an arylboronate ester to give the corresponding hydride complex. Another option is that the corresponding hydride complex is formed in a one-step "σ-bond metathesis" reaction as shown in Figure 71. σ-bond metathesis has been confirmed only for d^0 complexes of the early transition metal and lanthanides, where oxidative addition is precluded.
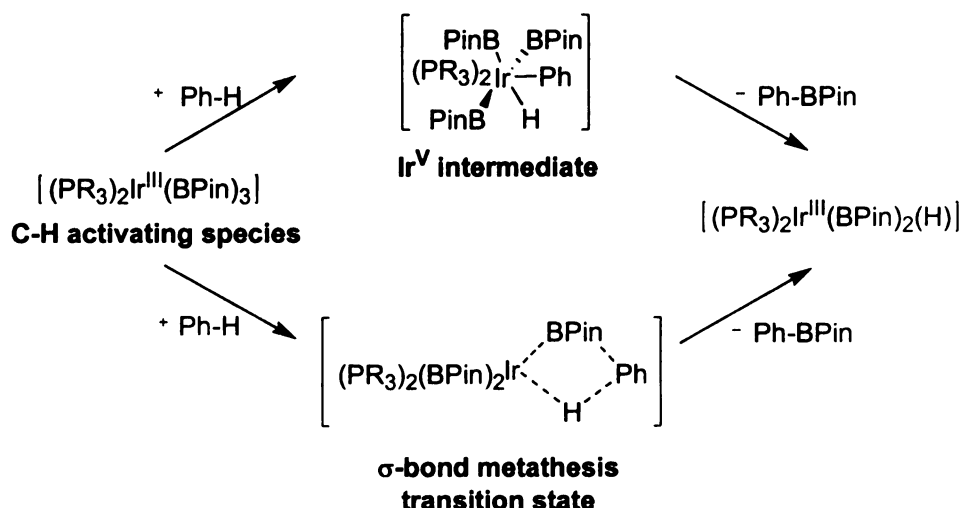
Figure 71. Possible mechanisms for Ir^{III} borylation reaction.

Although we have not yet investigated the mechanism of the borylation extensively, we have obtained qualitative information regarding this question. From the kinetic studies of the stoichiometric reaction of $(PMe_3)_4Ir(BPin)$ **(18)** with benzene, we established that the intermediate $[(PMe_3)_3Ir(BPin)]$ activates the C-H bond of benzene. Furthermore, in the stoichiometric reaction of fac-$(PMe_3)_3Ir(BPin)_3$ **(25)** with benzene, a transient species similar to $[(PMe_3)_2Ir(BPin)_3]$, presumably generated in the reaction mixture, activates the C-H bond of benzene. Therefore, oxidative addition of a C-H bond of an arene to an iridium boryl complex is a viable reaction pathway. In order to evaluate PhBPin reductive elimination, we examined the thermolysis of compound **28** in C_6D_6. Compound **28** has the BPin group *trans* to the phenyl group and it is stable at room temperature. Before reductive elimination of PhBPin occurs, compound **28** is expected to isomerize to another isomer with the BPin group and the phenyl group in a *cis* geometry. Thermolysis of compound **28** in C_6D_6 at 50 °C was carried out and the reaction was

monitored by ^{1}H, ^{11}B, and ^{31}P{^{1}H} NMR spectroscopy. At 50 °C, compound **28** was

converted to a mixture of *fac*-(PMe₃)₃Ir(C₆D₅)(D)(H) **(39)**, *fac*-(PMe₃)₃Ir(BPin)(H)₂ **(36)**,

and (PMe₃)₄Ir(H) **(37)**, and PhBPin was produced. After 55 hours, compound **28, 39, 36**,

and **37** were in the ratio of 16:73:11:<1 (Figure 72).

BPin
 | ,H
Me₃P—Ir—H
Me₃P |
      PMe₃

(36)

↑ HBPin

BPin   ⎡   ⎤
 | ,PMe₃   C₆D₆, - PhBPin | ,PMe₃ |
Me₃P—Ir—H   ————————————→   Me₃P—Ir—H
Me₃P | 50 °C, 55 h | Me₃P |
      Ph   ⎣   ⎦

(28)

│ C₆D₆
↓

C₆D₅
 | ,D
Me₃P—Ir—H
Me₃P |
      PMe₃

(39)

(28):(39):(36):(37) = 16:73:11:<1
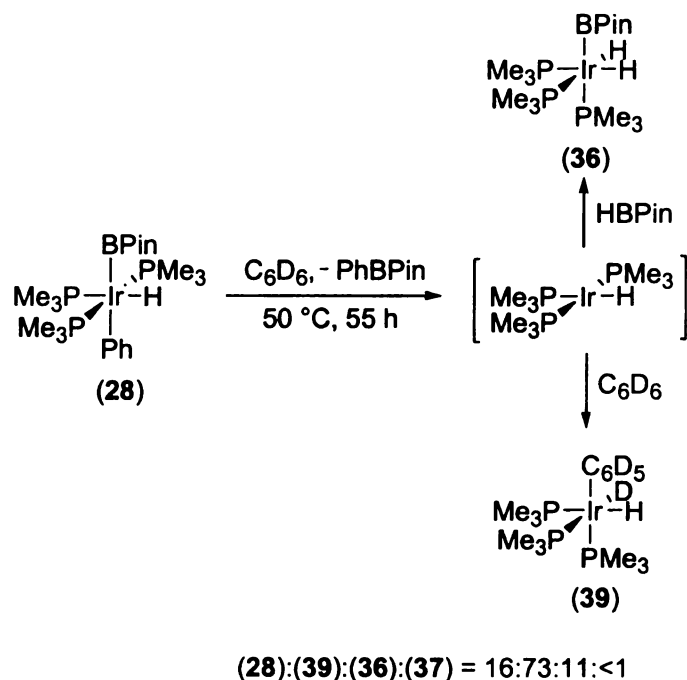
Figure 72. Thermolysis of compound **28** in C₆D₆ at 50 °C.

Presumably reductive elimination of PhBPin from compound **28** generates an

intermediate, [(PMe₃)₃Ir(H)], which can subsequently activate a C-D bond of C₆D₆ to

form compound **39**. Compound **36** most likely comes from the oxidative addition of

HBPin to the intermediate [(PMe₃)₃Ir(H)]. HBPin could come from a minor pathway

involving H-B reductive elimination from compound **28**. The generation of PhBPin from

the thermolysis of compound **28** in C_6D_6 shows that PhBPin reductive elimination is a viable pathway as well. In addition to some other observations discussed previously: (1) Borylation products of iodobenzene are not obtained when Ir^I sources are used under stoichiometric and catalytic conditions, whereas Ir^{III} complexes effect both stoichiometirc and catalytic borylations. (2) Improved catalytic activity is observed with chelating phosphines and inhibition is observed when [P]:[Ir] ratios equal or exceed 3:1, strongly supporting the viability of bisphosphine intermediates. (3) The 18-electron bisphosphine compound, $(PMe_3)_2Ir(H)_5$, is an effective pre-catalyst for borylation. Therefore, we presently favor the simple scheme which involves a direct oxidative addition of a C-H bond of an arene to the proposed active species, $[(PR_3)_2Ir^{III}(BPin)_3]$ to form an Ir^V intermediate, $[(PR_3)_2Ir^{III}(BPin)_3(H)(Ph)]$. Reductive elimination of PhBPin from the Ir^V intermediate, $[(PR_3)_2Ir^{III}(BPin)_3(H)(Ph)]$, gives $[(PR_3)_2Ir^{III}(BPin)_2(H)]$, which converts to $[(PR_3)_2Ir^V(BPin)_3(H)_2]$ in the presence of HBPin. After releasing H_2, the reaction regenerates $[(PR_3)_2Ir^{III}(BPin)_3]$, the proposed C-H activating species, to complete the catalytic cycle as shown in Figure 73.
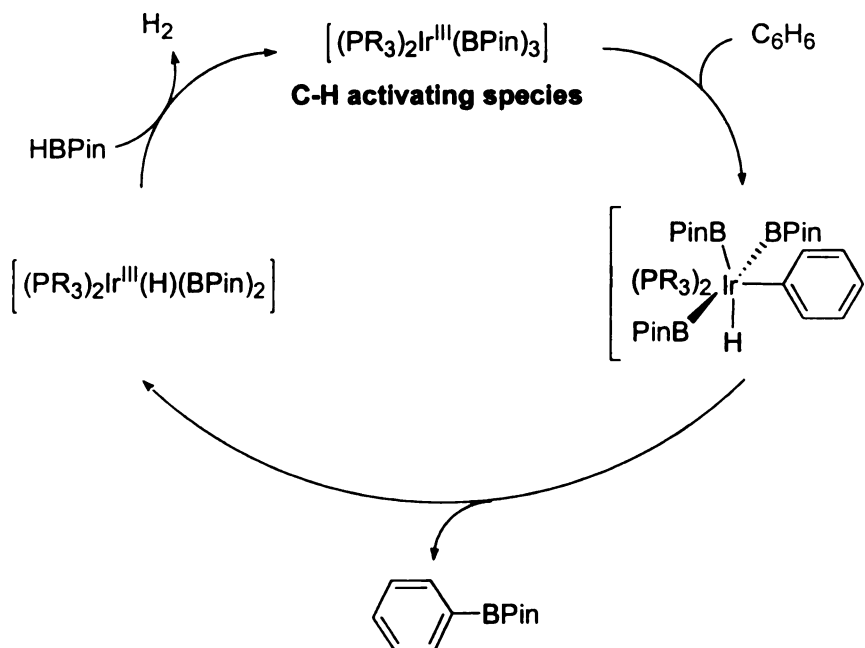
Figure 73. A putative mechanism for aromatic borylations catalyzed by iridium boryl complexes.

An interesting reactivity was observed in the thermolysis of *fac*-(PMe₃)₃Ir(BPin)₃ (25) in C₆D₆ in the presence of 10% of (MesH)Ir(BPin)₃ (14). The reaction proceeded at 100 °C instead of occurring at 150 °C to generate a mixture of *fac*-(PMe₃)₃Ir(BPin)₂(H/D) and *fac*-(PMe₃)₃Ir(BPin)(H)(D) in approximately 62:38 ratio and C₆D₅BPin after 33.5 hours. The hydride presumably comes from a PMe₃ ligand. As has been discussed earlier, the mesitylene ligand of compound 14 is very labile presumably due to the very strong trans influence of the BPin group, therefore, it is most likely that 14 acts as a phosphine trap, which facilitates the PMe₃ dissociation from compound 25 in the thermolysis

reaction of **25** in C_6D_6. The actual role of complex **14** in the reaction and the difference in terms of reactivity require further elucidation.

Miyaura, Ishiyama, and co-workers[60] recently developed a new catalyst system (1.5 mol% $[Ir(OMe)(COD)]_2$/ 3 mol% dtbpy) for borylation of arenes at room temperature with a stoichiometric amount of boron reagent (B_2Pin_2) and arene to produce the corresponding arylboronates in high yield. This new system has extended the functional group tolerance to a CN group. The high catalyst efficiency of $[Ir(OMe)(COD)]_2$ can be attributed to the more facile formation of iridium boryl complexes. Iridium triboryl complexes have been implied as possible intermediates in the borylation of arenes. Presumably, the transmetallation reaction between B_2Pin_2 and $[Ir(OMe)(COD)]_2$ results in the formation of an Ir^I boryl complex after releasing MeOBPin. The Ir^I boryl complex then undergoes oxidative addition of B_2Pin_2 to yield an Ir^{III} triboryl complex as shown in Figure 74.
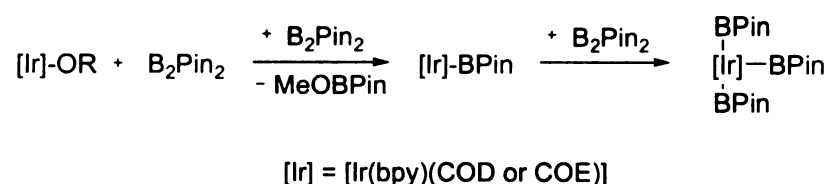
Figure 74. Iridium tris(boryl) intermediate in borylation reactions.

The results from preliminary mechanistic studies on the new iridium catalyst system indicate that a mechanism involving Ir^{III} and Ir^V intermediates in an $Ir^{III/V}$ catalytic cycle is most likely. Correlations between the stoichiometric and catalytic reactions provided a deeper insight into the mechanism of aromatic borylation.

Our studies allow arylboron species to be prepared in an economical fashion and also demonstrate that C-H bond activation and functionalization can be developed into a practical synthetic tool. Future work is needed to further elucidate the mechanism for aromatic borylations catalyzed by iridium boryl complexes in order to have a deeper understanding for this important transformation. With the rapid advances in this area, we expect that Ir-catalyzed borylations of aromatics will certainly find acceptance in the synthetic arsenal of organic chemists.

CHAPTER 6

EXPERIMENTAL

General Considerations

All manipulations were performed using glove box, Schlenk, or vacuum-line techniques. Pentane, diethyl ether, and tetrahydrofuran were pre-dried over $CaCl_2$ and distilled from Sodium/benzophenone ketyl. Toluene and benzene were pre-dried over $CaCl_2$ and distilled from Sodium metal. Methylene chloride was pre-dried over $CaCl_2$ and distilled from CaH_2. Cyclohexane was purified and dried according to the method reported by Perrin and Armarego.[61] Hexamethyldisiloxane, decane, and dodecane were distilled from sodium metal.

$CDCl_3$, tetrahydrofuran-d_8, p-xylene-d_{10}, cyclohexane-d_{12}, and $1,3,5$-$C_6D_3H_3$ were dried with and vacuum transferred from 3Å sieves. Benzene-d_6 and toluene-d_8 were dried with, vacuum transferred from 3Å sieves, and stored over a sodium mirror. CD_2Cl_2 was dried with 4Å sieves.

HBPin was purchased from Aldrich, further purified by stirring with PPh_3 to remove BH_3, and then vacuum distilled to give the borane as a clear viscous liquid. B_2Pin_2 was purchased from Frontier Scientific and used as received. PMe_3 and PMe_3-d_9 were purchased from Aldrich and vacuum transferred to an air-free flask respectively before use. PEt_3, P^iPr_3, P^tBu_3, PCy_3, PPh_3, 1,2-Bis(diphenylphosphino)ethane (dppe), 1,2-Bis(diphenylphosphino)propane (dppp), Bis(dimethylphosphino)methane (dmpm), 1,2-Bis(dimethylphosphino)ethane (dmpe), 1,2-Bis(dicyclohexylphosphino)ethane (dCype), 1,2-Bis(diphenylphosphino)benzene (dppb), 2,2'-dipyridyl (bpy), 4,4'-di-*tert*-butyl-2,2'-

126

dipyridyl (dtbpy), 2-(diphenylphosphino)-2'-(N,N-dimethylamino)biphenyl, 2-(dicyclohexylphosphino)-2'-(N,N-dimethylamino)biphenyl, 1,10-phenanthroline, and 2,2'-bithiophene were used as received from commercial sources. 1,2-dimethoxyethane, N,N,N,N-tetramethylethylenediamine (TMEDA), thiophene and triethylsilane were distilled prior to use.

Substrate: anisole, N,N-dimethylaniline, 2,6-lutidine, benzotrifluoride, N,N-diethylbenzamide, ethylbenzoate, 1,3,5-$C_6H_3F_3$, and 4-fluorobromobenzene were distilled and further dried by passing through a column of activated alumina prior to use. C_6HF_5 and 1,3-bis(trifluoromethyl)benzene were distilled and then dried over 4Å sieves, followed by vacuum transfer to an air-free flask. *m*-xylene, *p*-xylene, *o*-xylene, fluorobenzene, chlorobenzene, bromobenzene, 1,2-dichlorobenzene, 1,3-dichlorobenzene, 1,3-dibromobenzene, 4-chlorobenzotrifluoride, 4-fluoroanisole, 4-chloroanisole, 4-chlorotoluene, 2-chloroanisole, 2-chlorotoluene, and 2-methylanisole were distilled from Sodium metal. Veratrole and 1,4-bistrifluoromethylbenzene were distilled from CaH_2. 1,4-dichlorobenzene was sublimed prior to use.

Starting materials: [Ir(COD)Cl]$_2$,[62] [Ir(COE)$_2$Cl]$_2$,[62] (Ind)Ir(COD),[63] (PMe$_3$)$_4$Ir(Cl),[64] (PMe$_3$)$_4$Ir(H),[44] (PMe$_3$)$_4$Ir(Me),[52] (PMe$_3$)$_3$Ir(Ph),[55] Cp*Rh(η^4-C$_6$Me$_6$),[65] Cp*Ir(η^4-C$_6$Me$_6$),[66] Cp*Ir(PMe$_3$)(H)$_2$,[67] Cp*Ir(P(CD$_3$)$_3$)(H)$_2$,[67] (C$_5$Me$_4$Et)Ir(PMe$_3$)(H)$_2$,[67] (PMe$_3$)$_2$Ir(H)$_5$,[68] Cp*IrH$_4$,[69] and Cp*Ir(PMe$_3$)(H)(BPin)[21] were prepared according to literature methods.

^{1}H and ^{13}C{^{1}H} NMR spectra were recorded on Varian Inova–300, VXR–500, or Inova–600 spectrometers and referenced to residual proton solvent signals. ^{11}B, ^{19}F, and ^{31}P{^{1}H} spectra were recorded on Varian VXR–300 or Varian Inova–300 spectrometers,

operating at 96.29, 282.35, and 121.49 MHz respectively and referenced to external standards. Boron chemical shifts were referenced to a neat $BF_3 \cdot Et_2O$ external standard. Fluorine chemical shifts were referenced to a neat $CFCl_3$ external standard. Phosphorous chemical shifts were referenced to an 85% phosphoric acid external standard. Elemental analyses were performed at Michigan State University using a Perkin Elmer Series II CHNS/O Analyzer 2400. GC-MS data were obtained using a HP G1800A GCD system.

Syntheses

(MesH)Ir(BPin)₃ (14). Complex **13** (2.54 g, 6.11 mmol) and HBPin (3.91 g, 30.55 mmol) were dissolved in 32 mL mesitylene. The light brown solution was then heated at 75 °C for 48 h. The reaction mixture turned to dark brown after 24 h at 75 °C. Mesitylene was removed under high vacuum to give viscous dark brown oil. The crude mixture was then triturated with hexamethyldisiloxane (3 x 2 mL). A white solid (797 mg, 19%) was obtained after filtration and washed with cold hexamethyldisiloxane. mp 140 °C (dec). ^1H NMR (600 MHz, C_6D_6) δ 1.33 (s, 36H, 3 $BO_2C_6H_{12}$), 2.24 (s, 9H, 3 CH_3), 5.62 (s, 3H, 3 CH). ^{11}B NMR (C_6D_6) δ 32.5. $^{13}C\{^1H\}$ NMR (300 MHz, C_6D_6) δ 19.7 (s), 25.7 (s), 81.0 (s), 97.0 (s), 118.05 (s). Anal. Calcd for $C_{27}H_{48}IrB_2O_6$: C, 46.77; H, 6.98. Found: C, 47.13; H, 7.18.

***mer*-(PMe₃)₃Ir(BPin)(H)(Cl) (15).** A solution of PMe₃ (102 mg, 1.34 mmol) in 2 mL THF was added dropwise to a solution of $[Ir(COE)_2Cl]_2$ (200 mg, 0.22 mmol) in 4 mL THF solution. The reaction mixture was stirred at room temperature for 2 h. The solvent was then removed under reduced pressure. The residue was redissolved in 6mL

128

THF and a solution of HBPin (65 μL, 0.45 mmol) in 2 mL THF was added dropwise. The

reaction mixture was stirred at room temperature overnight. Next day, the solution was

filtered through celite to remove trace suspension. The filtrate was pumped down to give

a spectroscopically pure white solid (243.0 mg, 93%). The product can be recrystallized

from concentrated THF solution at −30 °C to give colorless crystals. mp 170-172 °C

(dec). ^{1}H NMR (C_6D_6) δ -9.66 (dt, J = 136.4 Hz, 21.8 Hz, 1H, hydride), δ 1.04 (s, 12H,

$BO_2C_6H_{12}$), 1.37 (d, J = 7.9 Hz, 9H, PMe_3 *trans* to hydride), 1.62 (t, J = 3.7 Hz, 18H, 2

PMe_3 *trans* to each other). $^{13}C\{^1H\}$ NMR (C_6D_6) δ 18.4 (d, J = 26.7 Hz), 20.7 (dt, J = 3.5

Hz, 19.1 Hz), 25.8 (s), 80.8 (s). ^{11}B NMR (C_6D_6) δ 28.5. $^{31}P\{^1H\}$ NMR (C_6D_6) δ −46.1

(t, J = 20.6 Hz, 1P, PMe_3 *trans* to hydride), −40.4 (d, J = 21.4 Hz, 2P, 2 PMe_3 *trans* to

each other). Anal. Calcd for $C_{15}H_{40}IrBClO_2P_3$: C, 30.86; H, 6.91. Found: C, 30.91; H,

7.06.

mer,cis-(PMe₃)₃Ir(BPin)₂(Cl) (17). A solution of B_2Pin_2 (191 mg, 0.75 mmol) in

5 mL THF was added to a suspension of $(PMe_3)_4Ir(Cl)$ (400 mg, 0.75 mmol) in 30 mL

THF in a schlenk tube. The reaction mixture was heated at 70 °C for 1 day. The orange

suspension gradually changed to a gray color suspension. The reaction mixture was

cooled down and filtered through celite to remove gray precipitates. The filtrate was then

pumped down to give a colorless crystalline solid. The crude product was recrystallized

from pentane at −30 °C. The product was collected as colorless crystals (390 mg, 73%).

mp 156-158 °C (dec). ^{1}H NMR (C_6D_6) δ 1.10 (s, 12H, $BO_2C_6H_{12}$), 1.22 (s, 12H,

$BO_2C_6H_{12}$), 1.31 (d, J = 6.9 Hz, 9H, PMe_3 *trans* to BPin), 1.72 (t, J = 3.6 Hz, 18H, 2

PMe_3 *trans* to each other). $^{13}C\{^1H\}$ NMR (C_6D_6) δ 15.9 (t, J = 19.1 Hz), 19.4 (d, J = 41.3

Hz), 25.4 (s), 81.9 (s). ^{11}B NMR (C_6D_6) δ 28.0, 36.5. $^{31}P\{^1H\}$ NMR (C_6D_6) δ -51.4 (br,

1P, PMe$_3$ *trans* to BPin), −41.1 (d, J = 26.9 Hz, 2P, 2 PMe$_3$ *trans* to each other). Anal.

Calcd for C$_{21}$H$_{51}$IrB$_2$ClO$_4$P$_3$: C, 35.53; H, 7.24. Found: C, 35.48; H, 7.60.

(PMe$_3$)$_4$Ir(BPin) (18). A solution of PMe$_3$ (161 mg, 2.12 mmol) in 4 mL THF

was added to a solution of **17** (500 mg, 0.7 mmol) in 5 mL THF in a schlenk tube. A

solution of KO^{t}Bu (158 mg, 1.4 mmol) in 5 mL THF was then added to the reaction

mixture. The reaction mixture was stirred at room temperature for 90 min. The solvent

was removed under reduced pressure. The product was extracted with 8 mL pentane. The

pentane filtrate was then pumped down to give a white solid (402 mg, 92%). The material

always contained a small amount of (PMe$_3$)$_4$Ir(H) **(37)** (ca. 3% by ^{1}H NMR) due to its

considerable moisture sensitivity). The product was recrystallized from a concentrated

pentane solution at −30 °C to give colorless crystals. mp 130-137 °C (dec). ^{1}H NMR

(C$_6$D$_6$, 25 °C) δ 1.24 (s, 12H, BO$_2$C$_6$H$_{12}$), 1.58 (br s, 36H, PMe$_3$). ^{13}C{^{1}H} NMR (C$_6$D$_6$,

25 °C) δ 26.8 (s), 28.9 (m), 81.0 (s). ^{11}B NMR (C$_6$D$_6$) δ 38. ^{31}P{^{1}H} NMR (C$_6$D$_6$, 25 °C)

δ −57.5 (br s, 4P). Anal. Calcd for C$_{18}$H$_{48}$IrBO$_2$P$_4$: C, 34.67; H, 7.76. Found: C, 34.76; H,

7.89.

fac-(PMe$_3$)$_3$Ir(BPin)$_3$ (25). A solution of PMe$_3$ (220 mg, 2.9 mmol) in 2 mL C$_6$H$_6$

was added a solution of **14** (400 mg, 0.58 mmol) in 4 mL C$_6$H$_6$ in a vial. The reaction

mixture was stirred at ambient temperature for 30 min and the solvent was removed

under reduced pressure to give a white solid (461 mg, 99%). The product was

recrystallized from a concentrated pentane solution at −30 °C to give colorless crystals.

mp 184 °C (dec). ^{1}H NMR (C$_6$D$_6$) δ 1.34 (s, 36H, BO$_2$C$_6$H$_{12}$), 1.52 (m, 27H, PMe$_3$).

^{13}C{^{1}H} NMR (C$_6$D$_6$) 23.7 (m), 26.5 (s), 80.4 (s). ^{11}B NMR (C$_6$D$_6$) δ 36.0. ^{31}P{^{1}H} NMR

(C_6D_6) δ −64 (br, 3P). Anal. Calcd for $C_{27}H_{63}IrB_3O_6P_3$: C, 40.47; H, 7.92. Found: C, 40.72; H, 8.01.

***fac*-(PMe₃)₃Ir(BPin)(H)(Me) (26).** A solution of HBPin (27 mg, 0.21 mmol) in 2 mL pentane was added to a solution of (PMe₃)₄Ir(Me) (100 mg, 0.21 mmol) in 4 mL pentane. The reaction mixture was stirred at ambient temperature for 5 min and the solvent was then removed under reduced pressure to give an isomer mixture of *fac*-(PMe₃)₃Ir(BPin)(H)(Me) (**26**) and *mer*-(PMe₃)₃Ir(Me)(H)(BPin) (**27**) in a ratio of 83:17 (94 mg, 75%). *fac*-(PMe₃)₃Ir(BPin)(H)(Me) (**26**). ^{1}H NMR (C_6D_6) δ -11.30 (dt, J = 140.4 Hz, 18.9 Hz, 1H, hydride), 0.40 (m, 3H, Me), 1.17 (d, J = 6.4 Hz, 9H, PMe₃ *trans* to BPin), 1.25 (s, 12H, $BO_2C_6H_{12}$), 1.35 (d, J = 7.3 Hz, 9H, PMe₃ *trans* to hydride), 1.47 (d, J = 7.9 Hz, 9H, PMe₃ *trans* to Me). ^{13}C{^{1}H} NMR (C_6D_6) δ -36.3 (dt, J = 62.5 Hz, 7.6 Hz, Me), 19.9 (ddd, J = 24.7 Hz, 5.5 Hz, 2.7 Hz), 20.9 (dt, J = 21.3 Hz, 2.7 Hz), 22.0 (td, J = 18.5 Hz, 4.1 Hz), 25.8 (s), 25.9 (s), 80.1 (s), 80.2 (s). ^{11}B NMR (C_6D_6) δ 38.6. ^{31}P{^{1}H} NMR (C_6D_6) δ -63.3 (br, 1P, PMe₃ *trans* to BPin), -56.83 (dd, J = 13.4 Hz, 23.2 Hz, 1P, PMe₃ *trans* to hydride), -55.16 (dd, J = 13.4 Hz, 18.3 Hz, 1P, PMe₃ *trans* to Me). *mer*-(PMe₃)₃Ir(Me)(H)(BPin) (**27**). ^{1}H NMR (C_6D_6) δ -11.98 (dt, J = 131.9 Hz, 23.0 Hz, 1H, hydride), -0.06 (m, 3H, Me), 1.19 (s, 12H, $BO_2C_6H_{12}$), 1.14 (d, J = 29.9 Hz, 9H, PMe₃ *trans* to hydride), 1.54 (t, J = 3.4 Hz, 18H, 2 PMe₃ *trans* to each other). ^{11}B NMR (C_6D_6) δ 38.6. ^{31}P{^{1}H} NMR (C_6D_6) δ - 57.8 (t, J = 22.9 Hz, 1P, PMe₃ *trans* to hydride), -48.2 (d, J = 22.9 Hz, 2P, 2 PMe₃ *trans* to each other). Anal. Calcd for $C_{16}H_{43}IrBO_2P_3$: C, 34.11; H, 7.69. Found: C, 33.64; H, 7.70.

***mer*-(PMe₃)₃Ir(BPin)(H)(Ph) (28).** A solution of HBPin (55 mg, 0.43 mmol) in 2 mL pentane was added to a solution of (PMe₃)₃Ir(Ph) (194 mg, 0.39 mmol) in 5 mL

pentane. The reaction mixture was stirred at ambient temperature for 30 min and the solvent was removed under reduced pressure to give *mer*-(PMe$_3$)$_3$Ir(BPin)(H)(Ph) (241 mg, 95%). The product was recrystallized from a concentrated pentane solution at –30 °C to give colorless crystals. mp 118 °C (dec). ^{1}H NMR (C$_6$D$_6$, 25 °C) δ -11.32 (dt, J = 131 Hz, 20 Hz, 1H, hydride), 1.16 (s, 12H, BO$_2$C$_6$H$_{12}$), 1.41 (m, 27H, PMe$_3$), 7.17-7.20 (m, 3H), 7.98 (br, 2H). ^{13}C{^{1}H} NMR (C$_6$D$_6$, 25 °C) δ 21.5 (d, J = 24.7 Hz), 22.2 (dt, J = 4.5 Hz, 19.1 Hz), 26.0 (s), 80.0 (s), 120.7 (s), 126.9 (s), 148.2 (br), 150.6 (br). ^{11}B NMR (C$_6$D$_6$) δ 35.8. ^{31}P{^{1}H} NMR (C$_6$D$_6$) δ –57.8 (t, J = 22.9 Hz, 1P), -45.6 (d, J = 22.0 Hz, 2P). Anal. Calcd for C$_{21}$H$_{45}$IrBO$_2$P$_3$: C, 40.32; H, 7.25. Found: C, 39.95; H, 7.38.

***fac*-(PMe$_3$)$_3$Ir(BPin)(H)(SiEt$_3$) (29).** A solution of HSiEt$_3$ (17 mg, 0.15 mmol) in 2 mL C$_6$H$_6$ was added to a solution of **18** (92 mg, 0.15 mmol) in 3 mL C$_6$H$_6$. The reaction mixture was stirred at ambient temperature for 2.5 days and the solvent was removed under reduced pressure to give colorless solid. The product was recrystallized from a concentrated pentane solution at –30 °C to give colorless crystals (83 mg, 86%). mp 134-136 °C. ^{1}H NMR (C$_6$D$_6$) δ -12.30 (dt, J = 117.0 Hz, 17.0 Hz, 1H, hydride), 0.84-0.95 (m, 3H, diastereotopic CH of CH$_2$ groups of SiEt$_3$), 1.25 (d, J = 6.7 Hz, 9H, PMe$_3$ *trans* to BPin), 1.29 (s, 12H, BO$_2$C$_6$H$_{12}$), 1.37 (d, J = 7.3 Hz, 9H, PMe$_3$ *trans* to SiEt$_3$), 1.46 (d, J = 7.6 Hz, 9H, PMe$_3$ *trans* to hydride), 1.35-1.45 (m, 12H, diastereotopic CH of CH$_2$ groups and CH$_3$ groups of SiEt$_3$). ^{11}B NMR NMR (C$_6$D$_6$) δ 36.3. ^{13}C{^{1}H} NMR (C$_6$D$_6$) δ 10.7 (d, J = 1.9 Hz), 13.1 (dd, J = 5.8 Hz, 7.7 Hz), 24.6 (dt, J = 25.9 Hz, 4.8 Hz), 25.3 (dt, J = 22.1 Hz, 3.8 Hz), 25.4 (dt, J = 24.0 Hz, 3.8 Hz), 27.2 (s), 27.4 (s), 81.32 (s), 81.34 (s). ^{31}P{^{1}H} NMR (C$_6$D$_6$) δ -66.4 (br, 1P, PMe$_3$ *trans* to BPin), -64.2 (dd, J = 31.3 Hz,

19.8 Hz, 1P, PMe₃ *trans* to SiEt₃), -58.1 (dd, J = 19.8 Hz, 19.8 Hz, 1P, PMe₃ *trans* to hydride). Anal. Calcd for $C_{21}H_{55}IrBO_2P_3Si$: C, 38.00; H, 8.35. Found: C, 38.38; H, 8.52.

mer-(PMe₃)₃Ir[B(NH)₂C₆H₄](H)(Cl) (31). A solution of PMe₃ (102 mg, 1.34 mmol) in 2 mL THF was added dropwise to a solution of [Ir(COE)₂Cl]₂ (200 mg, 0.22 mmol) in 4 mL THF. The reaction mixture was stirred at room temperature for 2 h. The solvent was then removed under reduced pressure. The residue was redissolved in 6mL THF and H[B(NH)₂C₆H₄] (51.7 mg, 0.44 mmol) was added to the mixture. The reaction mixture was stirred at ambient temperature for 12 h and then filtered through celite to remove trace suspension The filtrate was pumped down to give a white solid (226 mg, 88%). mp 170 °C (dec). ^{1}H NMR (CD₂Cl₂) δ -9.90 (dt, J = 138.2 Hz, 20.9 Hz, 1H, hydride), 1.53 (t, J = 3.6 Hz, 18H, 2 PMe₃ *trans* to each other), 1.63 (dd, J = 7.5 Hz, 0.9 Hz, 9H, PMe₃ *trans* to hydride), 5.83 (br, 2H, 2 NH), 6.64-6.66, 6.81-6.83 (m, 4H, C₆H₄). ^{13}C{^{1}H} NMR (CD₂Cl₂) δ 19.3 (d, J = 26.9 Hz), 20.4 (dt, J = 4.3 Hz, 18.9 Hz), 108.7 (s), 117.5 (s), 139.0 (s). ^{11}B NMR (CD₂Cl₂) δ 24.9. ^{31}P{^{1}H} NMR (CD₂Cl₂) δ –48.2 (t, J = 20.8 Hz, 1P, PMe₃ *trans* to hydride), -39.7 (d, J = 20.8 Hz, 2P, 2 PMe₃ *trans* to each other). Anal. Calcd for $C_{15}H_{34}IrBClN_2P_3$: C, 31.40; H, 5.97; N, 4.88. Found: C, 31.34; H, 5.79; N, 4.89.

mer-(PMe₃)₃Ir(BDAN)(H)(Cl) (32) and mer-(PMe₃)₃Ir(H)(BDAN)(Cl) (33). A solution of PMe₃ (102 mg, 1.3 mmol) in 2 mL THF was added dropwise to a solution of [Ir(COE)₂Cl]₂ (200 mg, 0.22 mmol) in 4 mL THF. The reaction mixture was stirred at room temperature for 2 h. The solvent was then removed under reduced pressure. The residue was redissolved in 6 mL THF and HBDAN (74.5 mg, 0.44 mmol) was added to the mixture. The reaction mixture was stirred at ambient temperature for 12 h and was

then filtered through celite to remove trace suspension. The filtrate was pumped down to give an isomer mixture of **32** and **33** in a ratio of 90.4:9.6 (200 mg, 72%). *mer*-(PMe₃)₃Ir(BDAN)(H)(Cl) (**32**). ^{1}H NMR (CD₂Cl₂) δ -10.60 (dt, J = 137.5 Hz, 20.8 Hz, 1H, hydride), 1.63 (d, J = 6.4 Hz, 9H, PMe₃ *trans* to hydride), 1.65 (t, J = 3.5 Hz, 18H, 2 PMe₃ *trans* to each other), 5.49 (br, 2H, 2 NH), 6.19 (d, J = 7.5 Hz, 2H, BDAN), 6.86 (d, J = 8.5 Hz, 2H, BDAN), 7.03 (dd, J = 7.6 Hz, 8.0 Hz, 2H, BDAN). ^{11}B NMR (CD₂Cl₂) δ 28.0. ^{13}C{^{1}H} NMR (CD₂Cl₂) δ 19.0 (d, J = 26.8 Hz), 20.3 (dt, J = 3.4 Hz, 18.9 Hz), 104.0 (s), 115.8 (s), 118.4 (s), 128.0 (s), 136.8 (s), 142.7 (d, J = 1.4 Hz). ^{31}P{^{1}H} NMR (CD₂Cl₂) δ -49.2 (t, J = 20.8 Hz, 1P, PMe₃ *trans* to hydride), -39.7 (d, J = 20.8 Hz, 2P, 2 PMe₃ *trans* to each other). *mer*-(PMe₃)₃Ir(H)(BDAN)(Cl) (**33**). ^{1}H NMR (CD₂Cl₂) δ -23.97 (td, J = 16.0 Hz, 10.1 Hz, 1H, hydride), 1.50 (d, J = 6.6 Hz, 9H, PMe₃ *trans* to BDAN), 1.56 (t, J = 3.3 Hz, 18H, 2 PMe₃ *trans* to each other), 5.74 (br, 2H, 2 NH), 6.18 (d, J = 7.3 Hz, 2H, BDAN), 6.82 (dd, J = 8.7 Hz, 12.4 Hz, 2H, BDAN), 6.99 (d, J = 8.0 Hz, 2H, BDAN). ^{11}B NMR (CD₂Cl₂) δ 38.6. ^{31}P{^{1}H} NMR (CD₂Cl₂) δ -52.4 (br, 1P, PMe₃ *trans* to BDAN), -43.1 (d, J = 26.9 Hz, 2P, 2 PMe₃ *trans* to each other). Anal. Calcd for C₁₉H₃₆IrBClN₂P₃: C, 36.58; H, 5.82; N, 4.49. Found: C, 36.62; H, 5.87; N, 4.43.

mer-(PMe₃)₃Ir[B(NMe)₂C₆H₄](H)(Cl) (34) and mer-(PMe₃)₃Ir(H)[B(NMe)₂C₆ H₄](Cl) (35). A solution of PMe₃ (102 mg, 1.3 mmol) in 2 mL THF was added dropwise to a solution of [Ir(COE)₂Cl]₂ (200 mg, 0.22 mmol) in 4 mL THF. The reaction mixture was stirred at room temperature for 2 h. The solvent was then removed under reduced pressure. The residue was redissolved in 6 mL THF and H[B(NMe)₂C₆H₄] (53.7 mg, 0.37 mmol) was added to the mixture. The reaction mixture was stirred at ambient temperature

for 12 h and then filtered through celite to remove trace suspension. The filtrate was pumped down to give an isomer mixture of **34** and **35** in a ratio of 14.4:85.6 (220 mg, 82%). *mer*-(PMe$_3$)$_3$Ir[B(NMe)$_2$C$_6$H$_4$](H)(Cl) (**34**). ^{1}H NMR (CD$_2$Cl$_2$) δ -10.75 (dt, J = 139.0 Hz, 19.6 Hz, 1H, hydride), 1.47 (t, J = 3.5 Hz, 18H, 2 PMe$_3$ *trans* to each other), 1.68 (dd, J = 6.9 Hz, 0.8 Hz, 9H, PMe$_3$ *trans* to hydride), 3.28 (s, 3H, Me), 3.55 (s, 3H, Me), 6.77-6.85 (m, 4H, C$_6$H$_4$). ^{11}B NMR (CD$_2$Cl$_2$) δ 28.6. ^{31}P{^{1}H} NMR (CD$_2$Cl$_2$) δ -54.9 (t, J = 22.0 Hz, 1P, PMe$_3$ *trans* to hydride), -39.4 (d, J = 22.0 Hz, 2P, 2 PMe$_3$ *trans* to each other). *mer*-(PMe$_3$)$_3$Ir(H)[B(NMe)$_2$C$_6$H$_4$](Cl) (**35**). ^{1}H NMR (CD$_2$Cl$_2$) δ -23.97 (td, J = 14.3 Hz, 12.2 Hz, 1H, hydride), 1.38 (t, J = 3.3 Hz, 18H, 2 PMe$_3$ *trans* to each other), 1.54 (d, J = 6.7 Hz, 9H, PMe$_3$ *trans* to [B(NMe)$_2$C$_6$H$_4$], 3.35 (s, 3H, Me), 3.68 (s, 3H, Me), 6.77-6.85 (m, 4H, C$_6$H$_4$). ^{11}B NMR (CD$_2$Cl$_2$) δ 38.3. ^{13}C{^{1}H} NMR (CD$_2$Cl$_2$) δ 20.0 (dt, J = 5.5 Hz, 18.9 Hz), 20.3 (d, J = 22.0 Hz), 32.1 (s), 32.8 (s), 106.2 (s), 106.6 (s), 117.0 (s), 117.2 (s), 140.6 (d, J = 3.4 Hz), 141.8 (d, J = 4.8 Hz). ^{31}P{^{1}H} NMR (CD$_2$Cl$_2$) δ -50.6 (br, 1P, PMe$_3$ *trans* to [B(NMe)$_2$C$_6$H$_4$], -40.6 (d, J = 26.9 Hz, 2P, 2 PMe$_3$ *trans* to each other). Anal. Calcd for C$_{17}$H$_{38}$IrBClN$_2$P$_3$: C, 33.92; H, 6.36; N, 4.66. Found: C, 34.10; H, 6.35; N, 4.57.

Screening Experiments

The general procedure for the synthesis of phenylboronate esters, catalyzed by **13** or **14**/a monodentate phosphine ligand, is illustrated by the following example. Decane (0.626 M in benzene, 50 μL, 0.031 mmol), HBPin (51 μL, 0.351 mmol) were charged into a J. Young NMR tube. **13** (3 mg, 7.3 x 10^{-3} mmol) was charged into a GC-vial and

dissolved in C_6H_6 (150 μL). PMe$_3$ (1.5 μL, 0.015 mmol) was added into the solution of

13 via a microsyringe. The mixture was then transferred into the J. Young NMR tube.

Benzene (150 μL x 2) was used to wash the residue to the J. Young NMR tube. The

reaction mixture was heated at 150 °C and monitored by ^{11}B NMR spectra. After HBPin

was consumed, an aliquot of the reaction mixture was diluted with CH_2Cl_2 and a GC-FID

chromatogram was obtained. From the calibration curve of PhBPin vs. decane, GC yield

of PhBPin formation was obtained. The results of borylation of benzene catalyzed by **13**

or **14**/a monodentate phosphine ligand are summarized in Table **3**.

The general procedure for the synthesis of phenylboronate esters, catalyzed by

13/a chelating phosphine ligand, is illustrated by the following example. Decane (0.626

M in benzene, 50 μL, 0.031 mmol), HBPin (51 μL, 0.351 mmol) were charged into a J.

Young NMR tube. **13** (2.9 mg, 7.0 x 10^{-3} mmol) and dppe (2.8 mg, 7.0 x 10^{-3} mmol) were

charged into two separate GC-vials and dissolved in C_6H_6 (150 μL x 2). The mixture was

then transferred into the J. Young NMR tube. Benzene (150 μL) was used to wash the

residue to the J. Young NMR tube. The reaction mixture was heated at 100 °C or 150 °C

and monitored by ^{11}B NMR spectra. After HBPin was consumed, an aliquot of the

reaction mixture was diluted with CH_2Cl_2 and a GC-FID chromatogram was obtained.

From the calibration curve of PhBPin vs. decane, GC yield of PhBPin formation was

obtained. The results of borylation of benzene catalyzed by **13**/a chelating phosphine

ligand are summarized in Table **4**.

The general procedure for the synthesis of phenylboronate esters, catalyzed by

13/a nitrogen or oxygen or sulfur containing ligand, is illustrated by the following

example. Dodecane (0.471 M in benzene, 50 μL, 0.024 mmol), HBPin (51 μL, 0.351

mmol) were charged into a J. Young NMR tube. **13** (2.9 mg, 7.0 x 10^{-3} mmol) and bpy

(1.1 mg, 7.0 x 10^{-3} mmol) were charged into two separate GC-vials and dissolved in C_6H_6

(150 μL x 2). The mixture was then transferred into the J. Young NMR tube. Benzene

(150 μL) was used to wash the residue to the J. Young NMR tube. The reaction mixture

was heated at 100 °C or 150 °C and monitored by ^{11}B NMR spectra. After HBPin was

consumed, an aliquot of the reaction mixture was diluted with CH_2Cl_2 and a GC-FID

chromatogram was obtained. From the calibration curve of PhBPin vs. dodecane, GC

yield of PhBPin formation was obtained. The results of borylation of benzene catalyzed

by **13**/a nitrogen or oxygen or sulfur containing ligand are summarized in Table **5**.

NMR Tube Reactions

Metathesis reaction between Cp*Ir(PMe₃)(Ph)(H) (5) and HBPin in C₆D₆.
Cp*Ir(PMe₃)(Ph)(H) (9 mg, 0.019 mmol) and HBPin (28.7 mg, 0.224 mmol) were

dissolved in C_6D_6 (540 μL) and the mixture was transferred to a J. Young NMR tube.

The reaction mixture was heated at 150 °C in an oil bath and monitored by ^1H, ^{11}B, and

$^{31}P\{^1H\}$ NMR.

Thermolysis of Cp*Ir(PMe₃)(H)(BPin) (1) in C₆D₆. Compound **1** (10 mg, 0.019

mmol) dissolved in C_6D_6 (550 μL) was transferred to a J. Young NMR tube. The solution

was heated at 200 °C in an oil bath for 2 weeks and 280 °C for 1 day. The reaction was

monitored by ^1H, ^{11}B, and $^{31}P\{^1H\}$ NMR.

Metathesis reaction between Cp*Rh(PMe₃)(Ph)(H) (4) and HBPin in C₆D₆.
Cp*Rh(PMe₃)(Ph)(H) (10 mg, 0.026 mmol) and HBPin (39 mg, 0.305 mmol) were

dissolved in C_6D_6 (550 μL) and the mixture was transferred to a J. Young NMR tube. The reaction mixture was heated at 95 °C in an oil bath and monitored by ^1H, ^{11}B, and $^{31}P\{^1H\}$ NMR.

Crossover experiment. $Cp*Ir(P(CD_3)_3)(H)_2$ (**8**) (10 mg, 0.024 mmol), $(C_5Me_4Et)Ir(PMe_3)(H)_2$ (**9**) (10.1 mg, 0.024 mmol), and HBPin (15.5 mg, 0.121 mmol) were dissolved in C_6H_6 (550 μL) and the reaction mixture was transferred to a J. Young NMR tube. The reaction mixture was heated at 150 °C in an oil bath and monitored by ^{11}B NMR. After HBPin was consumed, an aliquot of the reaction mixture was diluted with CH_2Cl_2 and a GC-MS chromatogram was obtained. From the chromatogram of the crude mixture there was no crossover products observed. Therefore, crossover during catalytic borylation was minimal.

Anisole borylation catalyzed by $Cp*IrH_4$ (11). $Cp*IrH_4$ (**11**) (10 mg, 0.030 mmol) and HBPin (23 mg, 0.180 mmol) were dissolved in a 1:2 (V/V) anisole/cyclohexane solution (500 μL). The reaction mixture was transferred to a J. Young NMR tube, heated at 150 °C in an oil bath, and monitored by ^{11}B NMR. After HBPin was consumed, an aliquot of the reaction mixture was diluted with CH_2Cl_2 and a GC-FID chromatogram was obtained. The isomer ratio of $C_6H_4(OMe)(BPin)$ (*o:m:p*) was determined to be 3:49:48.

Thermolysis of $(MesH)Ir(BPin)_3$ (14) in C_6H_6. $(MesH)Ir(BPin)_3$ (**14**) (15.2 mg, 0.022 mmol) dissolved in C_6H_6 (550 μL) was transferred to a J. Young NMR tube. The solution was heated at 150 °C in an oil bath and monitored by ^{11}B NMR. After complex **14** was consumed, an internal standard solution (decane/C_6H_6) was added to the reaction mixture. An aliquot of the mixture was diluted with CH_2Cl_2 and a GC-FID chromatogram

138

was obtained. Thermolysis of **14** in C_6H_6 produced 3 equivalents of PhBPin and black iridium metal.

14 + excess HBPin in C_6D_6. Compound **14** (10 mg, 0.014 mmol) and HBPin (11 mg, 0.086 mmol) dissolved in C_6D_6 (550 μL) was transferred to a J. Young NMR tube. The reaction mixture was heated at 150 °C in an oil bath and monitored by ^{11}B NMR. After 5 h at 150 °C, the reaction led to decomposition and PinB-O-BPin. No C_6D_5BPin was observed.

14 + excess HBPin in C_6D_6 in the presence of 2 equiv. of PMe₃. Compound **14** (10 mg, 0.014 mmol) and HBPin (11 mg, 0.086 mmol) dissolved in C_6D_6 (550 μL) was transferred to a J. Young NMR tube. PMe₃ (3 μL, 0.029 mmol) was added to the NMR tube via a microsyringe. The reaction mixture was heated at 150 °C in an oil bath and monitored by ^{11}B NMR. After 5 h at 150 °C, HBPin was completely converted to PhBPin.

14 + 2 equiv. PMe₃ in toluene-d_8. Compound **14** (10 mg, 0.014 mmol) dissolved in toluene-d_8 (500 μL) was transferred to a J. Young NMR tube. PMe₃ (3 μL, 0.029 mmol) was added to the NMR tube via a microsyringe. The reaction was monitored by ^{1}H, ^{11}B, and ^{31}P{^{1}H} NMR at room temperature. The reaction generated a mixture of compound **25** and $(\eta^6\text{-}C_7D_8)Ir(BPin)_3$ in a 2:1 ratio.

37 + HBPin in C_6D_6. $(PMe_3)_4Ir(H)$ (**37**) (15 mg, 0.030 mmol) dissolved in C_6D_6 (332 μL) in a GC vial was transferred to a J. Young NMR tube. Additional C_6D_6 (166 μL) was used to wash the residue into the NMR tube. HBPin (4.4 μL, 0.030 mmol) was added into the NMR tube via a microsyringe. At room temperature, the starting material was gradually converted into a mixture of *mer,cis*-$(PMe_3)_3Ir(H)_2(BPin)$ (**38**) and *fac-*

$(PMe_3)_3Ir(H)_2(BPin)$ **(36)**. The sample was allowed to stand at room temperature for 6 days to give compound **36** as the predominant species. *mer,cis*-$(PMe_3)_3Ir(H)_2(BPin)$ **(38)**. ^1H NMR (C_6D_6) δ -12.18 (dt, J = 114.7 Hz, 23.2 Hz, 1H, hydride *trans* to PMe_3), -10.46 (q, 1H, hydride *trans* to BPin), 1.21 (s, 12H, $BO_2C_6H_{12}$), 1.49 (d, 9H, PMe_3 *trans* to hydride), 1.69 (t, J = 3.5 Hz, 18H, 2 PMe_3 *trans* to each other). ^{11}B NMR (C_6D_6) δ 38.6. $^{31}P\{^1H\}$ NMR (C_6D_6) δ -58.1 (t, J = 22.6 Hz, 1P, PMe_3 *trans* to hydride), -48.1 (d, J = 22.6 Hz, 2P, 2 PMe_3 *trans* to each other). *fac*-$(PMe_3)_3Ir(H)_2(BPin)$ **(36)**. ^1H NMR (C_6D_6) δ -11.83 (symmetrical second order m, 2H, hydride), 1.25 (s, 12H, $BO_2C_6H_{12}$), 1.32 (d, J = 7.0 Hz, 9H, PMe_3 *trans* to BPin), 1.69 (d, J = 7.6 Hz, 18H, 2 PMe_3 *trans* to hydride). ^{11}B NMR (C_6D_6) δ 38.6. $^{31}P\{^1H\}$ NMR (C_6D_6) δ -62.0 (br, 1P, PMe_3 *trans* to BPin), -54.59 (d, J = 23.2 Hz, 2P, 2 PMe_3 *trans* to hydride).

37 + B$_2$Pin$_2$ in C$_6$D$_6$. B_2Pin_2 (7.9 mg, 0.031 mmol) dissolved in C_6D_6 (166 μL) was transferred to a J. Young NMR tube which was charged with $(PMe_3)_4Ir(H)$ **(37)** (15.4 mg, 0.031 mmol) in C_6D_6 (166 μL). Additional C_6D_6 (166 μL x 2) was used to wash the residue into the NMR tube. The reaction mixture was heated at 60 °C and monitored by ^1H, ^{11}B, and $^{31}P\{^1H\}$ NMR spectra. The starting material was gradually converted into a mixture of *mer,trans*-$(PMe_3)_3Ir(BPin)_2(H)$ **(20)** and *fac*-$(PMe_3)_3Ir(BPin)_2(H)$ **(21)**. *fac*-$(PMe_3)_3Ir(BPin)_2(H)$ **(21)** was the major species after the temperature was increased to 100 °C for 7 h. *mer,trans*-$(PMe_3)_3Ir(BPin)_2(H)$ **(20)**. ^1H NMR (C_6D_6) δ -12.36 (dt, J = 117.0 Hz, 21.7 Hz, 1H, hydride trans to PMe_3), 1.22 (s, 12H, $BO_2C_6H_{12}$), 1.49 (d, J = 8.0 Hz, 9H, PMe_3 *trans* to hydride), 1.74 (t, J = 3.4 Hz, 18H, 2 PMe_3 *trans* to each other). ^{11}B NMR (C_6D_6) δ 38.9. $^{31}P\{^1H\}$ NMR (C_6D_6) δ -59.6 (t, J = 22.0 Hz, 1P, PMe_3 *trans* to hydride), -50.8 (d, J = 22.0 Hz, 2P, 2 PMe_3 *trans* to each other). *fac*-$(PMe_3)_3Ir(BPin)_2(H)$

(21). mp 120-122 °C. ^{1}H NMR (C$_6$D$_6$) δ -11.66 (dt, J = 118.1 Hz, 18.1 Hz, 1H, hydride

trans to PMe$_3$), 1.29 (s, 24H, BO$_2$C$_6$H$_{12}$), 1.41 (vt, 18H, 2 PMe$_3$ *trans* to BPin), 1.58 (d, J

= 8.0 Hz, 9H, PMe$_3$ *trans* to hydride). ^{13}C{^{1}H} NMR (C$_6$D$_6$) δ 23.7 (dt, J = 26.9 Hz, 5.3

Hz), 25.1 (br), 25.8 (s), 26.3 (s), 80.3 (s). ^{11}B NMR (C$_6$D$_6$) δ 38.6. ^{31}P{^{1}H} NMR

(C$_6$D$_6$) δ -61.8 (br, 2P, 2 PMe$_3$ *trans* to BPin), -56.6 (t, J = 22.0 Hz, 1P, PMe$_3$ *trans* to

hydride). *fac*-(PMe$_3$)$_3$Ir(BPin)$_2$(H) **(21)** was independently synthesized and isolated in 80

% yield. Anal. Calcd for C$_{21}$H$_{52}$IrB$_2$O$_4$P$_3$: C, 37.34; H, 7.76. Found: C, 37.35; H, 7.72.

18 + dppe in C$_6$D$_6$. Dppe (8 mg, 0.020 mmol) dissolved in C$_6$D$_6$ (166 μL) was

transferred to a J. Young NMR tube, which was charged with **18** (12.5 mg, 0.020 mmol)

in C$_6$D$_6$ (166 μL). Additional C$_6$D$_6$ (166 μL) was used to wash the residue into the NMR

tube. The reaction mixture was allowed to stand at room temperature for 3 days to give

Ir(PMe$_3$)$_2$(dppe)(BPin) **(19)** as the predominant species. ^{1}H NMR (C$_6$D$_6$) δ 1.10 (s, 12H,

BO$_2$C$_6$H$_{12}$), 1.33 (t, J = 3.3 Hz, 18H, 2 PMe$_3$), 1.92-2.18 (m, 4H, CH$_2$), 6.98-7.12, 7.16-

7.28, 7.72-7.89, 7.91-7.98 (m, 20H, phenyl groups of dppe). ^{11}B NMR (C$_6$D$_6$) δ 38.8.

^{31}P{^{1}H} NMR (C$_6$D$_6$) δ -58.9 (dd, J = 141.6 Hz, 26.8 Hz, 2P, 2 PMe$_3$), 39.1 (dt, J =

141.6 Hz, 13.4 Hz, 1P, PPh$_2$ *cis* to BPin), 46.1 (br, 1P, PPh$_2$ *trans* to BPin).

18 + HBPin in C$_6$D$_6$. Compound **18** (12.8 mg, 0.021 mmol) dissolved in C$_6$D$_6$

(500 μL) was transferred to a J. Young NMR tube. HBPin (3 μL, 0.021 mmol) was added

to the NMR tube via a microsyringe. The reaction was monitored by ^{1}H, ^{11}B, and ^{31}P{^{1}H}

NMR at room temperature. *mer,trans*-(PMe$_3$)$_3$Ir(BPin)$_2$(H) **(20)** was the initial

predominant species, and it gradually isomerized to *fac*-(PMe$_3$)$_3$Ir(BPin)$_2$(H) **(21)** after

heating at 70 °C for 11h.

18 + ClBCat in C₆D₆. Compound **18** (12.1 mg, 0.019 mmol) and ClBCat (3 mg, 0.019 mmol) dissolved in C_6D_6 (500 μL) were transferred to a J. Young NMR tube. The reaction was monitored by ^1H, ^{11}B, and $^{31}P\{^1H\}$ NMR at room temperature. After 3 days at room temperature, the predominant species in the reaction mixture was *mer*-$(PMe_3)_3Ir(BPin)(BCat)(Cl)$ (**22**) with BPin group *trans* to Cl. ^1H NMR (C_6D_6) δ 1.18 (s, 12H, $BO_2C_6H_{12}$), 1.29 (d, J = 7.3 Hz, 9H, PMe_3 *trans* to BCat group), 1.47 (t, J = 3.7 Hz, 18H, 2 PMe_3 *trans* to each other), 6.84, 7.19 (AA'BB', 4H, BCat). ^{11}B NMR (C_6D_6) δ 28.1, 41.6. $^{31}P\{^1H\}$ NMR (C_6D_6) δ −56.2 (br, PMe_3 *trans* to BCat), −39.3 (d, J = 29.3 Hz, 2 PMe_3 *trans* to each other).

Thermolysis of 18 in C₆D₆. Compound **18** (10.2 mg, 0.016 mmol) dissolved in C_6D_6 (500 μL) was transferred to a J. Young NMR tube. The reaction mixture was heated at 100 °C in an oil bath and monitored by ^1H, ^{11}B, and $^{31}P\{^1H\}$ NMR. After 38 h at 100 °C, complex **18** was converted to $(PMe_3)_4Ir(D)$ and C_6D_5BPin.

Thermolysis of 25 in C₆D₆. Compound **25** (15 mg, 0.019 mmol) dissolved in C_6D_6 (500 μL) was transferred to a J. Young NMR tube. The reaction mixture was heated at 150 °C in an oil bath and monitored by ^1H, ^{11}B, and $^{31}P\{^1H\}$ NMR. The reaction gave *fac*-$(PMe_3)_3Ir(D)_3$ as the final iridium containing product and generated 3 equiv. of C_6D_5BPin.

Thermolysis of 18 in C₆H₅I. Complex **18** (12 mg, 0.019 mmol) dissolved in C_6H_5I (500 μL) was transferred to a J. Young NMR tube. The reaction resulted in immediate white precipitation. The reaction mixture was heated at 100 °C for 1 h in an oil bath. No isomer mixture of $C_6H_4(I)(BPin)$ was detected by GC-FID.

Thermolysis of 25 in C$_6$H$_5$I. Compound **25** (11.6 mg, 0.014 mmol) dissolved in C$_6$H$_5$I (500 μL) was transferred to a J. Young NMR tube. The reaction mixture was heated at 150 °C for 29 h in an oil bath. The reaction produced *m*- and *p*-C$_6$H$_4$(I)(BPin) in 54% GC yield, in addition to a 45% yield of PhBPin.

Kinetic Isotope Effect Experiments

Catalytic borylation in a molar ratio 1:1 mixture of C$_6$H$_6$/C$_6$D$_6$ with the Ir^I pre-catalyst (2 mol% 13 and 4 mol% PMe$_3$). A solution of (Ind)Ir(COD) (**13**) (6 mg, 0.014 mmol) in C$_6$H$_6$/C$_6$D$_6$ (1:1) (175 μL x 2) was mixed with a solution of PMe$_3$ (3 μL) in C$_6$H$_6$/C$_6$D$_6$ (1:1) (175 μL x 2). The solution mixture was then transferred to a J. Young NMR tube. Additional C$_6$H$_6$/C$_6$D$_6$ (1:1) (175 μL x 4) was used to wash the residue into the NMR tube. HBPin (104 μL, 0.717 mmol) was added to the NMR tube via an auto-pipette. The reaction mixture was heated at 150 °C in a constant temperature oil bath (Cole-Parmer Polystat Constant Temperature Circulator). The reaction was monitored by ^{11}B NMR. The ratio of C$_6$D$_5$BPin : C$_6$H$_5$BPin determined from GC-FID after calibration was 1.00:2.29.

Catalytic borylation in a molar ratio 1:1 mixture of C$_6$H$_6$/C$_6$D$_6$ with the Ir^{III} pre-catalyst (2 mol% 14 and 4 mol% PMe$_3$). A solution of (MesH)Ir(BPin)$_3$ (**14**) (10 mg, 0.014 mmol) in C$_6$H$_6$/C$_6$D$_6$ (1:1) (175 μL x 2) was mixed with a solution of PMe$_3$ (3 μL) in C$_6$H$_6$/C$_6$D$_6$ (1:1) (175 μL x 2). The solution mixture was then transferred to a J. Young NMR tube. Additional C$_6$H$_6$/C$_6$D$_6$ (1:1) (175 μL x 4) was used to wash the residue into the NMR tube. HBPin (104 μL, 0.717 mmol) was added to the NMR tube via

an auto-pipette. The reaction mixture was heated at 150 °C in a constant temperature oil bath (Cole-Parmer Polystat Constant Temperature Circulator). The reaction was monitored by ^{11}B NMR. The ratio of C_6D_5BPin : C_6H_5BPin determined from GC-FID after calibration was 1.00:2.28.

Catalytic borylation in 1,3,5-$C_6D_3H_3$ with the Ir^I pre-catalyst (2 mol% 13 and 4 mol% PMe$_3$). A solution of **13** (3 mg, 0.007 mmol) in 1,3,5-$C_6D_3H_3$ (166 μL) was mixed with a solution of PMe$_3$ (1.5 μL) in 1,3,5-$C_6D_3H_3$ (166 μL). The solution mixture was then transferred to a J. Young NMR tube. Additional 1,3,5-$C_6D_3H_3$ (166 μL) was used to wash the residue into the NMR tube. HBPin (52 μL, 0.358 mmol) was added to the NMR tube via an auto-pipette. The reaction mixture was heated at 150 °C in a constant temperature oil bath. The reaction was monitored by ^{11}B NMR. The ratio of 1,3,5-$C_6D_2H_3(BPin)$: 1,3,5-$C_6D_3H_2(BPin)$ determined by the ^{1}H NMR of the crude mixture was 1.00:2.06.

Catalytic borylation in 1,3,5-$C_6D_3H_3$ with the Ir^{III} pre-catalyst (2 mol% 14 and 4 mol% PMe$_3$). A solution of **14** (5 mg, 0.007 mmol) in 1,3,5-$C_6D_3H_3$ (166 μL) was mixed with a solution of PMe$_3$ (1.5 μL) in 1,3,5-$C_6D_3H_3$ (166 μL). The solution mixture was then transferred to a J. Young NMR tube. Additional 1,3,5-$C_6D_3H_3$ (166 μL) was used to wash the residue into the NMR tube. HBPin (52 μL, 0.358 mmol) was added to the NMR tube via an auto-pipette. The reaction mixture was heated at 150 °C in a constant temperature oil bath. The reaction was monitored by ^{11}B NMR. The ratio of 1,3,5-$C_6D_2H_3(BPin)$: 1,3,5-$C_6D_3H_2(BPin)$ determined from the ^{1}H NMR of the crude mixture was 1.00:1.94.

Thermolysis of 18 in a molar ratio 1:1 mixture of C_6H_6/C_6D_6. Compound **18** (25 mg, 0.060 mmol) dissolved in C_6H_6/C_6D_6 (1:1) (166 μL x 2) was transferred to a J. Young NMR tube. Additional C_6H_6/C_6D_6 (1:1) (166 μL) was used to wash the residue into the NMR tube. The reaction mixture was heated at 150 °C in an oil bath and monitored by ^{11}B and ^{31}P{^{1}H} NMR. The ratio of C_6D_5BPin : C_6H_5BPin determined from GC-FID after calibration was 1.00:2.67.

Thermolysis of 25 in a molar ratio 1:1 mixture of C_6H_6/C_6D_6. Compound **25** (32 mg, 0.040 mmol) dissolved in C_6H_6/C_6D_6 (1:1) (166 μL x 2) was transferred to a J. Young NMR tube. Additional C_6H_6/C_6D_6 (1:1) (166 μL) was used to wash the residue into the NMR tube. The reaction mixture was heated at 150 °C in an oil bath and monitored by ^{11}B and ^{31}P{^{1}H} NMR. The ratio of C_6D_5BPin : C_6H_5BPin determined from GC-FID after calibration was 1.00:2.53.

Thermolysis of 18 in 1,3,5-$C_6D_3H_3$. Compound **18** (25 mg, 0.060 mmol) dissolved in 1,3,5-$C_6D_3H_3$ (166 μL x 2) was transferred to a J. Young NMR tube. Additional 1,3,5-$C_6D_3H_3$ (166 μL) was used to wash the residue into the NMR tube. The reaction mixture was heated at 150 °C in an oil bath and monitored by ^{11}B and ^{31}P{^{1}H} NMR. The ratio of 1,3,5-$C_6D_2H_3$(BPin) : 1,3,5-$C_6D_3H_2$(BPin) determined from the ^{1}H NMR of the crude mixture was 1.00:2.37.

Thermolysis of 25 in 1,3,5-$C_6D_3H_3$. Compound **25** (32 mg, 0.040 mmol) dissolved in 1,3,5-$C_6D_3H_3$ (166 μL x 2) and transferred to a J. Young NMR tube. Additional 1,3,5-$C_6D_3H_3$ (166 μL) was used to wash the residue into the NMR tube. The reaction mixture was heated at 150 °C in an oil bath and monitored by ^{11}B and ^{31}P{^{1}H}

NMR. The ratio of 1,3,5-C$_6$D$_2$H$_3$(BPin) : 1,3,5-C$_6$D$_3$H$_2$(BPin) determined from the ^{1}H NMR of the crude mixture was 1.00:1.93.

Arylboronate Ester Syntheses

The general procedure for the synthesis of arylboronate esters, catalyzed by solutions of compound **1**, is illustrated for the synthesis of 1,3,5-C$_6$H$_3$(CF$_3$)$_2$(BPin). Compound **1**, (80 mg, 0.15 mmol) and HBPin (96 mg, 0.75 mmol) were dissolved in 4 mL 1,3-bis(trifluoromethyl)benzene and heated at 150 °C in a constant temperature circulator for 10 hours in a thick–walled, air–free flask. The solution was then transferred to a vial and the solvent was removed under vacuum at room temperature. The residue was chromatographed on a silica gel column, eluting with CH$_2$Cl$_2$, to yield 1,3,5-C$_6$H$_3$(CF$_3$)$_2$(BPin) as a colorless solid (182 mg, 81% based on HBPin). mp (65-66 °C). ^{1}H NMR (CDCl$_3$) δ 1.35 (s, 12H, BO$_2$C$_6$H$_{12}$), 7.92 (s, 1H), 8.22 (s, 2H). ^{13}C{^{1}H} NMR (CDCl$_3$) δ 24.8, 84.9, 123.5 (J = 272.4 Hz, 2C), 124.7, 130.9 (J = 32.7 Hz, 2C), 134.7 (2C). ^{11}B NMR (CDCl$_3$) δ 30. ^{19}F NMR (CDCl$_3$) δ –63. Anal. Calcd for C$_{14}$H$_{15}$BF$_6$O$_2$: C, 49.44; H, 4.45. Found: C, 49.55; H, 4.53. GC-MS (*m/z*) 340.

The general procedure for the synthesis of arylboronate esters, catalyzed by solutions of compound **1**, generated *in situ* from compound **2**, is illustrated for the synthesis of C$_6$H$_4$Me(BPin). Compound **2**, (70 mg, 0.17 mmol) and HBPin (133 mg, 1.04 mmol) were dissolved in 4 mL toluene and heated at 150 °C in a constant temperature circulator for 10 hours in a thick–walled, air–free flask. The solution was then transferred to a vial and the solvent was removed under vacuum at room temperature. The residue

146

was chromatographed on a silica gel column, eluting with CH_2Cl_2, to yield $C_6H_4Me(BPin)$. The reaction gave 3 isomers, m-$C_6H_4Me(BPin)$: p-$C_6H_4Me(BPin)$: o-$C_6H_4Me(BPin)$ in the ratio of 62:34:4 (173 mg, 91% based on HBPin). The identity of o-$C_6H_4Me(BPin)$ and p-$C_6H_4Me(BPin)$ were established by comparing spectroscopic data to those in the literature,[25] and by comparing GC-MS data for the mixture to data for the independently prepared pure isomers. The identity of m-$C_6H_4Me(BPin)$ was confirmed by independent synthesis of an authentic sample using the literature method.[2] m-$C_6H_4Me(BPin)$ was isolated as a colorless solid. mp 34-35 °C. ^{1}H NMR ($CDCl_3$) δ 1.33 (s, 12H, $BO_2C_6H_{12}$), 2.34 (s, 3H, Me), 7.25 (m, 2H), 7.59 (m, 1H), 7.62 (s, 1H). ^{11}B NMR ($CDCl_3$) δ 30.7. Anal. Calcd for $C_{13}H_{19}BO_2$: C, 71.59; H, 8.78. Found: C, 71.36; H, 9.33. GC-MS (m/z) 218.

The general procedure for the synthesis of arylboronate esters, catalyzed by solutions of compound **3**, is illustrated for the synthesis of 1,3,5-$C_6H_3(CF_3)_2(BPin)$. Compound **3**, (5 mg, 0.013 mmol) and HBPin (90 mg, 0.70 mmol) were dissolved in 550 μL 1,3-bis(trifluoromethyl)benzene and heated at 150 °C in a constant temperature circulator for 3 hours in a J. Young NMR tube. The solution was transferred to a vial and the solvent removed under vacuum at room temperature. The residue was chromatographed on a silica gel column, eluting with CH_2Cl_2, to yield 1,3,5-$C_6H_3(CF_3)_2(BPin)$ as a colorless solid (203 mg, 86% based on HBPin).
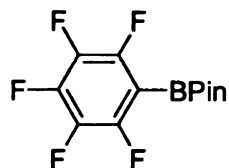
$C_6F_5(BPin)$. Catalytic addition of HBPin to C_6HF_5 using solutions of compounds **1** (generated *in situ* from compound **2**) and **3** gave $C_6F_5(BPin)$ as a colorless solid (205

mg, 81% based on HBPin, and 85 mg, 41% based on HBPin, for **1** and **3**, respectively).

mp 35-36 °C. ^{1}H NMR (CDCl$_3$) δ 1.36 (s, 12H, BO$_2$C$_6$H$_{12}$). ^{11}B NMR (CDCl$_3$) δ 29. ^{19}F

NMR (CDCl$_3$) δ –129.5 (m, 2F), –149.7 (m, 1F), –161.9 (m, 2F). Anal. Calcd for

C$_{12}$H$_{12}$BF$_5$O$_2$: C, 49.02; H, 4.11. Found: C, 48.33; H, 4.59. GC-MS (*m/z*) 294.
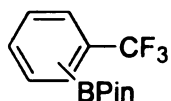
C$_6$H$_4$(CF$_3$)(BPin) (isomer mixture). Catalytic addition of HBPin to

benzotrifluoride using solutions of **1** gave 2 isomers, *m*-C$_6$H$_4$(CF$_3$)(BPin) : *p*-

C$_6$H$_4$(CF$_3$)(BPin) in a 2:1 ratio (202 mg, 99% based on HBPin). HBPin addition

catalyzed by solutions of **3** gave *m*-C$_6$H$_4$(CF$_3$)(BPin) : *p*-C$_6$H$_4$(CF$_3$)(BPin) in a 2:1 ratio

(161 mg, 84% based on HBPin). The proton chemical shifts of the two isomers were

determined by selective decoupling of peaks in the aromatic region. *m*-C$_6$H$_4$(CF$_3$)(BPin).

^{1}H NMR (CDCl$_3$) δ 1.34 (s, 12H, BO$_2$C$_6$H$_{12}$), 7.47 (t, 1H), 7.68 (d, 1H), 7.96 (d, 1H),

8.05 (s, 1H). ^{11}B NMR (CDCl$_3$) δ 30.2. ^{19}F NMR (CDCl$_3$) δ –62.9. *p*-C$_6$H$_4$(CF$_3$)(BPin).

^{1}H NMR (CDCl$_3$) δ 1.34 (s, 12H, BO$_2$C$_6$H$_{12}$), 7.59 (d, 2H), 7.89 (d, 2H). ^{11}B NMR

(CDCl$_3$) δ 30.2. ^{19}F NMR (CDCl$_3$) δ –63.3. Anal. Calcd for C$_{13}$H$_{16}$BF$_3$O$_2$: C, 57.39; H,

5.93. Found: C, 57.48; H, 6.40. GC-MS (*m/z*) 272.
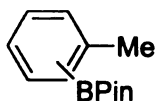
C$_6$H$_4$Me(BPin) (isomer mixture). Catalytic addition of HBPin to toluene using

solutions of **3** gave 3 isomers, *m*-C$_6$H$_4$Me(BPin) : *p*-C$_6$H$_4$Me(BPin) : *o*-C$_6$H$_4$Me(BPin) in

a 63:32:5 ratio (110 mg, 72% based on HBPin).
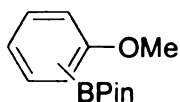
C₆H₄(OMe)(BPin) (isomer mixture). Catalytic addition of HBPin to anisole using solutions of **3** gave 3 isomers, *m*-C₆H₄(OMe)(BPin) : *p*-C₆H₄(OMe)(BPin) : *o*-C₆H₄(OMe)(BPin) in a 67:25:8 ratio (106 mg, 65% based on HBPin). The proton chemical shifts of the 2 major isomers were determined by selective decoupling experiments and by comparison to spectra of independently prepared authentic samples. *m*-C₆H₄(OMe)(BPin). ^{1}H NMR (CDCl₃) δ 1.33 (s, 12H, BO₂C₆H₁₂), 3.82 (s, 3H, OMe), 7.25-7.44 (m, 3H), 7.00 (m, 1H). ^{11}B NMR (CDCl₃) δ 30.8. *p*-C₆H₄(OMe)(BPin). ^{1}H NMR (CDCl₃) δ 1.31 (s, 12H, BO₂C₆H₁₂), 3.81 (s, 3H, OMe), 6.88 (d, 2H), 7.74 (d, 2H). ^{11}B NMR (CDCl₃) δ 30.8. Anal. Calcd for C₁₃H₁₉BO₃: C, 66.70; H, 8.18. Found: C, 66.69; H, 8.50. GC-MS (*m/z*) 234.
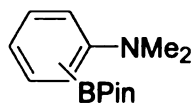
C₆H₄(NMe₂)(BPin) (isomer mixture). Catalytic addition of HBPin to N,N-dimethylaniline using solutions of **3** gave *m*-C₆H₄(NMe₂)(BPin) : *p*-C₆H₄(NMe₂)(BPin) : *o*-C₆H₄(NMe₂)(BPin) in the ratio 55:43:2 (113 mg, 65% based on HBPin). The proton chemical shifts of *p*-C₆H₄(NMe₂)(BPin) and *m*-C₆H₄(NMe₂)(BPin) isomers were determined by selective decoupling and NOE experiments. Resonances in the aromatic region were assigned to *m*- and *p*-C₆H₄(NMe₂)(BPin) isomers by selective decoupling experiments. Resonances for the methyl groups of NMe₂ in *m*- and *p*-C₆H₄(NMe₂)(BPin) were assigned to each isomer based on one-dimensional NOE experiments. In the NOE experiment, the methyl resonances of the NMe₂ groups were irradiated in order to establish through space relationships with their respective aromatic protons. Irradiation of

149

the methyl resonance at δ 2.97 resulted in an enhancement of the peak at δ 6.68, corresponding to the aromatic protons assigned to p-C$_6$H$_4$(NMe$_2$)(BPin). Irradiation of the second methyl resonance at δ 2.95 resulted in enhancement of the peaks at δ 6.85 and δ 7.21, corresponding to aromatic protons assigned to m-C$_6$H$_4$(NMe$_2$)(BPin). The integration of the methyl resonances of NMe$_2$ by deconvolution of the peaks, indicates a higher percentage of the *meta* isomer with respect to the *para* isomer. From the integration of the ^{1}H NMR spectrum, the peaks in the GC-MS were assigned accordingly to each isomer. m-C$_6$H$_4$(NMe$_2$)(BPin). ^{1}H NMR (CDCl$_3$) δ 1.33 (s, 12H, BO$_2$C$_6$H$_{12}$), 2.95 (s, 6H, N (CH$_3$)$_2$), 6.85 (m, 1H), 7.17-7.28 (m, 3H). ^{11}B NMR (CDCl$_3$) δ 31.1. p-C$_6$H$_4$(NMe$_2$)(BPin). ^{1}H NMR (CDCl$_3$) δ 1.32 (s, 12H, BO$_2$C$_6$H$_{12}$), 2.97 (s, 6H, NMe$_2$), 6.68 (d, 2H), 7.69 (d, 2H). ^{11}B NMR (CDCl$_3$) δ 31.1. Anal. Calcd for C$_{14}$H$_{22}$BNO$_2$: C, 68.04; H, 8.97. Found: C, 67.84; H, 9.11. GC-MS (m/z) 247.
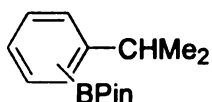
C$_6$H$_4$(CHMe$_2$)(BPin) (isomer mixture). Catalytic addition of HBPin to cumene using solutions of 3 gave 3 isomers, m-C$_6$H$_4$(CHMe$_2$)(BPin) : p-C$_6$H$_4$(CHMe$_2$)(BPin) : o-C$_6$H$_4$(CHMe$_2$)(BPin) in a 66:33:1 ratio (115 mg, 67% based on HBPin). The proton chemical shifts of the 2 major isomers were determined by selective decoupling experiments. m-C$_6$H$_4$(CHMe$_2$)(BPin). ^{1}H NMR (CDCl$_3$) δ 1.24 (d, 6H, 2Me), 1.33 (s, 12H, BO$_2$C$_6$H$_{12}$), 2.91 (m, 1H, CH), 7.27-7.33 (m, 2H), 7.62 (d, 1H), 7.65 (s, 1H). ^{11}B NMR (CDCl$_3$) δ 31.1. p-C$_6$H$_4$(CHMe$_2$)(BPin). ^{1}H NMR (CDCl$_3$) δ 1.23 (d, 6H, 2Me), 1.32 (s, 12H, BO$_2$C$_6$H$_{12}$), 2.91 (m, 1H, CH), 7.22 (d, 2H), 7.73 (d, 2H). ^{11}B NMR (CDCl$_3$) δ 31.1. GC-MS (m/z) 246.
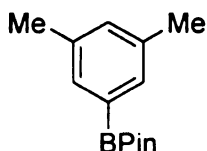
1,3,5-C₆H₃Me₂(BPin) Catalytic addition of HBPin to *m*-xylene using solutions of

3 gave 1 major product. 1,3,5-C$_6$H$_3$Me$_2$(BPin) was isolated as a white solid (119 mg,

73% based on HBPin). mp 90-91 °C. ^{1}H NMR (CDCl$_3$) δ 1.33 (s, 12H, BO$_2$C$_6$H$_{12}$),

2.30 (s, 6H, 2Me), 7.09 (s, 1H), 7.42 (s, 2H). ^{13}C{^{1}H} NMR (CDCl$_3$) δ 21.1, 24.8, 83.6,

132.4, 132.9, 137.1. ^{11}B NMR (CDCl$_3$) δ 30.9. Anal. Calcd for C$_{14}$H$_{21}$BO$_2$: C, 72.44; H,

9.12. Found: C, 72.38; H, 9.44. GC-MS (*m/z*) 232.
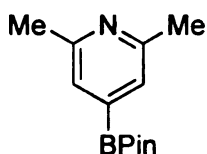
2,4,6-C₅NH₂Me₂(BPin) Catalytic addition of HBPin to 2,6-lutidine using

solutions of **3** gave 2,4,6-C$_5$NH$_2$Me$_2$(BPin), isolated as colorless crystals after

sublimation of the crude product under high vacuum at 70 °C (67 mg, 41% based on

HBPin). mp 82-83°C. ^{1}H NMR (CDCl$_3$) δ 1.32 (s, 12H, BO$_2$C$_6$H$_{12}$), 2.49 (s, 6H, 2Me),

7.28 (s, 2H). ^{11}B NMR (CDCl$_3$) δ 30.8. Anal. Calcd for C$_{13}$H$_{20}$BNO$_2$: C, 66.98; H, 8.65;

N, 6.01. Found: C, 66.79; H, 9.09; N, 6.40. GC-MS (*m/z*) 233.
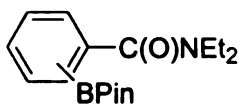
C₆H₄(C(O)NEt₂)(BPin) (isomer mixture). Catalytic addition of HBPin to

C$_6$H$_5$(C(O)NEt$_2$) using solutions of **3** gave *m*-C$_6$H$_4$(C(O)NEt$_2$)(BPin) : *p*-

C$_6$H$_4$(C(O)NEt$_2$)(BPin) : *o*-C$_6$H$_4$(C(O)NEt$_2$)(BPin) in the ratio 28:14:58. The product was

distilled from the reaction mixture using a Kugelrohr distillation apparatus and collected

as a colorless viscous liquid (106 mg, 50% based on HBPin). For isomer mixture: ^{1}H

NMR (CDCl$_3$) δ 1.04 (m, 3H, CH$_3$), 1.23 (m, 3H, CH$_3$), 1.28, 1.33, 1.34 (s, 12H,

BO$_2$C$_6$H$_{12}$), 3.20 (m, 2H, CH$_2$), 3.55 (m, 2H, CH$_2$), 7.23-7.26, 7.30-7.74, 7.75-7.81 (m,

4H). ^{13}C{^{1}H} NMR (CDCl$_3$) δ 12.36, 12.78 (br), 13.56, 14.05 (br) (NCH$_2$CH$_3$), 24.76

(BO$_2$C$_2$(CH$_3$)$_4$), 39.04 (br), 39.64, 42.87, 43.16 (br) (NCH$_2$CH$_3$), 83.23, 83.52, 83.82

(BO$_2$C$_2$(CH$_3$)$_4$), 125.27, 127.58, 128.08, 128.71, 130.34, 132.34, 134.64, 134.88, 135.16,

136.60, 139.74, 142.20 (aromatic resonances), 171.02, 171.17, 171.50 (carbonyl

resonances). ^{11}B NMR (CDCl$_3$) δ 28.7. IR (neat, cm^{-1}) 660 (m), 783 (w), 858 (m), 965

(m), 1103 (m), 1146 (s), 1223 (w), 1287 (m), 1321 (m), 1356 (s), 1428 (m), 1634 (s).

Satisfactory combustion analysis has not been obtained. GC-MS (*m/z*) 303. The identity

of isomer products was established by comparing spectroscopic data to the independent

synthesis of authentic samples using the literature method,[25] and by comparing GC-MS

data for the mixture to data for the independently prepared pure isomers. *m*-

C$_6$H$_4$(C(O)NEt$_2$)(BPin). ^{1}H NMR (CDCl$_3$) δ 1.07 (t, 3H, CH$_3$), 1.21 (t, 3H, CH$_3$), 1.32 (s,

12H, BO$_2$C$_6$H$_{12}$), 3.22 (br, 2H, CH$_2$), 3.52 (m, 2H, CH$_2$), 7.30-7.47 (m, 3H), 7.79 (s, 1H).

o-C$_6$H$_4$(C(O)NEt$_2$)(BPin). ^{1}H NMR (CDCl$_3$) δ 1.04 (br, 3H, CH$_3$), 1.28 (br, 3H, CH$_3$),

1.28 (s, 12H, BO$_2$C$_6$H$_{12}$), 3.20 (q, 2H, CH$_2$), 3.56 (q, 2H, CH$_2$), 7.27 (d, 1H), 7.30-7.40

(m, 2H), 7.79 (d, 1H). *p*-C$_6$H$_4$(C(O)NEt$_2$)(BPin). ^{1}H NMR (CDCl$_3$) δ 1.06 (br, 3H, CH$_3$),

1.23 (br, 3H, CH$_3$), 1.34 (s, 12H, BO$_2$C$_6$H$_{12}$), 3.19 (br, 2H, CH$_2$), 3.53 (br, 2H, CH$_2$), 7.34

(d, 2H), 7.81 (d, 2H).
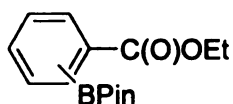
C₆H₄(C(O)OEt)(BPin) (isomer mixture). Catalytic addition of HBPin to $C_6H_5(C(O)OEt)$ using solutions of **3** gave m-$C_6H_4(C(O)OEt)(BPin)$: p-$C_6H_4(C(O)OEt)(BPin)$: o-$C_6H_4(C(O)OEt)(BPin)$ in the ratio 57:33:10. The identity of isomer products were established by comparing GC-MS data for the mixture to data for the independently prepared pure isomers using the literature method.[25] m-$C_6H_4(C(O)OEt)(BPin)$. ¹H NMR ($CDCl_3$) δ 1.34 (s, 12H, $BO_2C_6H_{12}$), 1.38 (t, 3H, CH_3), 4.36 (q, 2H, CH_2), 7.42 (t, 1H), 7.96 (d, 1H), 8.11 (d, 1H), 8.44 (s, 1H). ¹¹B NMR ($CDCl_3$) δ 30.8. p-$C_6H_4(C(O)OEt)(BPin)$. ¹H NMR ($CDCl_3$) δ 1.34 (s, 12H, $BO_2C_6H_{12}$), 1.38 (t, 3H, CH_3), 4.36 (q, 2H, CH_2), 7.84 (d, 2H), 8.00 (d, 2H). ¹¹B NMR ($CDCl_3$) δ 30.9. GC-MS (m/z) 276.
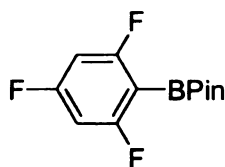
2,4,6-C₆H₂F₃(BPin). **3** (5 mg, 0.013 mmol) and HBPin (90 mg, 0.70 mmol) were dissolved in 550 μL of a 1:2 ratio of xylene-d_{10} and 1,3,5-$C_6H_3F_3$, and heated at 150 °C for 30 min in a J. Young tube. The solution was then transferred to a vial and the solvent removed under vacuum at room temperature. The residue was chromatographed on a silica gel column, eluting with CH_2Cl_2, to yield 2,4,6-$C_6H_2F_3(BPin)$ (83 mg, 46% based on HBPin). ¹H NMR ($CDCl_3$) δ 1.34 (s, 12H, $BO_2C_6H_{12}$), 6.58 (m, 2H). ¹¹B NMR ($CDCl_3$) δ 29.4. ¹⁹F NMR ($CDCl_3$) δ –103.8 (m, 2F), –97.1 (m, 1F). Anal. Calcd for $C_{12}H_{14}BF_3O_2$: C, 55.85; H, 5.47. Found: C, 56.08; H, 5.59. GC-MS (m/z) 258.

The general procedure for the syntheses of the following arylboronate esters: **13** (2.9 mg, 0.007 mmol) and dmpe (1 mg, 0.007 mmol) dissolved in an arene (166 μL x 2)

were transferred to a J-Young NMR tube, which was charged with HBPin (51 μL, 0.351 mmol). Additional arene (166 μL) was used to wash the residue to the NMR tube. The reaction mixture was then heated at 150 °C for xx h. The reaction was monitored by the disappearance of the resonance of pinacolborane in the ^{11}B NMR spectra. After the reaction was done, an aliquot was taken for GC-FID and GC-MS analyses. The reaction mixture was then transferred to a vial and the substrate was removed under vacuum (in some cases with gentle heating). The residue was dissolved in CH_2Cl_2 and passed through a silica gel column using CH_2Cl_2 as eluting solvent. The filtrate was then pumped down to give the corresponding spectroscopically pure arylboronate esters.

PinB—⟨benzene ring⟩—Cl
                    |
                    Cl
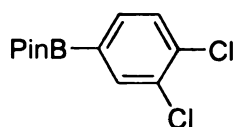
1,2,4-C₆H₃(Cl)₂(BPin). The borylation product was isolated as colorless oil (93.9 mg, 98%). ^{1}H NMR (CDCl₃) δ 1.32 (s, 12 H, BO₂C₆H₁₂), 7.41 (d, J = 8.0 Hz, 1H), 7.57 (dd, J = 8.0 Hz, 1.5 Hz, 1H), 7.84 (d, J = 1.5 Hz, 1H). ^{13}C NMR (125 MHz, CDCl₃) δ 24.8, 84.3, 130.0, 132.3, 133.8, 135.5, 136.6. ^{11}B NMR (CDCl₃) δ 30.0. Anal. Calcd for C₁₂H₁₅BCl₂O₂: C, 52.80; H, 5.54. Found: C, 53.09; H, 5.77. GC-MS (*m/z*) 273.

Cl—⟨benzene ring⟩—Cl
                    |
                   BPin
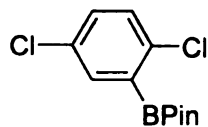
1,4,5-C₆H₃(Cl)₂(BPin). The borylation product was isolated as a colorless solid (72.6 mg, 76%). mp 46-48 °C. ^{1}H NMR (CD₂Cl₂) δ 1.35 (s, 12H, BO₂C₆H₁₂), 7.29 (d, J = 8.3 Hz, 1H), 7.33 (dd, J = 2.4 Hz, 8.8 Hz, 1H), 7.67 (d, J = 2.4 Hz, 1H). ^{13}C{^{1}H} NMR (CDCl₃) δ 24.8, 84.5, 130.7, 131.7, 132.1, 136.0, 137.7. ^{11}B NMR (CDCl₃) δ 29.9. Anal. Calcd for C₁₂H₁₅BCl₂O₂: C, 52.80; H, 5.54. Found: C, 53.19; H, 5.71. GC-MS (*m/z*) 273.
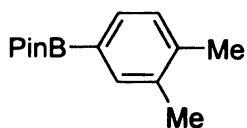
1,2,4-C₆H₃(Me)₂(BPin). The borylation product was isolated as colorless oil (69.2 mg, 85%). ^{1}H NMR (CDCl₃) δ 1.32 (s, 12H, BO₂C₆H₁₂), 2.25 (s, 3H, Me), 2.26 (s, 3H, Me), 7.12 (d, J = 7.3 Hz, 1H), 7.53 (d, J = 7.3 Hz, 1H), 7.57 (s, 1H). ^{13}C{^{1}H} NMR (CDCl₃) δ 19.4, 20.0, 24.8, 83.5, 129.1, 132.4, 135.8, 135.9, 140.1. ^{11}B NMR (CDCl₃) δ 30.6. Anal. Calcd for C₁₄H₂₁BO₂: C, 72.44; H, 9.12. Found: C, 72.26; H, 8.98. GC-MS (*m/z*) 232.
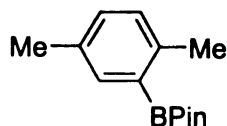
1,2,4-C₆H₃(BPin)(Me)₂. The borylation product was isolated as colorless oil (55.4 mg, 68%). ^{1}H NMR (CDCl₃) δ 1.33 (s, 12H, BO₂C₆H₁₂), 2.29 (s, 3H, Me), 2.48 (s, 3H, Me), 7.04 (d, J = 7.7 Hz, 1H), 7.11 (dd, J = 2.2 Hz, 7.7 Hz, 1H), 7.56 (d, J = 2.2 Hz, 1H). ^{13}C{^{1}H} NMR (CDCl₃) δ 20.7, 21.7, 24.8, 83.3, 129.7, 131.5, 133.8, 136.3, 141.7. ^{11}B NMR (CDCl₃) δ 30.9. Anal. Calcd for C₁₄H₂₁BO₂: C, 72.44; H, 9.12. Found: C, 72.00; H, 8.59. GC-MS (*m/z*) 232.
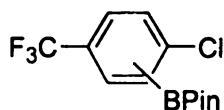
C₆H₃(Cl)(BPin)(CF₃) (isomer mixture). The borylation product was isolated as colorless oil (375 mg, 78%). The ratio of 1,2,4-C₆H₃(Cl)(BPin)(CF₃) to 1,3,4-C₆H₃(Cl)(BPin)(CF₃), determined by GC-FID of the crude reaction mixture, was 88:12. 1,2,4-C₆H₃(Cl)(BPin)(CF₃). ^{1}H NMR (CDCl₃) δ 1.36 (s, 12H, BO₂C₆H₁₂), 7.44 (d, J = 8.5 Hz, 1H), 7.56 (ddd, J = 8.3 Hz, 2.4 Hz, 0.7 Hz, 1H), 7.92 (d, 2.2 Hz, 1H). ^{13}C{^{1}H}

NMR (CDCl₃) δ 24.8, 84.7, 124.0 (q, J = 272.0 Hz, 1C), 128.4 (q, J = 3.5 Hz, 1C), 128.5

(q, J = 32.9 Hz, 1C), 129.9, 133.3 (q, J = 3.5 Hz, 1C), 143.5. ¹¹B NMR (CDCl3) δ 30.0.

¹⁹F NMR (CDCl₃) δ –62.8. Anal. Calcd for C₁₃H₁₅BClF₃O₂: C, 50.94; H, 4.93. Found: C,

51.27; H, 5.05. GC-MS (*m/z*) 306.
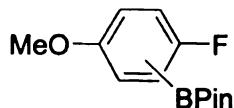
C₆H₃(F)(OMe)(BPin) (isomer mixture). The borylation product (55 mg, 62%)

was isolated as colorless oil. The ratio of 1,4,6-C₆H₃(F)(OMe)(BPin) to 1,4,5-

C₆H₃(F)(OMe)(BPin), determined by GC-FID of the crude reaction mixture, was 93:7.

1,4,6-C₆H₃(F)(OMe)(BPin). ¹H NMR (CDCl₃) δ 1.34 (s, 12H, BO₂C₆H₁₂), 3.78 (s, 3H,

OMe), 6.92 (m, 2H), 7.18 (m, 1H). ¹³C{¹H} NMR (CDCl₃) δ 24.8, 55.8, 83.9, 116.0 (d,

²J_{CF} = 25.9 Hz) 119.2 (d, ³J_{CF} = 8.6 Hz), 120.1 (d, ³J_{CF} = 8.6 Hz), 155.3 (d, ⁴J_{CF} = 1.9

Hz), 161.7 (d, ¹J_{CF} = 243.6 Hz). ¹¹B NMR (CDCl3) δ 29.8. ¹⁹F NMR (CDCl₃) δ –114.3.

1,4,5-C₆H₃(F)(OMe)(BPin). ¹H NMR (CDCl₃) δ 1.30 (s, 12H, BO₂C₆H₁₂), 3.88 (s, 3H,

OMe), 6.88 (d, J = 8.2 Hz, 1H), 7.64 (dd, J = 8.2 Hz, 1.5 Hz, 1H), 7.77 (d, J = 1.5 Hz,

1H). ¹³C{¹H} NMR (CDCl₃) δ 24.8, 56.7, 83.7, 112.2 (d, ³J_{CF} = 6.7 Hz) 118.3 (d, ²J_{CF} =

23.0 Hz), 122.4 (d, ²J_{CF} = 21.1 Hz), 157.0 (d, ¹J_{CF} = 238.8 Hz), 160.4 (d, ⁴J_{CF} = 1.9 Hz).

¹¹B NMR (CDCl₃) δ 29.8. ¹⁹F NMR (CDCl₃) δ –125.6. Anal. Calcd for C₁₃H₁₈BFO₃: C,

61.94; H, 7.20. Found: C, 61.83; H, 7.45. GC-MS (*m/z*) 252.
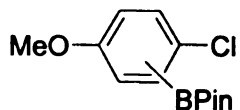
C₆H₃(Cl)(OMe)(BPin) (isomer mixture). The borylation product was isolated as

colorless oil (58 mg, 62%). The ratio of 1,4,6-C₆H₃(Cl)(OMe)(BPin) to 1,4,5-

156

$C_6H_3(Cl)(OMe)(BPin)$, determined by GC-FID of the crude reaction mixture, was 32:68.

1,4,6-$C_6H_3(Cl)(OMe)(BPin)$. ^1H NMR (CDCl$_3$) δ 1.35 (s, 12H, BO$_2$C$_6$H$_{12}$), 3.77 (s, 3H, OMe), 6.85 (dd, J = 8.6 Hz, 3.1 Hz, 1H), 7.17 (d, J = 3.3 Hz, 1H), 7.22 (d, J = 8.6 Hz, 1H). $^{13}C\{^1H\}$ NMR (CDCl$_3$) δ 24.7, 55.5, 84.1, 117.9, 120.9, 130.2, 130.9, 157.6. ^{11}B NMR (CDCl$_3$) δ 30.2. 1,4,5-$C_6H_3(Cl)(OMe)(BPin)$. ^1H NMR (CDCl$_3$) δ 1.33 (s, 12H, BO$_2$C$_6$H$_{12}$), 3.78 (s, 3H, OMe), 6.76 (d, J = 8.8 Hz, 1H), 7.30 (dd, J = 8.8 Hz, 2.9 Hz, 1H), 7.59 (d, J = 2.7 Hz, 1H). $^{13}C\{^1H\}$ NMR (CDCl$_3$) δ 24.7, 56.1, 83.7, 112.1, 125.4, 131.9, 136.0, 162.7. ^{11}B NMR (CDCl$_3$) δ 30.2. Anal. Calcd for C$_{13}$H$_{18}$BClO$_3$: C, 58.14; H, 6.76. Found: C, 58.20; H, 6.97. GC-MS (m/z) 268.
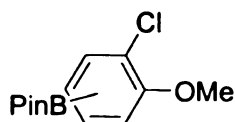
$C_6H_3(Cl)(OMe)(BPin)$ (isomer mixture). The borylation product was isolated as colorless oil (69 mg, 73%). The ratio of 1,2,4-$C_6H_3(Cl)(OMe)(BPin)$ to 1,2,5-$C_6H_3(Cl)(OMe)(BPin)$, determined by GC-FID of the crude reaction mixture, was 51:49.

1,2,5-$C_6H_3(Cl)(OMe)(BPin)$. ^1H NMR (CDCl$_3$) δ 1.31 (s, 12H, BO$_2$C$_6$H$_{12}$), 3.88 (s, 3H, OMe), 6.88 (d, J = 8.3 Hz, 1H), 7.65 (dd, J = 8.1 Hz, 1.5 Hz, 1H), 7.78 (d, J = 1.5 Hz, 1H). $^{13}C\{^1H\}$ NMR (CDCl$_3$) δ 24.8, 56.0, 83.8, 111.4, 122.3, 134.7, 136.5, 157.4. ^{11}B NMR (CDCl$_3$) δ 30.2. 1,2,4-$C_6H_3(Cl)(OMe)(BPin)$. ^1H NMR (CDCl$_3$) δ 1.32 (s, 12H, BO$_2$C$_6$H$_{12}$), 3.91 (s, 3H, OMe), 7.31-7.35 (m, 3H). $^{13}C\{^1H\}$ NMR (CDCl$_3$) δ 24.8, 56.1, 84.0, 117.7, 126.0, 127.9, 129.7, 154.6. ^{11}B NMR (CDCl$_3$) δ 30.2. Anal. Calcd for C$_{13}$H$_{18}$BClO$_3$: C, 58.14; H, 6.76. Found: C, 58.12; H, 6.84. GC-MS (m/z) 268.
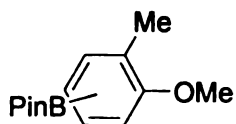
C₆H₃(OMe)(Me)(BPin) (isomer mixture). The borylation product was isolated as colorless oil (67 mg, 77%). The ratio of 1,2,5-C_6H_3(OMe)(Me)(BPin) to 1,2,4-C_6H_3(OMe)(Me)(BPin), determined by GC-FID of the crude reaction mixture, was 64:36. 1,2,5-C_6H_3(OMe)(Me)(BPin). ^{1}H NMR (CDCl₃) δ 1.34 (s, 12H, BO₂C₆H₁₂), 2.24 (s, 3H, Me), 3.87 (s, 3H, OMe), 7.15 (d, J = 7.3 Hz, 1H), 7.23 (s, 1H), 7.33 (d, J = 7.1 Hz, 1H). ^{13}C{^{1}H} NMR (CDCl₃) δ 16.4, 24.8, 55.4, 83.6, 115.5, 127.3, 130.2, 130.3, 157.4. ^{11}B NMR (CDCl3) δ 30.6. 1,2,4-C_6H_3(OMe)(Me)(BPin). ^{1}H NMR (CDCl₃) δ 1.33 (s, 12H, BO₂C₆H₁₂), 2.22 (s, 3H, Me), 3.84 (s, 3H, OMe), 6.82 (d, J = 8.2 Hz, 1H), 7.59 (s, 1H), 7.65(d, J = 8.2 Hz, 1H). ^{13}C{^{1}H} NMR (CDCl₃) δ 15.9, 24.8, 55.2, 83.5, 109.3, 125.9, 134.3, 137.2, 160.5. ^{11}B NMR (CDCl3) δ 30.6. Anal. Calcd for C₁₄H₂₁BO₃: C, 67.77; H, 8.53. Found: C, 67.76; H, 8.39. GC-MS (*m/z*) 248.
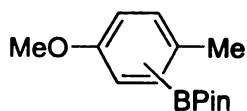
C₆H₃(OMe)(Me)(BPin) (isomer mixture). The borylation product was isolated as colorless oil (67 mg, 77%). The ratio of 1,4,6-C_6H_3(OMe)(Me)(BPin) to 1,4,5-C_6H_3(OMe)(Me)(BPin), determined by GC-FID of the crude reaction mixture, was 70:30. 1,4,6-C_6H_3(OMe)(Me)(BPin). ^{1}H NMR (CDCl₃) δ 1.34 (s, 12H, BO₂C₆H₁₂), 2.26 (s, 3H, Me), 3.78 (s, 3H, OMe), 6.74 (d, J = 8.4 Hz, 1H), 7.16 (ddd, J = 8.4 Hz, 2.4 Hz, 0.7 Hz, 1H), 7.45 (d, J = 2.4 Hz, 1H). ^{13}C{^{1}H} NMR (CDCl₃) δ 20.2, 24.8, 56.1, 83.3, 110.8, 129.2, 132.8, 137.0, 162.4. ^{11}B NMR (CDCl₃) δ 30.7. 1,4,5-C_6H_3(OMe)(Me)(BPin). ^{1}H NMR (CDCl₃) δ 1.32 (s, 12H, BO₂C₆H₁₂), 2.45 (s, 3H, Me), 3.78 (s, 3H, OMe), 6.85 (dd, J = 8.4 Hz, 3.1 Hz, 1H), 7.05 (d, J = 8.2 Hz, 1H), 7.28 (d, J = 2.9 Hz, 1H). ^{13}C{^{1}H} NMR (CDCl₃) δ 21.1, 24.8, 55.3 (d, J = 2.0 Hz), 83.4, 117.0, 120.3, 130.8, 136.8, 156.9. ^{11}B

NMR (CDCl₃) δ 30.7. Anal. Calcd for $C_{14}H_{21}BO_3$: C, 67.77; H, 8.53. Found: C, 67.50; H, 8.61. GC-MS (*m/z*) 248.
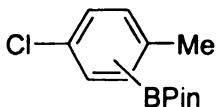
C₆H₃(Cl)(Me)(BPin) (isomer mixture). The borylation product was isolated as colorless oil (74 mg, 84%). The ratio of 1,4,5-C_6H_3(Cl)(Me)(BPin) to 1,4,6-C_6H_3(Cl)(Me)(BPin), determined by GC-FID of the crude reaction mixture, was 57:43.

1,4,5-C_6H_3(Cl)(Me)(BPin). ¹H NMR (CDCl₃) δ 1.32 (s, 12H, $BO_2C_6H_{12}$), 2.47 (s, 3H, Me), 7.06 (d, *J* = 8.3 Hz, 1H), 7.24 (dd, *J* = 8.3 Hz, 2.4 Hz, 1H), 7.69 (d, *J* = 2.4 Hz, 1H). ¹³C{¹H} NMR (CDCl₃) δ 21.5, 24.9, 83.8, 130.5, 130.8, 131.2, 135.4, 143.1. ¹¹B NMR (CDCl₃) δ 30.9. 1,4,6-C_6H_3(Cl)(Me)(BPin). ¹H NMR (CDCl₃) δ 1.35 (s, 12H, $BO_2C_6H_{12}$), 2.28 (s, 3H, Me), 7.11 (ddd, *J* = 8.3 Hz, 2.0 Hz, 0.7 Hz, 1H), 7.21 (d, *J* = 8.3 Hz, 1H), 7.46 (d, *J* = 2.0 Hz, 1H). ¹³C{¹H} NMR (CDCl₃) δ 20.6, 24.8, 84.1, 129.2, 132.5, 135.4, 136.6, 136.9. ¹¹B NMR (CDCl₃) δ 30.9. Anal. Calcd for $C_{13}H_{18}BClO_2$: C, 61.83; H, 7.18. Found: C, 62.15; H, 7.22. GC-MS (*m/z*) 252.
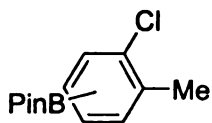
C₆H₄(Cl)(Me)(BPin) (isomer mixture). The borylation products (79 mg, 89%) were isolated as colorless oil. The ratio of 1,2,5-C_6H_3(Cl)(Me)(BPin) to 1,2,4-C_6H_3(Cl)(Me)(BPin), determined by GC-FID of the crude reaction mixture, was 62:38.

1,2,5-C_6H_3(Cl)(Me)(BPin). ¹H NMR (CDCl₃) δ 1.32 (s, 12H, $BO_2C_6H_{12}$), 2.38 (s, 3H, Me), 7.20 (d, *J* = 7.5 Hz, 1H), 7.52 (dd, *J* = 8.8 Hz, 0.9 Hz, 1H), 7.76 (s, 1H). ¹³C{¹H} NMR (125 MHz, CDCl₃) δ 20.2, 24.9, 84.0, 130.5, 132.8, 134.3, 135.2, 139.2. ¹¹B NMR

(CDCl3) δ 30.9. 1,2,4-C_6H_3(Cl)(Me)(BPin). ^{1}H NMR (CDCl$_3$) δ 1.33 (s, 12H, $BO_2C_6H_{12}$), 2.37 (s, 3H, Me), 7.32 (d, J = 8.0 Hz, 1H), 7.55 (dd, J = 7.5 Hz, 0.9 Hz, 1H), 7.65 (s, 1H). ^{13}C{^{1}H} NMR (125 MHz, CDCl$_3$) δ 19.7, 24.9, 83.9, 128.6, 133.5, 135.3, 137.3, 137.8. ^{11}B NMR (CDCl3) δ 30.9. Anal. Calcd for $C_{13}H_{18}BClO_2$: C, 61.83; H, 7.18. Found: C, 61.94; H, 7.42. GC-MS (m/z) 252.

Competitive Borylation Experiments

Competition between Toluene and Anisole Using Solutions of 2

Cp*Ir(PMe$_3$)H$_2$ (2) (15 mg, 0.037 mmol) was weighed in a test tube, and a pre-mixed 1:1 mole ratio of toluene (256 mg) and anisole (300 mg) was added to dissolve the catalyst. Then HBPin (27 μL, 0.185 mmol) was added to the test tube via syringe. The solution was transferred to a J. Young NMR tube, and the reaction was heated at 150 °C in a constant temperature circulator. The conversion of the reaction was monitored by the disappearance of the resonance for pinacolborane in the ^{11}B NMR spectrum. The isomer ratios were determined by integrating the peaks in the GC-MS spectra, after correcting for the response factors determined from equimolar mixtures of independently synthesized arylboronate esters. The ratio of o-, m-, p-C_6H_4Me(BPin) : o-, m-, p-C_6H_4(OMe)(BPin) is 38:62.

Competition between Toluene and Benzotrifluoride Using Solutions of 2

The procedure is the same as that in the competition between toluene and anisole using solutions of 2. Toluene (242 mg) and benzotrifluoride (383 mg) were used. The ratio of o-, m-, p-C_6H_4Me(BPin) : m-, p-C_6H_4(CF$_3$)(BPin) is 11:89.

Competition between Cumene and N,N-Dimethylaniline Using Solutions of 2

The procedure is the same as that in the competition between toluene and anisole using solutions of 2. Cumene (280 mg) and N,N-dimethylaniline (282 mg) were used. The ratio of $C_6H_4CH(CH_3)_2(BPin)$: o-, m-, p-$C_6H_4(NMe_2)(BPin)$ is 69:31.

Competition between Toluene and Anisole Using Solutions of 3

Cp*Rh(η^4-C_6Me_6) (3) (5 mg, 0.013 mmol) was weighed in a test tube, and a pre-mixed 1:1 mole ratio of toluene (256 mg) and anisole (300 mg) was added to dissolve the catalyst. Then HBPin (90 mg, 0.70 mmol) was added to the test tube via syringe. The solution was transferred to a J. Young NMR tube. The reaction was heated at 150 °C in a constant temperature circulator, and the reaction was judged to be complete by monitoring the disappearance of the resonance for pinacolborane in the ^{11}B NMR spectrum. The isomer ratios were determined by integrating the peaks in the GC-MS spectra, after correcting for the response factors determined from equimolar mixtures of independently synthesized arylboronate esters. The ratio of o-, m-, p-$C_6H_4Me(BPin)$: o-, m-, p-$C_6H_4(OMe)(BPin)$ is 46:54.

Competition between Toluene and Benzotrifluoride Using Solutions of 3

The procedure is the same as that in the competition between toluene and anisole using solutions of 3. Toluene (242 mg) and benzotrifluoride (383 mg) were used. The ratio of o-, m-, p-$C_6H_4Me(BPin)$: m-, p-$C_6H_4(CF_3)(BPin)$ is 27:73.

Competition between Cumene and N,N-Dimethylaniline Using Solutions of 3

The procedure is the same as that in the competition between toluene and anisole using solutions of 3. Cumene (280 mg) and N,N-dimethylaniline (282 mg) were used. The ratio of $C_6H_4CH(CH_3)_2(BPin)$: o-, m-, p-$C_6H_4(NMe_2)(BPin)$ is 60:40.

Competition between Toluene and N,N-Dimethylaniline Using Solutions of 3

The procedure is the same as that in the competition between toluene and anisole using solutions of 3. Toluene (250 mg) and N,N-dimethylaniline (329 mg) were used. The ratio of o-, m-, p-$C_6H_4Me(BPin)$: o-, m-, p-$C_6H_4(NMe_2)(BPin)$ is 59:41.

Competition Experiments Using Solutions of 13 and dmpe

The general procedure is illustrated by the competition reaction between m-xylene and 1,3-bis(trifluoromethyl)benzene using solutions of 13 and dmpe. (Ind)Ir(COD) (13) (2.9 mg, 0.007 mmol) and dmpe (1 mg, 0.007 mmol) were weighed into two separate GC vials, and a pre-mixed 1:1 molar ratio of m-xylene and 1,3-bis(trifluoromethyl)benzene solution (166 µL x 3) was added to dissolve the catalyst. The solution was transferred to a J. Young NMR tube, which was charged with HBPin (51 µL, 0.351 mmol) and the reaction mixture was heated at 150 °C in a constant temperature circulator. The conversion of the reaction was monitored by the disappearance of the resonance for pinacolborane in the ^{11}B NMR spectrum. The product ratios were determined by integrating the peaks in the GC-FID spectra. The ratio of $1,3,5$-$C_6H_3Me_2(BPin)$: 1,3,5-$C_6H_3(CF_3)_2(BPin)$ is 3.5:96.5. The results of borylation of equimolar mixtures of two different substituted arenes catalyzed by 13 (2 mol%)/dmpe (2 mol%) are summarized in Table 13.

Kinetics Experiments

A typical experimental run for the reaction of $Cp*Rh(PMe_3)(Ph)(H)$ (4) with 12 equiv. of HBPin in C_6D_6 is described as follows: Two samples were prepared at the same

time. In a drybox, compound **4** (18 mg, 0.046 mmol) and HBPin (80 μL, 0.55 mmol) were placed in a 1 mL volumetric flask and the flask was filled with C_6D_6 to the mark. The solution in the volumetric flask was mixed well and distributed equally to two J. Young NMR tubes. The kinetic experiments were run twice at different temperatures to ensure the reproducibility. The temperature range is from 65 °C to 115 °C. The kinetics was carried out at 65, 75, 85, 95, 105, and 115 °C. The reactions were heated in a constant temperature oil bath (Cole-Parmer Polystat Constant Temperature Circulator). At specific intervals the NMR tubes were removed from the oil bath and quenched by rapid cooling in an ice bath. The ^1H NMR spectra were then recorded at 25 ± 0.5 °C on a VXR-500 spectrometer. The progress of the reaction was monitored to 3 half-lives by measuring the ratio of the intensity of the Cp* of **4** versus the total "intensity" of the Cp* resonances of **4** and $Cp*Rh(PMe_3)(H)(BPin)$ (**7**).

A typical experimental run for the phosphine dependence on the thermolysis of **18** in C_6D_6 is described as follows: Four samples were prepared at the same time. In a drybox, compound **18** (60 mg, 0.096 mmol) was placed in a 1 mL volumetric flask and the flask was filled with C_6D_6 to the mark. The solution in the volumetric flask was mixed well and a 200 μL portion of the solution was added to four J. Young NMR tubes respectively via an auto-pipette (100 μL x 2). C_6Me_6 (15.6 mg, 0.096 mmol) was placed in a 1 ml volumetric flask and the flask was filled with C_6D_6 to the mark. The solution in the volumetric flask was mixed well and a 200 μL portion of the solution was added to the four J. Young NMR tubes respectively via an auto-pipette (100 μL x 2) as an internal standard. Pre-calculated amount of C_6D_6 was added into each of the four NMR tubes to make the total volume of the solution to 700 μL. In the end, different quantities of PMe₃

were added to the four NMR tubes respectively via a microsyringe. The experiments were carried out at 130 °C in a constant temperature oil bath (Cole-Parmer Polystat Constant Temperature Circulator). At specific intervals the NMR tubes were removed from the oil bath and quenched by rapid cooling in an ice bath. The ^{1}H NMR spectra were then recorded at 25 ± 0.5 °C on a Inova-600 spectrometer. The concentration range of PMe$_3$ is from 0.00828 M to 0.828 M. The progress of the reaction was monitored to 3 half-lives by measuring the ratio of the intensity of the PMe$_3$ of **18** versus the total "intensity" of the PMe$_3$ resonances of **18** and **37**-d_1.

Crystal Structure Determinations and Refinement

Crystals grown at –30 °C were covered in Paratone N and moved quickly from a scintillation vial to a microscope side. A suitable crystal was chosen and mounted on a glass fiber. The data collection were carried out at a sample temperature of 173(2) K on a Bruker AXS three-circle goniometer with a CCD detector. The data were processed and reduced utilizing the program SAINTPLUS supplied by Bruker AXS. The structure were solved by direct methods (SHELXTL v5.1, Bruker AXS) in conjunction with standard difference Fourier techniques. The figures shown were produced using ORTEP and ellipsoids are at the 25% probability level. Tables of pertinent data collection parameters for all compounds crystallographically characterized are given in appendix A.

Single crystals of **14** were grown from a pentane solution at –30 °C and the structure was further confirmed by single–crystal X-ray crystallographic analysis.

Single crystals of **17** and B$_2$Pin$_2$ co-crystallized from a pentane solution at –30 °C and the structures were established by X-ray crystallographic analysis.

Single crystals of **18** were grown from a pentane solution at −30 °C and the structure was further confirmed by single–crystal X-ray crystallographic analysis.

Crystals suitable for X-ray analysis of **25** were grown from a pentane solution at −30 °C.

Single crystals of **28** were grown from a pentane solution at −30 °C to give colorless crystals suitable for X-ray analysis.

Single crystals of **29** were grown from a concentrated pentane solution and the structure was further confirmed by single–crystal X-ray crystallographic analysis.

APPENDICES

Appendix A. Summary of crystal data and structure refinement for compound **14**.

Empirical formula	$C_{27}H_{45}B_3IrO_6$
Formula weight	690.26
Temperature (K)	173(2)
Wavelength (Å)	0.71073
Crystal system	Monoclinic
Space group	P2(1)/n
a (Å)	10.211(3)
b (Å)	16.822(4)
c (Å)	18.362(5)
α, deg	90
β, deg	92.907(5)
γ, deg	90
Volume ($Å^3$)	3150.2(14)
Z	4
Density (calculated) (Mg/m^3)	1.455
Absorption coefficient (mm^{-1})	4.273
F(000)	1388
Crystal size (mm^3)	0.32 x 0.30 x 0.28
Theta range for data collection, deg	1.64 to 23.28
Index ranges	-11<=h<=10, -18<=k<=18, -20<=l<=14
Reflections collected	14167
Independent reflections	4535 [R(int) = 0.1070]
Refinement method	Full-matrix least-squares on F^2
Data / restraints / parameters	4535 / 0 / 349
Goodness-of-fit on F^2	0.944
Final R indices [I>2sigma(I)]	R1 = 0.0453, wR2 = 0.1056
R indices (all data)	R1 = 0.0715, wR2 = 0.1146
Largest diff. peak and hole ($e.Å^{-3}$)	1.604 and -1.635

Appendix A (cont). Summary of crystal data and structure refinement for compound 17.

Empirical formula	$C_{21}H_{51}B_2ClIrO_4P_3$
Formula weight	557.84
Temperature (K)	173(2)
Wavelength (Å)	0.71073
Crystal system	Monoclinic
Space group	P2(1)/c
a (Å)	11.4474(13)
b (Å)	17.2608(19)
c (Å)	19.579(2)
α, deg	90
β, deg	92.162(2)
γ, deg	90
Volume ($Å^3$)	3865.9(8)
Z	6
Density (calculated) (Mg/m^3)	1.438
Absorption coefficient (mm^{-1})	3.681
F(000)	1708
Crystal size (mm^3)	0.42 x 0.40 x 0.38
Theta range for data collection, deg	1.57 to 23.28
Index ranges	-12<=h<=12, -19<=k<=19, -21<=l<=21
Reflections collected	31832
Independent reflections	5555 [R(int) = 0.1432]
Refinement method	Full-matrix least-squares on F^2
Data / restraints / parameters	5555 / 0 / 391
Goodness-of-fit on F^2	1.052
Final R indices [I>2sigma(I)]	R1 = 0.0320, wR2 = 0.0874
R indices (all data)	R1 = 0.0363, wR2 = 0.090
Largest diff. peak and hole ($e.Å^{-3}$)	1.786 and -1.656

Appendix (cont). Summary of crystal data and structure refinement for compound **18**.

Empirical formula	$C_{18}H_{48}BIrO_2P_4$
Formula weight	311.73
Temperature (K)	173(2)
Wavelength (Å)	0.71073
Crystal system	Triclinic
Space group	P-1
a (Å)	9.290(3)
b (Å)	12.408(5)
c (Å)	12.458(5)
α, deg	90.107(5)
β, deg	99.436(6)
γ, deg	90.221(6)
Volume (Å^3)	1416.4(9)
Z	4
Density (calculated) (Mg/m^3)	1.462
Absorption coefficient (mm^{-1})	4.949
F(000)	628
Crystal size (mm^3)	0.43 x 0.31 x 0.28
Theta range for data collection, deg	1.64 to 23.31
Index ranges	-10<=h<=7, -13<=k<=13, -12<=l<=13
Reflections collected	6368
Independent reflections	4039 [R(int) = 0.0226]
Refinement method	Full-matrix least-squares on F^2
Data / restraints / parameters	4039 / 0 / 252
Goodness-of-fit on F^2	1.103
Final R indices [I>2sigma(I)]	R1 = 0.0380, wR2 = 0.1022
R indices (all data)	R1 = 0.0394, wR2 = 0.1035
Largest diff. peak and hole (e.Å^{-3})	2.484 and -1.546

Appendix (cont). Summary of crystal data and structure refinement for compound **25**.

Empirical formula	$C_{27}H_{63}B_3IrO_6P_3$
Formula weight	801.31
Temperature (K)	173(2)
Wavelength (Å)	0.71073
Crystal system	Monoclinic
Space group	P2(1)/c
a (Å)	17.808(4)
b (Å)	11.073(3)
c (Å)	19.023(5)
α, deg	90
β, deg	90.106(4)
γ, deg	90
Volume ($Å^3$)	3751.0(15)
Z	5
Density (calculated) (Mg/m^3)	1.774
Absorption coefficient (mm^{-1})	4.651
F(000)	2050
Crystal size (mm^3)	0.44 x 0.28 x 0.26
Theta range for data collection, deg	2.13 to 23.28
Index ranges	-19<=h<=18, -12<=k<=12, -12<=l<=21
Reflections collected	16587
Independent reflections	5396 [R(int) = 0.0595]
Refinement method	Full-matrix least-squares on F^2
Data / restraints / parameters	5396 / 0 / 362
Goodness-of-fit on F^2	1.037
Final R indices [I>2sigma(I)]	R1 = 0.0743, wR2 = 0.1796
R indices (all data)	R1 = 0.1012, wR2 = 0.1971
Largest diff. peak and hole ($e.Å^{-3}$)	3.058 and -1.864

Appendix (cont). Summary of crystal data and structure refinement for compound **28**.

Empirical formula	$C_{21}H_{44}BIrO_2P_3$
Formula weight	499.59
Temperature (K)	173(2)
Wavelength (Å)	0.71073
Crystal system	Monoclinic
Space group	P2(1)/n
a (Å)	10.740(2)
b (Å)	16.687(3)
c (Å)	15.145(3)
α, deg	90
β, deg	90.069(4)
γ, deg	90
Volume ($Å^3$)	2714.3(10)
Z	5
Density (calculated) (Mg/m^3)	1.528
Absorption coefficient (mm^{-1})	5.109
F(000)	1252
Crystal size (mm^3)	0.42 x 0.35 x 0.24
Theta range for data collection, deg	1.82 to 23.28
Index ranges	-11<=h<=11, -17<=k<=18, -16<=l<=16
Reflections collected	12074
Independent reflections	3908 [R(int) = 0.0288]
Refinement method	Full-matrix least-squares on F^2
Data / restraints / parameters	3908 / 0 / 266
Goodness-of-fit on F^2	1.119
Final R indices [I>2sigma(I)]	R1 = 0.0282, wR2 = 0.0647
R indices (all data)	R1 = 0.0346, wR2 = 0.0669
Largest diff. peak and hole ($e.Å^{-3}$)	1.110 and -0.912

171

Appendix A (cont). Summary of crystal data and structure refinement for compound **29**.

Empirical formula	$C_{21}H_{54}BIrO_2P_3Si$
Formula weight	530.12
Temperature (K)	173(2)
Wavelength (Å)	0.71073
Crystal system	Monoclinic
Space group	P2(1)/c
a (Å)	19.733(8)
b (Å)	10.280(4)
c (Å)	16.119(7)
α, deg	90
β, deg	110.168(7)
γ, deg	90
Volume (Å^3)	3069(2)
Z	5
Density (calculated) (Mg/m^3)	1.434
Absorption coefficient (mm^{-1})	4.559
F(000)	1348
Crystal size (mm^3)	0.36 x 0.34 x 0.26
Theta range for data collection, deg	2.20 to 23.28
Index ranges	-21<=h<=21, -7<=k<=11, -16<=l<=17
Reflections collected	9405
Independent reflections	4175 [R(int) = 0.1122]
Refinement method	Full-matrix least-squares on F^2
Data / restraints / parameters	4175 / 0 / 278
Goodness-of-fit on F^2	1.056
Final R indices [I>2sigma(I)]	R1 = 0.0472, wR2 = 0.1208
R indices (all data)	R1 = 0.0506, wR2 = 0.1238
Largest diff. peak and hole (e. Å^{-3})	3.122 and -2.075

APPENDIX B. Derivation of Rate Expressions for Chapter 5

$$[18] \underset{k_{-1}}{\overset{k_1}{\rightleftharpoons}} \left[(PMe_3)_3Ir(BPin) + PMe_3 \right] \underset{k_{-2}}{\overset{k_2}{\rightleftharpoons}} \left[(PMe_3)_2Ir(BPin) + PMe_3 \right]$$

$$\mathbf{[B]} \qquad k_3 \downarrow C_6D_6 \qquad \qquad \mathbf{[C]} \qquad k_4 \downarrow C_6D_6$$

$$(PMe_3)_4Ir(D) + C_6D_5BPin \qquad (PMe_3)_4Ir(D) + C_6D_5BPin$$
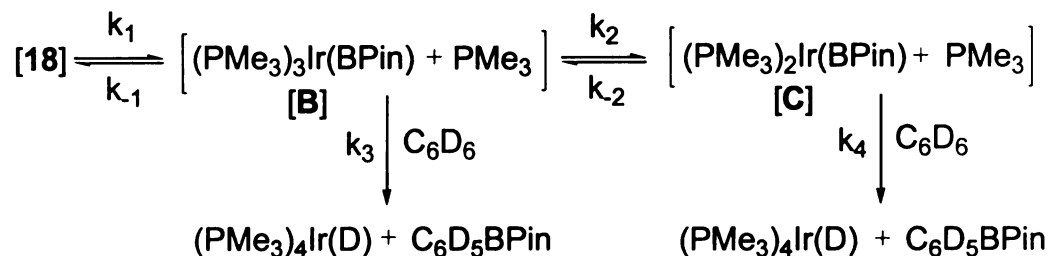
From the Figure above, the time dependent concentrations for **18**, **B**, and **C** are governed by the Equations B1, B2, and B-3:

$$-\frac{d[18]}{dt} = k_1[18] - k_{-1}[B][PMe_3]$$

(B1)

$$\frac{d[B]}{dt} = k_1[18] - k_{-1}[B][PMe_3] - k_2[B] + k_{-2}[C][L] - k_3[B][C_6D_6]$$

(B2)

$$\frac{d[C]}{dt} = k_2[B] - k_{-2}[C][L] - k_4[C][C_6D_6]$$

(B3)

Application of the steady state approximation to [**C**] yields Equation B4, and combination of the steady state expression for [**B**] and Equation B4 gives B5.

$$\frac{d[C]}{dt} = 0 \implies [C] = \frac{k_2[B]}{k_{-2}[PMe_3] + k_4[C_6D_6]}$$

$$\frac{d[B]}{dt} = 0 \implies k_1[18] = k_{-1}[B][PMe_3] + k_2[B] + k_3[B][C_6D_6] \frac{k_{-2}k_2[B][L]}{k_{-2}[PMe_3] + k_4[C_6D_6]}$$

(B5)

Rearrangement of Equation B5 gives Equation B6. The first order rate law in Equation B7 follows from substitution of the expression for [B] (Equation B6) in Equation B1:

$$[B] = \left(\frac{k_1(k_{-2}[PMe_3] + k_4[C_6D_6])}{k_{-1}k_{-2}[PMe_3]^2 + (k_{-1}k_4[C_6D_6] + k_{-2}k_3[C_6D_6])[PMe_3] + k_4[C_6D_6](k_2 + k_3[C_6D_6])} \right) [18]$$

(B6)

$$-\frac{d[18]}{dt} = \left(\frac{k_1 k_{-2} k_3[C_6D_6][PMe_3] + k_1 k_4[C_6D_6](k_2 + k_3[C_6D_6])}{k_{-1}k_{-2}[PMe_3]^2 + (k_{-1}k_4[C_6D_6] + k_{-2}k_3[C_6D_6])[PMe_3] + k_4[C_6D_6](k_2 + k_3[C_6D_6])} \right) [18]$$

(B7)

From Equation B7, k_{obs} (Equation B8) and $1/k_{obs}$ (Equation B9) can be extracted:

$$k_{obs} = \frac{k_1 k_{-2} k_3[C_6D_6][PMe_3] + k_1 k_4[C_6D_6](k_2 + k_3[C_6D_6])}{k_{-1}k_{-2}[PMe_3]^2 + (k_{-1}k_4 + k_{-2}k_3)[C_6D_6][PMe_3] + k_4[C_6D_6](k_2 + k_3[C_6D_6])}$$

(B8)

$$\frac{1}{k_{obs}} = \frac{1}{k_1} + \frac{k_{-1}k_{-2}[PMe_3]^2 + k_{-1}k_4[C_6D_6][PMe_3]}{k_{-1}[C_6D_6](k_{-2}k_3[PMe_3] + k_4k_2 + k_4k_3[C_6D_6])}$$

(B9)

If the reaction only goes through intermediate **B** to yield products ($k_4 = 0$), $1/k_{obs}$ can be derived in Equation B10. If the reaction only passes through intermediate **C** to yield products ($k_3 = 0$), $1/k_{obs}$ can be derived in Equation B11.

$$\frac{1}{k_{obs}} = \frac{1}{k_1} + \frac{k_{-1}}{k_1k_3[C_6D_6]}[PMe_3]$$

(B10)

$$\frac{1}{k_{obs}} = \frac{1}{k_1} + \frac{k_{-1}k_{-2}[PMe_3]^2 + k_{-1}k_4[C_6D_6][PMe_3]}{k_1k_2k_4[C_6D_6]}$$

(B11)

APPENDIX C. Kinetic Details

Data for the reaction of Cp*Rh(PMe₃)(Ph)(H) (4) with 12 equiv. HBPin in C₆D₆.

The progress of the reaction was monitored to 3 half-lives by measuring the ratio of the intensity of the Cp* of **4** versus the total "intensity" of the Cp* resonances of **4** and **7**. The experiments were performed at various temperatures in a constant temperature oil bath.

[4] = 0.046 M; [HBPin] = 0.551 M

Temperature (°C)	k_{obs} (sec^{-1})
65	1.27×10^{-5}
75	4.0×10^{-5}
85	1.38×10^{-4}
95	3.37×10^{-4}
105	9.8×10^{-4}
115	2.0×10^{-3}

Data for the reaction of Cp*Rh(PMe₃)(Ph)(H) (4) with 24 equiv. HBPin in C₆D₆.

The progress of the reaction was monitored to 3 half-lives by measuring the ratio of the intensity of the Cp* of **4** versus the total "intensity" of the Cp* resonances of **4** and **7**. The experiments were performed at 95 ± 0.5 °C in a constant temperature oil bath.

176

[HBPin]	k_{obs} (sec^{-1})
0.551 M	3.37 x 10^{-4}
1.103 M	6.80 x 10^{-4}

Data for the phosphine dependence on the thermolysis of (PMe₃)₄Ir(BPin) (18) in

Data for the phosphine dependence on the thermolysis of $(PMe_3)_4Ir(BPin)$ (18) in C_6D_6 at 130 °C.

The progress of the reaction was monitored to 3 half-lives by measuring the ratio of the intensity of the PMe₃ of **18** versus the total "intensity" of the PMe₃ resonances of **18** and **37-d_1**. The experiments were performed at 130 ± 0.5 °C in a constant temperature oil bath.

[**18**] = 0.0275 M; [C_6Me_6] = 0.0275 M

[PMe₃] (M)	k_{obs} (sec^{-1})
0	0.0417
0.0083	0.0170
0.0138	0.0138
0.0207	0.0097
0.0276	0.0072
0.0552	0.0044
0.1380	0.0021

BIBLIOGRAPHY

BIBLIOGRAPHY

(1) (a) Bergman R. G. *Science* **1984**, *223*, 902-908. (b) Jones, W. D.; Feher, F. J. *Acc. Chem. Res.* **1989**, *22*, 91-100. (c) Arndtsen, B. A.; Bergman, R. G.; Mobley, T. A.; Peterson, T. H. *Acc. Chem. Res.* **1995**, *28*, 154-162. (d) Crabtree R. H. *Chem. Rev.* **1995**, *95*, 987-1007. (e) Bengali, A. A.; Arndtsen, B. A.; Burger, P. M.; Schulta, R. H.; Weiller, B. H.; Kyle, K. R.; Moore, C. B.; Bergman, R. G. *Pure Appl. Chem.* **1995**, *67*, 281-288. (f) Stahl, S. S.; Labinger, J. A.; Bercaw, J. E. *Angew. Chem., Int. Ed. Engl.* **1998**, *37*, 2180-2192. (g) Crabtree R. H. *J. Chem. Soc., Dalton Trans.* **2001**, 2437-2450. (h) Labinger J. A.; Bercaw, J. E. *Nature* **2002**, *417*, 507-514.

(2) Olah, G. A.; Schleyer, P. v. R.;, Eds. "Carbonium Ions"; Wiley: New York, Vol. *1*, **1968**; Vol. *2*, **1970**; Vol. *3*, **1972**; Vol. *4*, **1973**; Vol. *5*, **1976**.

(3) Olah, G. A.; Yoneda, N.; Parker, D. G. *J. Am. Chem. Soc.* **1976**, *98*, 5261-5268.

(4) (a) *Selective Hydrocarbon Activation* (Eds.: Davies, J. A.; Watson, P. L..; Liebman, J. F.; Greenberg, A.), VCH, New York, **1990**. (b) Shilov, A. E. *Activation of Saturated Hydrocarbons by Transition Metal Complexes*, Reidel, Dordrecht, **1984**. (c) Labinger, J. A., *Fuel Process, Technol.* **1995**, *42*, 325-338. (d) Shilov, A. E.; Shul'pin *Chem. Rev.* **1997**, *97*, 2879-2932.

(5) (a) Farinas, E. T.; Schwaneberg, U.; Glieder, A.; Arnold, F. H. *Advanced Synthesis & Catalysis* **2001**, *343*, 601-606. (b) Costas, M.; Chen, K.; Que, L., Jr. *Coord. Chem. Rev.* **2000**, *200-202*, 517-544. (c) Mansuy, D.; Battioni, P. *Act. Funct. Alkanes* **1989**, 195-218. (d) Atkins, W. M.; Sligar, S. G. *J. Am. Chem. Soc.* **1989**, *111*, 2715-2717.

(6) (a) Neimann, K.; Neumann, R.; Rabion, A.; Buchanan, R. M.; Fish, R. H. *Inorg. Chem.* **1999**, *38*, 3575-3580. (b) Rabion, A.; Chen, D. S.; Wang, J.; Buchanan, R. M.; Seris, J.-L.; Fish, R. H. *J. Am. Chem. Soc.* **1995**, *117*, 12356-12357.

(7) Kitajima, N.; Fukui, H.; Moro-oka, Y. *J. Chem. Soc., Chem. Commun.* **1988**, 485.

(8) Janowicz, A. H.; Bergman, R. G. *J. Am. Chem. Soc.* **1982**, *104*, 352-354.

(9) (a) Watson, T. L. *J. Am. Chem. Soc.* **1983**, *105*, 6491-6493. (b) Thompson, M. E.; Baxter, S. M.; Bulls, A. R.; Burger, B. J.; Nolan, M. C.; Santarsiero, B. D.; Schaefer, W. P.; Bercaw, J. E. *J. Am. Chem. Soc.* **1987**, *109*, 203-219.

(10) (a) Cummins, C. C.; Baxter, S. M.; Wolczanski, P. T. *J. Am. Chem. Soc.* **1988**, *110*, 8731-8733. (b) Walsh, P. J.; Hollander, F. J.; Bergman, R. G. *J. Am. Chem. Soc.* **1988**, *110*, 8729-8731. (c) Bennett, J. L.; Wolczanski, P. T. *J. Am. Chem. Soc.* **1997**, *119*,

10696-10719. (d) Schaefer, W. P.; Wolczanski, P. T. *J. Am. Chem. Soc.* **1998**, *120*, 4881-4882.

(11) (a) Sherry, A. E.; Wayland, B. B. *J. Am. Chem. Soc.* **1990**, *112*, 1259-1261. (b) Wayland, B.B.; Sherry, A. E. *J. Am. Chem. Soc.* **1991**, *113*, 5305-5311.

(12) Crabtree, R. H.; Mihelcic, J. M.; Quirk, J. M. *J. Am. Chem. Soc.* **1979**, *101*, 7738-7739.

(13) (a) Fisher, B. J.; Eisenberg, R. *Organometallics* **1983**, *2*, 764-767. (b) Sakakura, T.; Sodeyama, T.; Sasaki, K.; Wada, K.; Tanaka, M. *J. Am. Chem. Soc.* **1990**, *112*, 7221-7229.

(14) Sakakura, T.; Tanaka, M. *J. Chem. Soc., Chem. Commun.* **1987**, *10*, 758-759.

(15) (a) Jenson, C. M. *J. Chem. Soc., Chem. Commun.* **1999**, 2443-2449. (b) Liu, F. C.; Pak, E. B.; Singh, B.; Jensen, C. M.; Goldman, A. S. *J. Am. Chem. Soc.* **1999**, *121*, 4086-4087.

(16) (a) Rablen, P. R.; Hartwig, J. F. *J. Am. Chem. Soc.* **1994**, *116*, 4121-4122. (b) Rablen, P. R.; Hartwig, J. F. *J. Am. Chem. Soc.* **1996**, *118*, 4648-4653.

(17) Waltz, K. M.; He, X.; Muhoro, C.; Hartwig, J. F. *J. Am. Chem. Soc.* **1995**, *117*, 11357-11358.

(18) (a) Westcott, S. A.; Blom, H. P.; Marder, T. B.; Baker, R. T. *J. Am. Chem. Soc.* **1992**, *114*, 8863-8869. (b) Burgess, K.; van der Donk, W. A.; Westcott, S. A.; Marder, T. B.; Baker, R. T. Calabrese, G. C. *J. Am. Chem. Soc.* **1992**, *114*, 9350-9359. (c) Brown, J, M.; Lloyd-Jones, G. C. *J. Chem. Soc., Chem. Commun.* **1993**, 710.

(19) Waltz, K. M.; Hartwig, J. F. *Science* **1997**, *277*, 211-213.

(20) Waltz, K. M.; Muhoro, C. N.; Hartwig, J. F. *Organometallics* **1999**, *18*, 3383-3393.

(21) Iverson, C. N.; Smith M. R. III *J. Am. Chem. Soc.* **1999**, *121*, 7696-7697.

(22) (a) Periana, R. A.; Taube, D. J.; Evitt, E. R.; Loffler, D. G.; Wentrcek, P. R.; Voss, G.; Masuda, T. *Science* **1993**, *259*, 340-343. (b) Periana, R. A.; Taube, D. J.; Gamble, S.; Taube, H.; Satoh, T.; Fujii, H. *Science* **1998**, *280*, 560-564.

(23) (a) Miyaura, N.; Suzuki, A. *Chem. Rev.* **1995**, *95*, 2457-2483. (b) Suzuki, A. *J. Organomet. Chem.* **1999**, *576*, 147-168.

(24) Chen, H; Hartwig, J. F. *Angew. Chem. Int. Ed. Engl.* **1999**, *38*, 3391-3393.

(25) Ishiyama, T.; Murata, M.; Miyaura, N. *J. Org. Chem.* **1995**, *60*, 7508-7510.

(26) (a) Chen, H; Schlecht, S.; Semple, T. C.; Hartwig, J. F. *Science*, **2000** *287*, 1995-1997. (b) Cho, J.-Y., Iverson, C. N.; Smith, M. R. III *J. Am. Chem. Soc.* **2000** *122*, 12868-12869. (c) Tse, M. K.; Cho, J.-Y.; Smith M. R. III *Org. Lett.* **2001** *3*, 2831-2833. (d) Shimada, S.; Batsanov, A. S.; Howard, J. A. K.; Marder, T. B. *Angew. Chem. Int. Ed. Engl.* **2001**, *40*, 2168-2171. (e) Cho, J.-Y.; Tse, M. K.; Holmes, D.; Maleczka, R. E. Jr.; Smith, M. R. III *Science* **2002**, *295*, 305-308. (f) Ishiyama, T.; Takagi, J.; Ishida, K.; Miyaura, N.; Anastasi, N. R.; Hartwig, J. F. *J. Am. Chem. Soc.* **2002** *124*, 390-391. (g) Takagi, J.; Kazuaki, S.; Hartwig, J. F.; Ishiyama, T.; Miyaura, N. *Tetrahedron Lett.* **2002** *43*, 5649-5651.

(27) Goldfuss, B.; Knochel, P.; Bromm, L. O.; Knapp K. *Angew. Chem. Int. Ed. Engl.* **2000**, *39*, 4136-4139.

(28) Aizenberg, M.; Milstein, D. *Science* **1994**, *265*, 359-361.

(29) Jones, W. D.; Feher, F. J. *J. Am. Chem. Soc.* **1984**, *106*, 1650-1663.

(30) Kawamura, K.; Hartwig, J. F. *J. Am. Chem. Soc.* **2001**, *123*, 8422-8423.

(31) Nguyen, P.; Blom, H. P.; Westcott, S. A.; Taylor, N. J.; Marder, T. B. *J. Am. Chem. Soc.* **1993**, *115*, 9329-9330.

(32) The approach was first demonstrated by Dr. Man Kin Tse.

(33) Some of the experiments were carried out by Dr. Man Kin Tse.

(34) Anastasi, N. R.; Hartwig, J. F. *J. Am. Chem. Soc.* **2002**, *124*, 390-391.

(35) Ezbiansky, K.; Djurovich, P. I.; LaForest, M.; Sinning, D. J.; Zayes, R.; Berry, D. H. *Organometallics* **1998**, *17*, 1455-1457.

(36) Murata, M.; Oyama, T.; Watanabe, S.; Masuda, Y. *J. Org. Chem.* **2000**, *65*, 164-168.

(37) White, D. P.; Anthony, J. C.; Oyefeso, A. O. *J. Org. Chem.* **1999**, *64*, 7707-7716.

(38) Winstein, S.; Holness, N. *J. Am. Chem. Soc.* **1955**, *77*, 5562-5578.

(39) CRC Handbook of Chemistry and Physics, 83rd Edition **2002**, Lide, D. L. CRC Press.

(40) (a) Dawans, F.; Morel, D. *J. Mol. Catal.* **1977-78**, *3*, 403. (b) Halpem, J.; Okamoto, T.; Zakhariev, A. *J. Mol. Catal.* **1976**, *2*, 65. (c) Chan, A. S. C.; Halpem, J. *J. Am. Chem.*

Soc. **1980**, *102*, 838. (d) Halpern, J. *Inorg. Chim. Acta.* **1981**, *50*, 11. (e) Halpern, J.; Riley, D. P.; Chan, A. C. S.; Pluth, J. J. *J. Am. Chem. Soc.* **1977**, *99*, 8055. (f) Halpern, J. *Science* **1982**, *217*, 401.

(41) Harper, T. G. P.; Desrosiers, P. J.; Flood, T. C. *Organometallics* **1990**, *9*, 2523-2528.

(42) Knorr, J. R.; Merola, J. S. *Organometallics* **1990**, *9*, 3008-3010.

(43) Dai, C; Stringer, G; Marder, T. B.; Scott, A. J.; Clegg, W; Norman, N. C. *Inorg. Chem.* **1997**, *36*, 272-273.

(44) Thorn, D. L.; Tulip, T. H. *Organometallics* **1982**, *1*, 1580-1586.

(45) Harris, R. K. *In* Nuclear Magnetic Resonance Spectroscopy. Longman Scientific and Technical, Essex, U.K. 1986

(46) Dai, C.; Stringer, G.; Marder, T. B.; Baker, R. T.; Scott, A. J.; Clegg, W.; Norman, N. C. *Can. J. Chem.* **1996**, *74*, 2026-2031.

(47) Cleary, B.; Eisenberg, R. *Organometallics* **1995**, *14*, 4525-4534.

(48) (a) Johnson, C. E.; Eisenberg, R. *J. Am. Chem. Soc.* **1985**, *107*, 3148-3160. (b) Johnson, C. E.; Eisenberg, R. *J. Am. Chem. Soc.* **1985**, *107*, 6531-6540.

(49) Sargent, A. L.; Hall, M. B.; Guest, M. F. *J. Am. Chem. Soc.* **1992**, *114*, 517-522.

(50) Lu, Z.; Jun, C.-H.; de Gala, S. R.; Sigalas, M.; Eisenstein, O; Crabtree, R. H. *J. Chem. Soc., Chem. Commun.* **1993**, 1877-1880.

(51) Rickard, C. E. F.; Roper, W. R.; Williamson, A.; Wright, L. J. *Angew. Chem. Int. Ed.* **1999**, *38*, 1110-1113.

(52) Thorn, D. L. *Organometallics* **1982**, *1*, 197-204.

(53) The ratio was determined from the integrations of pinacol resonance in the ^{1}H NMR spectrum.

(54) Baker, R. T.; Ovenall, D. W.; Calabrese, J. C.; Westcott, S. A.; Taylor, N. J.; Williams, I. D.; Marder, T. B. *J. Am. Chem. Soc.* **1990**, *112*, 9399-9400.

(55) Aizenberg, M.; Milstein, D. *J. Am. Chem. Soc.* **1995**, *117*, 6456-6464.

(56) Sakaki S.; Satoru, K.; Manabu, S. *Organometallics* **1999**, *18*, 4825-4837.

182

(57) See Table 4 in the Chapter 3.

(58) Jones, W. D.; Feher, F. J. *J. Am. Chem. Soc.* **1986**, *108*, 4814-4819.

(59) The product distribution between C_6D_5BPin and C_6H_5BPin was determined by integrating the peaks in the GC-FID spectra, after correcting for the response factors determined from equimolar mixtures of independently synthesized arylboronate esters. The product distribution between $C_6D_2H_3(BPin)$ and $C_6D_3H_2(BPin)$ was extracted from ^1H NMR spectrum of the crude mixture. T1 measurement experiments were conducted before acquiring ^1H NMR spectra.

(60) Ishiyama, T.; Takagi, J.; Hartwig, J. F.; Miyaura, N. *Angew. Chem. Int. Ed.* **2002**, *41*, 3056-3058.

(61) Armarego, W. L. F.; Perrin, D. D. Purification of Laboratory Chemicals, Fourth Edition, Butterworth Heinemann.

(62) Herde, J. L.; Lambert, J. C.; Senoff, C. V. *Inorg. Synth.* **1974**, *15*, 18-20.

(63) Merola, J. S.; Kacmarcik, R. T. *Organometallics* **1989**, *8*, 778-784.

(64) Herskovitz, T. *Inorg. Synth.* **1982**, *21*, 99-102.

(65) Bowyer, W. J.; Merkert, J. W.; Geiger, W. E. *Organometallics* **1989**, *8*, 191- 198.

(66) Bowyer, W. J.; Geiger, W. E. *J. Am. Chem. Soc.* **1985**, *107*, 5657-5663.

(67) Janowicz, A. H.; Bergman, R. G. *J. Am. Chem. Soc.* **1983**, *105*, 3929-3939.

(68) Barefield, E. K. *Inorg. Synth.* **1974**, *15*, 34-38.

(69) Gilbert, T. M.; Bergman, R. G. *Organometallics* **1983**, *2*, 1458-1460.